

Characterization of Multi-Phase Performance-Based Passive Control Systems

by

Taylor A. Rawlinson

A thesis submitted to the Graduate Faculty of
Auburn University
in partial fulfillment of the
requirements for the Degree of
Master of Science

Auburn, Alabama
December 12th, 2011

Keywords: performance-based, earthquake, multi-phase,
structures, engineering

Copyright 2011 by Taylor Rawlinson

Approved by

Justin D. Marshall, Chair, Assistant Professor of Civil Engineering
Mary L. Hughes, Instructor of Civil Engineering
James S. Davidson, Associate Professor of Civil Engineering

Abstract

Typical passive control devices have inherent strengths and weaknesses as seismic protection systems. A Multi-phase Passive Control System (MPCS) combines two types of passive control devices in a system in order to offset the weaknesses of each system individually and to optimize structural performance. The performance-based nature of a MPCS in structural design allows the structure to respond effectively to varying levels of lateral loading. Previous work indicates the effectiveness of combining passive control devices but the fundamental understanding of the system is lacking. A single-degree-of-freedom (SDOF) non-linear dynamic study was performed in order to more clearly define multi-phase behavior and identify important parameters affecting response. Seismic hazard, system arrangement, system strength, system components, and material properties were all varied in order to fundamentally understand which parameters had significant effects on response. An incremental dynamic analysis was performed on the SDOF systems for a suite of scaled strong ground motions representing an array of site characteristics. Important response quantities included total acceleration, base shear, element ductility demand, and drift. Compared to the baseline systems, overall structural performance showed improved behavior with multi-phase configurations. The results of this study offer significant insight towards future work involving MPCS.

Acknowledgments

First, I would like to thank Dr. Marshall for giving me the opportunity to further myself at Auburn University. His advice and guidance throughout this research has been very beneficial to my success. Always making himself available and offering valuable feedback and passion towards the research, Dr. Marshall has been a very enjoyable person to work alongside. I look forward to our continued research over the next few years as I continue my studies.

I would also like to acknowledge the rest of my committee. Dr. Hughes has been a tremendous help throughout the duration of my graduate career. Whether it be a research question, class work question, or just general chit-chat, her positive attitude and willingness to help is extremely appreciated. Dr. Davidson has provided me with useful information applied throughout this research in the 3 courses I have taken with him here at Auburn. I truly appreciate the time and feedback they have devoted to this project. In addition to my committee members, I would also like to thank Dr. LaMondia who devoted time to helping me when I was struggling with the statistical aspects of the research.

I would also like to thank my family, especially my mother, whose love and support throughout the duration of my schooling have helped me grow as an individual.

My mother's strong work ethic and determination have provided me a strong disposition for success. In addition to my mother, my girlfriend Alana Resmini has provided me with a tremendous amount of support. I would also like to thank my fellow graduate students and friends whose camaraderie has made Auburn a very enjoyable place to study and live the last two years.

Table of Contents

| | |
|--|------|
| Abstract..... | ii |
| Acknowledgments | iii |
| List of Tables..... | viii |
| List of Figures | ix |
| Chapter 1 Introduction..... | 1 |
| 1.1 Defining the Problem..... | 1 |
| 1.2 The Proposed Solution..... | 2 |
| 1.3 Scope of Work..... | 4 |
| 1.4 Organization of Thesis..... | 5 |
| Chapter 2 Literature Review | 7 |
| 2.1 Introduction..... | 7 |
| 2.2 Active Control Devices..... | 8 |
| 2.3 Semi-Active Control Devices | 9 |
| 2.4 Passive Control Devices | 11 |
| 2.5 Hybrid Control Devices | 23 |
| 2.6 Multi-Phase Passive Control Devices | 23 |
| 2.7 Multi-Phase Behavior | 24 |
| 2.8 Summary..... | 33 |
| Chapter 3 Parametric Study Development and Analysis Plan | 34 |

| | | |
|--|--------------------------------------|----|
| 3.1 | Introduction | 34 |
| 3.2 | Velocity-Dependent Device | 35 |
| 3.3 | Displacement-Dependent Device | 36 |
| 3.4 | System Arrangement | 37 |
| 3.5 | Baseline Systems | 41 |
| 3.6 | Transition Phase (Gap Size)..... | 46 |
| 3.7 | Seismic Hazard..... | 46 |
| 3.8 | Natural Period | 48 |
| 3.9 | Experimental Design | 49 |
| 3.10 | System Names | 51 |
| 3.11 | Summary | 51 |
| Chapter 4 Nonlinear SDOF Response History Analysis | | 53 |
| 4.1 | Introduction | 53 |
| 4.2 | System Parameters | 53 |
| 4.3 | Earthquake Records..... | 54 |
| 4.4 | Modeling Details | 58 |
| 4.5 | Incremental Dynamic Analysis | 65 |
| 4.6 | Response Quantities | 66 |
| 4.7 | Summary | 67 |
| Chapter 5 Preliminary Analysis | | 69 |
| 5.1 | Introduction | 69 |
| 5.2 | Preliminary Analysis | 69 |
| 5.2 | Reduction of the Research Scope..... | 76 |

| | | |
|---|--|-----|
| 5.3 | Summary | 83 |
| Chapter 6 Full Factorial Analysis | | 85 |
| 6.1 | Introduction | 85 |
| 6.2 | Comparison to Baselines | 85 |
| 6.3 | Comparison Between Natural Periods..... | 91 |
| 6.4 | Comparison Between Multi-Phase Systems | 96 |
| 6.5 | Acceleration Spikes | 127 |
| 6.6 | Residual Drifts | 131 |
| 6.7 | Summary | 132 |
| Chapter 7 Summary and Conclusions | | 135 |
| 7.1 | Summary | 135 |
| 7.2 | Conclusions | 137 |
| 7.3 | Future Work | 140 |
| References | | 143 |
| Appendix A. | Preliminary Design | 148 |
| Appendix B. | Final Design | 170 |

List of Tables

| | |
|---|----|
| Table 3-1: Multi-Phase Systems and Abbreviations | 37 |
| Table 3-2: Dual System Stiffness Derivation..... | 45 |
| Table 3-3: System Naming Scheme | 51 |
| Table 4-1: Los Angeles Record Selection Summary..... | 55 |
| Table 4-2: Memphis Record Selection Summary | 56 |
| Table 4-3: Link Element Backbone Curve Values (ASCE/SEI, 2007)..... | 60 |
| Table 4-4: Response Quantity Summary | 67 |
| Table 5-1: Connecting Letters Report | 79 |

List of Figures

| | |
|---|----|
| Figure 2-1: Typical Performance Curve (Ghobarah, 2001)..... | 7 |
| Figure 2-2: Magnetorheological Fluid Damper (Spencer Jr. & Nagarajaiah, 2003)..... | 10 |
| Figure 2-3: Velocity-dependent Hysteresis Comparison..... | 12 |
| Figure 2-4: Typical Viscous Fluid Damper (Lee & Taylor, 2001) | 14 |
| Figure 2-5: Viscoelastic Device Configuration (Aiken et al., 1993)..... | 15 |
| Figure 2-6: VE Devices in All Stories (Kim et al., 2006) | 16 |
| Figure 2-7: Displacement-Dependent Hysteresis Comparison | 17 |
| Figure 2-8: Typical ADAS Configuration (Alehashem et al., 2008) | 18 |
| Figure 2-9: Acceleration Response Comparison with ADAS Device (Tehranizadeh, 2001) | 19 |
| Figure 2-10: BRB Schematic with Hysteretic Behavior (Sabelli et al, 2003) | 20 |
| Figure 2-11: Typical Slotted Bolted Connection (Balendra et al., 2001) | 22 |
| Figure 2-12: Pall Friction Device (Aiken et al., 1993) | 23 |
| Figure 2-13: Sequential Connection Schematics (Weidlinger & Ettouney, 1993) | 25 |
| Figure 2-14: Benefits of Sequential Coupling (Weidlinger & Ettouney, 1993) | 26 |
| Figure 2-15: Stiffening Single-Degree-of-Freedom System (Motlagh & Saadeghvaziri, 2001) | 27 |
| Figure 2-16: Stiffening Single-Degree-of-Freedom Comparison to Baseline (Motlagh & Saadeghvaziri, 2001)..... | 27 |
| Figure 2-17: Finite Element Model of the VPD (Ibrahim et al., 2007) | 28 |

| | |
|--|----|
| Figure 2-18: Multi-Phase Passive Control Device (Marshall, 2008) | 29 |
| Figure 2-19: High-damping Rubber Sandwich Damper Schematic (Marshall, 2008) | 30 |
| Figure 2-20: Possible Arrangements of Multi-Phase Systems (Marshall, 2008)..... | 31 |
| Figure 2-21: Acceleration Response Comparison (Marshall, 2008) | 32 |
| Figure 2-22: DBE Residual Displacement Comparison (Marshall, 2008) | 32 |
| Figure 3-1: BRB Yield Length (Lopez & Sabelli, 2004) | 37 |
| Figure 3-2: Multi-Phase Passive Control Systems | 38 |
| Figure 3-3: Elastomeric Device (Karavasilis et al., 2010)..... | 41 |
| Figure 3-4: Comparison of Two Systems with Different Baselines (Marshall, 2008)..... | 42 |
| Figure 3-5: Moment Frame Stiffness/Strength Comparison..... | 43 |
| Figure 3-6: Buckling Restrained Brace Frame Stiffness/Strength Comparison | 44 |
| Figure 3-7: Comparison of the Design Response Spectrums | 48 |
| Figure 3-8: Design Spectrums with System Natural Periods..... | 49 |
| Figure 3-9: System Combinations | 50 |
| Figure 4-1: Rayleigh Damping..... | 54 |
| Figure 4-2: Los Angeles Ground Motion Selection and Scaling | 57 |
| Figure 4-3: Memphis Ground Motion Selection and Scaling | 58 |
| Figure 4-4: Special Moment Frame Component Breakdown | 59 |
| Figure 4-5: Link Backbone Behavior (ASCE/SEI, 2007) | 60 |
| Figure 4-6: Modeled Baseline System..... | 61 |
| Figure 4-7: Gap Element Modeling..... | 62 |
| Figure 4-8: Modeling of the Series Systems..... | 63 |
| Figure 4-9: EMD Hysteretic Slip Behavior | 64 |

| | |
|--|-----|
| Figure 4-10: Modeling of the Parallel Systems..... | 65 |
| Figure 5-1: Acceleration Results for 0.5T Los Angeles Systems | 71 |
| Figure 5-2: Base Shear Results for 0.5T Los Angeles Systems..... | 71 |
| Figure 5-3: Moment Frame Ductility Results for 0.5T Los Angeles Systems | 72 |
| Figure 5-4: BRB Ductility Results for 0.5T Los Angeles Systems..... | 72 |
| Figure 5-5: Hierarchal Nesting Issue..... | 75 |
| Figure 5-6: 1T-M70B30-1.0-HYFR Seismic Hazard Comparison..... | 77 |
| Figure 5-8: Moment Frame Ductility Comparison between Dual System Ratios | 80 |
| Figure 5-9: M-S-2.5T-M50B50-HPCD-VFD Gap Size Comparison | 81 |
| Figure 5-10: Full Factorial Experimental Design..... | 83 |
| Figure 6-1: Multi-Phase System Acceleration Comparison to Baseline (1T-M50B50) .. | 87 |
| Figure 6-2: Multi-Phase System Base Shear Comparison to Baseline (1T-M50B50) | 87 |
| Figure 6-3: Multi-Phase System Moment Frame Ductility Comparison to Baseline (1T-M50B50)..... | 88 |
| Figure 6-4: Multi-Phase System Brace Ductility Comparison to Baseline (1T-M50B50)..... | 89 |
| Figure 6-5: Acceleration Comparison of Multi-Phase Systems to Baselines (0.25T) | 92 |
| Figure 6-6: Acceleration Comparison of Multi-Phase Systems to Baselines (2.5T) | 93 |
| Figure 6-7: Brace Ductility Comparison of Multi-Phase Systems to Baselines (0.25T) .. | 93 |
| Figure 6-8: Brace Ductility Comparison of Multi-Phase Systems to Baselines (2.5T) ... | 94 |
| Figure 6-9: Gap Element Displacement Comparison..... | 95 |
| Figure 6-10: HPCD 1T Comparison to Baselines | 98 |
| Figure 6-11: HPCD 1T Moment Frame Ductility | 99 |
| Figure 6-12: HPCD 1T Acceleration Response | 101 |

| | |
|---|-----|
| Figure 6-13: HPCD 1T Base Shear Response..... | 101 |
| Figure 6-14: HPCD 1T Brace Ductility | 102 |
| Figure 6-15: HPCD-VFD 1T Comparison to Baselines | 103 |
| Figure 6-16: HPCD-VFD 1T Moment Frame Ductility | 105 |
| Figure 6-17: HPCD-VFD 1T Acceleration Response | 106 |
| Figure 6-18: HPCD-VFD 1T Base Shear Response..... | 107 |
| Figure 6-19: Gap Element Comparison for M50B50-1T (DZC270 DBE)..... | 107 |
| Figure 6-20: HPCD-VFD 1T Brace Ductility | 108 |
| Figure 6-21: HPCD-VFD Damping Ratio Comparison | 110 |
| Figure 6-22: HPCD vs. HPCD-VFD (M40B60-1.0-1T) | 111 |
| Figure 6-23: HYFR 1T Comparison to Baselines | 112 |
| Figure 6-24: HYFR 1T Moment Frame Ductility | 113 |
| Figure 6-25: HYFR 1T Acceleration Response | 115 |
| Figure 6-26: HYFR 1T Base Shear Response..... | 116 |
| Figure 6-27: HYFR 1T Brace Ductility Response | 117 |
| Figure 6-28: HPCD vs. HYFR Performance | 118 |
| Figure 6-29: HYFR-VFD Comparison to Baselines | 119 |
| Figure 6-30: HYFR-VFD 1T Moment Frame Ductility | 121 |
| Figure 6-31: HYFR-VFD 1T Acceleration Response | 122 |
| Figure 6-32: HYFR-VFD 1T Base Shear Response..... | 123 |
| Figure 6-33: HYFR-VFD 1T Brace Ductility | 124 |
| Figure 6-34: HYFR-VFD Damping Ratio Comparison | 125 |
| Figure 6-35: System Arrangement Comparison..... | 126 |

| | |
|--|-----|
| Figure 6-36: a) HYFR-VFD-0.25T-1.0 Gap-M40B60 Acceleration Response History b) HYFR-VFD-1T-1.0 Gap-M40B60 Acceleration Response History | 128 |
| Figure 6-37: a) HPCD-0.25T-1.0 Gap-M40B60 Acceleration Response History b) HPCD-1T-1.0 Gap-M40B60 Acceleration Response History | 130 |
| Figure 6-38: Residual Deformations | 132 |
| Figure A- 1: Los Angeles 0.25T Acceleration | 148 |
| Figure A- 2: Los Angeles 0.25T Base Shear | 148 |
| Figure A- 3: Los Angeles 0.25T Moment Frame Ductility | 149 |
| Figure A- 4: Los Angeles 0.25T Brace Ductility | 149 |
| Figure A- 5: Memphis 0.25T Acceleration | 150 |
| Figure A- 6: Memphis 0.25T Base Shear | 150 |
| Figure A- 7: Memphis 0.25T Moment Frame Ductility | 151 |
| Figure A- 8: Memphis 0.25T Brace Ductility | 152 |
| Figure A- 9: Los Angeles 0.5T Acceleration | 152 |
| Figure A- 10: Los Angeles 0.5T Base Shear | 153 |
| Figure A- 11: Los Angeles 0.5T Moment Frame Ductility | 153 |
| Figure A- 12: Los Angeles 0.5T Brace Ductility | 154 |
| Figure A- 13: Memphis 0.5T Acceleration | 154 |
| Figure A- 14: Memphis 0.5T Base Shear | 155 |
| Figure A- 15: Memphis 0.5T Moment Frame Ductility | 155 |
| Figure A- 16: Memphis 0.5T Brace Ductility | 156 |
| Figure A- 17: Los Angeles 1T Acceleration | 156 |
| Figure A- 18: Los Angeles 1T Base Shear | 157 |
| Figure A- 19: Los Angeles 1T Moment Frame Ductility | 157 |

| | |
|---|-----|
| Figure A- 20: Los Angeles 1T Brace Ductility | 158 |
| Figure A- 21: Memphis 1T Acceleration..... | 159 |
| Figure A- 22: Memphis 1T Base Shear | 159 |
| Figure A- 23: Memphis 1T Moment Frame Ductility | 160 |
| Figure A- 24: Memphis 1T Brace Ductility..... | 160 |
| Figure A- 25: Los Angeles 2.5T Acceleration | 161 |
| Figure A- 26: Los Angeles 2.5T Base Shear | 161 |
| Figure A- 27: Los Angeles 2.5T Moment Frame Ductility | 162 |
| Figure A- 28: Los Angeles 2.5T Brace Ductility | 162 |
| Figure A- 29: Memphis 2.5T Acceleration..... | 163 |
| Figure A- 30: Memphis 2.5T Base Shear | 163 |
| Figure A- 31: Memphis 2.5T Moment Frame Ductility | 164 |
| Figure A- 32: Memphis 2.5T Brace Ductility | 164 |
| Figure A- 33: Los Angeles 4T Acceleration | 165 |
| Figure A- 34: Los Angeles 4T Base Shear | 165 |
| Figure A- 35: Los Angeles 4T Moment Frame Ductility | 166 |
| Figure A- 36: Los Angeles 4T Brace Ductility | 167 |
| Figure A- 37: Memphis 4T Acceleration..... | 167 |
| Figure A- 38: Memphis 4T Base Shear | 168 |
| Figure A- 39: Memphis 4T Moment Frame Ductility | 168 |
| Figure A- 40: Memphis 4T Brace Ductility..... | 169 |
| Figure B- 1: Los Angeles 0.25T HYFR Acceleration | 170 |
| Figure B- 2: Los Angeles 0.25T HYFR-VFD Acceleration | 170 |

| | |
|---|-----|
| Figure B- 3: Los Angeles 0.25T HPCD Acceleration | 171 |
| Figure B- 4: Los Angeles 0.25T HPCD-VFD Acceleration | 171 |
| Figure B- 5: Los Angeles 0.25T HYFR Base Shear | 172 |
| Figure B- 6: Los Angeles 0.25T HYFR-VFD Base Shear..... | 172 |
| Figure B- 7: Los Angeles 0.25T HPCD Base Shear | 173 |
| Figure B- 8: Los Angeles 0.25T HPCD-VFD Base Shear..... | 173 |
| Figure B- 9: Los Angeles 0.25T HYFR Moment Frame Ductility | 174 |
| Figure B- 10: Los Angeles 0.25T HYFR-VFD Moment Frame Ductility | 174 |
| Figure B- 11: Los Angeles 0.25T HPCD Moment Frame Ductility | 175 |
| Figure B- 12: Los Angeles 0.25T HPCD-VFD Moment Frame Ductility | 175 |
| Figure B- 13: Los Angeles 0.25T HYFR Brace Ductility | 176 |
| Figure B- 14: Los Angeles 0.25T HYFR-VFD Brace Ductility | 176 |
| Figure B- 15: Los Angeles 0.25T HPCD Brace Ductility | 177 |
| Figure B- 16: Los Angeles 0.25T HPCD-VFD Brace Ductility | 177 |
| Figure B- 17: Los Angeles 0.5T HYFR Acceleration | 178 |
| Figure B- 18: Los Angeles 0.5T HYFR-VFD Acceleration | 178 |
| Figure B- 19: Los Angeles 0.5T HPCD Acceleration | 179 |
| Figure B- 20: Los Angeles 0.5T HPCD-VFD Acceleration | 179 |
| Figure B- 21: Los Angeles 0.5T HYFR Base Shear | 180 |
| Figure B- 22: Los Angeles 0.5T HYFR-VFD Base Shear..... | 180 |
| Figure B- 23: Los Angeles 0.5T HPCD Base Shear | 181 |
| Figure B- 24: Los Angeles 0.5T HPCD-VFD Base Shear..... | 181 |
| Figure B- 25: Los Angeles 0.5T HYFR Moment Frame Ductility | 182 |

| | |
|--|-----|
| Figure B- 26: Los Angeles 0.5T HYFR-VFD Moment Frame Ductility | 182 |
| Figure B- 27: Los Angeles 0.5T HPCD Moment Frame Ductility | 183 |
| Figure B- 28: Los Angeles 0.5T HPCD-VFD Moment Frame Ductility | 183 |
| Figure B- 29: Los Angeles 0.5T HYFR Brace Ductility | 184 |
| Figure B- 30: Los Angeles 0.5T HYFR-VFD Brace Ductility | 184 |
| Figure B- 31: Los Angeles 0.5T HPCD Brace Ductility | 185 |
| Figure B- 32: Los Angeles 0.5T HPCD-VFD Brace Ductility | 185 |
| Figure B- 33: Los Angeles 1T HYFR Acceleration | 186 |
| Figure B- 34: Los Angeles 1T HYFR-VFD Acceleration | 186 |
| Figure B- 35: Los Angeles 1T HPCD Acceleration | 187 |
| Figure B- 36: Los Angeles 1T HPCD-VFD Acceleration | 187 |
| Figure B- 37: Los Angeles 1T HYFR Base Shear | 188 |
| Figure B- 38: Los Angeles 1T HYFR-VFD Base Shear | 188 |
| Figure B- 39: Los Angeles 1T HPCD Base Shear | 189 |
| Figure B- 40: Los Angeles 1T HPCD-VFD Base Shear | 189 |
| Figure B- 41: Los Angeles 1T HYFR Moment Frame Ductility | 190 |
| Figure B- 42: Los Angeles 1T HYFR-VFD Moment Frame Ductility | 190 |
| Figure B- 43: Los Angeles 1T HPCD Moment Frame Ductility | 191 |
| Figure B- 44: Los Angeles 1T HPCD-VFD Moment Frame Ductility | 191 |
| Figure B- 45: Los Angeles 1T HYFR Brace Ductility | 192 |
| Figure B- 46: Los Angeles 1T HYFR-VFD Brace Ductility | 192 |
| Figure B- 47: Los Angeles 1T HPCD Brace Ductility | 193 |
| Figure B- 48: Los Angeles 1T HPCD-VFD Brace Ductility | 193 |

| | |
|--|-----|
| Figure B- 49: Los Angeles 2.5T HYFR Acceleration | 194 |
| Figure B- 50: Los Angeles 2.5T HYFR-VFD Acceleration | 194 |
| Figure B- 51: Los Angeles 2.5T HPCD Acceleration | 195 |
| Figure B- 52: Los Angeles 2.5T HPCD-VFD Acceleration | 195 |
| Figure B- 53: Los Angeles 2.5T HYFR Base Shear | 196 |
| Figure B- 54: Los Angeles 2.5T HYFR-VFD Base Shear..... | 196 |
| Figure B- 55: Los Angeles 2.5T HPCD Base Shear | 197 |
| Figure B- 56: Los Angeles 2.5T HPCD-VFD Base Shear..... | 198 |
| Figure B- 57: Los Angeles 2.5T HYFR Moment Frame Ductility | 198 |
| Figure B- 58: Los Angeles 2.5T HYFR-VFD Moment Frame Ductility | 198 |
| Figure B- 59: Los Angeles 2.5T HPCD Moment Frame Ductility | 199 |
| Figure B- 60: Los Angeles 2.5T HPCD-VFD Moment Frame Ductility | 199 |
| Figure B- 61: Los Angeles 2.5T HYFR Brace Ductility | 200 |
| Figure B- 62: Los Angeles 2.5T HYFR-VFD Brace Ductility | 201 |
| Figure B- 63: Los Angeles 2.5T HPCD Brace Ductility | 201 |
| Figure B- 64: Los Angeles 2.5T HPCD-VFD Brace Ductility | 201 |

Chapter 1 Introduction

1.1 Defining the Problem

Catastrophic seismic events in recent times have received global attention and have increased concern about the resilience of structures. While engineers are prepared to design for life safety for such events, the need and motivation to evolve design to be more efficient and create greater resiliency is stronger than ever.

The two primary types of loading engineers are faced with in designing a structure include gravity and lateral loads. Within the scope of lateral loading, design is focused on elastic design for service level wind conditions and relies on inelastic behavior for the dissipation of energy for earthquake loading. Relying on elastic behavior for design level earthquake resistance is impractical and uneconomical given the large inertial forces exerted on the structure and the relatively infrequent occurrence of seismic events within the life of the structure. For these reasons, the emphasis of the design codes is primarily on life safety rather than structural resilience after an event. The 1994 Northridge and 1995 Kobe earthquakes demonstrated the need for a monumental shift in the design philosophy. More recently, 2011 New Zealand and 2011 Japan events have commanded worldwide attention for the protection of structures from seismic events. Although structures provided adequate life safety, the economic losses were far too great.

This research seeks to find a solution to seismic design that is able to provide life safety in addition to damage control. Limiting damage to a replaceable element and

minimizing non-structural damage would be an attractive option to building owners who want to return to business as quickly as possible after a seismic event.

Most structures rely on the structural system to dissipate the majority of the earthquake energy while ensuring post-event safety. When additional energy dissipation is needed, supplemental passive control devices such as viscous fluid dampers, viscoelastic solid dampers, metallic yielding devices, and friction dampers are paired with the structural system. However, the problem lies within the inherent strengths and weaknesses of these devices. Each device performs well under certain loading conditions but is not ideal for a range of loadings. For instance, viscous dampers are efficient at dissipating energy for wind and small to moderate seismic events but can become uneconomical when they are needed for a larger amount of supplemental damping. Alternatively, braces are efficient at dissipating large amounts of energy and are relatively inexpensive, but experience large accelerations, base shears, and possible inelastic deformations in small to moderate seismic events. This could require costly replacement following an event.

1.2 The Proposed Solution

The solution proposed in this work combines two different passive control devices working together as a system to create multi-phase behavior that utilizes the strengths of each device. There are three primary elements of a multi-phase passive control system: 1) a velocity-dependent damper, 2) a displacement-dependent energy dissipation device, and 3) a phase transition mechanism. Combining these elements with a moment frame creates two-phased behavior. The first phase involves the velocity-

dependent damper paired with a special moment frame for initial stiffness which reduces response through supplemental damping for severe wind events and low to moderate seismic events. The second phase involves the transition mechanism which engages at a displacement less than the yield displacement of the moment frame. After the transition, the displacement-dependent device adds significant stiffness and energy dissipation capability in the final phase. This phase would be utilized in moderate to severe events.

Many options exist for the multi-phase passive control systems and there is a need for research to understand the fundamental system behavior. The type of velocity-dependent or displacement-dependent energy dissipation devices needed in a multi-phase system is unclear. An extensive review of passive control devices to be included in a multi-phase system needs to be completed in order to find a solution. Many combinations of devices are available but the best-performing, most practical, reliable and economical combination is largely unknown. Arrangement of the phases in parallel or series also provides an interesting aspect to the research. By combining the phases in parallel, the damping in the first phase can happen concurrently with the significant energy dissipation in the second phase, a potentially appealing attribute. Other system characteristics, such as the transitional gap size and moment-frame-to-hysteretic-device strength ratio have a potential to largely affect response. All of these options need to be thoroughly researched in order to work towards an effective multi-phase passive control system.

The result of the multi-phase behavior is essentially a structure that is pre-programmed to respond to varying levels of lateral loading, ranging from service level wind conditions to major seismic events. A system that responds to varying levels of

loading is not a unique idea. However, a multi-phase *passive* control system which requires no electricity, maintenance, or controllers has tremendous potential to impact seismic design. The improvement in structural response would result in a decrease in the likelihood of structural damage within the design life of the structure while improving life safety. From an engineering standpoint, this is a marketable and viable option.

1.3 Scope of Work

Previous research demonstrates the effectiveness of combining passive control systems but the fundamentals of system behavior are unclear. A single-degree-of-freedom (SDOF) non-linear dynamic study was performed to clearly define multi-phase behavior and to identify important parameters affecting response. Because most structures respond primarily in the first mode of vibration, a SDOF study is initially sufficient to examine the fundamental system behavior. The research is completed in three main stages: 1) parametric development and analysis plan, 2) model development and nonlinear dynamic SDOF analytical study, and 3) interpretation of results.

The parametric development involves choosing the parameters and their range of acceptable values. An extensive literature review provides insight as to the type of parameters and values that should be involved in the study. The analysis plan involves a statistical experimental design in which the number of system combinations is reduced, yet the interactions are still captured between the parameters and the response. The model development is completed using SAP 2000 Version 14 (CSI, 2009). Models include linear and nonlinear elements to represent system and material behavior. The nonlinear dynamic SDOF study is completed using an incremental dynamic analysis for a suite of scaled ground motions representing various site conditions (Vamvatsikos &

Cornell, 2002). The interpretation of results evaluates the statistical significance of parameters on total acceleration, base shear, moment frame ductility, and displacement-dependent device ductility. The systems are also compared against baseline models to illustrate the benefits of adding supplemental damping and a transitional gap element. Other areas of concern such as acceleration spikes and residual deformations are also investigated.

The study seeks to reduce the range of possible combinations of devices to be combined in a multi-phased system. With a reduction in the range of qualified devices, the study can be expanded into a multi-degree of freedom (MDOF) study and then tested within a lab setting. This research provides the groundwork for a system that could largely change design philosophy.

1.4 Organization of Thesis

Chapter 2 provides a literature review on the development of passive control systems and their application to structures. Various types of passive control systems are reviewed in order to illustrate strengths and weaknesses of the systems. The need for multi-phase behavior of the systems is also demonstrated.

Chapter 3 presents the single-degree-of-freedom system development. Each parameter of the study is briefly discussed and an acceptable range of response values are chosen. Arrangement of the multi-phase systems are also discussed and illustrated. The statistical basis for the research is also described.

Chapter 4 describes the analytical study. The modeling of the system and material behavior is discussed. Details on ground motion selection and scaling are also presented.

Chapter 5 organizes the results from the preliminary SDOF study and investigates the statistical significance. The scope of the study is reduced to a reasonable range for a full factorial study to be completed.

Chapter 6 shows the results from the full factorial study developed in Chapter 5. Systems are compared to each other and also to baseline systems in order to demonstrate the benefits of multi-phase behavior. Other behavior elements, such as acceleration spikes and residual deformations are analyzed for a select group of systems.

Chapter 7 summarizes the findings of the study and offers recommendations for future work involving multi-phase passive control systems.

Chapter 2 Literature Review

2.1 Introduction

Conventional structural design provides life safety but in recent years there has been a push towards performance-based design. The 1994 Northridge and 1995 Kobe earthquakes were very significant seismic events, yet structures performed well from a life safety point-of-view. Unfortunately, the economic loss and cost of repair was much higher than expected, leading to a need for a fundamental change in the code towards performance-based design. Creating performance objectives in response to certain seismic hazards, a performance-based design seeks to provide additional life safety in addition to damage control (Ghobarah, 2001). The typical performance curve for a structure is indicated in Figure 2-1.

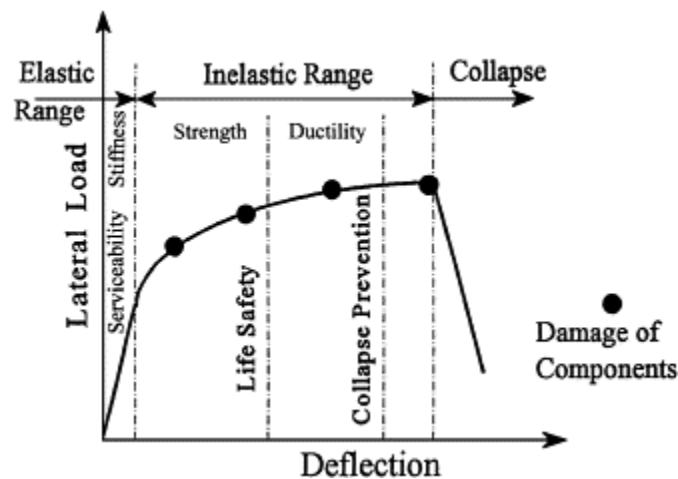


Figure 2-1: Typical Performance Curve (Ghobarah, 2001)

The Japanese seismic design code has already moved towards a performance-based engineering approach, first concerned with life safety and secondly with damage-

limitation levels. The life safety limit state is concerned with preventing an individual story and entire structure from collapsing. The damage limit state seeks to prevent damage and limit inelastic behavior only to the energy dissipation devices (Midorikawa, et al., 2000). Performance-based design essentially breaks design into three main parts: the seismic hazard, the structural system, and loss. The hazard and loss domains provide design constraints while the structural system provides design alternatives (Krawinkler et al., 2006).

The multi-phase passive control systems analyzed in this research are a prime example of performance-based design oriented lateral systems. Since the field of performance-based seismic engineering is relatively new, the results from the multi-phase passive control study could provide great strides towards improved design. A performance-based system could involve a large array of structural control systems. The following is an in-depth look at structural control systems in order to more clearly understand the options available for multi-phase control systems.

2.2 Active Control Devices

Active control devices utilize actuators, such as an active mass damper, to add or dissipate energy in a structure. Physical sensors relay information to the actuators which respond accordingly to reduce structural response. The first full-scale use of an active control device was in 1989 in Tokyo, using two active mass dampers. The role of this system was to reduce building vibration for strong winds and moderate earthquakes and to increase the comfort of the building occupants (Spencer Jr. & Nagarajaiah, 2003).

The primary problem with an active control device is that it uses an external power source to run the system. In load cases in which structural control would be most critical, such as strong wind or earthquakes, it is likely that electricity would be lost, making the building very vulnerable to damage (Asteris, 2008). The reliability and stability of the sensor system is an area of concern in active control and for most structures, the systems are not always cost effective or necessary for energy dissipation, leading to the use of semi-active or passive control devices.

2.3 Semi-Active Control Devices

Semi-active control is a rapidly developing area in the field of civil engineering. The devices do not add any mechanical energy to the structural system, but have properties that can be altered in order to reduce the structural response. Examples include controllable fluid dampers, controllable friction devices, variable stiffness devices, and variable-orifice fluid dampers. Many semi-active devices are able to operate on battery power, making it an appealing option because of the adaptability of the systems without the use of an external power source (Asteris, 2008).

Controllable fluid dampers offer simplicity and reliability to semi-active control in the form of electrorheological (ER) and magnetorheological (MR) devices. Reversible behavior between a viscous fluid and a semi-solid fluid is achieved by inducing an electric or magnetic field as needed to dissipate energy (Spencer Jr. & Nagarajaiah, 2003). ER fluids have been thoroughly researched and remain limited in use due to a limited yield stress range, high voltage requirements, low level of safety, and intolerability to fluid impurities. In recent years, magnetorheological (MR) fluid

dampers, as illustrated in Figure 2-2, have become a more attractive option for semi-active controllable fluid dampers. MR fluid is able to achieve much higher yield stresses than ER fluids in addition to requiring much less power, and exhibiting resilience to temperature changes and fluid impurities (Spencer Jr. & Sain, 1997).

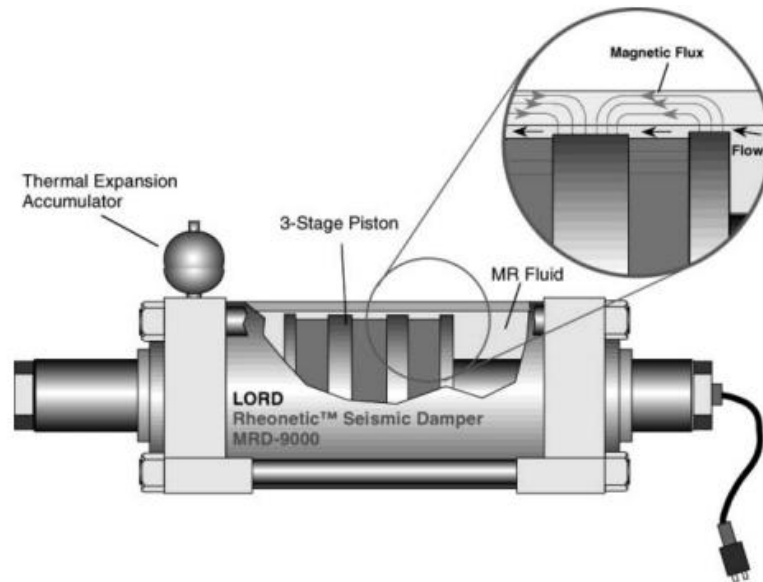


Figure 2-2: Magnetorheological Fluid Damper (Spencer Jr. & Nagarajaiah, 2003)

Due to that fact that this is a developing field, there are still many inherent problems to be resolved. Complex algorithms that are not yet optimal are involved in relaying information from sensors to the control center. Also, when using a displacement-dependent or accumulated semi-active hydraulic damper, the time delay between the sensor and controller is about 0.11 to 0.13 seconds. Therefore, when the frequency is greater than 1.0 Hz, the device will lose the efficiency of semi-active control and could possibly amplify response (Shih & Sung, 2010). Maintenance costs, design costs, and the reliability of vibration sensors over time are other issues that could deter the use of a semi-active system in its current state.

2.4 Passive Control Devices

Passive control devices, the first and most common structural control device, utilize relative displacement between two attachment points to dissipate energy. Examples of passive control devices include base isolation systems, viscoelastic dampers, viscous fluid dampers, tuned mass dampers, metallic yielding devices, and friction devices. These devices are often favored in design due to low maintenance costs, stability, and absence of an external power source (Spencer Jr. & Nagarajaiah, 2003). The use of passive control devices also minimizes structural damage by restricting the energy dissipation and damage to the device, making it favorable for post-event repairs. Behavior of passively controlled systems is also widely understood and accepted in structural design for dynamic resistance. The major drawback of typical passive control devices is that they are unable to adapt to structural load changes, from service level loading to extreme wind or seismic events. Design of a passive system that effectively handles all of these load conditions is currently far from optimal, yet necessary for life safety (Asteris, 2008).

2.4.1 Base Isolation

Base isolation is a passive control mechanism used in low-to-mid-rise structures. In the most common base isolation system, the structure is connected to the ground using layers of material that are stiff under gravity loads, yet flexible under lateral loads. The horizontal flexibility gives the structure a much longer natural period than a fixed-base structure. This substantially reduces the expected forces within the first mode of

response. Deformation is primarily concentrated in the isolation system and therefore the structural system experiences minimal drifts (Chopra, 2007). Problems associated with the large deformations in the isolation system are the mechanical, electrical, and plumbing materials at the base which must be specially detailed to avoid damage. The cost of this isolation system is often a deterrent for a typical structure. Base isolation is typically used for historical retrofits and important structures in areas of high seismicity.

2.4.2 Velocity-Dependent Passive Control Devices

Velocity-dependent, often referred to as rate-dependent, passive control devices rely on relative motion for energy dissipation. They are typically cost effective and can be used in the design of a new structure or added to existing structures to provide additional protection (Chopra, 2007). The two most typical rate-dependent devices are viscous fluid dampers (VFD) and viscoelastic dampers (VED). The typical hysteretic behavior of these devices is found in Figure 2-3. Damping values can vary largely depending on the type and implementation of damping device. The damping coefficients used in this research will be discussed within the parametric development in Chapter 3.

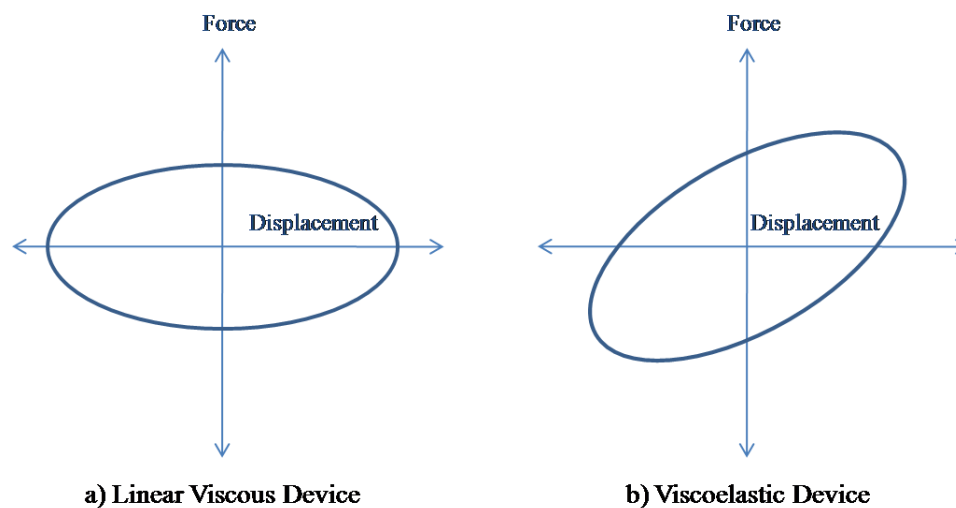


Figure 2-3: Velocity-dependent Hysteresis Comparison

2.4.2.1 Viscous Fluid Dampers

Viscous fluid dampers consist of a cylinder filled with a fluid, typically silicon, and a piston with orifices on the face (Figure 2-4). The travel of the piston through the fluid inside the cylinder dissipates energy. Although the device is operational and stable at various temperatures and frequencies, the viscous properties of the damper do vary (Reinhorn et al., 1995). Viscous fluid dampers can be either linear or nonlinear depending on the arrangement of the orifices on the face of the piston. The linear hysteresis loop has an elliptical shape (Figure 2-3) but as the nonlinear exponent approaches 0.3, the hysteresis loop is nearly rectangular (Lee & Taylor, 2001). Inclusion of viscous fluid dampers in an elastic steel structure shaking table experiment have shown to reduce story drift and shear forces by 30% to 70% in addition to improving drift response in inelastic systems (Reinhorn et al., 1995).

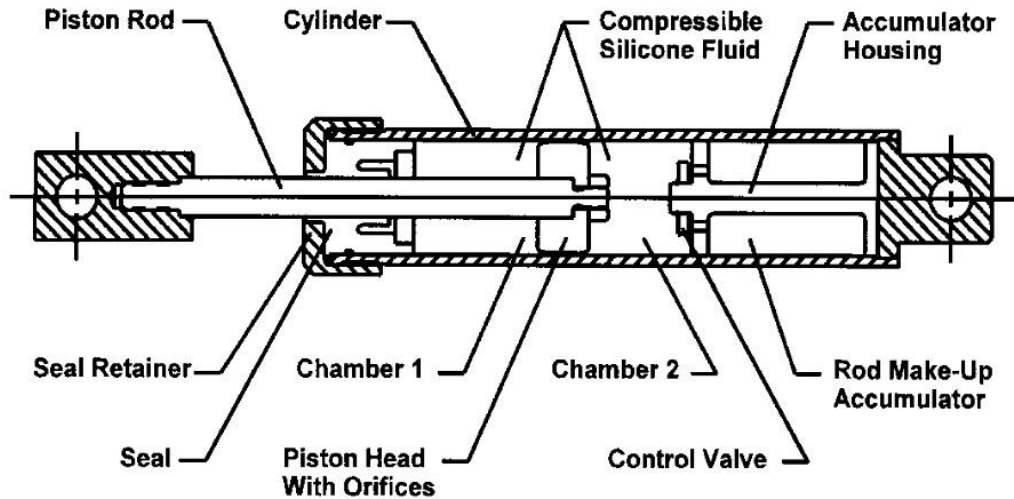


Figure 2-4: Typical Viscous Fluid Damper (Lee & Taylor, 2001)

2.4.2.2 Viscoelastic Dampers

Viscoelastic devices utilize layers of polymers to dissipate energy in shear deformation (Chopra, 2007). Figure 2-5 illustrates a typical configuration for a VE device which utilizes a viscoelastic material, such as high-damping natural rubber, sandwiched between two metal plates. That ability to reach strains up to 500% before failure means that the device can dissipate energy over a large range of deformation (Marshall, 2008).

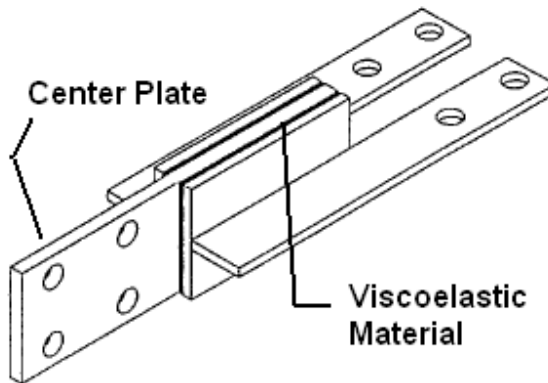


Figure 2-5: Viscoelastic Device Configuration (Aiken et al., 1993)

Variation in temperature can significantly impact the performance of a viscoelastic device. An increase of 10°C can alter material storage and loss modulus from 30% to 50% at low frequencies and even more at higher frequencies, meaning that a fluctuation in temperature could largely affect the energy dissipation capability (Reinhorn et al., 1995). This is typically not an issue for seismic events because of the short duration but can cause problems for strong wind events due to a build-up of heat over repeated strain cycles. The development of newer rubber materials has decreased the variability in performance and increased the energy dissipation capacity (Marshall, 2008). As evident in Figure 2-3, viscoelastic devices do provide additional stiffness to a system. Although this could decrease the natural period of the structure and thus increase the seismic response, the period is typically only shortened by about 10% to 20%, which is much less than the effect of most metallic displacement-dependent devices (Chopra, 2007).

Although primarily used for wind excitation, considerable research has been performed in recent years on VE dampers for seismic protection. One dynamic analysis demonstrates the effectiveness of installing VE dampers between seismic joints or sky bridges between structures. As evident in Figure 2-6, displacements were significantly decreased, especially if the natural frequencies of the connected structures were different (Kim et al., 2006).

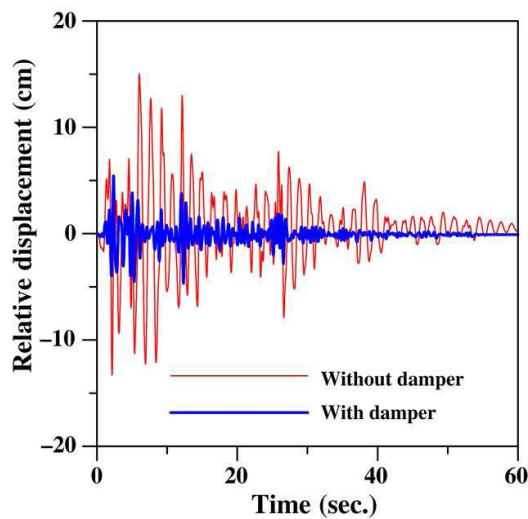


Figure 2-6: VE Devices in All Stories (Kim et al., 2006)

2.4.3 Displacement-Dependent Passive Control Devices

Another type of passive control, which is rate-independent (or velocity-independent), is often referred to as “hysteretic”. Use of these rate-independent devices significantly affects seismic response due to a high elastic stiffness which can drastically shorten the natural period of the structure. Although the seismic hazard may significantly increase, the large inelastic capabilities are appealing for energy dissipation. The two

most common classes of hysteretic devices are metallic yielding devices and friction devices. The hysteretic behavior of each is represented in Figure 2-7.

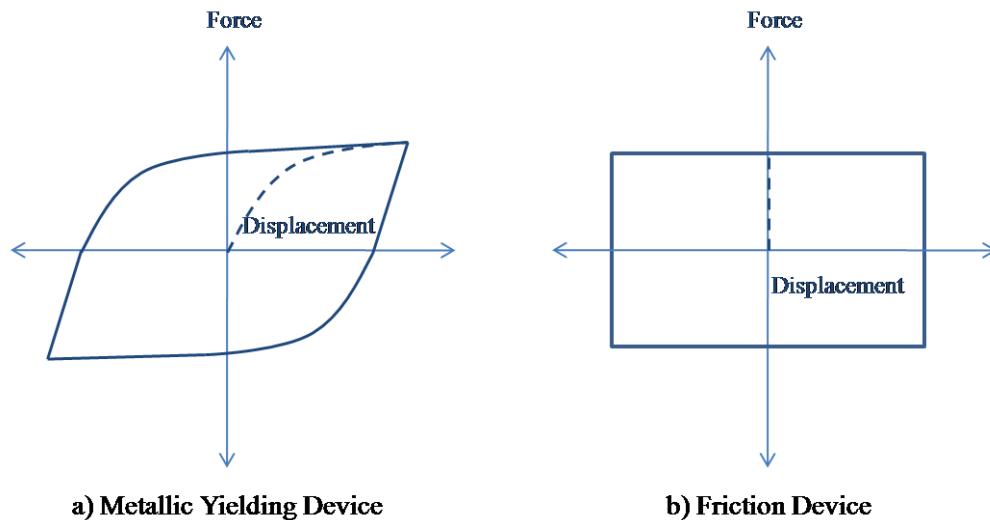


Figure 2-7: Displacement-Dependent Hysteresis Comparison

2.4.3.1 Metallic Yielding Devices

Metallic yielding devices rely heavily on the inelastic action of the metal, typically mild steel, to dissipate energy. Numerous devices and configurations have been designed, researched, and implemented with success. One such application involves adding damping and stiffness (ADAS) elements as a link at the top of a chevron braced configuration (Figure 2-8).

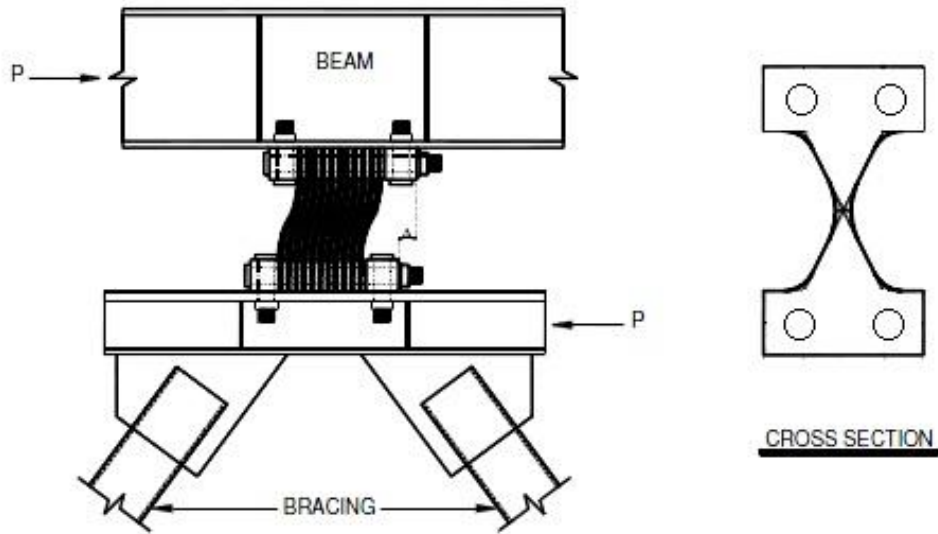


Figure 2-8: Typical ADAS Configuration (Alehashem et al., 2008)

Multiple plates are arranged in a parallel formation and dissipate energy through flexural yielding. The unique tapered design of the plate is intended so that the plates can act in double curvature, yielding across the entirety of the plate and therefore dissipating more energy (Alehashem et al., 2008). A reduction of almost 50% in acceleration can be seen in Figure 2-9 with the addition of an ADAS device to a 4-story building (Tehranizadeh, 2001). The TADAS (Triangular Added Damping and Stiffness) device is similar except it utilizes a triangular shaped plate and therefore single curvature to dissipate energy.

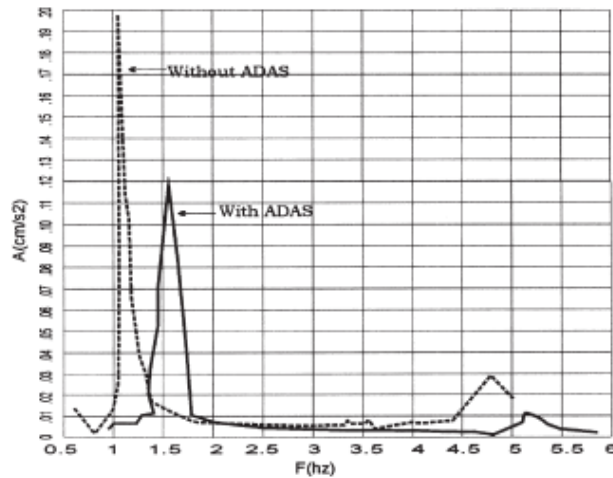


Figure 2-9: Acceleration Response Comparison with ADAS Device (Tehranizadeh, 2001)

Recent seismic events such as Northridge 1994 and Loma Prieta 1989 raised concerns about typical braced frames due to poor performance under cyclic loading (Sabelli et al., 2003). Buckling restrained braces (BRB) offer a solution to this problem by encasing a steel core in a concrete filled tube in order to restrain the brace from lateral buckling. BRBs are beneficial because they are able to dissipate roughly the same amount of energy in both tension and compression, eliminating the erratic and inefficient behavior of typical concentrically braced frames. Figure 2-10 shows the typical arrangement and hysteresis loops for a typical BRB. The design of the steel core may vary depending on the manufacturer but the fundamentals of behavior remain the same. Nonlinear dynamic analyses and experimental testing of the braces have demonstrated reliable behavior with improved interstory drifts and substantial ductility capability (Sabelli et al., 2003).

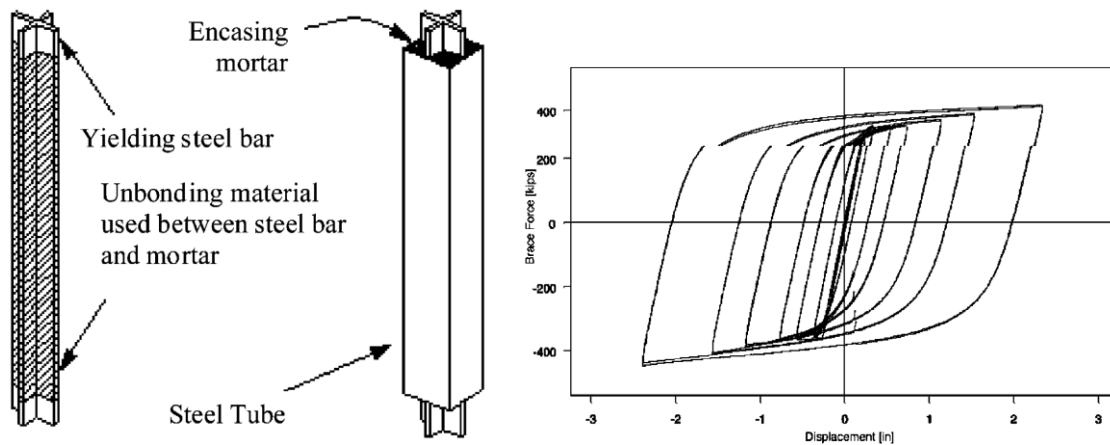


Figure 2-10: BRB Schematic with Hysteretic Behavior (Sabelli et al, 2003)

Another metallic device involves the use of shape memory alloys (SMA), utilized in wire braces installed diagonally in a frame. During excitation, the braces dissipate energy through stress-induced solid-to-solid phase transformation (Song et al., 2006). Change in stress causes a phase transition from austenite to martensite and then back again to austenite, resulting in a hysteretic behavior. SMAs perform well in large strain cycle fatigue, are corrosion resistant, and require no maintenance. The main advantage of using a SMA system is the self-centering capability which would provide safety after a seismic event. Unfortunately, the energy dissipation achieved by the SMA devices is not sufficient to limit deformation to the SMA element itself. Costly strengthening of other structural elements would be a deterrent to most structural applications (Dolce et al., 2000).

2.4.3 Friction Devices

Friction devices are another commonly used means for dissipating large amounts of energy. Once the device reaches a “slip force”, friction is utilized as two solid bodies slide against one another. The mechanism slips in both tension and compression and

creates a rectangular hysteresis behavior, which is evident in Figure 2-7. Although the devices do add stiffness to the system, the natural periods are only shortened by about 10% to 20% (Chopra, 2007). The devices are often favored in design due to reliable behavior under varying load amplitude and frequencies (Reinhorn et al., 1995).

Slotted bolted connections (SBC) are a type of friction device often used due to the relative ease of design, construction, and availability of commercial materials (Levy et al., 2000). As seen in Figure 2-11, the bolts connect two plates together with a compression force. Once the slip force is reached, the coefficient of friction and bolt compression dissipate energy through heat. Initially SBCs used two steel surfaces to generate friction but experimental results showed that brass on steel contact creates a more uniform behavior (Levy et al., 2000). Retrofit of a moment resisting frame building with a SBC in a chevron configuration provided a much greater energy dissipation capacity and limited inelastic action in the friction device (Aiken et al., 1993). More recently, SBCs have been utilized at the beam-to-column moment connection in order to dissipate energy and provide self-centering capabilities after a seismic event (Tsai et al., 2008).

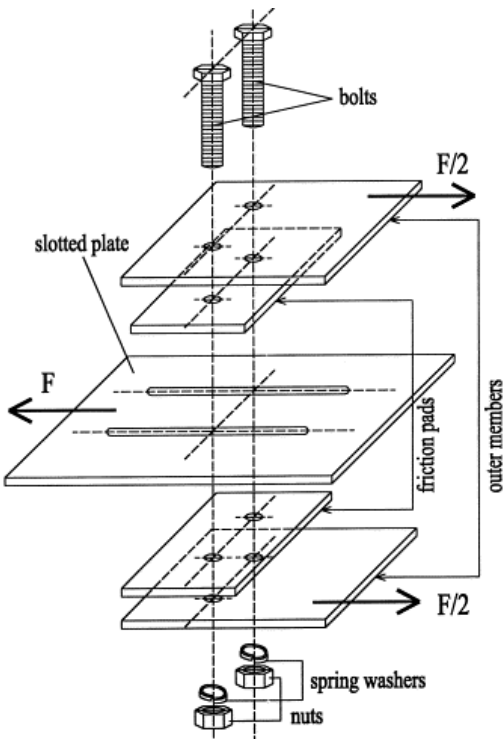


Figure 2-11: Typical Slotted Bolted Connection (Balendra et al., 2001)

A specific type of friction damper known as a Pall friction damper is located at the intersection of diagonal brace elements, utilizing friction at the interface of the two cross braces, as shown in Figure 2-12. Horizontal and vertical links attach the two braces to ensure that the slip deformation is equal in both compression and tension in order to maintain stability (Aiken et al., 1993). The performance of a 9-story steel moment resisting frame structure showed marked improvement by the addition of Pall devices, with reliable behavior and increasing energy absorption with increasing input energy (Aiken et al., 1993).

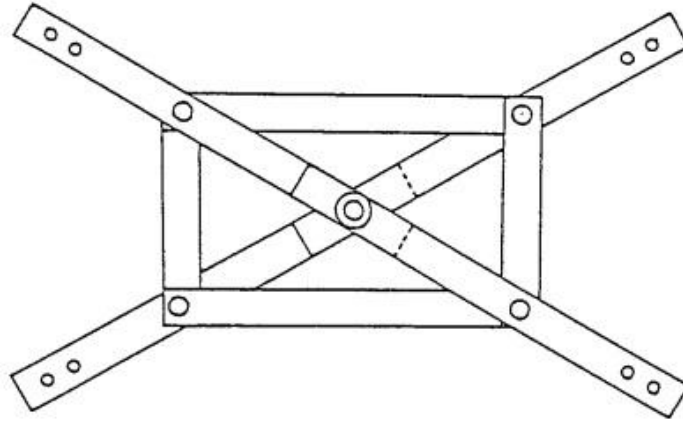


Figure 2-12: Pall Friction Device (Aiken et al., 1993)

2.5 Hybrid Control Devices

Hybrid control devices combine active and passive control systems in order to offset inherent weaknesses of each system. An example of a hybrid system is a base isolated system with supplemental actively controlled actuators to enhance the overall performance of the system. Although the active system is still subject to power failure, the major benefit of the hybrid system is that the passive component is still present for backup protection (Asteris, 2008). The demand for external energy is also reduced because of the presence of the passive control systems (Marshall, 2008). Similar to active control systems, hybrid control systems are simply not cost effective for most structures.

2.6 Multi-Phase Passive Control Devices

Typical passive control devices have inherent strengths and weaknesses that are considered in design. A multi-phase passive control device seeks to combine two types

of passive control devices in a system in order to offset the weaknesses of each and to optimize structural performance (Marshall, 2008). This can essentially create a performance-based approach that can allow the structure to react differently to varying levels of lateral force. If implemented correctly, a multi-phase passive control system could potentially have all the benefits of a semi-active active system without need for an external power source, control algorithm, and structural monitoring system. The low maintenance cost and improved reliability are appealing features in comparison to semi-active devices.

As previously discussed, the more commonly used passive control devices include viscous fluid dampers, viscoelastic solid dampers, metallic yielding devices, and friction dampers. The focus of the research involves combining these more commonly used devices into a multi-phase system in order to improve structural response.

2.7 Multi-Phase Behavior

The multi-phase nature of multi-phase passive control systems has been explored in the past, showing promising results in many different applications. A sequential coupling system was one of the first introductions of dynamic slip and multi-phase behavior in order to improve response. Using a repeated slip-resistance sequence within a structural system, a significant reduction in deformation response was achieved. This can be accomplished by properly detailing special connections, such as bolts in slotted holes, in steel, reinforced concrete, and prestressed concrete structures, as illustrated in Figure 2-13 (Weidlinger & Ettouney, 1993).

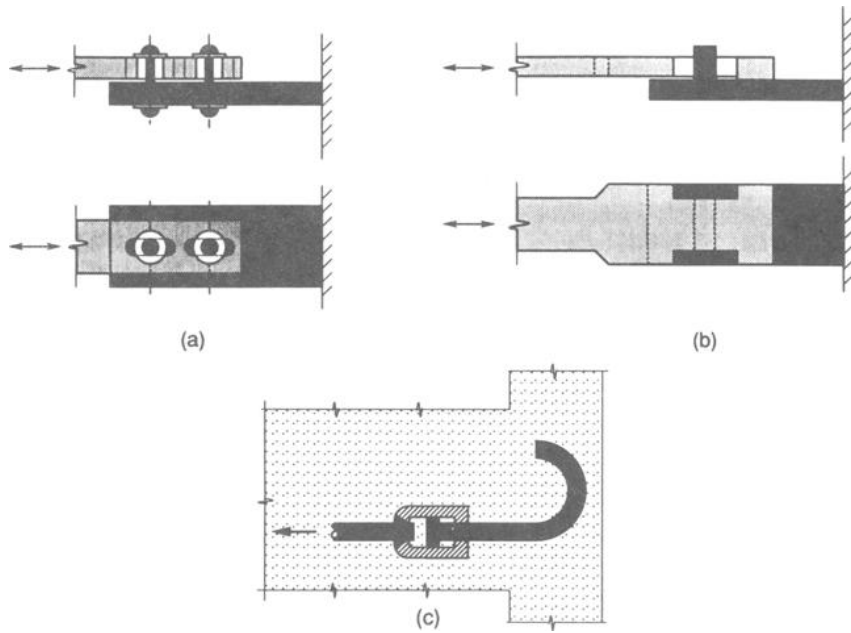


Figure 2-13: Sequential Connection Schematics (Weidlinger & Ettouney, 1993)

A relatively simple SDOF example of this sequential coupling is evident in Figure 2-14. System A, which is representative of a parallel (conventional) system and system B, which is representative of a sequential system, are equivalent in both strength (R_0) and mass (M). Combinations of the α value (secondary stiffness value) and γ (percentage of yield displacement) were optimized in order to achieve the best response. Both systems were subjected to the same seismic event and the results of the sequential connection had a displacement response of 70% of the standard system and a residual displacement that was only 10% of the standard system (Weidlinger & Ettouney, 1993).

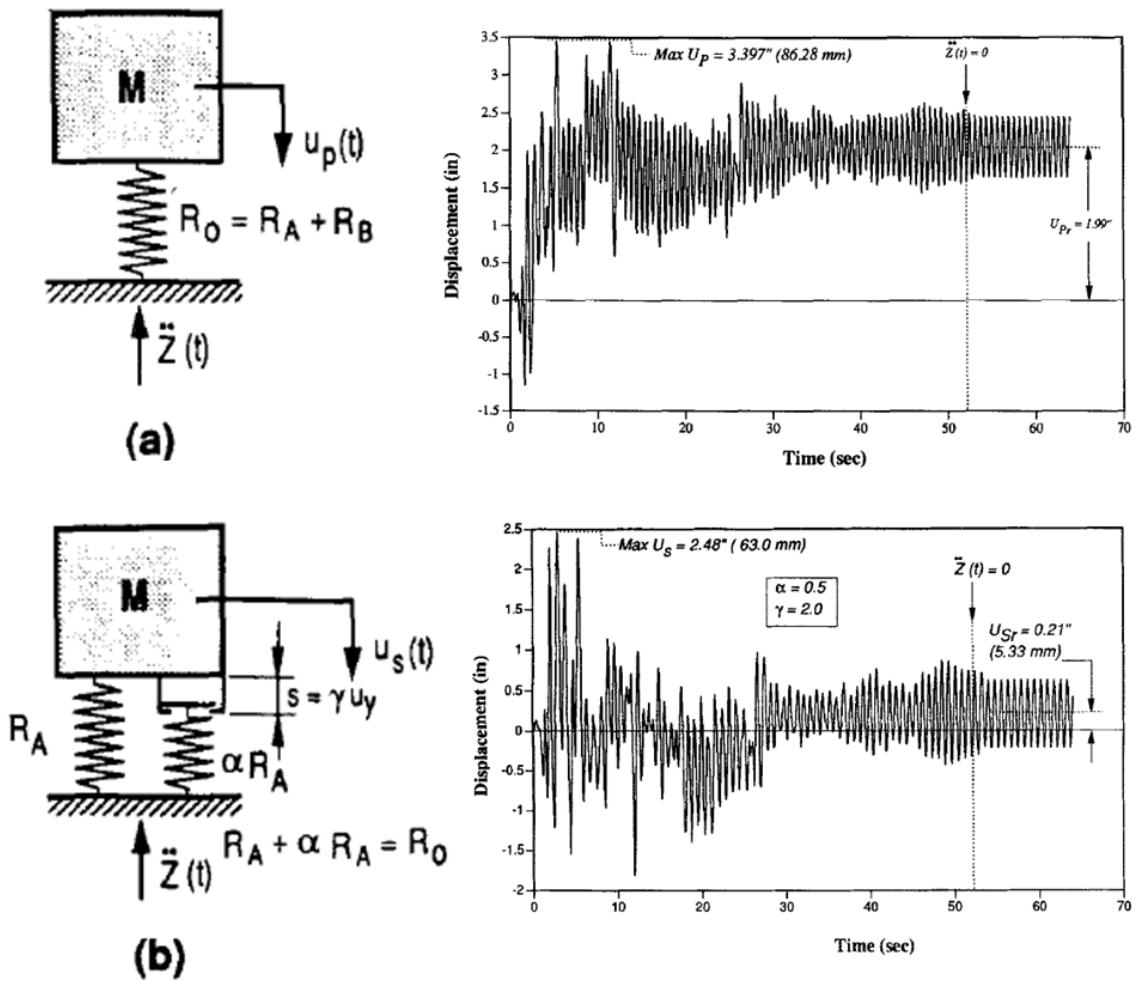


Figure 2-14: Benefits of Sequential Coupling (Weidlinger & Ettouney, 1993)

Another example of multi-phased passive control behavior involves an analysis performed on a multi-span simply supported bridge (Figure 2-15). When excited, the system increases in stiffness as the displacement increases, which mainly results from the closure of the gap between the end span and abutment (Motlagh & Saadeghvaziri, 2001). This is referred to as a stiffening single-degree-of-freedom system whereas a baseline single-degree-of-freedom system would only consist of the bridge without the stiffness added from the abutment.

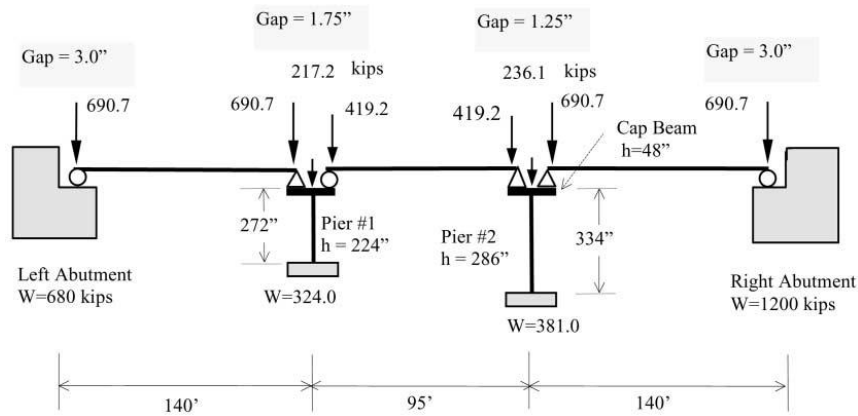


Figure 2-15: Stiffening Single-Degree-of-Freedom System (Motlagh & Saadeghvaziri, 2001)

Figure 2-16 clearly demonstrates the multi-phase nature of the stiffening SDOF system in comparison to the baseline system. For most periods, the stiffening system had much lower ductility demands than the baseline system yet the hysteretic energy and damage index were often higher (Motlagh & Saadeghvaziri, 2001). Further research was recommended to quantify the effects of yield strength, stiffness, and gap size on response in order to minimize damage while maintaining the decreased ductility demand.

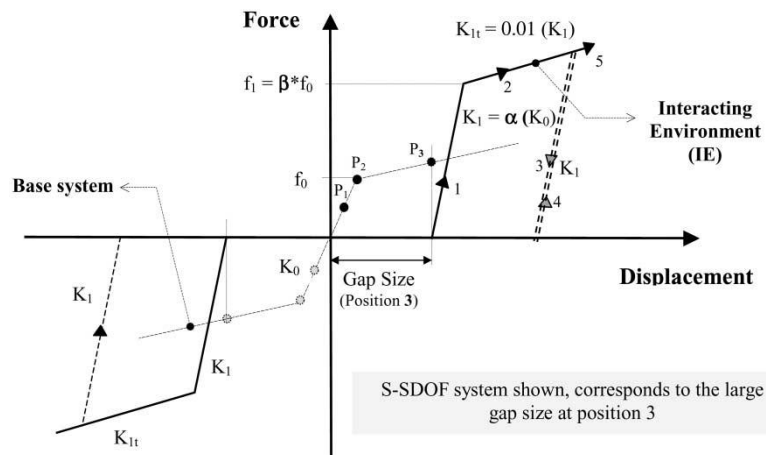


Figure 2-16: Stiffening Single-Degree-of-Freedom Comparison to Baseline (Motlagh & Saadeghvaziri, 2001)

More recently, a structural application of a multi-phase passive system has been developed that sandwiches a high-damping viscoelastic material between two steel plates or channels, as shown in Figure 2-17. The visco-plastic device (VPD) utilizes the displacements across the viscoelastic material to increase damping as the steel plates subject it to tension and compression forces. As the forces increase, the steel elements yield in order to dissipate more energy. The primary benefit of this system is that it will respond elastically to low level excitation yet still possess the energy dissipation capability for large events (Ibrahim et al., 2007). The cost of manufacturing this device is a potential drawback of this system.

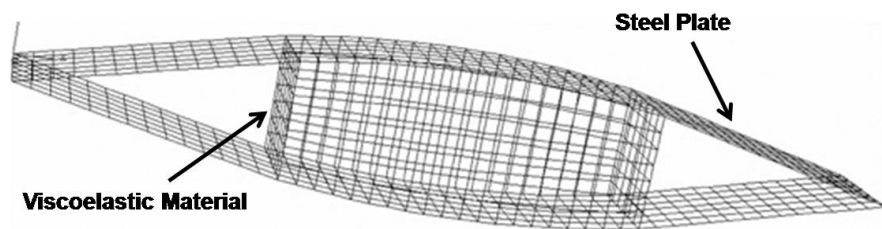


Figure 2-17: Finite Element Model of the VPD (Ibrahim et al., 2007)

Stemming from the visco-plastic research, a multi-phase passive control device was developed combining a viscoelastic high-damping rubber sandwich damper and a buckling restrained brace in series in order to utilize the strengths of each system (Figure 2-18). The system is backed up with a moment resisting frame in order to provide initial stiffness and redundancy to the system. Although other passive control devices and arrangements were considered, the VE and BRB provided the most reliable and practical option for construction (Marshall, 2008).

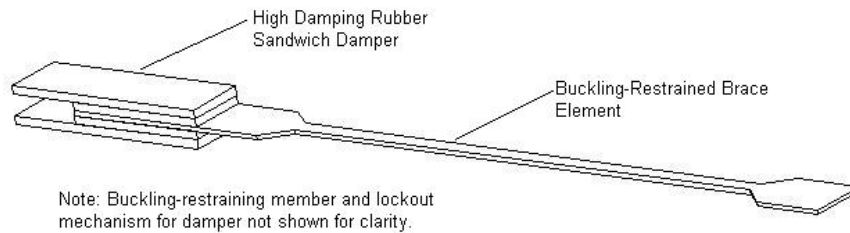


Figure 2-18: Multi-Phase Passive Control Device (Marshall, 2008)

The behavior of the system is comprised of three main phases. The first phase, involving the VE sandwich damper and moment frame, is designed to provide sufficient stiffness and damping for service level wind conditions and small to moderate seismic events. The next phase involves the transition from the VE device to the BRB, which occurs at a specified gap size that is a percentage of the moment frame yield displacement. The lockout of the secondary phase occurs due to a slotted bolted connection on the outer plates of the sandwich damper (Figure 2-19). The final phase involves the BRB, which adds significant stiffness and energy dissipation capacity to the system for larger seismic events. The overall result is a device that can variably respond to levels of lateral force and primarily restrict damage to a replaceable BRB (Marshall, 2008).

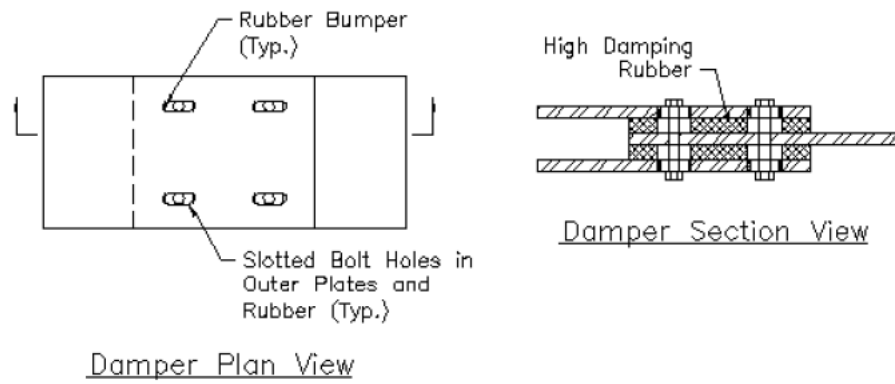


Figure 2-19: High-damping Rubber Sandwich Damper Schematic (Marshall, 2008)

An analytical study was performed on a 9-story steel moment frame designed with a hybrid passive control device (HPCD) and other multi-phase arrangements. Viscous fluid dampers as well as a range of transition gap sizes were also considered. Other arrangements of the system were also considered (Figure 2-20). Arranging a system in a parallel formation provides damping throughout the entire duration of excitation, whereas the series formation only allows damping in the first phase (Marshall, 2008).

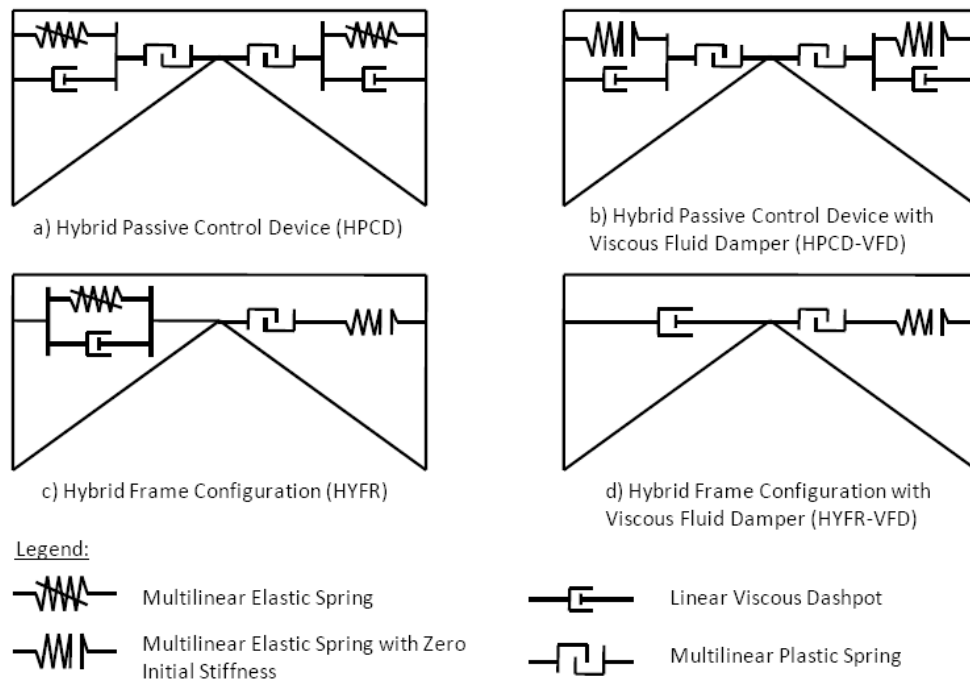


Figure 2-20: Possible Arrangements of Multi-Phase Systems (Marshall, 2008)

Response parameters such as acceleration, base shear, drift, and residual displacements all showed marked improvement over conventional systems. Figure 2-21 shows the results of an incremental dynamic analysis (IDA) that demonstrates significant decreases in acceleration response of an HPCD system in comparison to the baseline buckling restrained brace framed system. Figure 2-22 demonstrates the re-centering capability of a parallel system (HYFR) due to the presence of the elastic high-damping rubber throughout the entirety of the excitation (Marshall, 2008). This could provide tremendous post-event safety after a design basis earthquake in which secondary moments are often a concern for taller structures.

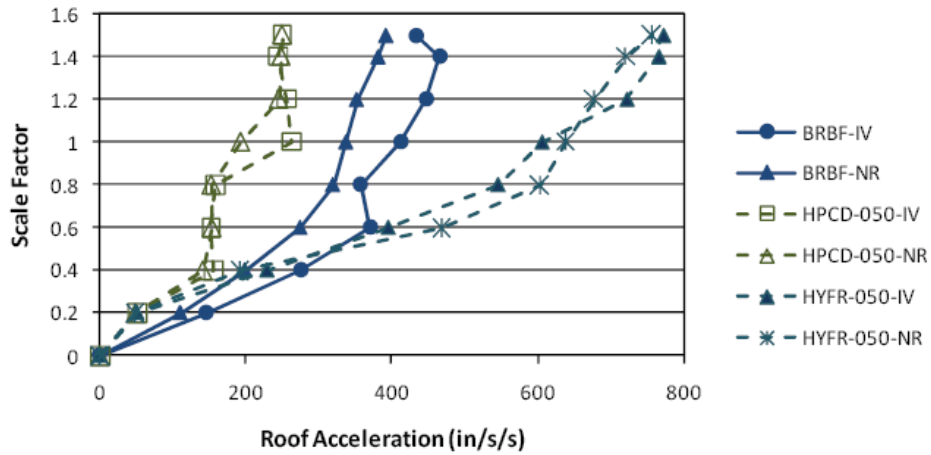


Figure 2-21: Acceleration Response Comparison (Marshall, 2008)

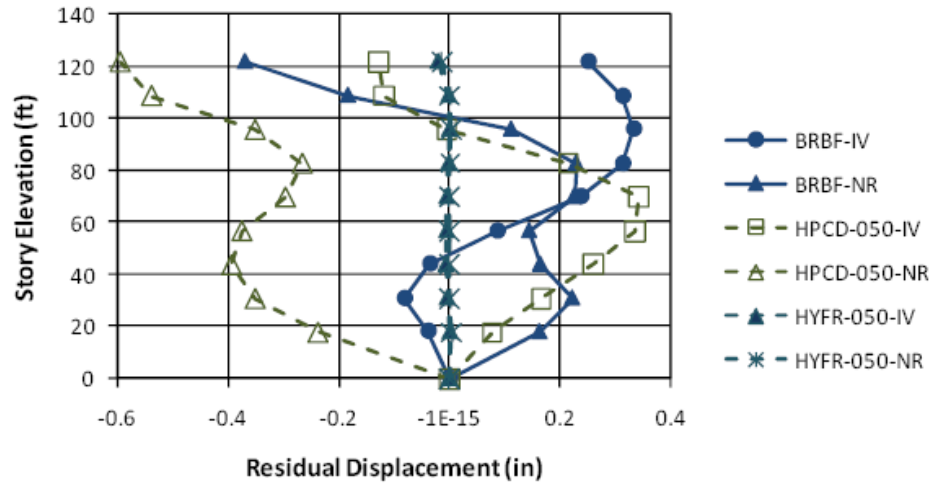


Figure 2-22: DBE Residual Displacement Comparison (Marshall, 2008)

Although the research produced many beneficial results, the fundamental understanding of the systems was lacking. In order to find a better performing device, it was recommended that an exhaustive SDOF study be performed to identify some of the more important variables influencing response (Marshall, 2008). A larger range of gap sizes, natural periods, and hysteretic-device-to-moment-frame strength ratios need to be

investigated in different system arrangements and subjected to a larger suite of ground motions. In doing this, a range of values could be established for a given situation.

2.8 Summary

The potential for multi-phase passive control devices to improve structural performance is clearly demonstrated within the literature. Ideally a system could be optimized to remain elastic for the duration of a small to moderate seismic event, while still providing life safety, and to minimize damage for a large scale seismic event. Multiple options exist for multi-phase passive devices but the best-performing combination is still unknown. Although multi-phase systems have shown improved structural response, the fundamental understanding of this improvement is unclear. This SDOF study seeks to explore these multi-phase system combinations and clarify important variables that affect response. By accomplishing this feat, the study can be expanded into a multi degree-of-freedom study with a much smaller range of variables. Subsequently, lab testing and implementation would provide results leading to a device that could substantially change the way structures react to seismic loading. This research can provide valuable insight and lay the groundwork for these goals.

Chapter 3 Parametric Study Development and Analysis Plan

3.1 Introduction

Numerous factors are involved in each multi-phase control system: a velocity-dependent damping device, displacement-dependent device, system arrangement, hysteretic-device-to-moment-frame strength ratio, seismic hazard, natural period, and transition gap size. The feasibility of testing all combinations of these factors and the ranges of values is simply impractical. Therefore, an analysis of all the variables was performed and narrowed down to an acceptable range. Passive control devices reviewed in Chapter 2 were analyzed and chosen based on energy dissipation capability, damping characteristics, reliability, and constructability within a multi-phase device.

Each multi-phase system should be subjected to various seismic hazards to show the versatility of the systems. This chapter details the selection of the seismic hazards and natural periods to be tested within the scope of the research. The hysteretic-device-to-moment-frame strength ratio and the corresponding transitional gap size are thought to be important factors in the response of the multi-phase control systems. The ranges of values for these variables are also discussed within this chapter. With the large number of variables present in each multi-phase system, a systematic naming scheme had to be developed in order to keep the extensive data organized. The details of this naming scheme are also detailed in this chapter.

3.2 Velocity-Dependent Device

Two main types of velocity-dependent damping devices were reviewed and considered for a multi-phase system: viscous fluid dampers (VFD) and viscoelastic dampers (VED). Both systems can provide substantial damping within a multi-phase system. Marshall (2008) demonstrated the potential of both systems but a clear favorite was not evident. For this reason, both devices were examined within the scope of this research. As a control, some systems were designed with no supplemental damping, so that show the benefits of a velocity-dependent device could be shown in comparison.

The VFD used in the multi-phase system was similar to the one in Figure 2-4, utilizing a piston displacing fluid in an enclosed cylinder. A linear viscous damper was used for simplicity in analysis. For a nonlinear damper, a range of nonlinear exponents would have to be tested as well. Since the results prove that a multi-phase system with a VFD is beneficial, further study should be conducted to investigate the possible benefits of a nonlinear VFD. The VED used utilized high-damping rubber as the viscoelastic material, in the form of a sandwich damper, as illustrated in Figure 2-19, and other configurations to be discussed in Section 3.4.

Once the damping device is established, appropriate damping values have to be determined for the system. Typical buildings have about 2%-3% inherent damping but the addition of a supplemental damper significantly adds to the damping capacity. For a structure with a uniform distribution of mass and stiffness, a necessary assumption for a SDOF system, total damping of 16% of critical damping is expected for a viscous damper (Occhiuzzi, 2009). This recommended value would suggest that the viscous damper is contributing about 13% of the damping, which was the value used for design of the multi-

phase systems. Using this damping ratio, along with the mass and stiffness of the system, the damping coefficient for the systems can be calculated.

As part of Marshall's (2008) investigation, extensive material testing was performed on the viscoelastic high-damping rubber (HDR) component utilized in the sandwich damper. The butyl rubber tested had a loss factor of about 0.36 at a frequency of 2.0 hertz which is able to provide about 8% of critical damping, a value used for this analysis (Marshall, 2008). Although damping values for the VED are less than the VFD, the initial stiffness provided by the high-damping rubber could help to reduce displacements.

3.3 Displacement-Dependent Device

Buckling restrained braces (BRBs), slotted bolted friction devices, and Pall friction devices were all considered for displacement-dependent elements of the multi-phase system. For simplicity, only one device was chosen. A device with reliable hysteresis behavior, large energy dissipation, and a large ductility capacity for moderate to large seismic events was desirable. Therefore, a BRB was chosen as the displacement-dependent device.

Once the BRB was chosen, some important parameters had to be established. The hysteresis loop for the BRB is not quite symmetric for tension and compression, resulting in the need for adjustment factors. The tension strength adjustment factor, ω , was taken as 1.0 while the compression overstrength adjustment factor, β , was taken as 1.1 to account for slightly larger compression stresses typically seen in BRBs. Additionally, a generally accepted range of core yield strengths is 38 ksi to 46 ksi; therefore, 42 ksi was

used in design (Robinson, 2009). A BRB core yield length varies between manufacturers depending on connection detail and frame configuration (Figure 3-1). A standard connection length of 48” from work point to yielding core was used on each side of the brace to calculate the yield length for each frame configuration. Average yield length was 60% of the work-point length, a reasonable approximation for a chevron configuration. These design values are important for the development of the strength and stiffness relationships developed later in the research.

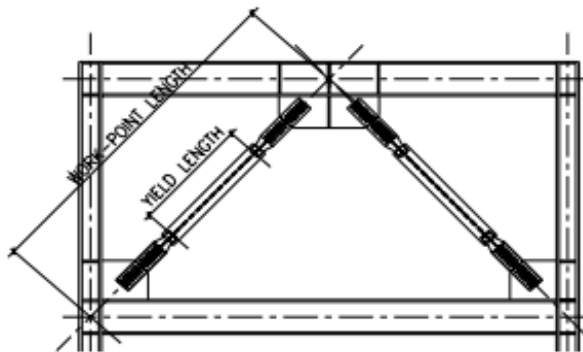


Figure 3-1: BRB Yield Length (Lopez & Sabelli, 2004)

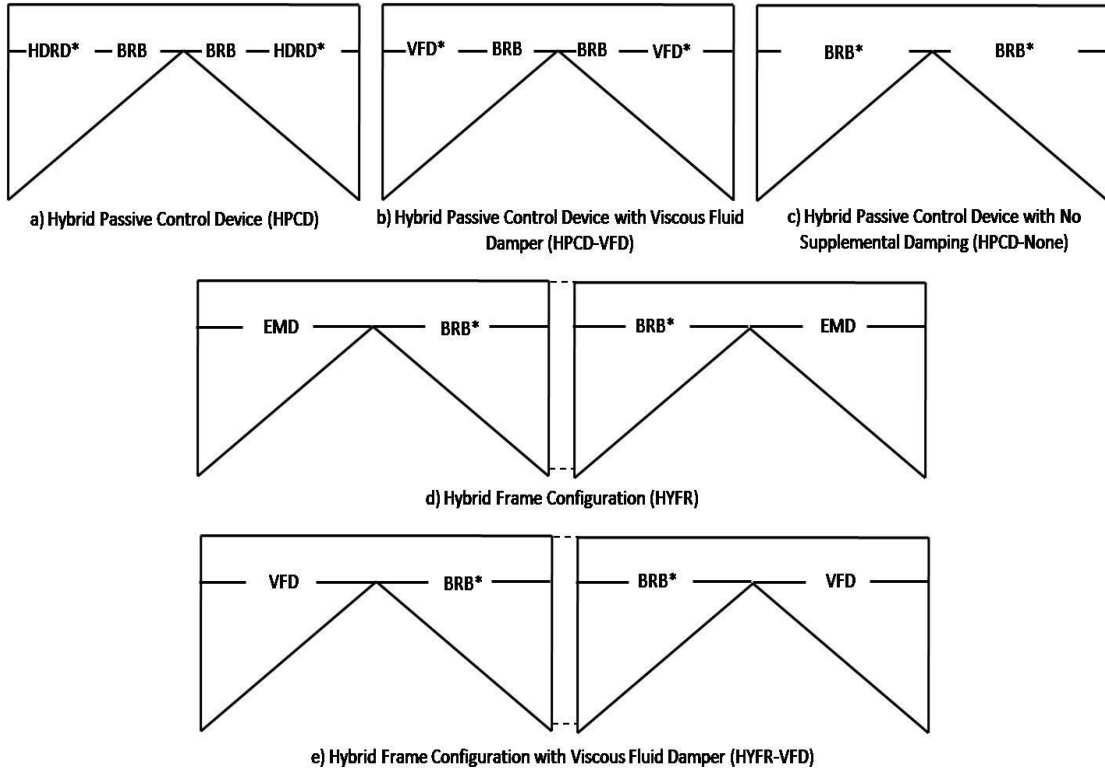
3.4 System Arrangement

Using the variables defined above, essentially 5 multi-phase systems were created, the details of which are outlined in Table 3-1 and shown in Figure 3-2.

Table 3-1: Multi-Phase Systems and Abbreviations

| Abbreviation | System Description |
|---------------------|--|
| HPCD | Special moment frame with a multi-phase passive control device utilizing a BRB and high-damping rubber sandwich damper |
| HPCD-VFD | Special moment frame with a multi-phase passive control device utilizing a BRB and linear viscous fluid damper |
| HPCD-None | Special moment frame with a multi-phase passive control device with no damper |

| | |
|----------|--|
| HYFR | Special moment frame with a multi-phase frame configuration utilizing an BRB and compressed elastomeric device |
| HYFR-VFD | Special moment frame with a multi-phase frame configuration utilizing a BRB and viscous fluid damper |



Legend:

HDRD – High Damping Rubber Damper
VFD – Viscous Fluid Damper

BRB – Buckling Restrained Brace
EMD – Elastomeric Device

Note – ‘*’ denotes the element with a locking mechanism.

Note – All systems are backed up with a Special Moment Frame

Note – The hybrid systems shown in d and e, both bays are part of the same system.

Figure 3-2: Multi-Phase Passive Control Systems

The HPCD is composed of a high-damping rubber damper in series with a buckling restrained brace. The transition from viscoelastic damping to BRB yielding is dependent upon a lockout mechanism, which is a slotted bolted rubber sandwich damper as illustrated in Figure 2-11. The initial stiffness of the system is provided by the

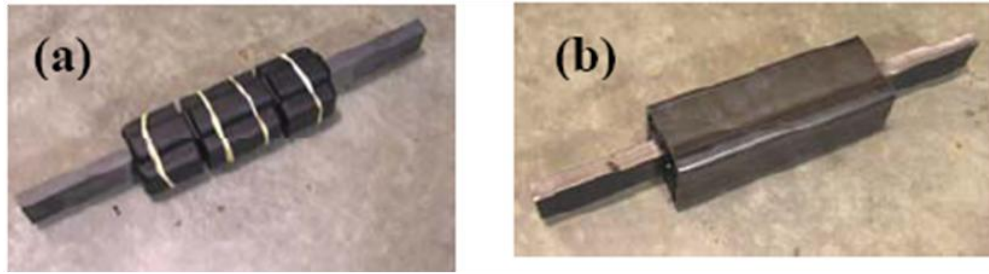
moment frame and damper stiffness. This transition mechanism is reliant upon a displacement-based gap size which can be varied in design. Damping is only present before the mechanism is locked out. The HPCD-VFD is exactly the same as the HPCD system except a VFD is utilized as a means of damping instead of the high-damping rubber. The difference between the two systems is that the high-damping rubber provides initial stiffness, while the VFD does not provide initial static stiffness but can achieve higher damping capacity at a lower cost. The importance of these inherent properties was investigated in this research effort. The HPCD-None system is only a BRB in series with a lockout mechanism; no supplemental damping is provided. Simple schematics of the systems are provided in Figure 3-2a, 3-2b, and 3-2c.

The HYFR and HYFR-VFD configurations are considered to be parallel systems because the damping device is utilized throughout the duration of excitation, even while the BRB is yielding. The damper and BRB on opposite sides of the chevron configuration means that one is in tension and one is in compression, requiring two frames and symmetry for equal action in each direction. The ability to model and utilize a high-damping rubber for large displacements and corresponding strains is not very practical due to the highly nonlinear behavior of rubber. A parallel arrangement with a HDR could experience large strains and complex nonlinear rubber behavior. The SDOF study demands simplicity to understand the fundamental behavior of the multiphase systems, so modeling the complex nonlinear behavior of the high-damping rubber is not desirable, and was not attempted in this study.

A new system was investigated for parallel action of damping and yielding for the HYFR configuration in order to reduce the complexity of the model. Karavasilis et al.

(2010) offered a system that could be utilized in a parallel design. The device proved beneficial in reducing drifts and floor acceleration and could be substantially beneficial when paired with a BRB. This device consists of precompressed high-damping rubber wrapped around a longitudinal bar and wrapped in a steel tube (Figure 3-3). The rubber is bonded to the longitudinal bar, which is subsequently wrapped in a steel tube but not bonded to the steel tube. At a specified force and displacement the steel tube slips until the load is reversed. Behavior is very similar to a friction device, with the added benefit of VE damping prior to slipping. Since the rubber remains elastic, a simple linear model gives a reasonable approximation. The BRB element of this arrangement has a specified gap size before the yielding takes place. Similar to the HPCD, the damping and stiffness provided could significantly reduce response except the HYFR high-damping rubber can be utilized throughout the duration of excitement.

The HYFR-VFD system is the same as the HYFR configuration except a VFD is used as the damping device instead of a high-damping rubber (Figure 3-2d and Figure 3-2e). Every system is backed up by a special moment frame that resists a portion of the lateral force in addition to the BRB. The details of the “baseline” system are given in the next section.



- a) Elastomeric material wrapped around longitudinal bar
- b) Elastomeric material and bar compressed in the steel tube

Figure 3-3: Elastomeric Device (Karavasilis et al., 2010)

3.5 Baseline Systems

The baseline systems considered consisted of conventional lateral force resisting systems; a special moment frame, a braced frame, and a combination of the two in a dual frame. These systems are often favored in seismic design due to their large ductility capacity and corresponding reduction in design forces (response modification factor of 8 in some cases). Special moment frames are often controlled by drift rather than strength due to inherent flexibility and a deflection amplification factor (C_d) of 5.5. Pairing the special moment frame with a buckling restrained brace adds stiffness and redundancy to the system and reduces the C_d to 5, allowing the system to be controlled by strength rather than stiffness. Code minimum requires that the moment frame must resist at least 25% of the lateral force in a dual frame (ASCE, 2006). Previous research indicates that a special moment frame resisting 25% of the force is inadequate in a multi-phase passive system because it does not provide enough initial stiffness to allow the first phase of the multi-phase system to be active long enough to provide sufficient damping (Marshall & Charney, 2010).

Figure 3-4 illustrates the inadequacy of a system with a relatively weak moment frame. The dual system with the smaller portion of the lateral force being resisted by the moment frame (VFD10-3-M25B75) experiences larger displacements. For this reason, the range of stiffness ratios for dual systems used in this study were limited to 5 values: Moment frame resisting 40% of the lateral force and buckling restrained brace resisting 60% of the lateral force (M40B60), M50B50, M60B40, M70B30, and M80B20. This provides a large range of dual system arrangements but if it becomes evident that another combination may provide better performance within the study, the range can be modified.

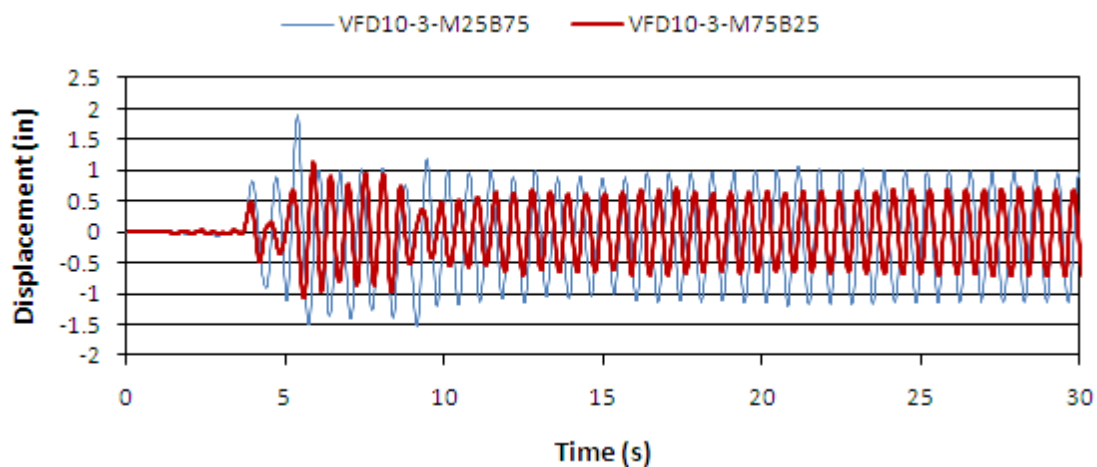


Figure 3-4: Comparison of Two Systems with Different Baselines (Marshall, 2008)

The inherent behavior of a moment frame coupled with a buckling restrained brace creates different strength-to-stiffness ratios for each of the baseline systems. A moment frame is more flexible than a buckling restrained brace therefore a multi-phase system containing a M80B20 dual system would be more flexible than a M40B60 system designed for the same seismic hazard. To clearly define the properties of these dual systems, it was important to find the numerical relationship between the strength and

stiffness of each component in the system. Once the relationship was found, separate force-displacement plots could be developed for the moment frame and BRB elements. Together, the overall strength of these elements will equal the required design strength, yet the overall stiffness will vary depending on the baseline ratios. In order to find the strength/stiffness ratios, moment frames were designed at 7 different strength levels for 5 typical bent sizes. The resulting stiffness from the models were recorded and plotted against strength (Figure 3-5). Strength and stiffness increase in a linear fashion. The relationship between strength and stiffness is given in the legend for each bent size.

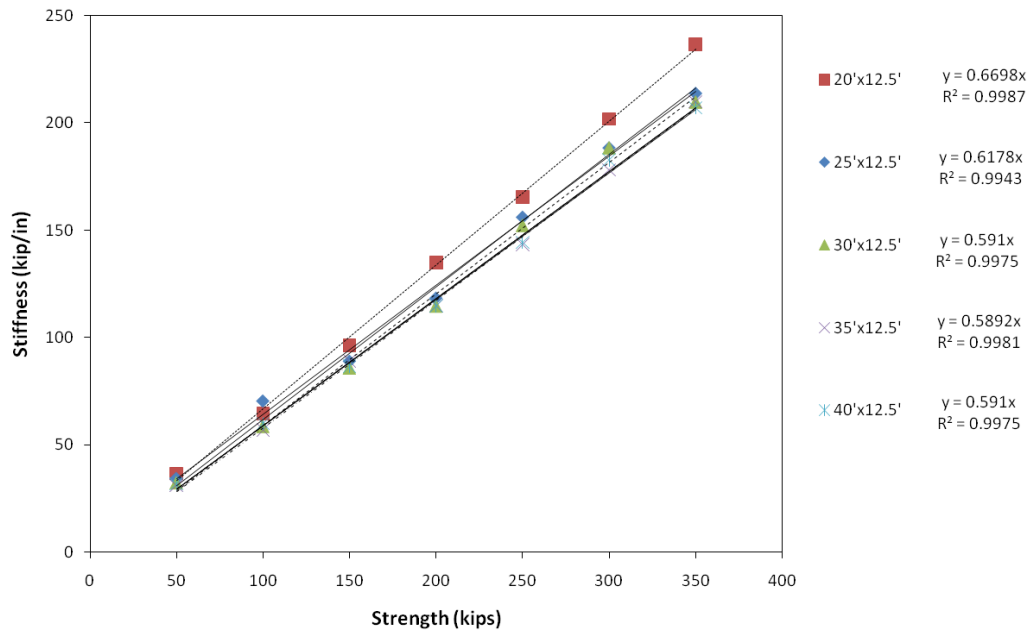


Figure 3-5: Moment Frame Stiffness/Strength Comparison

Similar to the moment frame analysis, buckling restrained brace frames (BRBFs) were designed for 7 different strength levels and 5 different frame configurations. The design of the frames was carried out using the BRB design parameters defined earlier.

The resulting stiffness was plotted against strength in Figure 3-6. A linear relationship between strength and stiffness was also found for the BRBFs.

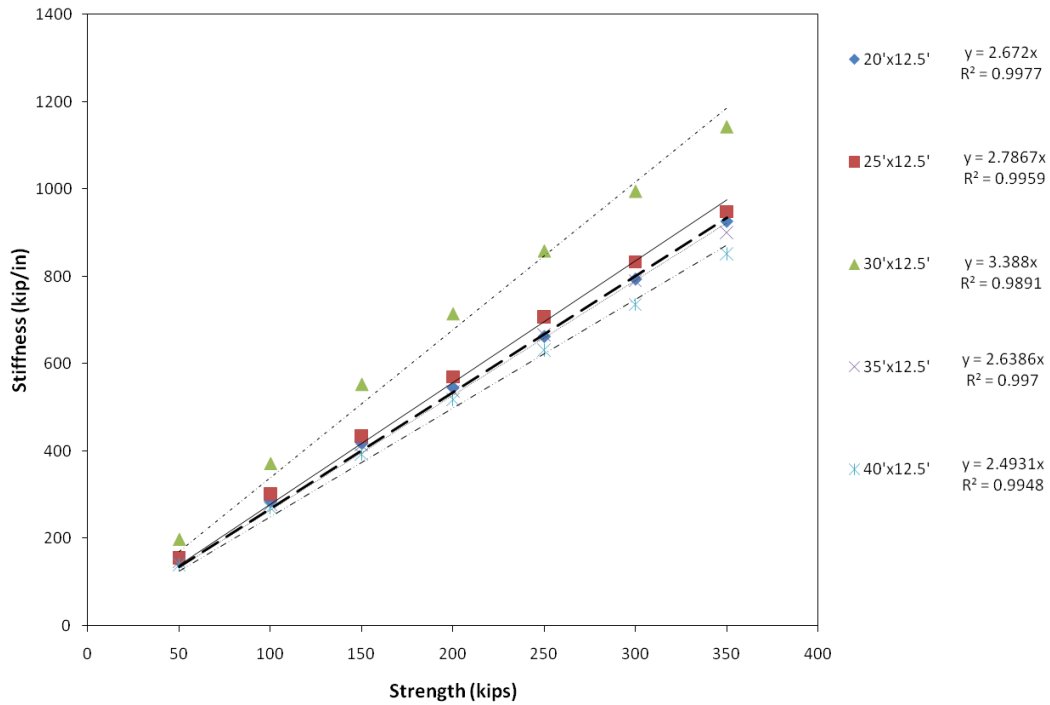


Figure 3-6: Buckling Restrained Brace Frame Stiffness/Strength Comparison

After the relationship between strength and stiffness for each component was established, the same relationship had to be created for a dual system. One could infer that the strength and stiffness relationship in a dual system would simply be a weighted average of system components but this hypothesis was tested to ensure its validity. Twelve systems were designed and the strength and stiffness of the dual frames were compared to a weighted average. The values for strength, frame size, and dual frame ratio were generated randomly and designed accordingly. **Error! Reference source not**

found. shows the relationship between the design stiffness and weighted average stiffness.

Table 3-2: Dual System Stiffness Derivation

| System | | | Results | | |
|-----------------|-------------|---------------------------|---------------------------|---------------------------|------------------------|
| Strength (kips) | Frame Size | Dual System Configuration | Designed Stiffness (k/in) | Weighted Stiffness (k/in) | Percent Difference (%) |
| 213 | 25' x 12.5' | M62.5B37.5 | 323.56 | 329.35 | -1.76 |
| 351 | 20' x 12.5' | M25B75 | 756.14 | 760.16 | -0.53 |
| 347 | 30' x 12.5' | M62.5B37.5 | 512.8 | 519.73 | -1.33 |
| 289 | 40' x 12.5' | M75BM25 | 326.66 | 329.64 | -0.90 |
| 341 | 35' x 12.5' | M62.5B37.5 | 477.7 | 476.16 | 0.32 |
| 199 | 20' x 12.5' | M37.5B62.5 | 399.3 | 394.35 | 1.26 |
| 295 | 35' x 12.5' | M37.5B62.5 | 558.66 | 558.06 | 0.11 |
| 211 | 35' x 12.5' | M62.5B37.5 | 305.29 | 304.53 | 0.25 |
| 274 | 30' x 12.5' | M50B50 | 478.97 | 472.32 | 1.41 |
| 122 | 30' x 12.5' | M62.5B37.5 | 188.29 | 202.42 | -6.98 |
| 393 | 35' x 12.5' | M50B50 | 636.9 | 639.82 | -0.46 |
| 205 | 25' x 12.5' | M37.5B62.5 | 437.3 | 423.56 | 3.24 |

The 99% confidence interval was -2.28 to 1.38 percent for the difference between a weighted average stiffness and designed system stiffness. This small range indicates that a weighted average is a good indicator of the stiffness to strength ratio of a dual system. The stiffness-to-strength ratios used for the design of the baseline systems were chosen based on the 30' x 12.5' bent size, a typical structural frame size.

Once the weighted average issue was resolved, a simple multi-phase design process was used for the moment frame and BRB strength-to-stiffness ratios. The dual system design strength was comprised of the appropriate ratio for a given multi-phase system (i.e. M50B50), while the stiffness for the elements were calculated using a

weighted average of the linear equations in Figure 3-5 and Figure 3-6. Once the strength-to-stiffness ratio of the elements was developed, the transitional gap size was considered.

3.6 Transition Phase (Gap Size)

As stated before, each multi-phase system has a transition phase before the BRB becomes active. The gap needs to be less than the yield displacement of the moment frame in an attempt to limit yielding to the replaceable BRB. The gap also has to be large enough to allow damping to be effective before the mechanism locks out. This research looks to strike a balance in order to increase damping of the system and reduce moment frame yielding, which is designed to first occur in the beam element. These gap sizes are specified as a percentage of the moment frame yield displacement: 20%, 40%, 60%, 80%, and 100%. Depending on the dual system used in the multi-phase control system, the yield displacement varies depending on the strength of the moment frame required for lateral resistance. A gap in a high-damping rubber system has a stiffness that is a function of the damper size while the VFD has no initial stiffness. All of the gap size properties are a function of the design strength, which is dependent on the seismic hazard, the next topic of discussion..

3.7 Seismic Hazard

The systems were designed to resist two different seismic hazard levels: those of Los Angeles, CA and Memphis, TN. The systems were designed with an Occupancy Importance Factor of II, on Site Class D soil, and were considered vertically and

horizontally regular. Los Angeles, CA (34.05°, -118.25°) was chosen to evaluate the seismic hazard of a populous city near the San Andreas Fault, a transform fault located in California. The 1994 M6.7 Northridge earthquake caused \$20-\$40 billion dollars in damage in the Los Angeles area, and the potential for another earthquake of significance is relatively large (U.S. Geological Survey 2008). For a Site Class B soil, short period spectral acceleration is 2.17g and the 1 second period spectral acceleration is 0.727g. Modified for site class and the design basis earthquake, short period and 1 second period spectral accelerations changed to 1.447g and 0.727g, respectively (ASCE, 2006). The design spectrum according to ASCE 7-05 provisions is shown in Figure 3-7.

Memphis, TN (35.65, -90.22) was chosen to evaluate the seismic hazard induced in a populous city near the New Madrid Fault, an intra-plate fault near the border of Tennessee and Missouri. The largest seismic event in the continental United States (M8.7) occurred at the New Madrid Fault in 1812. Although the reoccurrence of events is over a much larger time scale than the San Andreas Fault, the seismic hazard is still an important issue for design in this populous area. For a Site Class B soil, short period acceleration is 1.415g and the 1 second period acceleration is 0.385g. Modified for site class and the design basis earthquake, short period and 1 second period spectral accelerations are 0.943g and 0.444g, respectively (ASCE, 2006). The design spectrum according to ASCE 7-05 provisions is shown in Figure 3-7.

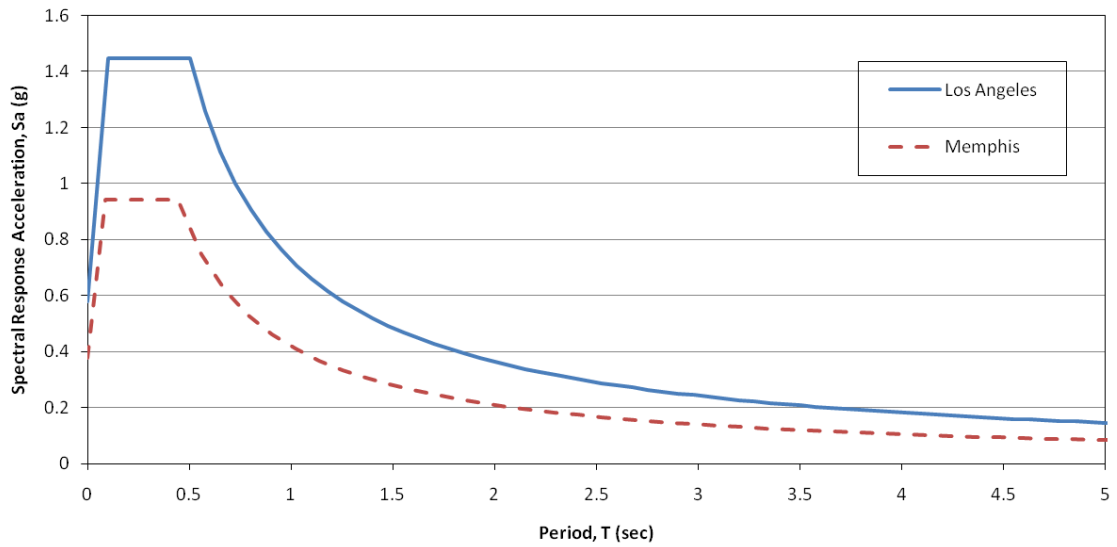


Figure 3-7: Comparison of the Design Response Spectrums

3.8 Natural Period

After evaluating the design response spectrums for each location, it was determined that systems should be designed for 5 different natural periods. The periods chosen were: 0.25 seconds, 0.5 seconds, 1 seconds, 2.5 seconds, and 4 seconds. These natural periods are representative of most buildings within these seismic locations and were chosen to test the feasibility of multi-phase behavior in both long and short periods. The design accelerations for these periods are indicated in Figure 3-8.

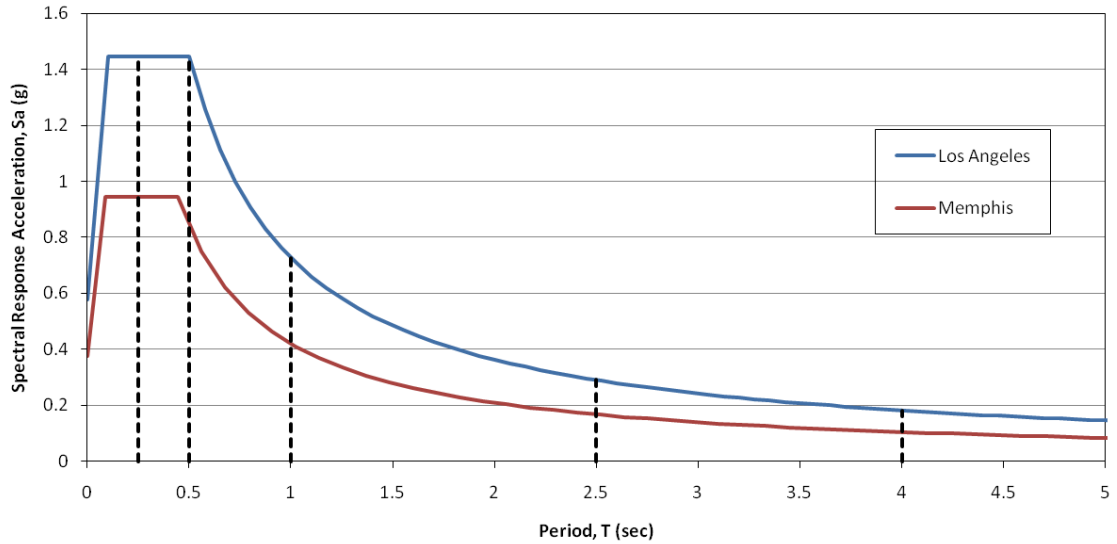


Figure 3-8: Design Spectrums with System Natural Periods

3.9 Experimental Design

After the variables and range of their characteristic values to use in the study were established, the next step was to choose the multi-phase systems for the analytical study. A full factorial design in which all the combinations of variables would be tested would involve 1250 systems (Montgomery, 2009). Modeling, analyzing, and organizing data from 1250 systems is simply impractical, therefore an experimental design had to be performed in order to reduce this number, while still maintaining statistical significance. The hierarchy showing all the possible combinations of systems is shown in Figure 3-9 for clarity.

The statistical software used for analysis was JMP Version 8 (SAS Institute Inc., 2009). Using a D-Optimal experimental design, the number of systems needed to capture all the main effects and two-way interactions of the variables was 103, a much more

reasonable scope for this study. To include more statistical evidence, 135 systems were ultimately analyzed.

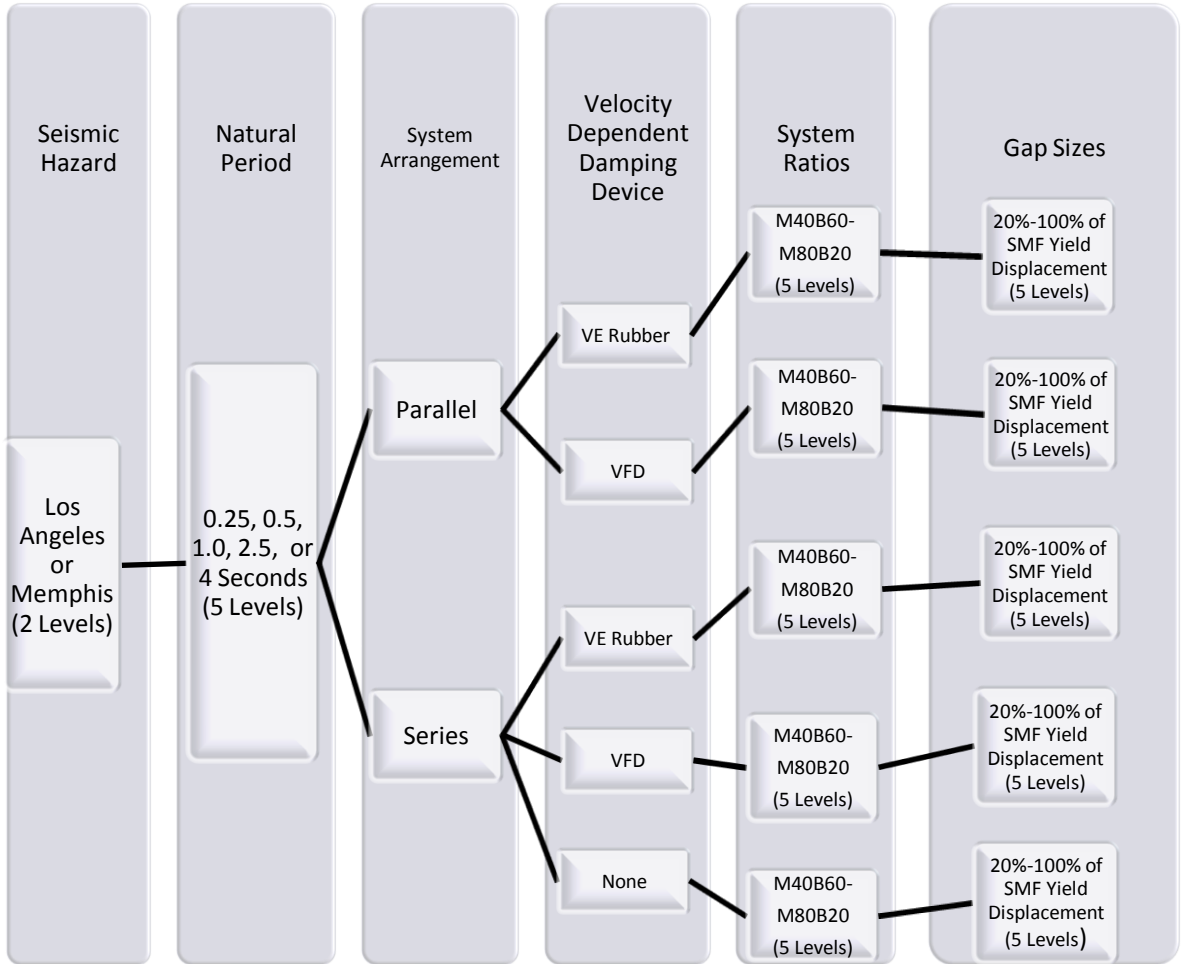


Figure 3-9: System Combinations

3.10 System Names

After the systems were generated in an experimental design, it was important to come up with a naming convention in order to effectively organize the extensive data. As outlined in the previous sections, each system contains a seismic hazard, multi-phase system arrangement, natural period, gap size, baseline system, and velocity-dependent damping device. Examples of the naming scheme are outlined in Table 3-3.

Table 3-3: System Naming Scheme

| Seismic Hazard | System Arrangement | Natural Period (sec) | Gap Size | Strength Ratio | System Configuration | System Name |
|----------------|--------------------|----------------------|----------|----------------|----------------------|------------------------------|
| Los Angeles | Parallel | 0.25 | 40% | M50B50 | HYFR | LA-P-0.25T-0.4-M50B50-HYFR |
| Los Angeles | Series | 2.5 | 80% | M60B40 | HPCD | LA-S-2.5T-0.8-M60B40-HPCD |
| Los Angeles | Series | 1 | 60% | M80B20 | HPCD-None | LA-S-1T-0.6-M80B20-HPCD-None |
| Memphis | Parallel | 4 | 100% | M40B60 | HYFR-VFD | M-P-4T-1.0-M40B60-HYFR-VFD |
| Memphis | Series | 0.5 | 20% | M70B30 | HPCD-VFD | M-S-0.5-0.2-M70B30-HPCD-VFD |

3.11 Summary

This chapter has provided a thorough explanation of the parametric development and analysis plan. Velocity-dependent devices, such as a viscous fluid damper and viscoelastic damper, were chosen, and the corresponding properties were discussed. A BRB was chosen as the displacement-dependent device and the pertinent properties to include in the analysis were also discussed. Once the two damping device types were chosen, the multi-phase arrangements were developed and discussed in detail. Other system components such as the dual frame strength ratios were reduced to an acceptable

range of values. Relationships between the strength and stiffness of the dual frame components were developed. The gap size responsible for the transition of phases was also briefly discussed. The seismic locations, which are indicative of the seismic hazard level, and natural periods included in the scope of the research were chosen to adequately represent an array of seismic hazards. A naming scheme was also formed so that data collection could be performed in an organized manner. Once the parametric development was complete, the modeling and response history analysis criteria were developed and the analysis was performed.

Chapter 4 Nonlinear SDOF Response History Analysis

4.1 Introduction

Measuring the earthquake response of buildings using a single degree of freedom system is common. This research is intended to identify the fundamental behavior of multi-phase systems; therefore, an approximation of a regular building as a single-degree of freedom system is desirable. An analysis of system parameters and their affect on structural response was used to reduce the number of viable multi-phase systems. The analysis of fundamental system behavior provided insight towards a MDOF analysis. Considering the multi-phase control device's current state of knowledge, statistical inferences of a MDOF system would be exhaustive, clouded, and difficult to comprehend. Additionally, attributing response to a certain system parameter would not be nearly as straightforward as it would be for a SDOF system because of the relatively complex behavior involved with a MDOF system. This chapter details the SDOF system parameters, in addition to the modeling process. Other aspects such as ground motion selection and scaling are also detailed in this chapter.

4.2 System Parameters

The SDOF system seeks to represent the whole structure but fails to account for the significant redundancy that would be present in a MDOF system. Since the first yield of a structure may happen early in a SDOF system, rendering it relative weak in seismic capacity, the use of an overstrength factor ($\Omega = 2.5$) was justified for modeling the systems (NEHRP, 2003). Inherent damping, another item to be included in SDOF

modeling, was represented using mass and stiffness proportional damping (Rayleigh damping). The damping ratio was kept between 1.5% and 2.3% of critical damping from a 0.25 second natural period (T_n) to $1.5T_n$ of the system (Figure 4-1).

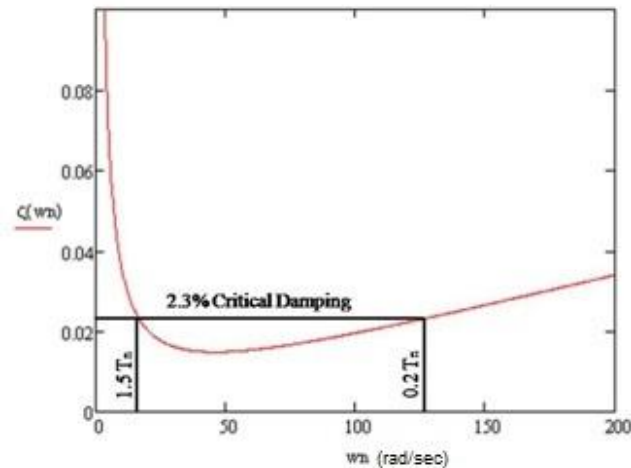


Figure 4-1: Rayleigh Damping

4.3 Earthquake Records

A suite of ground motions had to be selected that represented a variety of ground motion types: far field, near field with an acceleration pulse, and near field without an acceleration pulse. Eleven ground motions were chosen for each seismic hazard location and three sources were used for the selection of the ground motions. The Los Angeles ground motions were chosen from a list of motions recommended in FEMA-P695 based on characteristics such as source magnitude, source type, site conditions, and distance from source (FEMA, 2009). The eleven records chosen for response history analysis were comprised of 5 far field records, 3 near field with acceleration pulse records, and 3 near field without acceleration pulse records and were downloaded from the PEER

database (PEER, 2000). The records chosen for the response history analysis of the multi-phase systems are detailed in Table 4-1.

Table 4-1: Los Angeles Record Selection Summary

| Earthquake Record | Location | Source | Year | Magnitude | Duration (Seconds) | Scale Factor |
|--|--------------------|--------|------|-----------|--------------------|--------------|
| Far Field Records | | | | | | |
| DZC270 | Duzce, Turkey | PEER | 1999 | 7.5 | 27.19 | 1.924 |
| BPOE270 | Superstition Hills | PEER | 1987 | 6.5 | 22.3 | 1.861 |
| HE11140 | Imperial Valley | PEER | 1979 | 6.5 | 39.04 | 2.06 |
| BICC000 | Superstition Hills | PEER | 1987 | 6.5 | 40 | 2.233 |
| ABBARL | Manjil, Iran | PEER | 1990 | 7.4 | 53.52 | 1.624 |
| Near Field with Pulse Acceleration | | | | | | |
| DZC180 | Duzce, Turkey | PEER | 1999 | 7.1 | 25.89 | 1.146 |
| ERZEW | Erzican, Turkey | PEER | 1992 | 6.7 | 20.78 | 1.672 |
| STG090 | Loma Prieta | PEER | 1989 | 6.9 | 39.955 | 2.036 |
| Near Field without Pulse Acceleration | | | | | | |
| CPM000 | Cape Mendocino | PEER | 1992 | 7.0 | 30 | 1.409 |
| TCU067N | Chi-Chi, Taiwan | PEER | 1999 | 7.6 | 90 | 1.66 |
| STC180 | Northridge | PEER | 1994 | 6.7 | 30 | 1.782 |

The approach for record selection in the Memphis location was slightly different than for the Los Angeles area due to the unavailability of historic ground motion data.

The use of near field ground motions is not practical in the Memphis area because of the

distance from the New Madrid Fault. Numerous synthetic motions have been developed for the Memphis area by Fernandez (2007) and the Engineering Seismology Laboratory (2005) and were included in the suite of motions. Of the eleven ground motions, 5 were far-field motions obtained from FEMA-P695, 4 were Memphis synthetic records, and 2 were Charleston, SC synthetic records, chosen to represent another East coast seismic hazard. The records chosen for the Memphis response history analysis of the multi-phase systems are detailed in Table 4-2.

Table 4-2: Memphis Record Selection Summary

| Earthquake Record | Location | Source | Year | Magnitude | Duration (Seconds) | Scale Factor |
|-------------------------------------|-----------------|-----------|------|-----------|--------------------|--------------|
| Far Field Records | | | | | | |
| BOL000 | Duzce, Turkey | PEER | 1999 | 7.1 | 55.9 | 1.21 |
| ABBARL | Manjil, Iran | PEER | 1990 | 7.4 | 53.52 | 1.348 |
| DZC270 | Kocaeli, Turkey | PEER | 1999 | 7.5 | 27.19 | 1.432 |
| CHY101N | Chi-Chi, Taiwan | PEER | 1999 | 7.6 | 90 | 1.016 |
| TCU045W | Chi-Chi, Taiwan | PEER | 1999 | 7.6 | 90 | 1.686 |
| Charleston Synthetic Records | | | | | | |
| Cacc401bc | Charleston, SC | MCEER | N/A | 7.3 | 21.78 | 1.685 |
| Cacc105bc | Charleston, SC | MCEER | N/A | 7.3 | 22.78 | 1.061 |
| Memphis Synthetic Records | | | | | | |
| Acc510bc | Memphis | MCEER | N/A | 8.0 | 51.34 | 1.234 |
| Acc101bc | Memphis | MCEER | N/A | 8.0 | 51.34 | 1.25 |
| MEM97507 | Memphis | Fernandez | N/A | 7.65 | 59.715 | 1.802 |

| | | | | | | |
|----------|---------|-----------|-----|------|-------|-------|
| MEM97504 | Memphis | Fernandez | N/A | 7.65 | 85.63 | 1.513 |
|----------|---------|-----------|-----|------|-------|-------|

Once a suite of motions was selected, each had to be scaled appropriately to match the design spectrum. The geometric mean of the motions had to be kept above the design spectrum from a natural period of 0.25 seconds to 4 seconds to ensure that the input energy was greater than the design strength at all levels modeled. The scaled earthquake records for the Los Angeles and Memphis ground motions are detailed in Figure 4-2 and Figure 4-3. Each scaled record was input as an acceleration function in SAP2000.

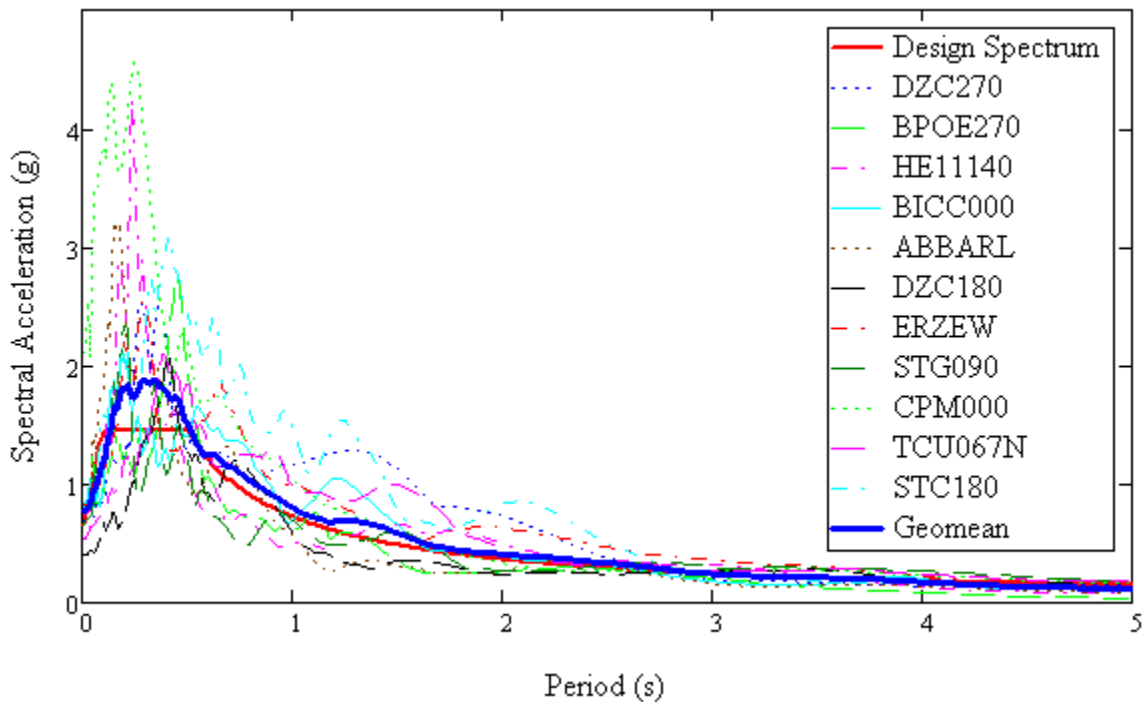


Figure 4-2: Los Angeles Ground Motion Selection and Scaling

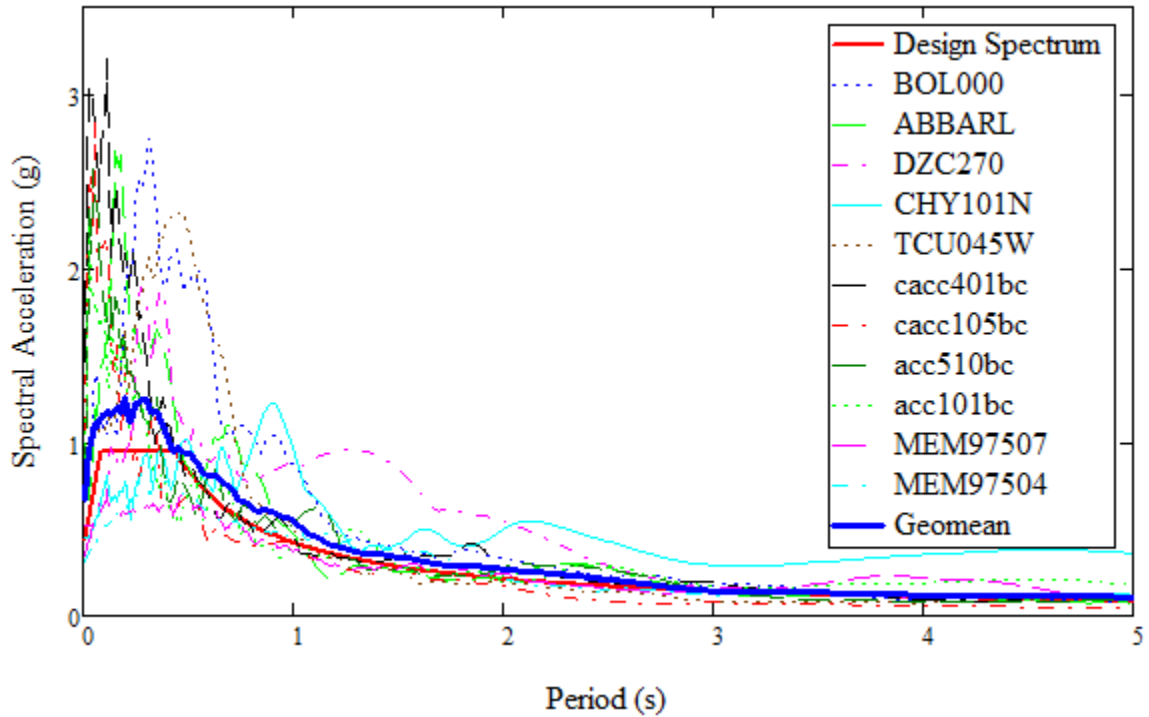


Figure 4-3: Memphis Ground Motion Selection and Scaling

4.4 Modeling Details

With the ground motions and systems selected, the details of the modeling had to be established. Each element had to be accurately represented so that system behavior could be analyzed. The following sections detail the modeling process for each system.

4.4.1 Baseline Systems

The baseline systems consisted of a dual seismic resisting system and were analyzed to demonstrate the benefits of adding a transitional gap phase. The multi-phase systems also contain the baseline elements, but included the addition of other elements representing gap, rubber, and damping behavior, depending on the system arrangement. Each baseline system has a moment frame and buckling restrained brace element, represented with a multilinear plastic link in SAP2000. Using data from the moment

frame design discussed earlier in the research, a “backbone” curve was developed off the link elements. A trilinear force-displacement relationship would be expected as the beam yields first, the column yields, then both strain harden together. Since it would be somewhat difficult to represent this sequential yielding with strain hardening, two bilinear relationships, one for the moment frame beam and one for the column were used in parallel instead (Figure 4-4).

Post-yield p-delta effects were neglected because the practicality of use within a SDOF study is simply not realistic. P-delta effects can add large secondary moments to the structure throughout the duration of excitement, especially after yielding because of the decrease of system stiffness. Because, for a SDOF system, the mass is lumped at a single point, including secondary moments associated the displacement is not realistic. Although neglecting p-delta effects improves system performance, it is a necessary assumption within the scope of the research. Investigating p-delta effects would be an area of interest, especially with longer period structures, in a MDOF study.

Similar to the moment frame, the buckling restrained brace frame backbone curve was generated using the strength and stiffness data presented in the previous chapter.

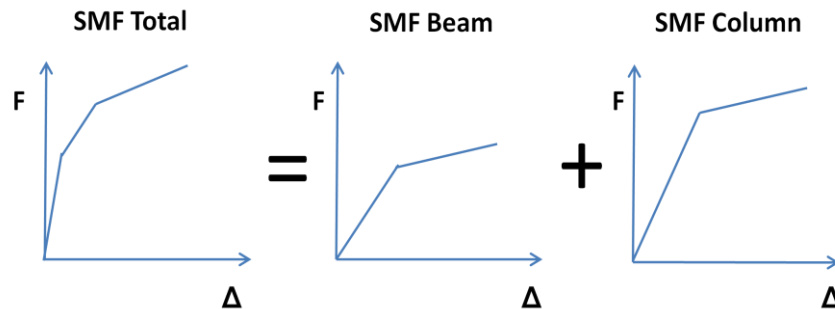


Figure 4-4: Special Moment Frame Component Breakdown

The backbone curves for the links in the models were created in accordance with *ASCE Standard 41-06 "Seismic Rehabilitation of Existing Buildings"* (ASCE, 2007). Figure 4-5 details the typical behavior of the elements, including criteria for yielding, strain hardening (3% of the elastic slope), plastic deformation, and residual strength. Values taken from Table 5-6 and Table 5-7 in *ASCE Standard 41-06* are outlined in Table 4-3.

Table 4-3: Link Element Backbone Curve Values (ASCE/SEI, 2007)

| Link Element | Plastic Rotation Angle or Deformation | | Residual Strength Ratio |
|--------------------------------------|---------------------------------------|--------------|-------------------------|
| | a | b | c |
| Moment Frame Beam for Flexure | $9\theta_y$ | $11\theta_y$ | 0.6 |
| Moment Frame Column for Flexure | $9\theta_y$ | $11\theta_y$ | 0.6 |
| Buckling Restrained Brace in Tension | $11\Delta_T$ | $14\Delta_T$ | 0.8 |

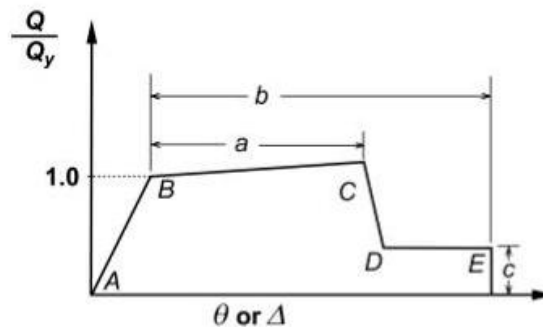


Figure 4-5: Link Backbone Behavior (ASCE/SEI, 2007)

In the model, the multilinear plastic links for the SMRF and BRB are situated on either side of the SDOF mass (Figure 4-6). These plastic links are comprised of elastic

and inelastic behavior and are representative of the force-displacement behavior of the SMRF and BRB elements. Varying the SDOF mass and the link stiffnesses, the natural period of the system can be changed. Other modeling elements will be detailed in further sections as they are encountered in the multi-phase systems.

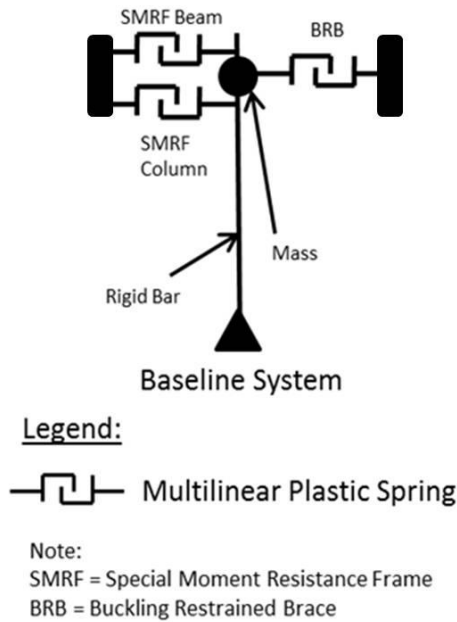


Figure 4-6: Modeled Baseline System

4.4.2 Series Systems

The three series systems to be modeled include the HPCD, HPCD-VFD, and HPCD-None systems. These systems include the link elements previously described for the SMRF and BRBF, with the addition of a gap element and linear viscous damper. The gap element for the HPCD system is represented with a multilinear elastic link element that accounts for the high-damping rubber stiffness and lockout mechanism. The stiffness during the transition action is dependent on the damper size but after the desired

displacement is reached, the element essentially becomes infinitely stiff when the mechanism locks out. Marshall (2008) found the shear storage modulus (G') to be 87 psi during the mechanical testing of a high-damping butyl rubber to be utilized in an HPCD; therefore this value was used in this research as well. The gap for the HPCD-VFD and HPCD-None (also represented with a multilinear elastic link element) theoretically has no stiffness but a value of 0.5 kips/inch was used to account for friction in the slotted connection. Detailed gap element behavior can be found in Figure 4-7.

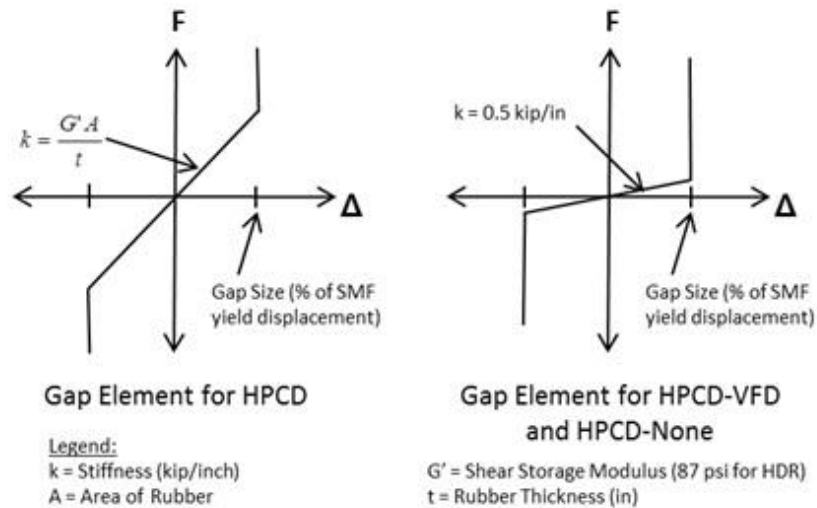


Figure 4-7: Gap Element Modeling

Damping in the high-damping rubber and viscous fluid damper was modeled using a linear viscous dashpot element. The damping coefficient, c , is changed depending on the system properties and damping material (8% for the HDR and 13% for the VFD). In the series systems, viscous or viscoelastic damping is only present while the gap is active; therefore it is placed in parallel with the gap element. The HPCD-None

system has no supplemental damping and therefore no linear viscous damper. Details of the system arrangements are shown in Figure 4-8.

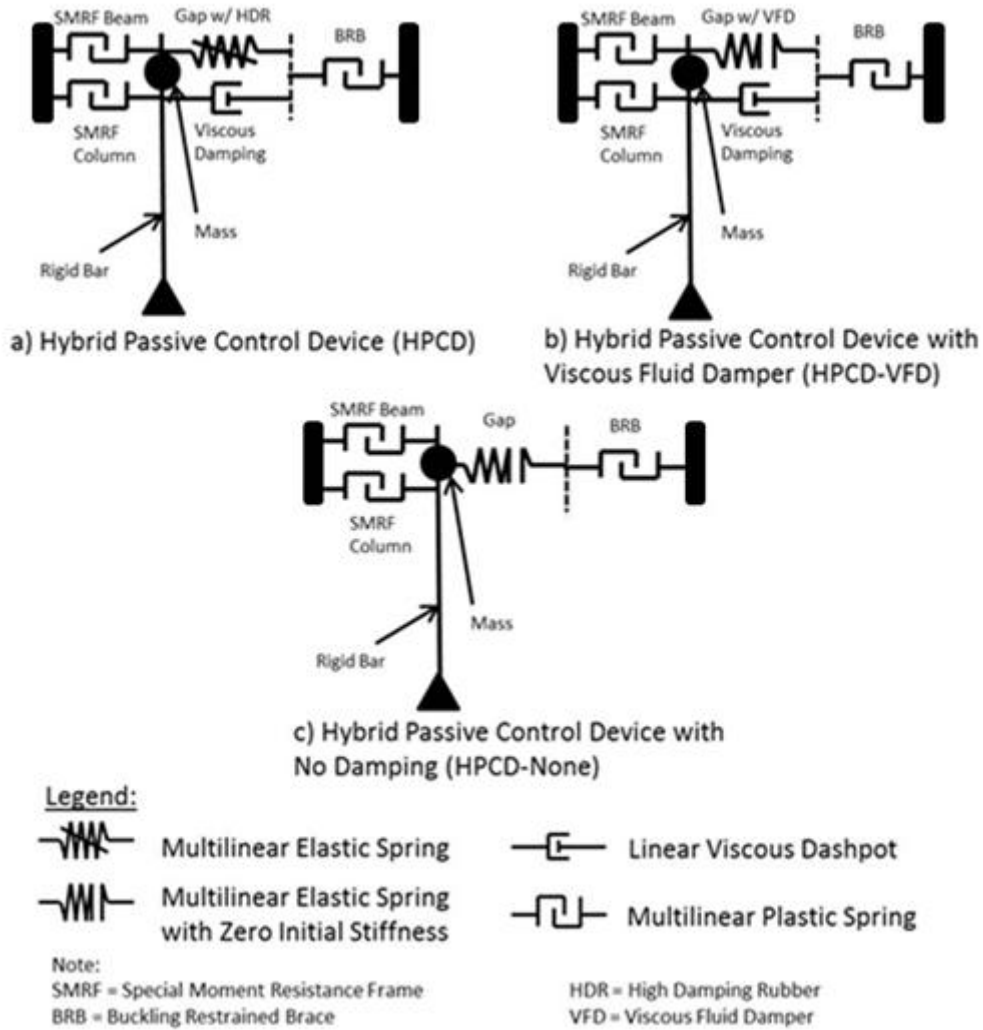


Figure 4-8: Modeling of the Series Systems

4.4.3 Parallel Systems

The parallel systems were a little more complex to model and had to allow for damping during all phases of excitation. The HYFR system included the SMRF elements in parallel with a BRB and gap element in series on one side of the system. The other side

included the compressed elastomeric device (EMD) described in Chapter 3. The encased high-damping rubber in the EMD is represented using a multilinear elastic link element, linear viscous dashpot, and a multilinear plastic element. The HDR stiffness is represented the same as it was in the HPCD system, in parallel with the viscous damper with a damping coefficient that creates 8% of critical damping. Karavasilis et al. (2010) found slip behavior in the EMD to occur at approximately 2/3 of an inch, meaning that a “slip force” can be found that would initiate a friction device behavior with little resistance until force direction reverses. This slip behavior is represented with a multilinear plastic link element that does not become active until the slip force is reached; this behavior is evident in a hysteresis loop resulting from a representative model in Figure 4-9.

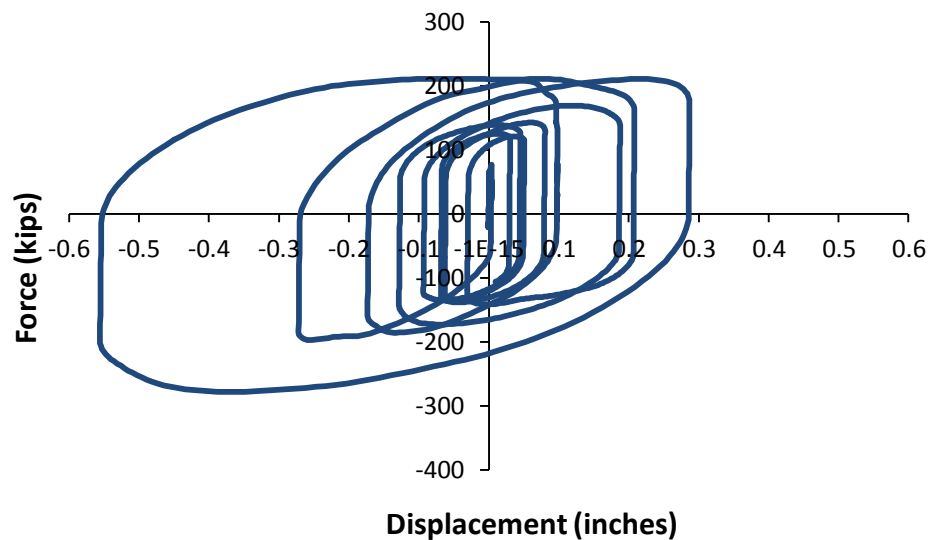


Figure 4-9: EMD Hysteretic Slip Behavior

The HYFR-VFD system utilizes a VFD placed in parallel with a BRB and gap element acting in series. The other side of the system is the typical moment frame

configuration seen in all the other systems. The modeling schematics for the parallel systems are represented in Figure 4-10. Both systems can utilize damping even while the BRBF link is yielding, a potentially appealing option that was investigated in this study.

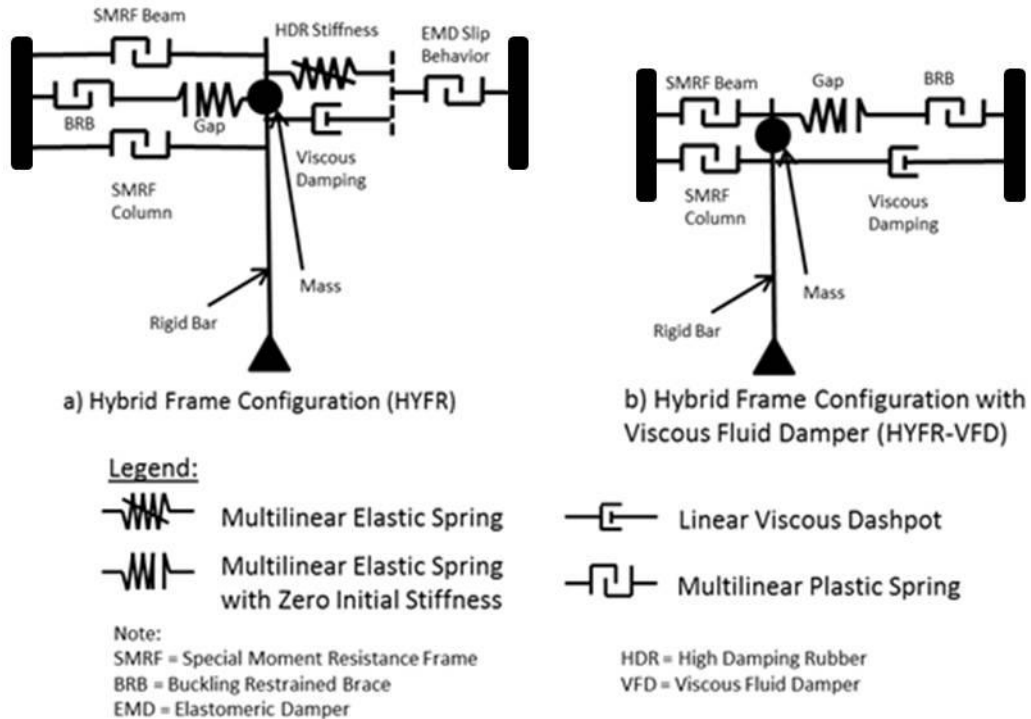


Figure 4-10: Modeling of the Parallel Systems

4.5 Incremental Dynamic Analysis

The primary means for analyzing the data was in the form of an incremental dynamic analysis (IDA). This method is widely accepted and has been adopted as an acceptable means of analysis in the FEMA guidelines (Vamvatsikos & Cornell, 2002). In the scope of this research, the IDAs were created by 1) scaling the ground motions as detailed earlier in the chapter, 2) scaling the ground motions further by factors of 0.1, 0.2, 0.3, 0.4, 0.5, 0.6, 0.7, 0.8, 0.9 and 1.0 (DBE), 3) running each scale factor for the model,

and 4) plotting the maximum absolute value for each response quantity. The values used in the IDAs were typically an average response of the 11 ground motions at each scale factor. General trends, such as yielding of an element, were noticed as the IDA plots changed shape. Comparing multi-phase system IDAs to baseline system IDAs is also a useful means of analysis. Observing response in an IDA is a great means for evaluating a large set of data in a quick fashion. As better performing multi-phase systems were identified using the IDA data, more rigorous comparisons were made. Acceleration spikes and residual displacements were also analyzed using a representative set of response histories.

4.6 Response Quantities

The four primary response quantities used to evaluate the systems were acceleration, base shear, moment frame ductility, and buckling restrained brace ductility. It was felt that the magnitudes of these four characteristics could adequately describe the overall performance of the multi-phase systems. In order to compare the systems, normalization of the response parameters into unitless quantities was desirable. Acceleration response consisted of the total nodal acceleration divided by the gravitational constant ($386.4 \frac{\text{in.}}{\text{sec}^2}$). Base shear response was determined by dividing the lateral base reaction (kips) by the weight (kips) of the system.

Since the moment frames were designed to ensure strong column-weak beam response, the moment frame ductility was determined using the moment frame beam link response. The moment frame ductility is also a measure of drift since the moment frame displacement is the absolute displacement of the system. The normalized moment frame

ductility value (μ_M) consisted of the actual beam displacement value divided by the beam yield displacement. Similarly, the buckling restrained brace ductility (μ_B) was calculated by dividing the buckling restrained brace link displacement by the brace yield displacement. The quantities used to determine these normalized responses are detailed in Table 4-4.

Table 4-4: Response Quantity Summary

| Response Quantity | Unitless Response |
|---|--|
| Acceleration (g) | $\frac{\text{Total Acceleration Response}}{\text{Gravity}}$ |
| Base Shear | $\frac{\text{Base Shear Response}}{\text{Weight}}$ |
| Moment Frame Ductility (μ_M) | $\frac{\text{Moment Frame Beam Link Response}}{\text{Moment Frame Beam Yield Displacement}}$ |
| Buckling Restrained Brace Ductility (μ_B) | $\frac{\text{Buckling Restrained Brace Link Response}}{\text{Buckling Restrained Brace Yield Displacement}}$ |

4.7 Summary

This chapter provided a description for the response history analysis that was performed for the multi-phase passive control systems. Important aspects of the study were established such as the suite of ground motions and the appropriate scaling levels for the ground motion records. Modeling aspects for all of the multi-phase systems were discussed, and the arrangement of the systems was described. Multi-linear plastic link elements, multi-linear elastic link elements, and linear viscous dashpots were all used to represent the multi-phase behavior. In addition to modeling techniques, analysis criteria were described for the results of the response history analyses. Four primary response

quantities were chosen to be analyzed in the form of an incremental dynamic analysis.

After the completion of the model development, the multi-phase system models were run in SAP2000 and the results are discussed within the next section.

Chapter 5 Preliminary Analysis

5.1 Introduction

The groundwork for the study has been clearly defined in the previous chapters. Multiple multi-phase passive control device combinations have been proposed and demonstrated to be beneficial in previous studies (Marshall, 2008). The goal of this study was to identify the important factors controlling response. This chapter provides the results of the study outlined in the previous chapters and some conclusions are drawn about the behavior of passive multi-phase systems. The chapter consists of the description a preliminary analysis, in which the range of variables was narrowed down into a reasonable range, for which a full factorial analysis could be conducted. The ultimate goal was to narrow the scope of the research into an acceptable range of values so that a MDOF study may be performed in the next part of the multi-phase system development. In doing so, important system responses were identified and fundamental multi-phase behavior was uncovered. As outlined in previous chapters, an extensive nonlinear response history analysis was completed using SAP2000. The graphical results of data collected in the preliminary analyses can be found in Appendix A.

5.2 Preliminary Analysis

As described in Chapter 3, the scope of the study potentially involved 1250 possible combinations for the multi-phase systems. In order to complete the study in a timely manner and still capture the significance of the results, the results of an experimental design reduced the scope of the study to 135 systems. This representative

subset of the 1250 possible systems was meant to capture the statistical significance of each of the system parameters. This was difficult to determine due to the hierarchal structure inherently present within the multi-phase systems. The factors are statistically “nested” within each other, an important variable that was unintentionally ignored in the experimental design. This means that individually variable performance could not be compared to each other because the performance was dependent on other variables within the hierarchal structure. The scope of this analysis was simply too large to draw finite conclusions about the statistical significance of multi-phase systems, but general conclusions were made. In this section, some results from the preliminary analysis are presented, general observations about multi-phase systems are provided, and a solution to the nesting issue is offered.

Figure 5-1 through 5-4 show representative sets of data generated from the preliminary analysis with the four response quantities of concern are plotted. The system names follow the convention given in Section 3.10.

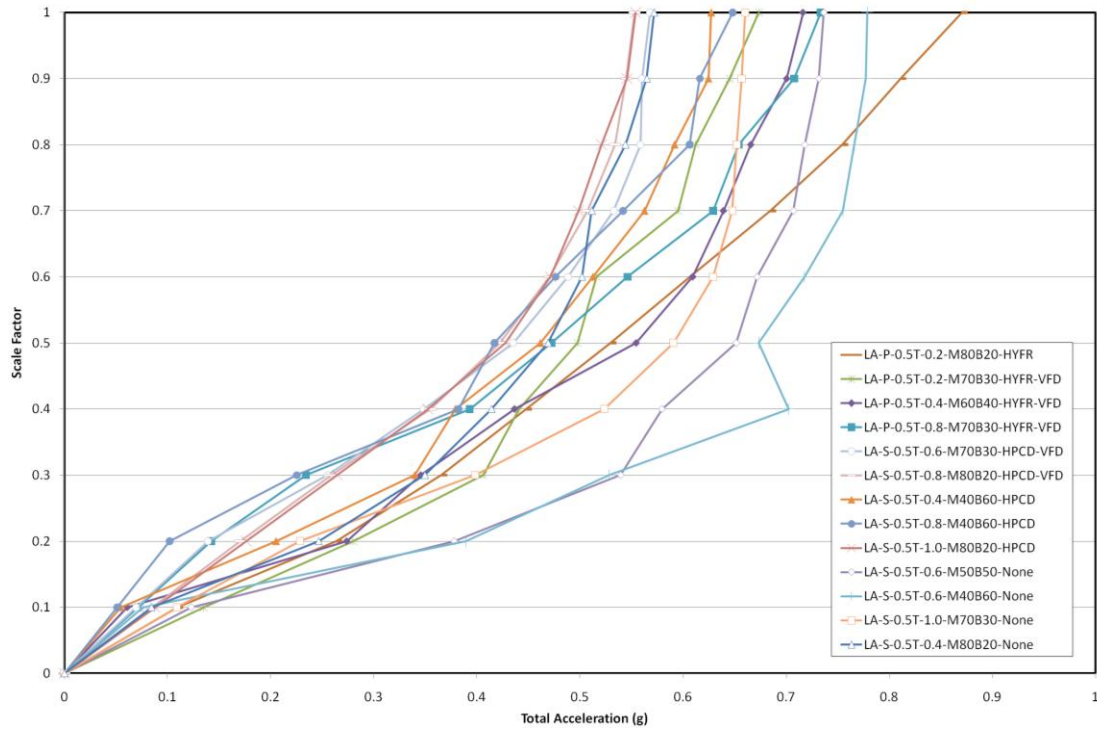


Figure 5-1: Acceleration Results for 0.5T Los Angeles Systems

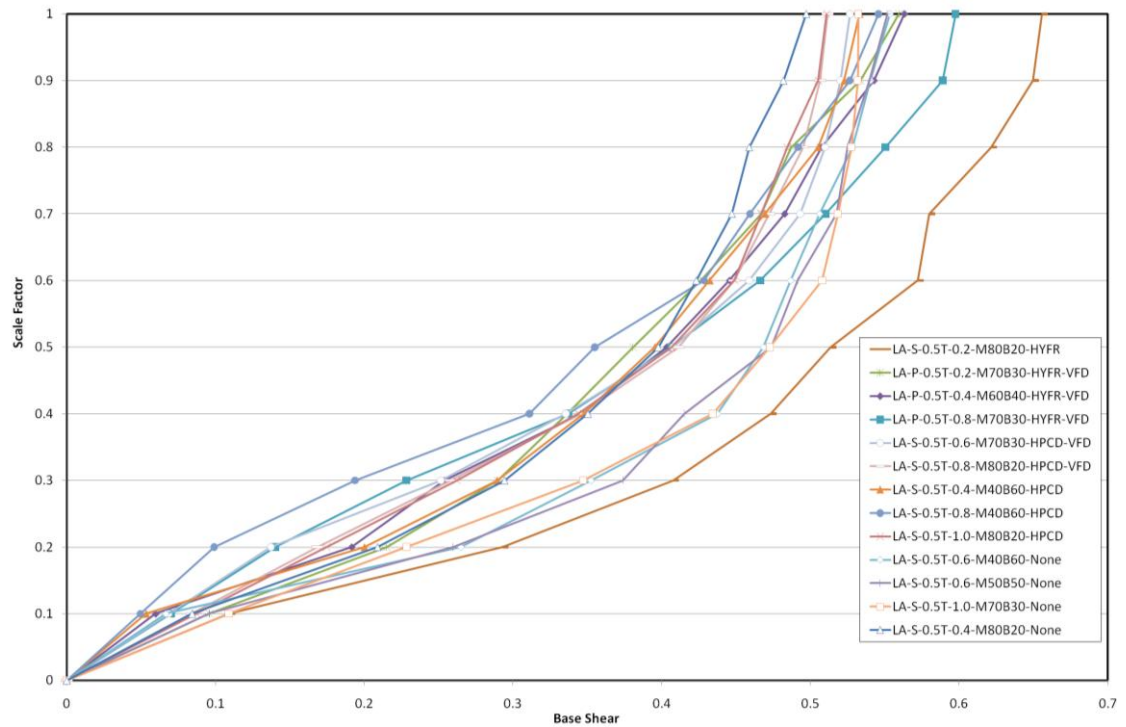


Figure 5-2: Base Shear Results for 0.5T Los Angeles Systems

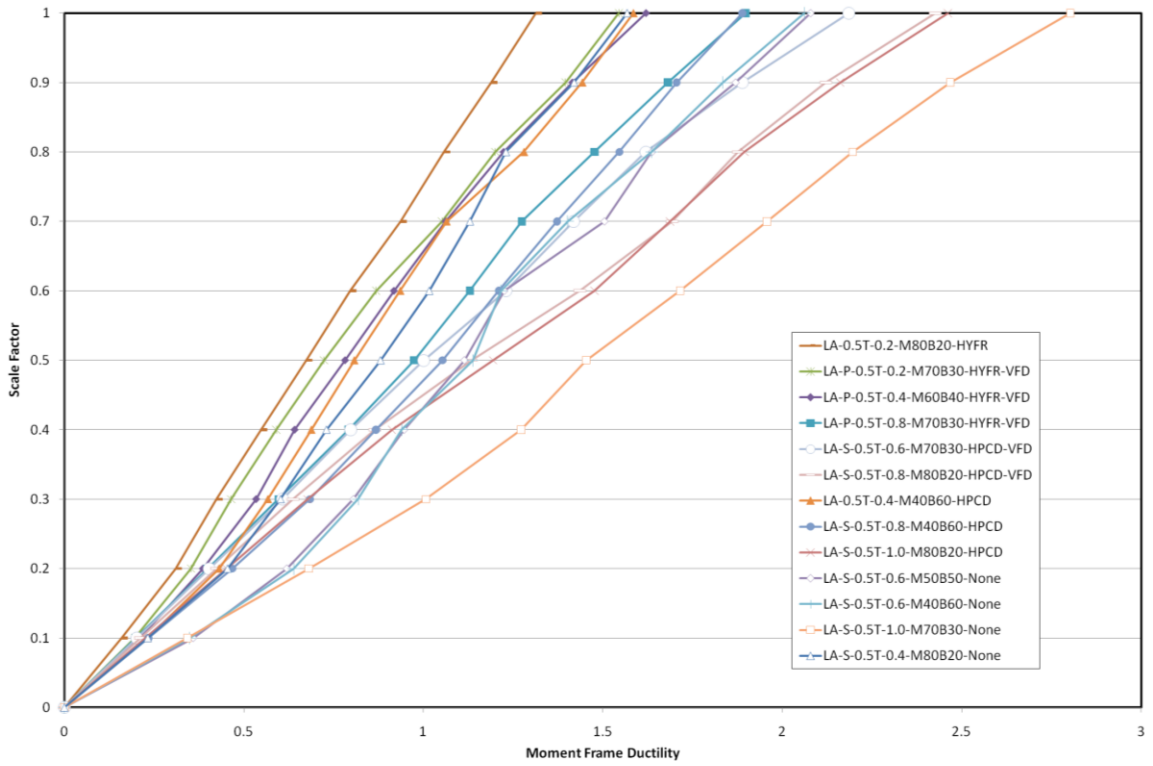


Figure 5-3: Moment Frame Ductility Results for 0.5T Los Angeles Systems

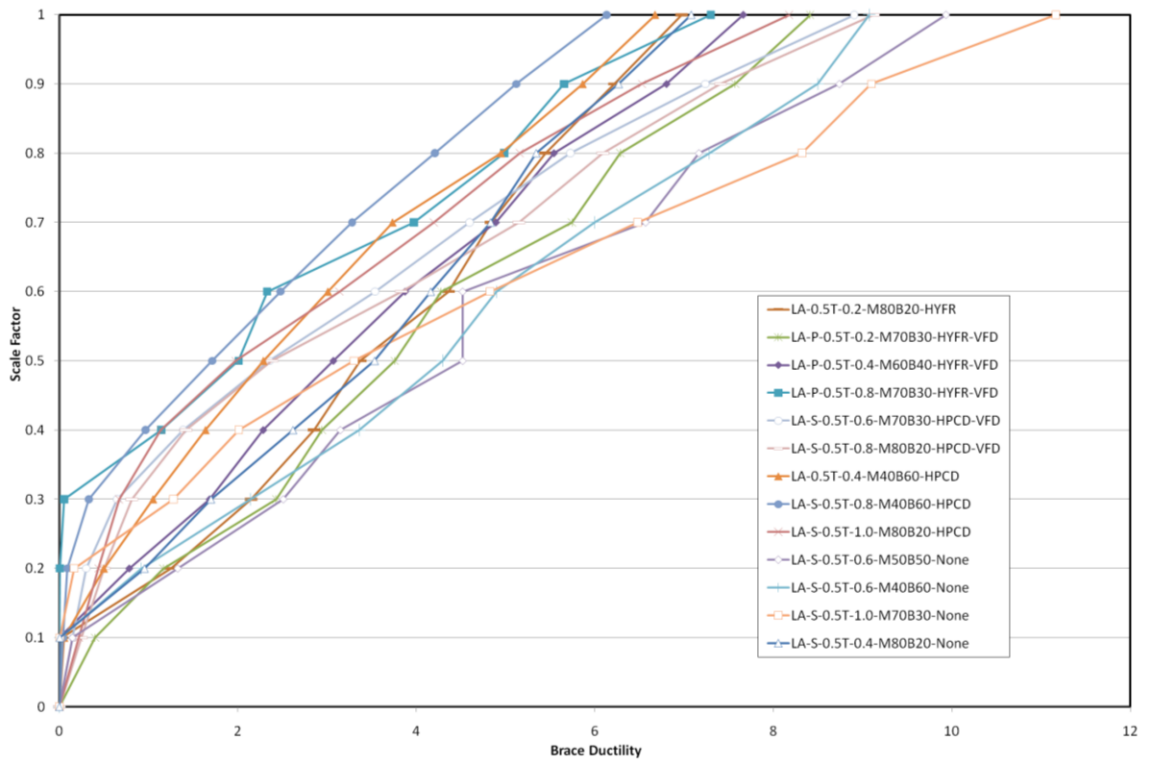


Figure 5-4: BRB Ductility Results for 0.5T Los Angeles Systems

In comparing the graphical results, there were no multi-phase systems that clearly stood out as outstanding performers across all scale factors and response quantities, but general trends were noticed. Even though systems had noticeable differences in response, the reasons for the differences were difficult to pinpoint due to the nesting of the system variables. For many of the multi-phase systems, better performance in one of the response quantity amounts to sacrificial performance in another.

Generally speaking, the transition gap allows for better acceleration and base shear performance in the lower scale factors. This was noticed as the plots with the larger gap sizes have a lower acceleration response in the lower scale factors and delayed transition into higher acceleration values in the upper scale factors. To a degree, this is noticed across all natural periods, multi-phase systems, and both hazards. The presence of supplemental damping and a reduction in initial stiffness would be present in a dual system is the reason for this marked improvement in Figure 5-1 and

Figure 5-2: Base Shear Results for 0.5T Los Angeles Systems

show the poor performance of the HPCD-None systems, demonstrating the need for supplemental damping and therefore a transition gap phase with supplemental damping. Yielding in the HPCD-None systems occurs quicker than the systems with supplemental damping. The overall performance seems to be very sensitive to the strength/stiffness ratio and gap size pairing.

No discernable difference could be found between the two types of supplemental damping. The high-damping rubber provides more stiffness, and therefore higher

acceleration, in the lower scale factors for the series systems, but also potentially delays the transition into the secondary phase and reduces displacements. The high-damping rubber in the parallel arrangement provides more stiffness throughout all scale factors and therefore can experience a larger acceleration throughout all scale factors. Although this is a drawback of a parallel multi-phase system, it also means that more damping and energy dissipation is present to protect the system elements.

Although these general observations are helpful in understanding the fundamental multi-phase behavior, statistical significance and proof of beneficial multi-phase behavior was not evident. The difficulty in identifying the beneficial factors arose because of the great independence of each of the factors on one another. Figure 5-5 illustrates the hierarchical path taken to get to two plausible multi-phase systems: LA-S-4T-0.4-M50B50-HPCD-None and LA-P-0.5T-0.6-M80B20-HYFR-VFD. Simply comparing the response parameters from the two gap sizes or system ratios is not feasible because the response is also reliant on the higher levels in the hierarchal structure. Trying to find statistical significance this far down the hierarchal arrangement with data from 135 systems out of the 1250 combinations was not possible due to this nesting issue.

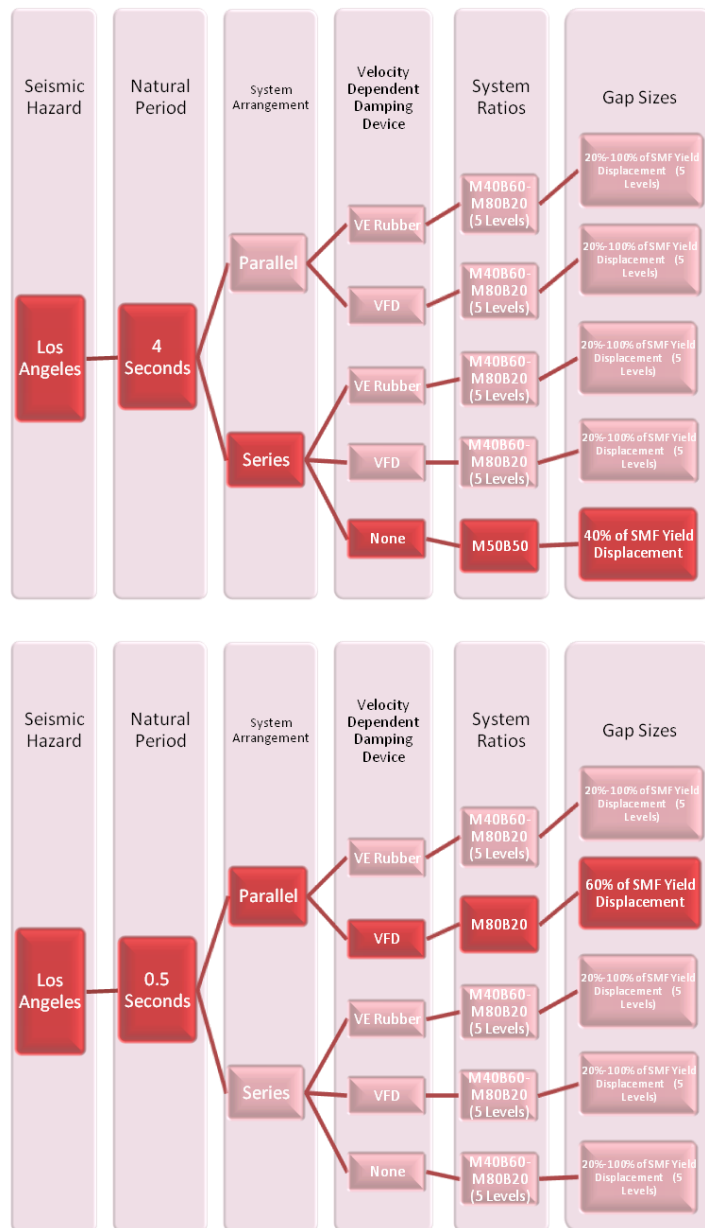


Figure 5-5: Hierarchal Nesting Issue

A full factorial design on a smaller range of variables would allow statistical observations to be made if significance were present. At the very least, since the research was deterministic in nature and all the multi-phase combinations were exhausted, the data from a full factorial design would allow one to make observations between the systems,

knowing that a better performing multi-phase system is not available within the scope the research variables. The following sections detail the reduction of the research scope in order to accomplish these goals.

5.2 Reduction of the Research Scope

Although the analysis was intended to be the only analysis, it ultimately served as a preliminary analysis used to narrow the scope of the study into a more useful range of values. Instead of performing another experimental design and analyzing a representative set of the multi-phase system population, the goal was to eliminate certain factors, and perform a full factorial analysis using the remaining factors, for which the whole population was analyzed. Since the analysis was deterministic in nature, this full factorial analysis was a desirable option for determining the variables that controlled the response, and for identifying the systems that showed superior performance. As stated in Chapter 3, a full factorial design which exhausts all possible options would consist of 1250 systems. The following sections details the techniques used to systematically reduce the number of factors varied in the study.

5.2.1 Seismic Hazard

Results of the preliminary analysis demonstrated similar response magnitudes for the two seismic hazards, as evident in Figure 5-6a through Figure 5-6d. In this figure, results for two multi-phase systems that had the same multi-phase configuration, but were designed and exposed to both seismic hazards, are compared. Although the systems were subjected to a different suite of ground motions, the general shape of the IDA curves is somewhat similar, suggesting similar behavior across seismic hazards. Ductility values

were also found to be statistically similar for the analysis, further backing this assertion. These observations hold true across the preliminary analyses for multi-phase systems with differing gap sizes.

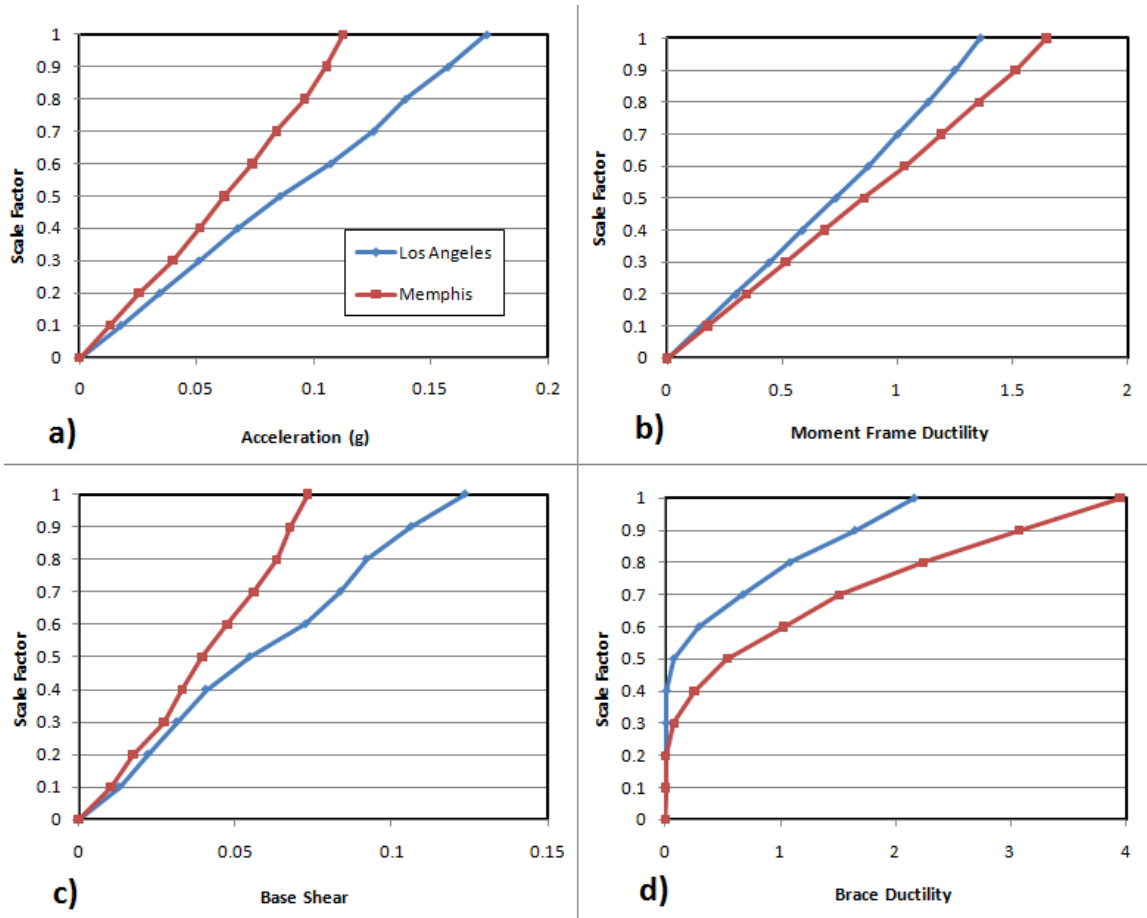


Figure 5-6: 1T-M70B30-1.0-HYFR Seismic Hazard Comparison

Since there are only two seismic hazards and seismic hazard is near the top of the hierarchy, reducing the seismic hazard to one location would reduce the number of possible systems from 1250 to 625 systems. Evaluating the responses for the seismic hazard of each location, it was determined that Los Angeles would be a more suitable

location for the rest of the analyses, because the intensity and frequency of seismic events in Los Angeles make the location a more marketable and viable option for the multi-phase systems. Once a range of multi-phase systems are identified as good performers at the end of the study, their performance can be validated in other locations.

5.2.2 Natural Period

The preliminary analysis included 5 natural periods of interest: 0.25, 0.5, 1.0, 2.5, and 4.0 seconds. In order to reduce the number of natural periods, similarities in response behavior were sought.

Error! Reference source not found. shows a connecting letters report for the longer natural periods for the report. A Tukey is used test to compare the means and to test for significant differences. The Tukey test has been demonstrated as an excellent post-hoc test method for an Analysis of Variance (ANOVA) (Montgomery, 2009). The report shows that moment frame and brace ductilities are not significantly different for the two periods, suggesting that only one of the periods needs to be tested in the future. The total acceleration and base shear responses are not connected in a similar manner, which is expected due to different input energies at the two natural periods. Conclusions drawn for a 2.5 second period could reasonably be extended for a 4 second period in the next analysis. Once a range of acceptable multi-phase systems are established at the end of the study, their performance can be validated for a 4 second natural period if needed. This would probably not be the case within the scope of an MDOF study, but for the scope of this research it is no longer necessary to include both periods. Eliminating the 4 second period from the study reduced the scope of interest from 625 to 500 systems.

Table 5-1: Connecting Letters Report

| Moment Frame Ductility | | | Buckling Restrained Brace Ductility | | |
|------------------------|---|---------------|-------------------------------------|---|---------------|
| Level | | Least Sq Mean | Level | | Least Sq Mean |
| [Memphis]2.5 | A | 0.99540847 | [Memphis]2.5 | A | 3.0125158 |
| [Memphis]4 | A | 0.95086615 | [Memphis]4 | A | 2.8254972 |
| [Los Angeles]2.5 | B | 0.71350320 | [Los Angeles]2.5 | B | 2.0072952 |
| [Los Angeles]4 | B | 0.64386006 | [Los Angeles]4 | B | 1.5073349 |

Levels not connected by same letter are significantly different. Levels not connected by same letter are significantly different.

5.2.3 System Arrangement

The preliminary analysis involved 5 different multi-phase system HPCD, HPCD-VFD, HPCD-None, HYFR, and HYFR-VFD. As alluded to earlier shown in Figure 5-1 and

Figure 5-2: Base Shear Results for 0.5T Los Angeles Systems

, the HPCD-None system demonstrated poor acceleration and base shear performance in comparison to the other systems. Yielding of elements, as the ductility values exceed 1, also occurred earlier in comparison to the other multi-phase systems. For these reasons, the HPCD-None system was eliminated from further analyses. As expected, damping does play a valuable role in the protection of structures using the multi-phase systems.

No valid arguments could be made for the elimination of other systems. The parallel systems did experience high acceleration and base shear response in the higher scale factors in comparison to the series systems, but the great ductility response made those systems a viable to option to be included in the next analysis. The elimination of the HPCD-None system reduced the scope of the study from 500 to 400 systems.

5.2.4 System Ratios

The preliminary analysis involved 5 different dual system ratios: M40B60, M50B50, M60B40, M70B30, and M80B20. Moment frame ductility is largely dependent on the moment frame strength and gap size. The larger the portion of the dual system resisted by the moment frame, the more ductility is present in the moment frame element. Since the primary goal of the study was to limit the ductile behavior to a replaceable “link” element, the ductile behavior of the moment frame was not desirable. This ductility could be reduced by limiting the gap size to 20%-40% of the moment frame yield, but that would not allow the supplemental damping to be fully utilized to reduce accelerations.

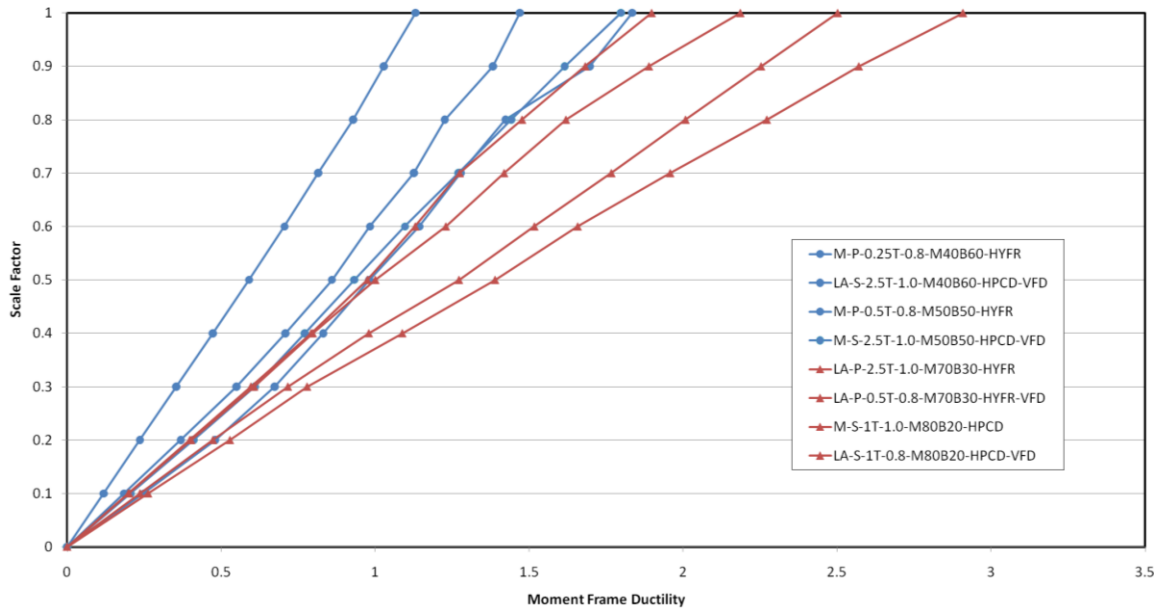


Figure 5-7: Moment Frame Ductility Comparison between Dual System Ratios

Figure 5-7 is a random sample of ductility responses of multi-phase systems at different system ratios. The IDA curves illustrate the relatively poor performance of the systems with a larger moment frame percentage (M70B30 and M80B20). Moment frame yielding occurs as early as 40% of the design basis earthquake (DBE) for these systems

as opposed to 60%-90% of the DBE for the M40B60 and M50B50 systems. For this reason, the secondary analysis was concentrated on the range of M40B60 to M60B40 in order to reduce moment frame ductility. This reduced the scope of the study from 400 to 240 multi-phase systems.

5.2.5 Transitional Gap Size

The preliminary analysis involved 5 different transitional gap sizes: 20%, 40%, 60%, 80%, and 100% of the special moment frame yield displacement. The multi-phase system behavior was very sensitive to the system ratio paired with the gap size.

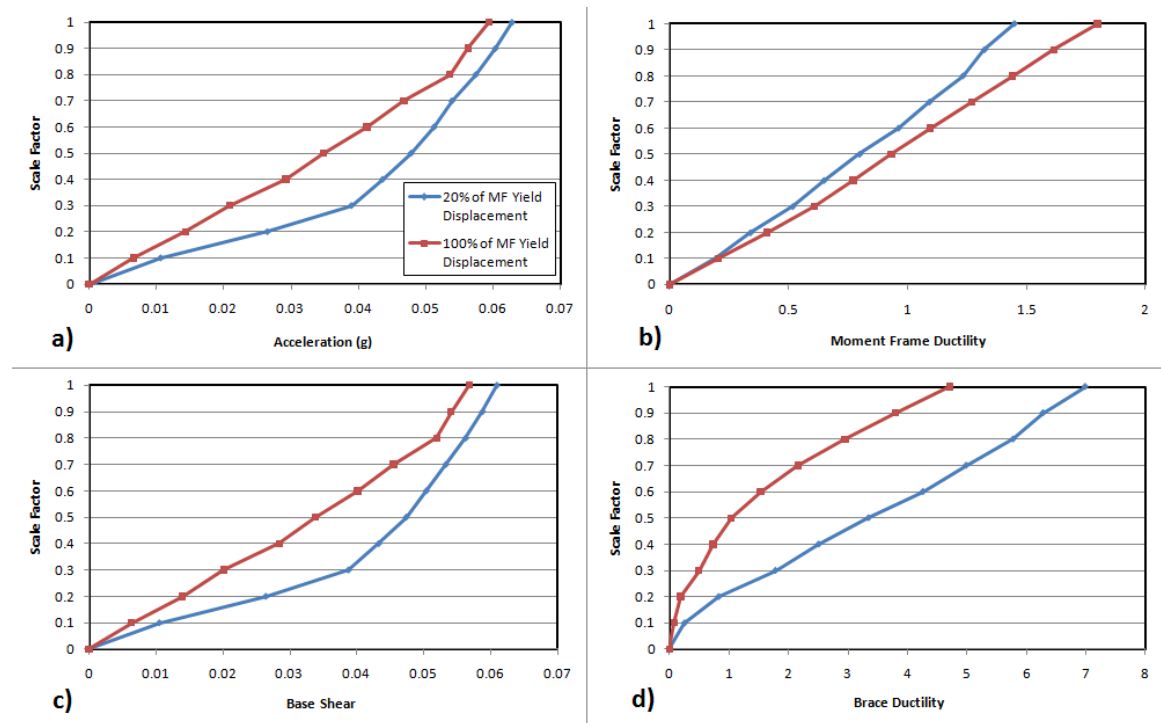


Figure 5-8: M-S-2.5T-M50B50-HPCD-VFD Gap Size Comparison

Figure 5-8a through Figure 5-8d demonstrate the importance of the gap size on the response of the multi-phase systems, comparing the same multi-phase arrangement with two different gap sizes. Significant differences in magnitude can be seen between

the two systems across all of the response quantities. The smaller gap size does not allow for significant damping because it closes too quickly and increases acceleration and base shear due to the increase in stiffness. Buckling restrained brace behavior is also much more desirable for the larger gap size, delaying yielding until about 50% of the DBE as opposed to 20% of the DBE in the multi-phase system with the smaller gap size. The one drawback of the larger gap size is the slightly worse moment frame ductility behavior, a response quantity identified earlier as very important. This problem could potentially be resolved with a smaller gap size, such as 60% or 80% of moment frame yield displacement, which should still allow for significant damping but also protect the moment frame. Similar behavior was observed across all of the multi-phase systems, and therefore justified the reduction of the scope of the study to only include gap sizes from 60%-100% of moment frame yield displacement.

This decision reduced the scope of the study from 240 to 144 systems, a number that was much more reasonable to analyze in a timely manner than 1250 systems. With the reduction of variable levels to a reasonable scope for a full factorial analysis, the next set of analyses was completed. The hierarchal structure of the full factorial analysis is given in Figure 5-9. Although nesting was still present due to the inherent hierarchal structure of the data, the overall multi-phase system performance was more evident at the end of the analysis.

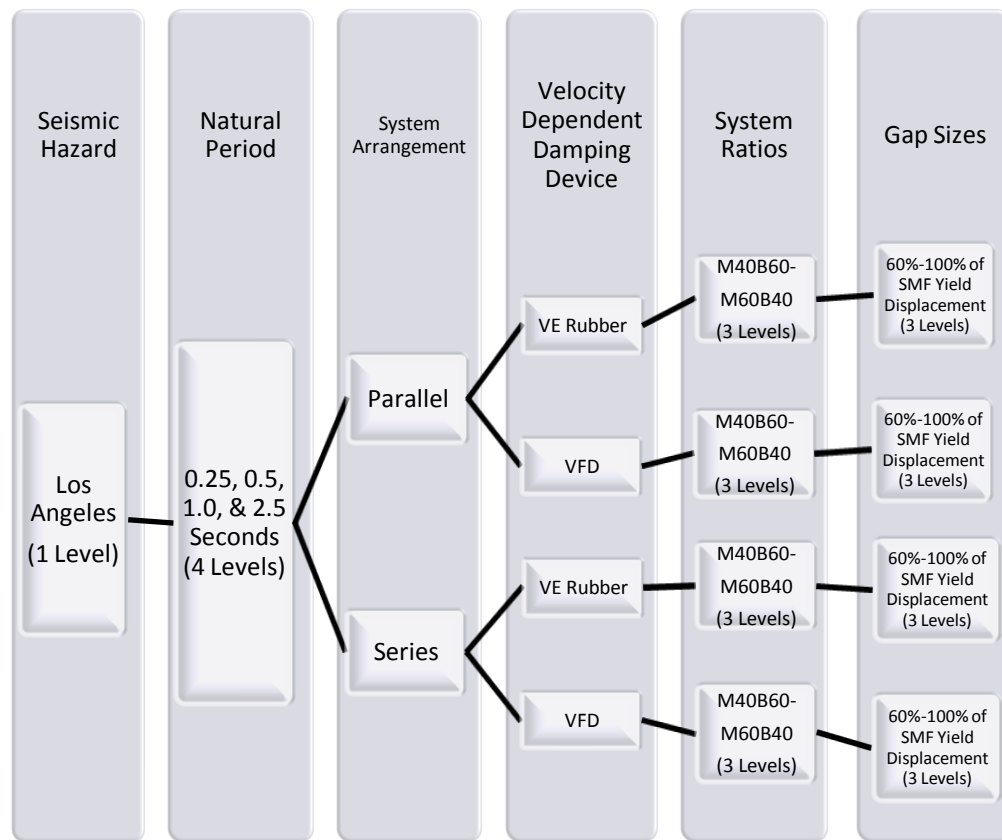


Figure 5-9: Full Factorial Experimental Design

5.3 Summary

This chapter provided a significant amount of preliminary information for multi-phase systems. Although the work was intended to be the only analysis, the results were unclear, and an additional analysis was required. Some general observations were made but the fundamental understanding of multi-phase behavior was still lacking. The preliminary analysis did help in reducing the range of variables to an acceptable range for a full factorial analysis to be performed. Each variable was analyzed and the range of variable values to be studied was reduced using a statistical analysis or empirical observations. The number of possible systems was reduced from 1250 to 144 multi-

phase arrangements, a number reasonable for a full factorial analysis. Similar to models described in this chapter, the new models required for the full factorial analysis were assembled and run in SAP2000. The following chapter details the results of this analysis.

Chapter 6 Full Factorial Analysis

6.1 Introduction

Chapter 6 describes the steps taken to identify the fundamental behavior of multi-phase systems. With the range of variables narrowed as detailed in the previous chapter, a full factorial analysis was completed in order to find significant differences in the system responses. The original intention of the research was to provide a statistical analysis of the system results, but since the data is deterministic in nature, a full factorial analysis will allowed a direct comparison between systems. First, an overall comparison of the multi-phase systems to baseline systems was accomplished to demonstrate the benefits of a multi-phase system. Once this was completed, the ultimate goal became narrowing the scope of the study into an acceptable range of values so that a MDOF study can be performed in the next phase of multi-phase system development. This goal was accomplished by comparing the responses of multi-phase systems in a variety of ways. Responses for different natural periods, system arrangements, and system strength ratio and gap size combinations were all compared in order to identify the systems that performed the best. Other aspects of multi-phase behavior, such as acceleration spikes and residual deformations, were also investigated. The complete set of data collected for the full factorial analysis can be found in Appendix B.

6.2 Comparison to Baselines

In order to demonstrate the benefits of a multi-phased system, their performances were compared to the baseline systems for all response quantities. For appropriate

comparisons to be made, all multi-phase systems were compared to their corresponding baseline system, which were comprised of only the dual frames. Figure 6-1 through Figure 6-4 show the performance of all the multi-phase systems for a 1 second natural period with an M50B50 dual frame. This is a representative selection of multi-phase systems but similar observations were made across all of the multi-phase systems evaluated in this analysis.

The responses of the baseline systems were represented with a solid line. Box plots were used to depict the spread in the multi-phase system responses. Using the five number summary (minimum value, lower quartile, median, upper quartile, and maximum value), variability and skewness in the responses were readily identified. Since these comparisons included all of the multi-phase systems, large error bars or a high level of skewness may be apparent in some system combinations, indicating poor performance. Initially, this was a useful means to evaluate the multi-phase performance, but more detailed analyses were used in further sections to further evaluate system behavior.

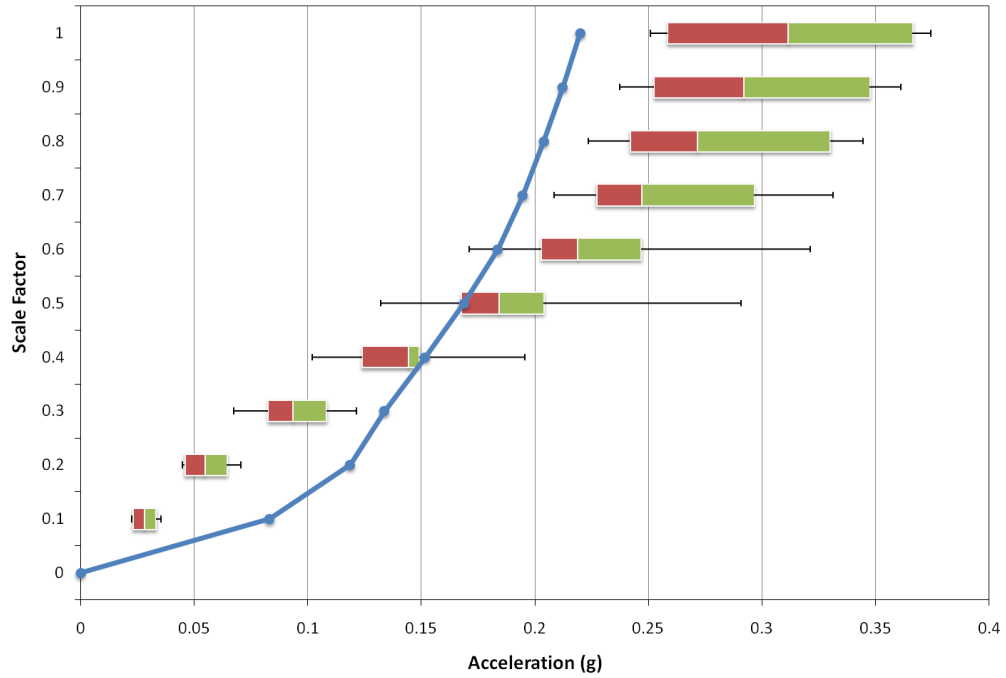


Figure 6-1: Multi-Phase System Acceleration Comparison to Baseline (1T-M50B50)

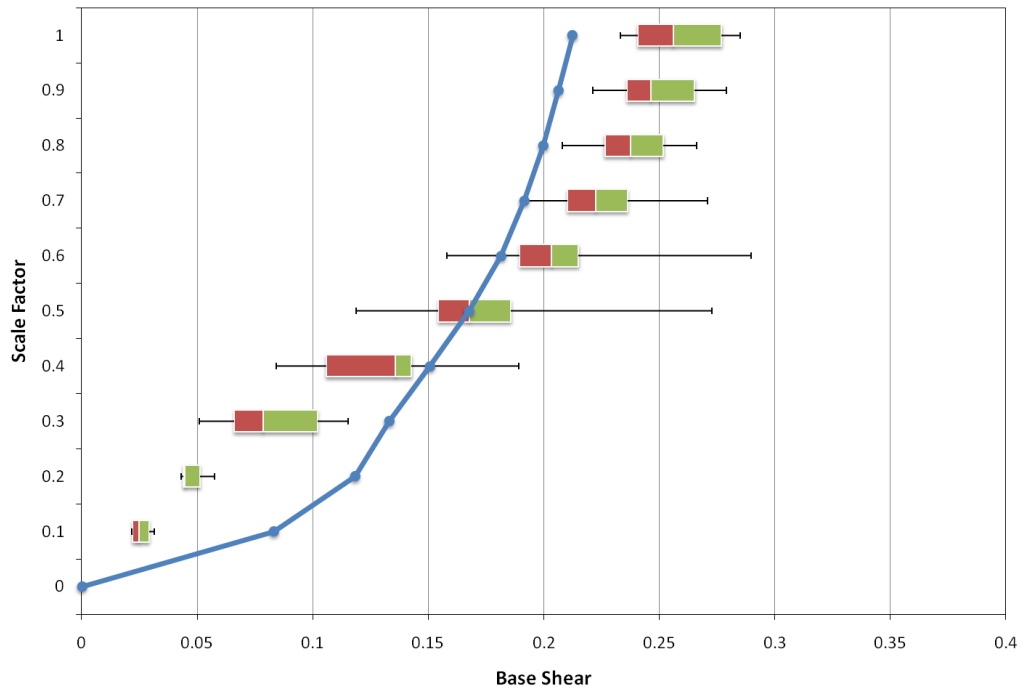


Figure 6-2: Multi-Phase System Base Shear Comparison to Baseline (1T-M50B50)

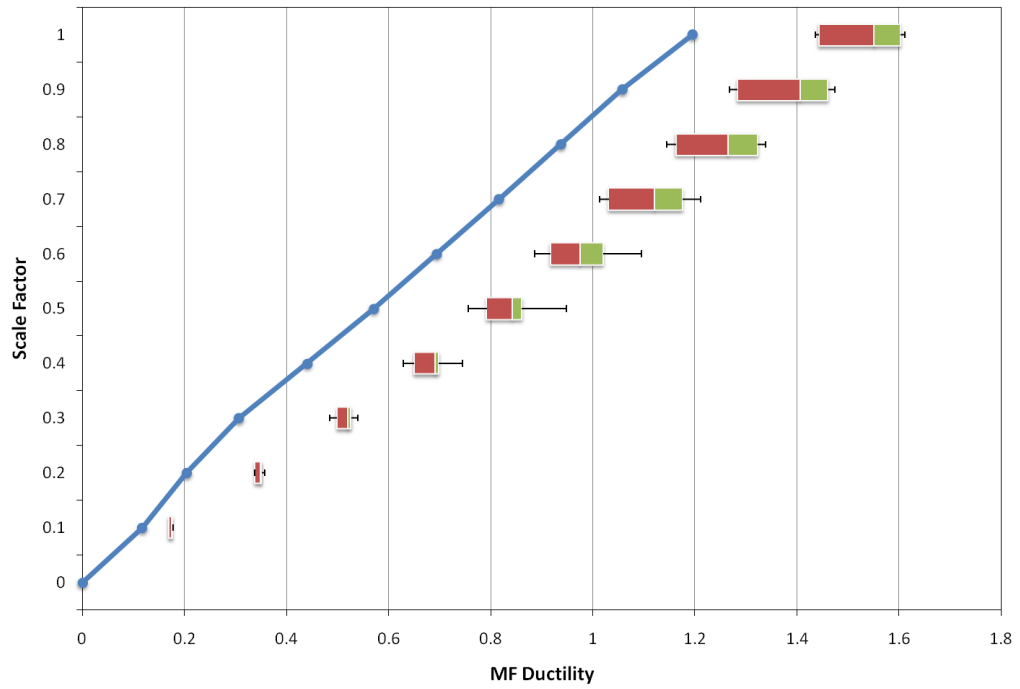


Figure 6-3: Multi-Phase System Moment Frame Ductility Comparison to Baseline (1T-M50B50)

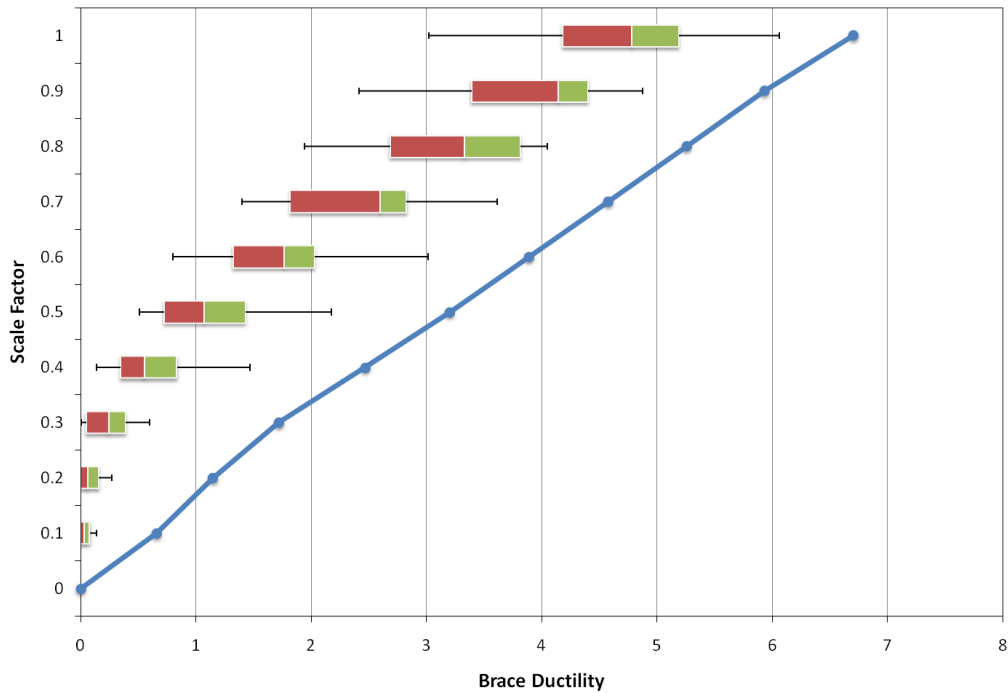


Figure 6-4: Multi-Phase System Brace Ductility Comparison to Baseline (1T-M50B50)

As seen in Figure 6-1, relative to the baseline system (solid line), poor performance was seen for the upper scale factors with 40% more acceleration for the median multi-phase system. This poor performance is probably partially due to larger second phase stiffness present once the gap is closed and yielding of the displacement device takes place. Another reason for the poor performance could also be a result of large acceleration spikes that may occur as the multi-phase systems transition from the first to second phase. These acceleration spikes were evaluated in more detail later in the study to determine if they were a controlling factor in acceleration performance of the multi-phase systems.

The mid-scale factors exhibited a tremendous amount of variability in acceleration response, depending on the system arrangement. Some systems performed better than the baselines, while others performed worse. This is due to the transition of

phases as the gap locks out and the system becomes stiffer. The most evident and convincing benefit of the multi-phase systems is present in the lower scale factors. Regardless of the multi-phase arrangement, improved performance was observed from 10% to 40% of the DBE. The supplemental damping and lower stiffness present in the initial phase of the multi-phase arrangements is probably responsible for the improved behavior.

Base shear performance for the multi-phase systems, in comparison to the baseline dual frame, was very similar to that for the acceleration performance, as seen in Figure 6-2. Relatively poor performance was seen in the upper scale factors but the systems were not as variable and median performance was only about 20% worse than the baseline system. Similar to acceleration response, the mid-scale factors showed the most variability in response due to the transition of phases. Responses for lower scale factors had very little variability and demonstrated as low as 35% of baseline shear responses in some cases.

Although the variability in moment frame ductility response was relatively low and therefore led to somewhat predictable performances, overall performance of the multi-phase systems for moment frame ductility was worse than the baseline performance across all of the scale factors. Ductility values ranged from 20% to 70% higher than the baseline ductility values, with the multi-phase systems remaining elastic up to a 60% DBE, as opposed to 80% of the DBE with the baseline system. The response is sensitive to the frame stiffness ratio and gap size pairing, but even if optimized in this regard, moment frame ductility was worse than baseline values. Although the displacement device performs extremely well in the multi-phase system, it is at a slight cost to the

performance of the moment frame. A few solutions to be discussed later could improve the moment frame integrity, while also maintaining the improved displacement device behavior.

The brace ductility performance in comparison to the performance of the baseline system is by far the most appealing aspect of the multi-phase systems. Unfortunately, this outstanding performance often comes at the cost of moment frame ductility. Every system remained elastic at 40% of the DBE, and about half of them remained elastic up to 50% of the DBE which is much better than the baseline system, which yields before 20% of the DBE. Even beyond the elastic range, brace ductility was still markedly improved in comparison to the baseline system, with median ductility values of only 70% of the baseline value at the DBE.

In conclusion, the multi-phase systems offer many advantages in comparison to the baseline dual frames. This better performance comes at the cost, though, of higher accelerations and base shears in the mid to high scale factors, and of poor moment frame ductility response. Since the displacement device is the replaceable link in the system, more investigation into limiting the moment frame ductility will need to be performed. The multi-phase system arrangements offer too many advantages in comparison to the baseline dual systems to be ignored as an option for seismic protection. The following sections describe the narrowing of a range of multi-phase systems to those that offer the best performance across all response quantities. A reduction into a smaller range of multi-phase systems will allow further research into optimizing system performance.

6.3 Comparison Between Natural Periods

Multi-phase system performance has been proven to be beneficial in some cases, but the extent of the benefits and the variability of performance across natural periods were not evident. This section describes the effort to clarify the relationship between multi-phase system performance and natural period. Figure 6-5 through Figure 6-8 show comparisons of multi-phase system responses from a 0.25 second period system and 2.5 second period system, the two extremes of the analysis.

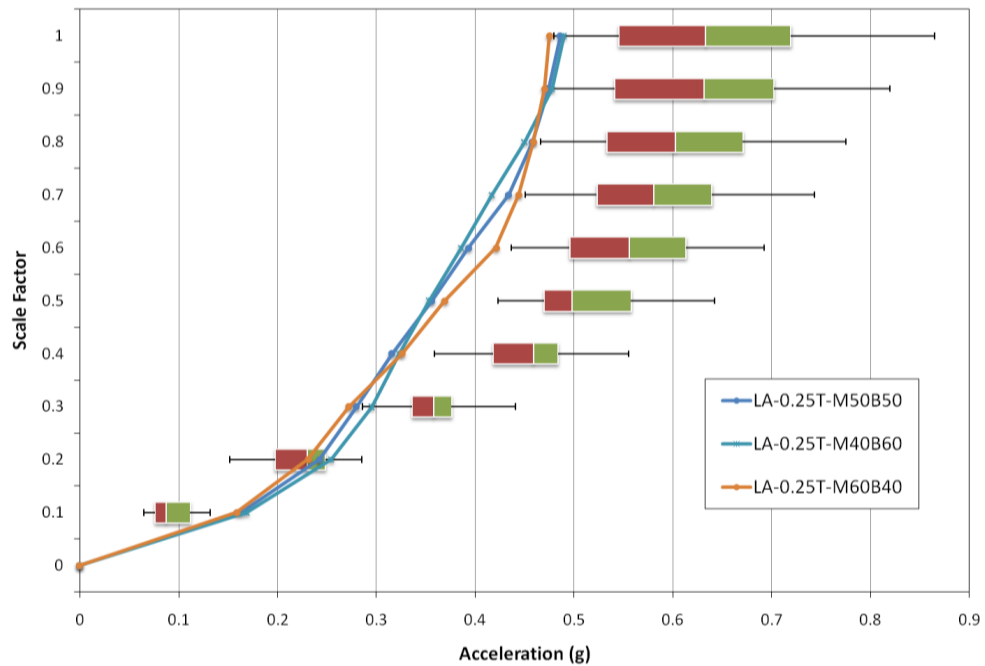


Figure 6-5: Acceleration Comparison of Multi-Phase Systems to Baselines (0.25T)

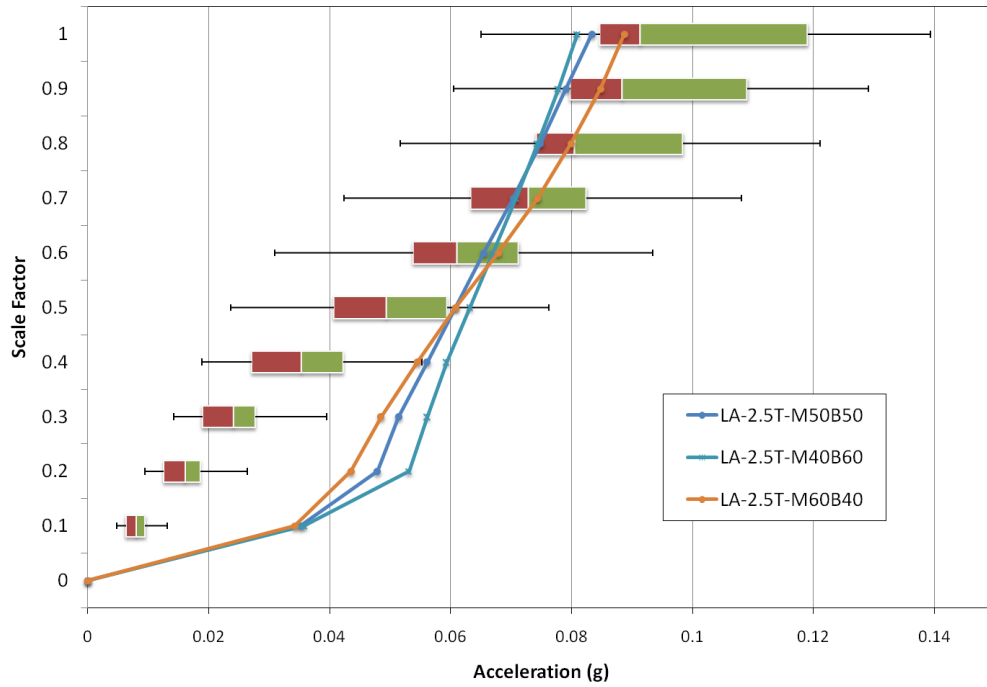


Figure 6-6: Acceleration Comparison of Multi-Phase Systems to Baselines (2.5T)

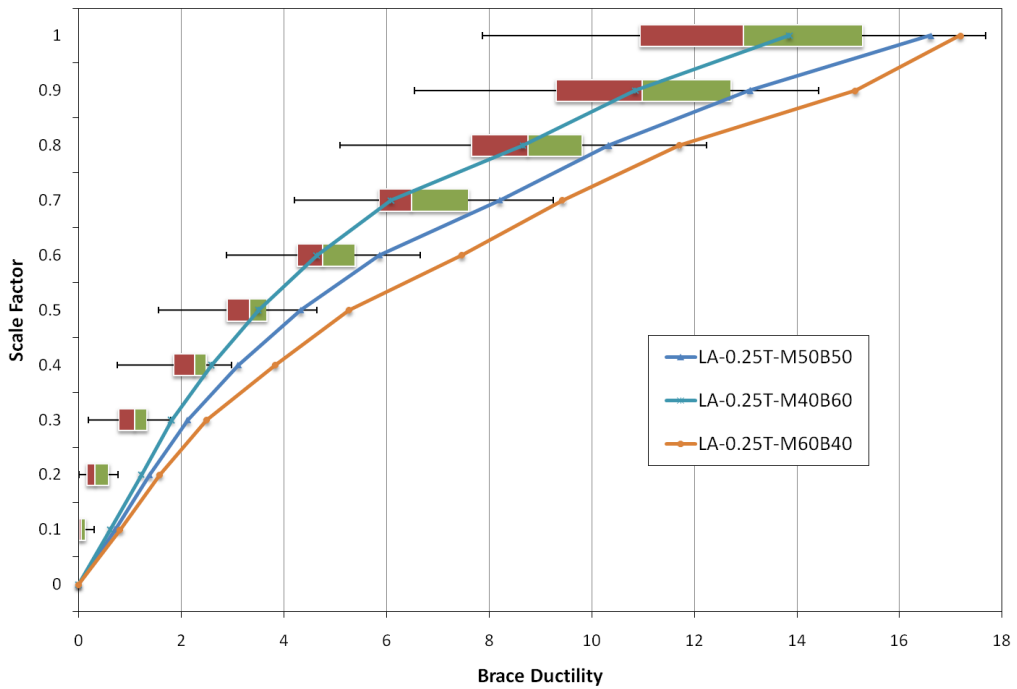


Figure 6-7: Brace Ductility Comparison of Multi-Phase Systems to Baselines (0.25T)

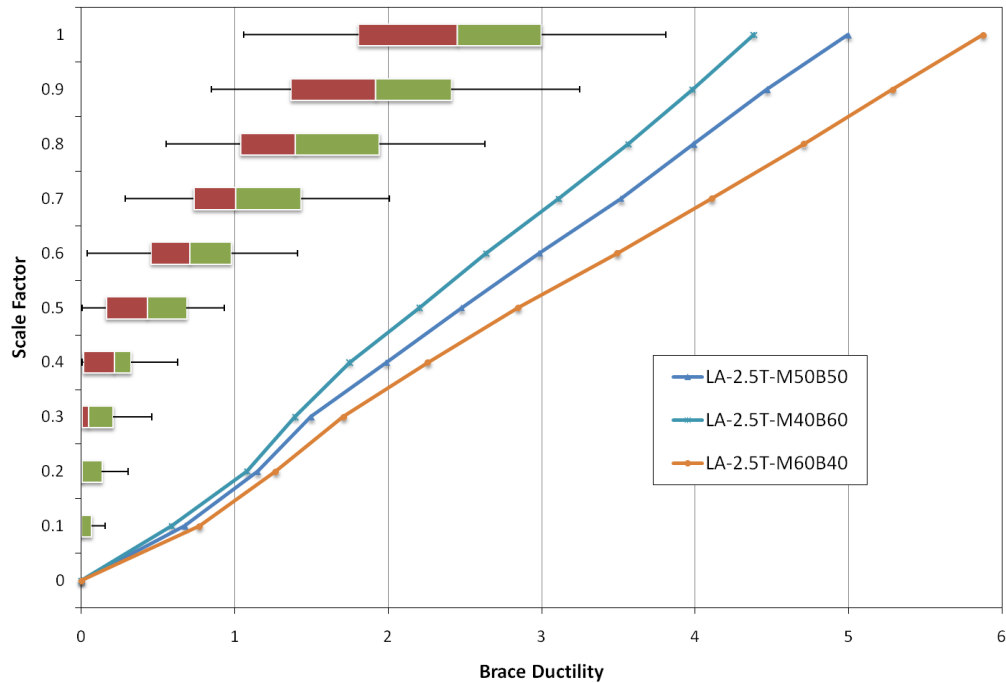


Figure 6-8: Brace Ductility Comparison of Multi-Phase Systems to Baselines (2.5T)

The acceleration performances of the 0.25 second period multi-phase systems were worse than the baseline dual system for almost all scale factors, whereas the 2.5 second system showed improved performance up to 50% of the DBE, as evident in Figure 6-5 & Figure 6-6, respectively. Similar results were observed for the brace element ductility responses for the multi-phase systems. The shorter period systems barely outperformed the baseline systems, while the longer period systems experienced up to only 30% of the baseline ductility in some cases, as shown in Figure 6-7 & Figure 6-8, respectively. These observations lead to question the validity of using multi-phase systems for shorter period systems, an issue that needs to be further investigated.

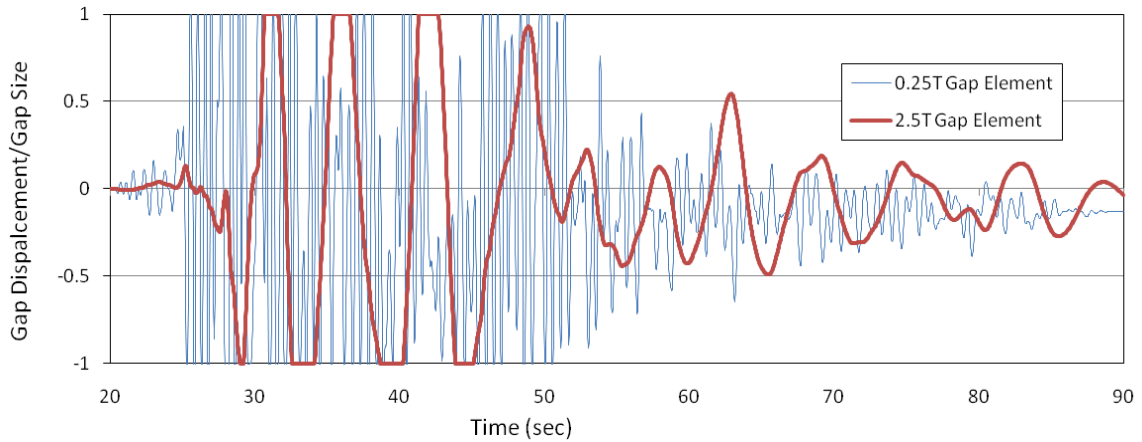


Figure 6-9: Gap Element Displacement Comparison

Figure 6-9 shows a comparison of the gap element behavior of two of the same multi-phase arrangements designed with different natural periods and subjected to the same ground motion. Each plateau represents the changing of phases as the gap element locks out and the secondary phase begins. The 0.25 second period system experiences about 50 phase transitions throughout the duration of the 90 second ground motion, compared to 8 phase changes for the 2.5 second period multi-phase system. Ultimately, the greater number of phase transitions could lead to reliability issues with repeated closing of the link and large acceleration spikes for the lower periods. Failure of the transition element could lead to catastrophic failure of the overall system, therefore the 0.25 second period systems may not be a viable option for the rest of the multi-phase system analysis. Also, overall performance of the shorter period systems did not offer many benefits in contrast to the baseline systems making the multi-phase systems an undesirable option, especially considering the higher costs associated with the fabrication and design of the devices. Further research could provide a solution for multi-phase behavior in shorter period systems but that is beyond the scope of this study.

Performance of the 0.5 and 1.0 second period systems were statistically different than the 0.25 second period systems for all response quantities. Overall results were also observed to be much better than 0.25 period systems; therefore it was determined to include the 0.5 and 1.0 period systems in the rest of the analysis.

6.4 Comparison Between Multi-Phase Systems

With the scope of the multi-phase systems reduced into a reasonable range, it became important to establish selection criteria for the systems. Because there are four response quantities of interest, good performance in one was often offset by poor performance in another. Setting criteria for the selection of the better-performing systems created a consistent, systematic way of analyzing the data.

The first, and most important criteria, is moment frame protection. As stated earlier, the goal of a multi-phase system is to efficiently dissipate energy as well as to limit yielding to a replaceable element. Damage to the moment frame requires expensive and time-consuming repairs after an event. Another important criterion is good performance in the low-to-mid scale factors for the acceleration and base shear responses. Protection of acceleration and shear sensitive elements in the low-to-mid scale factors could mean immediate occupancy after an event. Lastly, the BRB ductility performance must be checked. Most of the multi-phase systems showed great performance in this regard, remaining elastic anywhere from 30%-70% of the design basis earthquake. Similar to the previous criterion, protecting a displacement-dependent device in the low-to-midscale factors would allow immediate occupancy after an event.

Although this type of performance is ideal in regards to occupancy, as the ground motion intensity increases, it becomes important to strike a balance between brace ductility and other response quantities. Higher brace ductility values in the mid-to-upper scale factors would be acceptable because of the extensive energy dissipation capabilities and the ability to replace the device after an event.

This section looks at each system arrangement and follows the selection criteria outlined above in order to identify the better performing systems. If a system demonstrated potential but was lacking in a certain response quantity, solutions were investigated and the results are discussed. The 1 second natural period systems were analyzed as a representative set for this next section but observations made were similar for each natural period. Generally speaking, as natural period increased, the performance of the multi-phase systems increased.

6.4.1 HPCD Analysis

The HPCD systems described in Table 3-1 were the first to be analyzed. Figure 6-10 illustrates the system performance relative to the baseline systems.

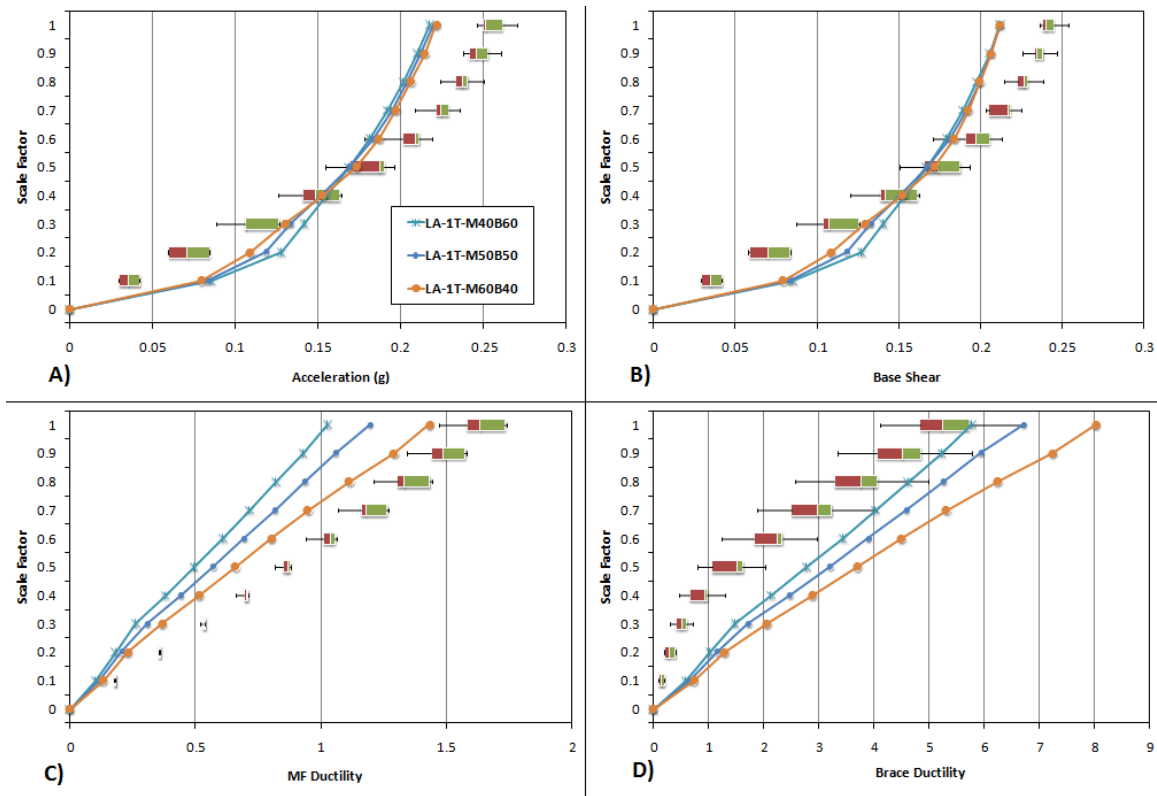


Figure 6-10: HPCD 1T Comparison to Baselines

Median moment frame ductility was over 30% more than the baseline response for each scale factor, but was still reasonable at 1.6 times the yield displacement at the DBE. The plots show that yielding of the moment frame would be expected at about 60% of the DBE, as opposed to 80% to 100% of DBE for the baselines. Acceleration and base shear responses were much better for the low scale factors when compared to the baseline systems. A median response of 50% of the baseline response for the 0.1 and 0.2 scale factors can be attributed to the significant supplemental damping provided by the high-damping rubber. Greater responses than the baseline responses were exhibited at high scale factors, but only by about 10%-15%. Brace behavior remained elastic up to

almost 50% of the DBE, and far exceeded baseline performance in the upper scale factors.

In regards to the system-to-system comparisons, Figure 6-12 through Figure 6-14 demonstrate the relationships for the four response quantities. The moment frame ductility presented in Figure 6-11 shows relatively no difference in response until about 40% of the DBE, and then a slight dispersion is noticed. Regardless of the gap size, the larger system ratio (M60B40) performed the worst out of all the systems. As one would expect, the larger gap sizes also performed the worst. Moment frame ductility values were very close for the lower scale factors and showed only a 20% difference from the worst performer to the best performer for the upper scale factors. The M40B60 paired with the 0.6 gap size was the best overall performer in terms of moment frame ductility.

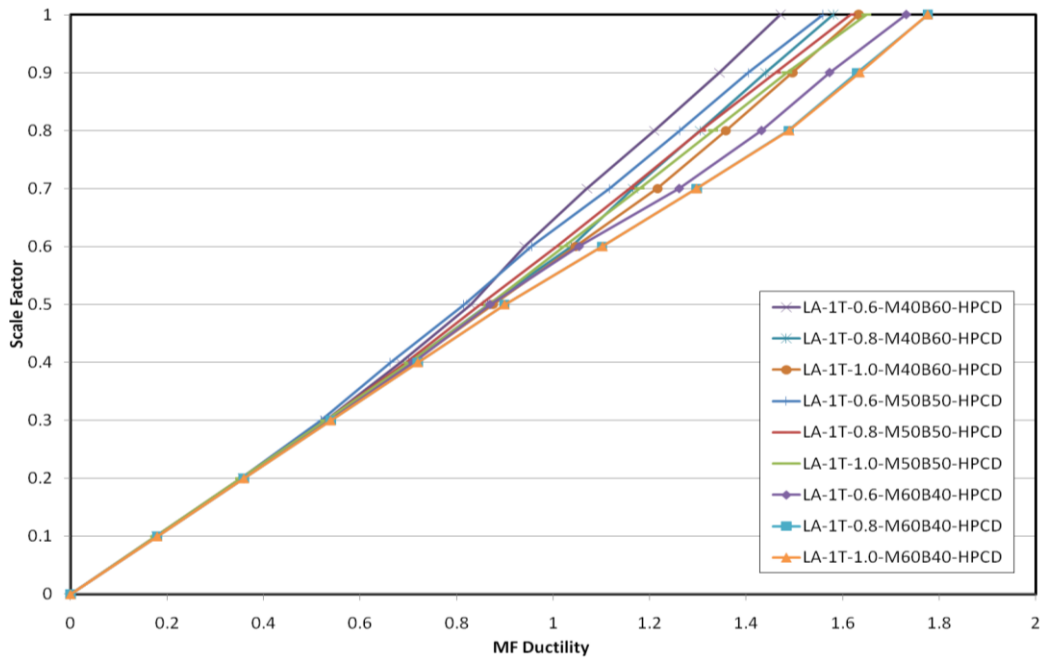


Figure 6-11: HPCD 1T Moment Frame Ductility

Acceleration and base shear responses were very similar across all of the scale factors, as shown in Figure 6-12 and Figure 6-13. For the lower scale factors, the lower system ratio (M40B60) performed the best due to the flexibility present in the first phase. As the scale factor increased, the higher system ratios became the more attractive option, probably due to a lower stiffness present in the second phase of the control device. The dispersion between the responses for the various systems for the upper scale factors is not very significant, exhibiting approximately a 10% difference between the best and worst performers for acceleration. As far as gap size is concerned, the larger the gap, the better the performance across all of the scale factors. This is probably due to a longer first phase duration which allows more damping from the high-damping rubber. Overall, the best performer in regards to acceleration and base shear is the M40B60, paired with the 1.0 gap size.

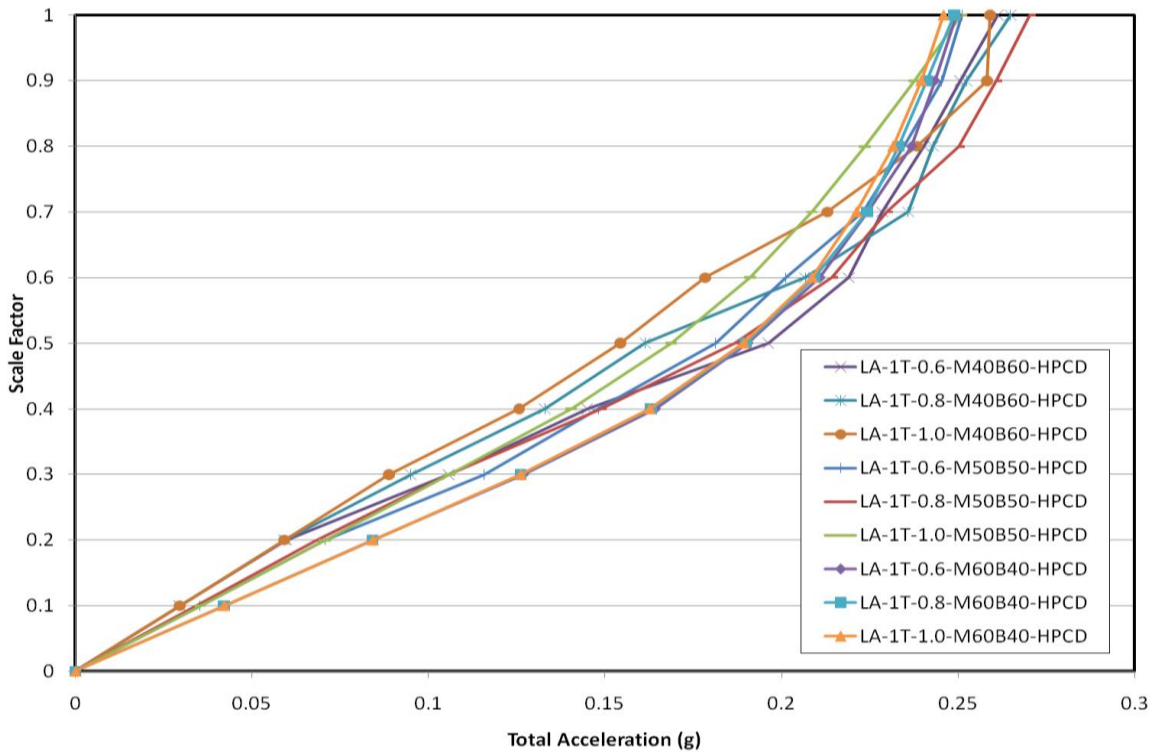


Figure 6-12: HPCD 1T Acceleration Response

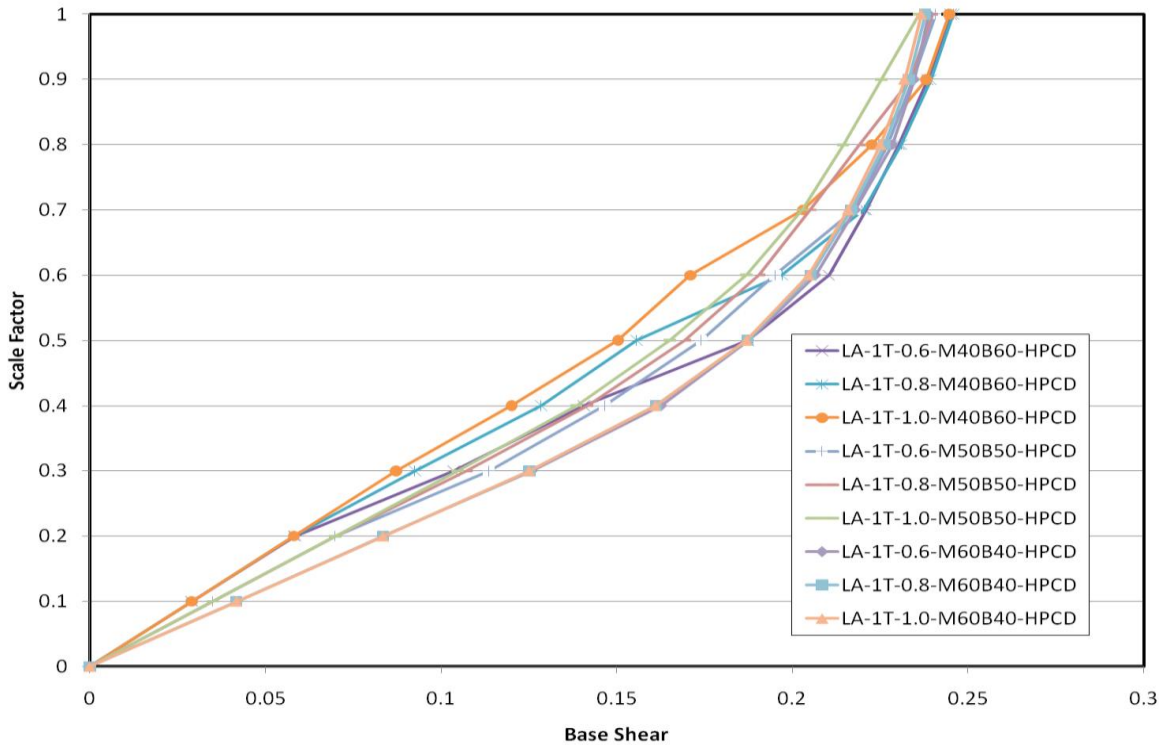


Figure 6-13: HPCD 1T Base Shear Response

Lastly, the brace ductility behavior exhibited much more dispersion between systems than the other response quantities, with over 70% difference in response in the upper scale factors. Yielding occurs anywhere from 40% to 60% of the DBE, depending on the system ratio and gap size combination. The smaller system ratios performed the best out of all of the systems. As the gap size increased, the brace ductility decreased, due to less energy dissipation required from the hysteretic braces. Combining the observations regarding system ratios and gap sizes, the M40B60 system with the 1.0 gap size is the best performer regarding brace ductility of the group of HPCD systems for all scale factors.

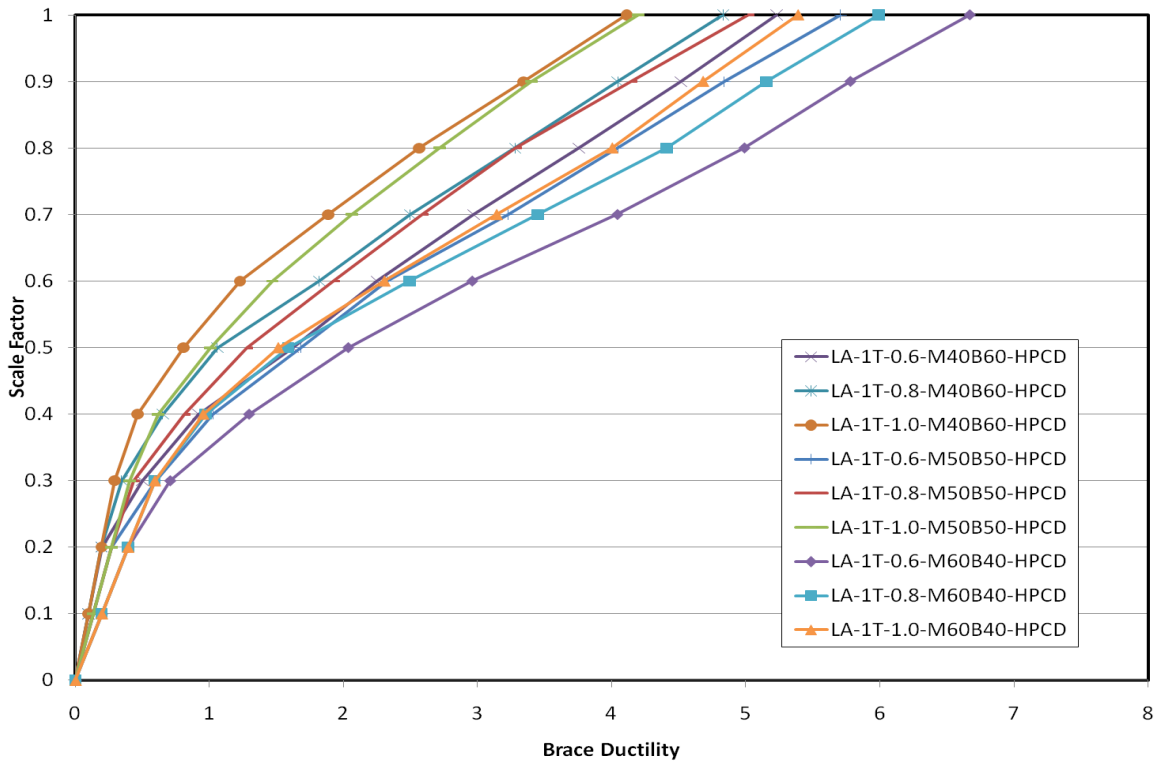


Figure 6-14: HPCD 1T Brace Ductility

Notwithstanding a slight compromise in the moment frame ductility (less than 10% of the best performing system), the M40B60 system with the 1.0 gap size is clearly the best performer for the HPCD systems. The large gap size allows for more damping in the first phase and a significant improvement in response in the low-to-mid scale factors in comparison to the baseline system. The only drawback of the system is the yielding of the moment frame at 60% of the DBE, as opposed to yielding at 100% of the DBE for the baseline system (M40B60). A solution to address moment frame ductility is a must for all of the HPCD systems before they are completely viable for implementation.

6.4.2 HPCD-VFD Analysis

Many of the observations made for the HPCD system would be expected to be the same for the HPCD-VFD systems. Any differences would be attributed to higher damping present in the VFD relative to the high-damping rubber, and the lack of stiffness present in the first phase of the VFD devices. Figure 6-15 presents the HPCD-VFD system responses compared to the baseline system responses for a system period of 1 second.

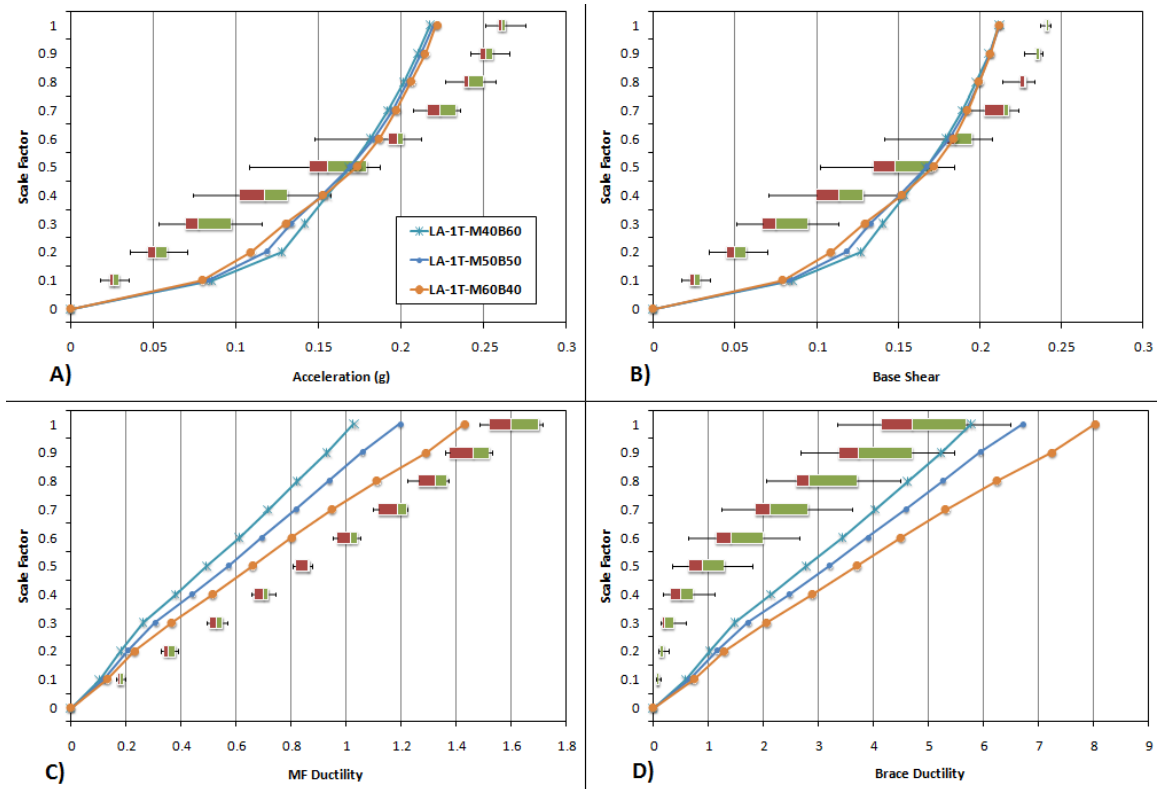


Figure 6-15: HPCD-VFD 1T Comparison to Baselines

Similarly to the HPCD systems, the median moment frame ductility was over 30% more than the baseline response at the DBE but was still reasonable at about 1.6 times the yield displacement. Yielding of the moment frame was exhibited at about 60% to 70% of the DBE as opposed to 80% to 100% of DBE for the baselines. Acceleration

and base shear responses were much better in the low-to-mid scale factors when compared to the baseline systems. Although there was a large dispersion for the lower scale factors, the median acceleration and base shear responses did not become larger than the baseline systems until about 60% of the DBE. The higher scale factors exhibited a higher response than the baselines but only by about 15%-20%. Brace behavior remained elastic up to almost 60% of the DBE and far exceeded baseline performance for the upper scale factors.

Also, similar to the HPCD systems, the moment frame ductility (Figure 6-16) shows relatively no difference in response until about 40% of the DBE, and then a slight dispersion is noticed. Regardless of the gap size, the larger system ratio (M60B40) performed the worst out of all the systems. Similar to the HPCD systems, the larger gap sizes also performed the worst but the difference was small for each system ratio. Moment frame ductility values were very close in the lower scale factors and showed only a 15% difference from the worst performer to the best performer in the upper scale factors. Very little difference between the M40B60 systems was noticed across all the scale factors and each of those systems could be considered the best performers. The M50B50 system with the smallest gap size also offered comparable moment frame protection.

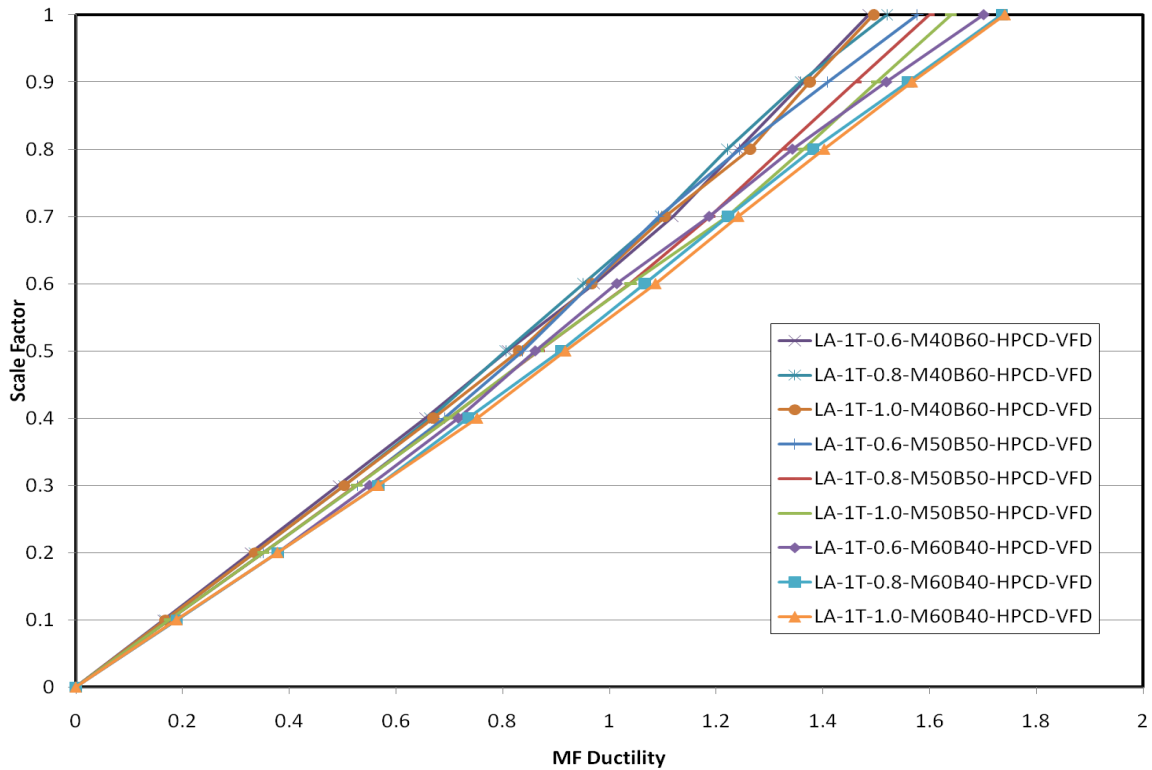


Figure 6-16: HPCD-VFD 1T Moment Frame Ductility

Acceleration and base shear responses were very similar across all of the scale factors (Figure 6-17 & 6-18). The lower system ratio (M40B60) performed the best due to the flexibility present in the first phase. The dispersion between the systems in the upper scale factors is not very significant, exhibiting approximately a 10% difference between the best and worst performers for acceleration, and virtually no difference at the DBE for base shear response. As far as gap size goes, the larger the gap, the better the performance across all of the scale factors. The 0.6 gap size consistently performed the worst out of the systems most likely due to the relatively small amount of damping in the first phase compared to that for the larger gap size. The VFD provides very little stiffness to the system and therefore allows the transition into the second phase to happen

quicker with smaller gap sizes. This is illustrated in Figure 6-19, in which the gap displacement response histories are presented for two M50B50 HPCD-VFD systems with different gap sizes. The smaller gap size goes through over 10 phase transitions, as opposed to 5 transitions for the larger gap size. Overall, the best performer in regards to acceleration and base shear is the M40B60, paired with the 1.0 gap size.

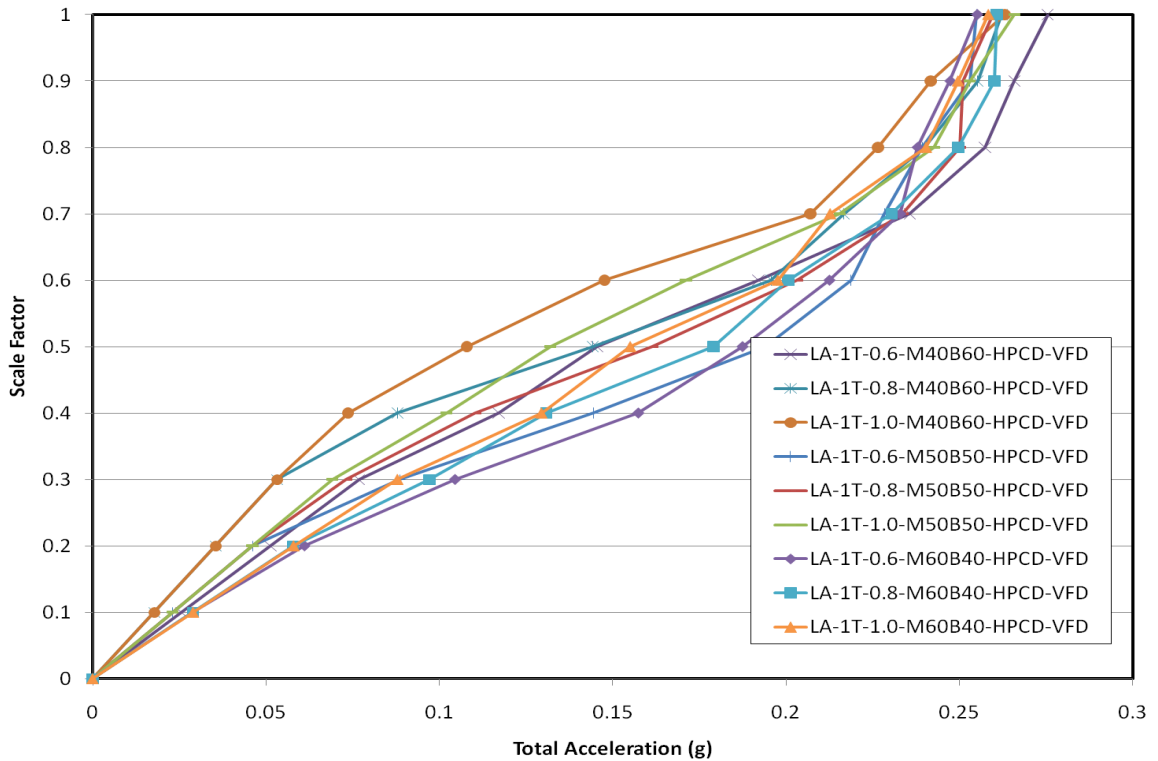


Figure 6-17: HPCD-VFD 1T Acceleration Response

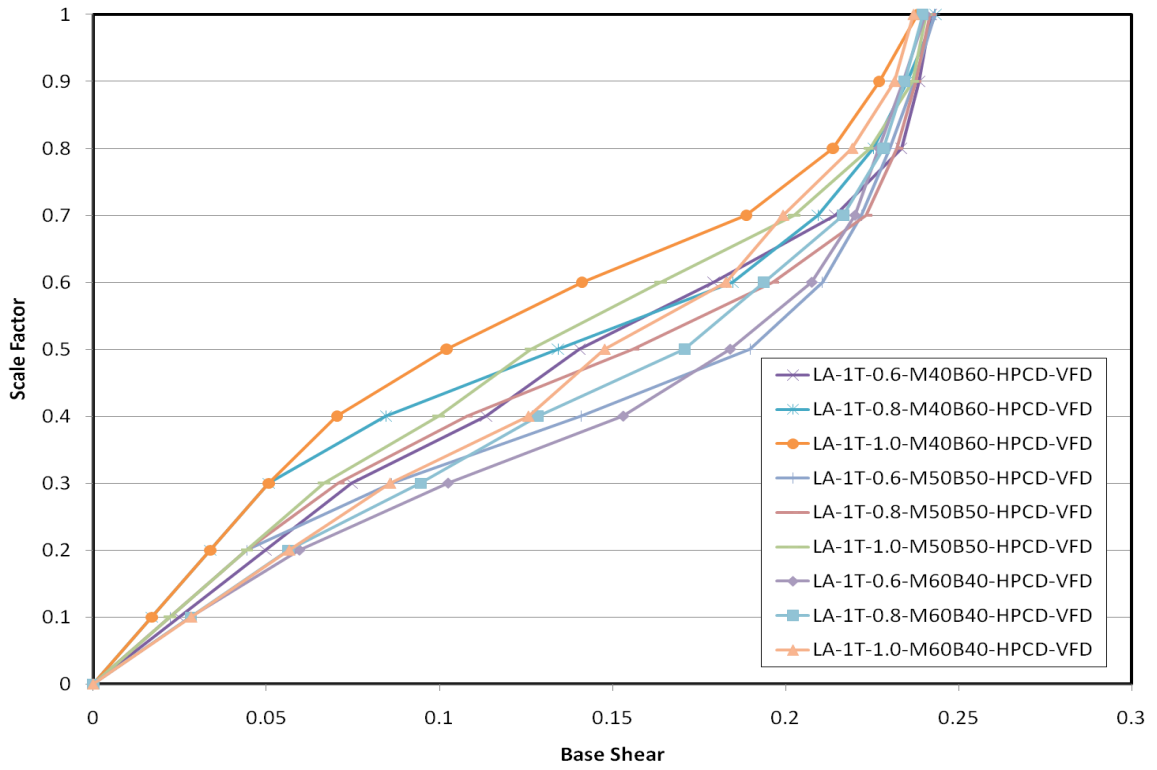


Figure 6-18: HPCD-VFD 1T Base Shear Response

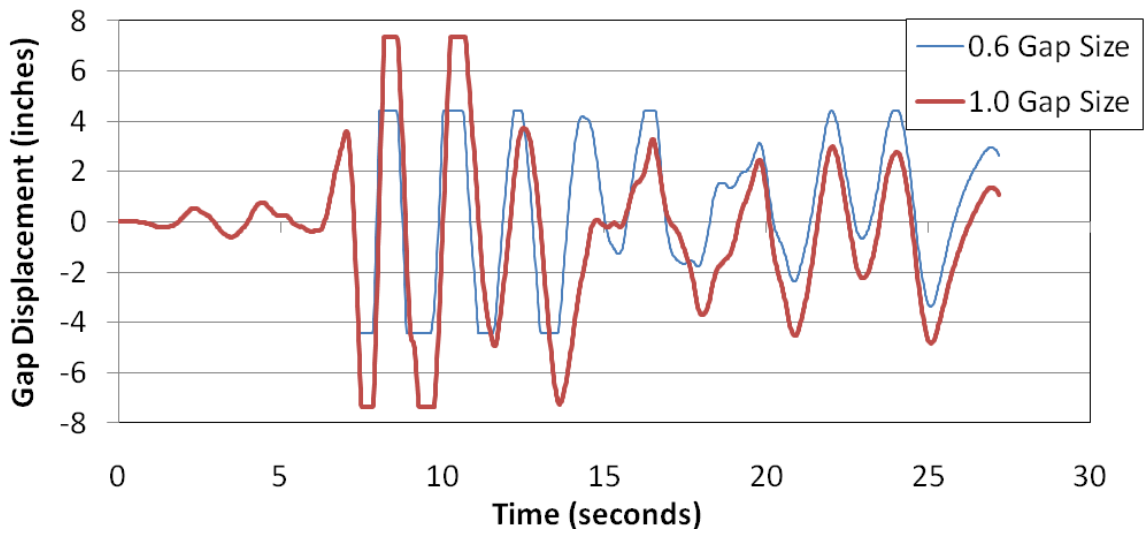


Figure 6-19: Gap Element Comparison for M50B50-1T (DZC270 DBE)

Similar to the HPCD system response, the brace ductility behavior for the HPCD-VFD systems exhibited much more dispersion than the other response quantities, with over 90% difference in response for the upper scale factors. Yielding occurred anywhere from 40% to 70% of the DBE, depending on the system ratio and gap size combination. The smaller system ratios performed the best out of all of the systems. As the gap size increased, the brace ductility decreased due to less energy dissipation required from the hysteretic braces. Similar to the HPCD systems, the M40B60 system with the 1.0 gap size was the best performer out of the group of HPCD-VFD systems for all scale factors regarding brace ductility.

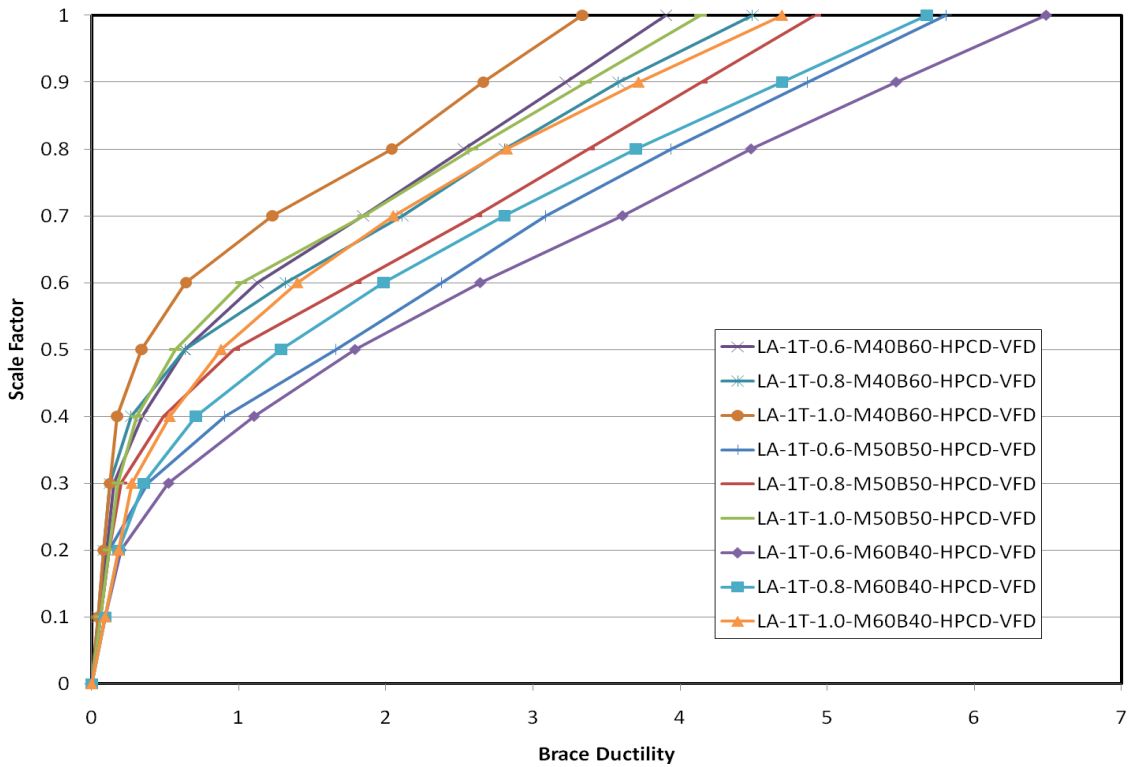


Figure 6-20: HPCD-VFD 1T Brace Ductility

The M40B60 system with the 1.0 gap size is clearly the best performer for the HPCD-VFD systems. The large gap size allows for more damping in the first phase, and a significant improvement in response in the low-to-mid scale factors when compared to the same responses for the baseline system.

Similar to the HPCD system, the only drawback of the M40B60 HPCD-VFD system is the yielding of the moment frame at 70% of the DBE, as opposed to 100% of the DBE for the baseline system (M40B60). One possible solution to this issue is to add more damping to the system, an option that is feasible for a VFD. The systems with the smallest gap sizes were analyzed again with a damping ratio equal to 25% including inherent damping, as opposed to the 15% value used in the original models, to see if there was a significant increase in performance (Figure 6-21). Improved performance was seen across all response quantities, but only approximately a 10% improvement in moment ductility performance was realized. More significant improvements were seen in other response quantities, but the extra costs associated with a higher damping ratio may not be worthwhile, especially since the moment frame performance wasn't significantly improved. Other solutions for moment frame protection need to be investigated.

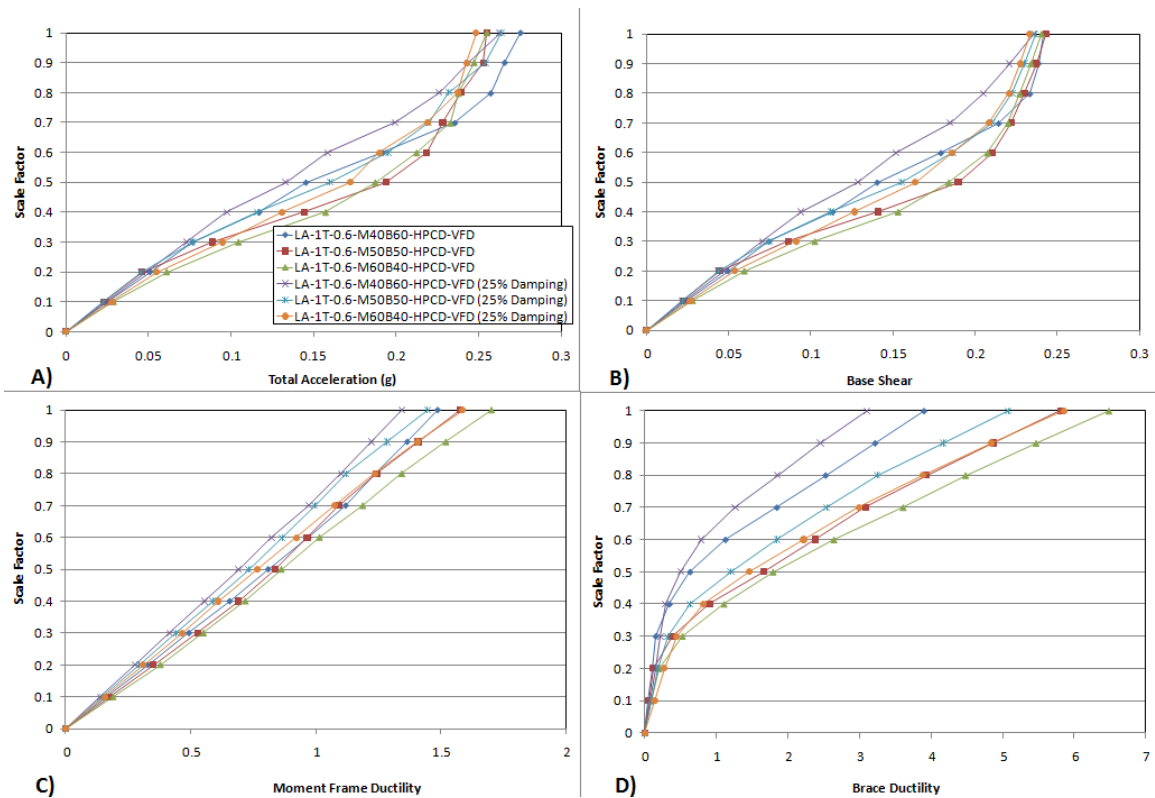


Figure 6-21: HPCD-VFD Damping Ratio Comparison

Although the performance of the HPCD and HPCD-VFD systems were very similar, there were some differences. Figure 6-22 shows a comparison of responses for the two best systems (M40B60 with 1.0 gap size) from both series configurations. The HPCD-VFD outperformed the HPCD systems for all response quantities. Moment frame ductility response was about 10% better in the upper scale factors, yielding at 70% of the DBE, as opposed to yielding at 60% of the DBE with the HPCD system. Acceleration response was up to 70% better for mid-scale factors. The brace remained elastic up to 70% of the DBE as opposed to 60% for the HPCD system. These results suggest that the damping capability is the most important aspect of the series configurations.

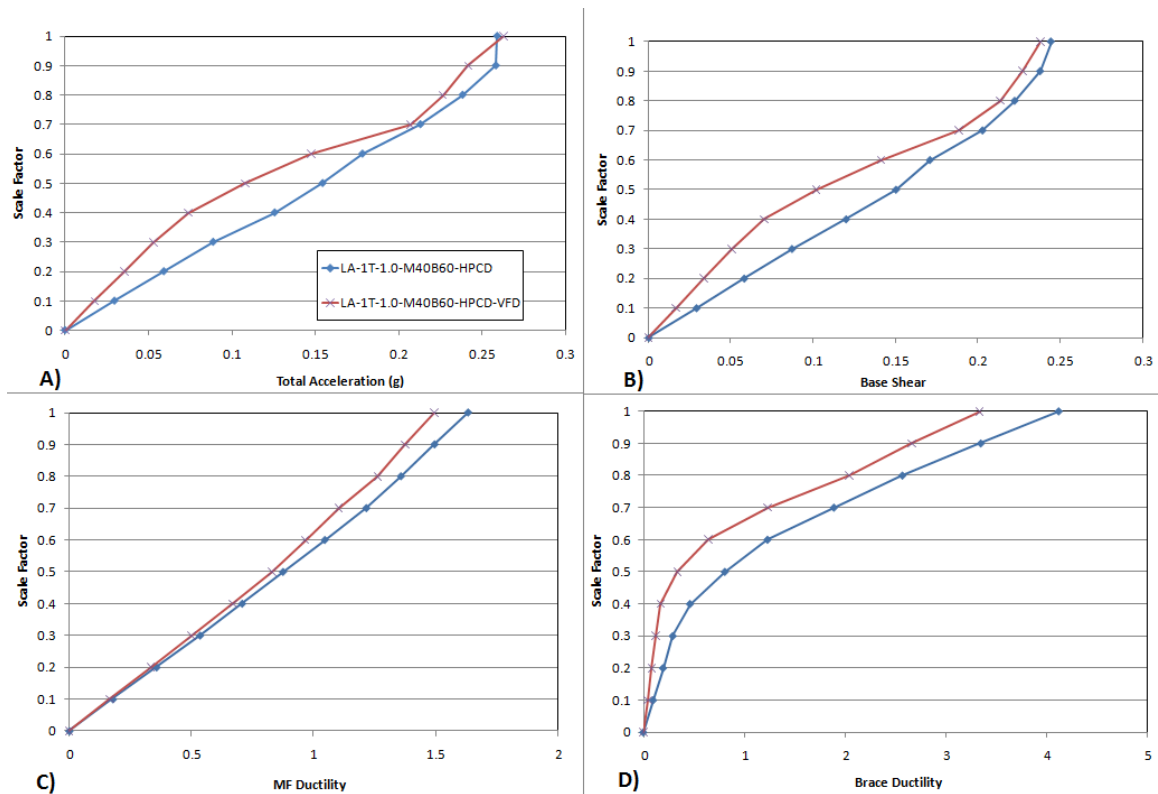


Figure 6-22: HPCD vs. HPCD-VFD (M40B60-1.0-1T)

6.4.3 HYFR Analysis

Although the series systems needed to be fundamentally analyzed, their behavior was somewhat intuitive. The parallel systems add another element to the multi-phase behavior that may not be as intuitive, but could be potentially advantageous. The damping present throughout the duration of the ground motion offers both positive and negative attributes that are described in the HYFR and HYFR-VFD sections.

The HYFR performance compared to baseline performance is presented in Figure 6-23. Slightly better than the two series systems, the median moment frame ductility at the DBE was only about 15% more than the baseline response, measuring approximately 1.4 times the yield displacement. From the plot it can be seen that yielding of the

moment frame would be expected at about 70% to 80% of the DBE, as opposed to 80% to 100% of DBE for the baselines. Acceleration and base shear responses were much better for the lower factors when compared to the baseline systems. A large variability in acceleration in the mid-to-upper scale factors suggests that HYFR systems are more sensitive to system ratio and gap size than the series systems. The median acceleration response is much larger than the baseline response for the upper scale factors, up to over 60% larger. Similar to the series systems, the HYFR brace ductility behavior remained elastic up to almost 60% of the DBE and far exceeded baseline performance for the upper scale factors.

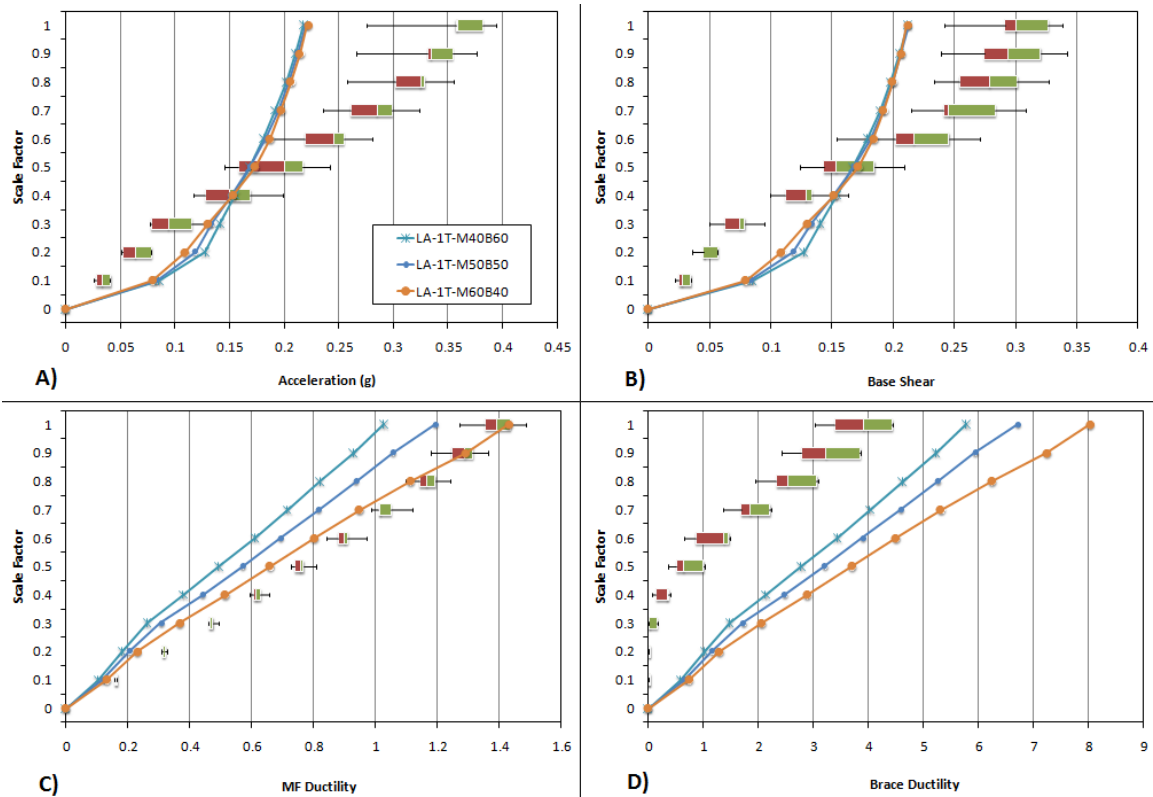


Figure 6-23: HYFR 1T Comparison to Baselines

Data for moment frame ductility for the various HYFR systems, presented in Figure 6-24, shows relatively no difference in response until about 60% of the DBE, and then a slight dispersion is noticed. Regardless of the gap size, the larger system ratio (M60B40) performed the worst out of all the systems. The larger gap sizes also performed the worst but the difference was small for each system ratio. The two best performers were the M40B60 and M50B50 systems with the 0.6 gap size, but the variance between the best and worst performers was less than 15%.

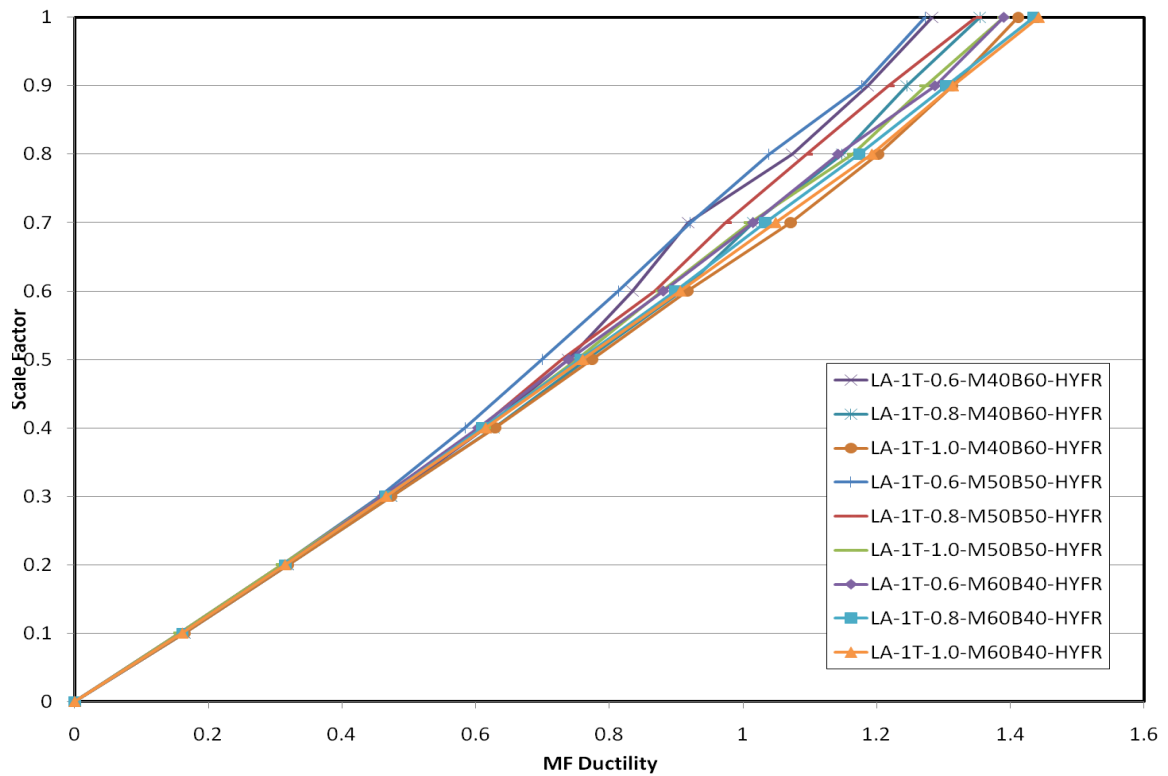


Figure 6-24: HYFR 1T Moment Frame Ductility

Acceleration and base shear responses showed a large amount of variability across all of the scale factors, especially the base shear response (Figure 6-25 & Figure

6-26). Unlike the series systems, the acceleration and base shear responses differed slightly for a system-to-system comparison. In regards to acceleration, the lower system ratios performed the best throughout all scale factors. Base shear performance was the best for the lower-to-mid scale factors with the lower system ratio (M40B60), but this performance trend was reversed in the upper scale factors. Similar to the series systems, the largest gap size allowed for better response regarding both acceleration and base shear.

Because of the variability in response and difference between acceleration and base shear, it is difficult to pick the best overall system for this selection criterion.

Although not the best performing system at all times, the M50B50 system with a 1.0 gap size offers the best overall performance.

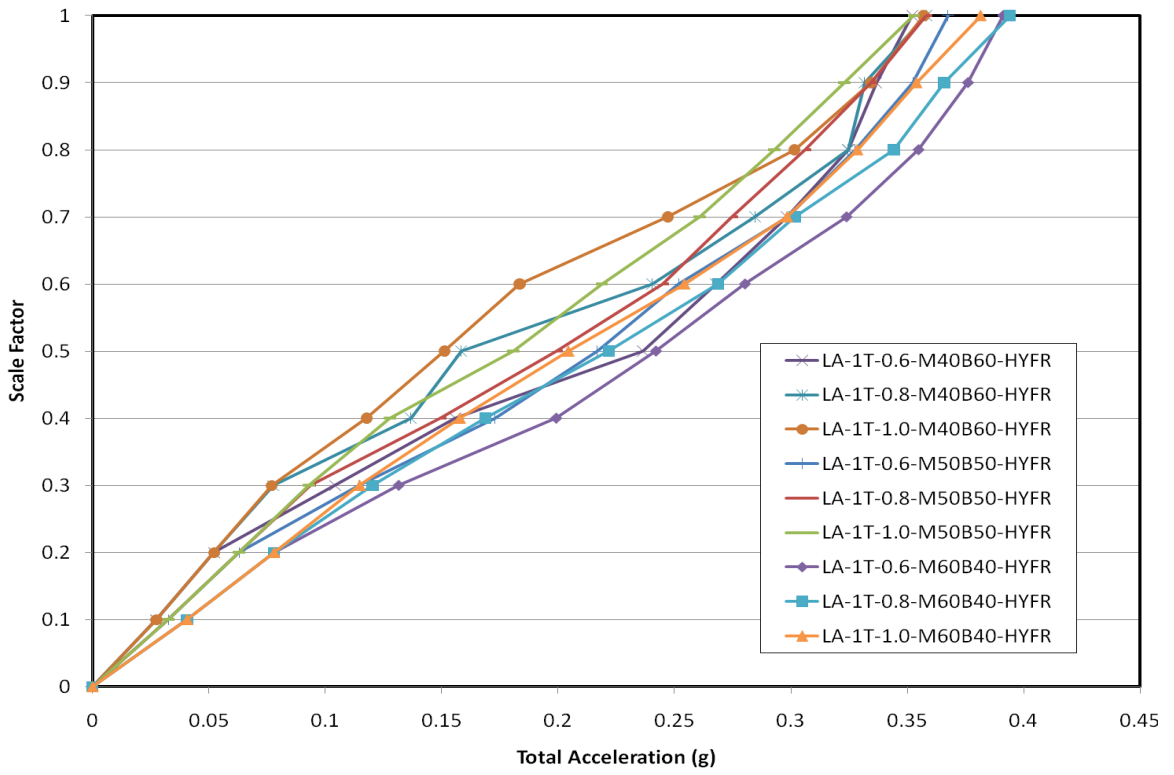


Figure 6-25: HYFR 1T Acceleration Response

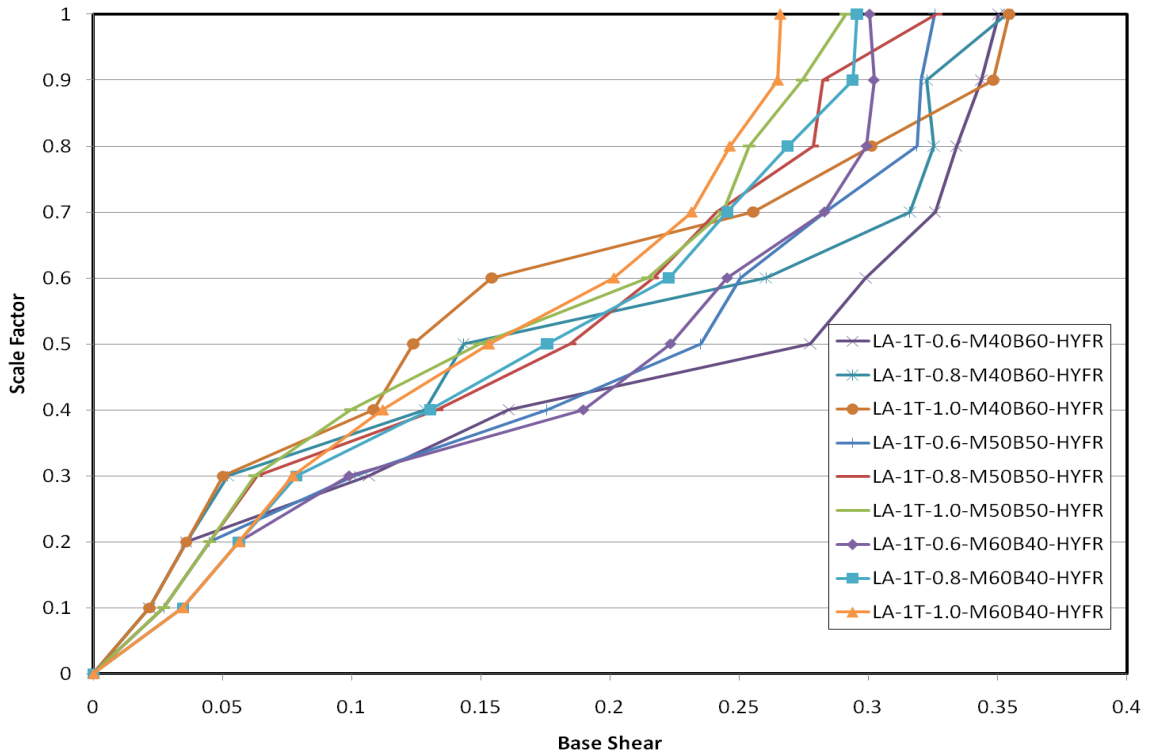


Figure 6-26: HYFR 1T Base Shear Response

The brace ductility response, presented in Figure 6-27, showed a significant amount of dispersion through the mid-to-upper scale factors. Yielding occurred anywhere from 50% to 70% of the DBE, depending on the system ratio and gap size combination. The brace ductility performance is largely dependent on the gap size, with the largest gap sizes performing the best. The performance was much less dependent on the system ratio, although the M50B50 system showed a slightly better response for all three gap sizes. All three system ratios with the largest gap size would be a viable option in regards to brace ductility, with yielding delayed beyond 60% of the DBE.

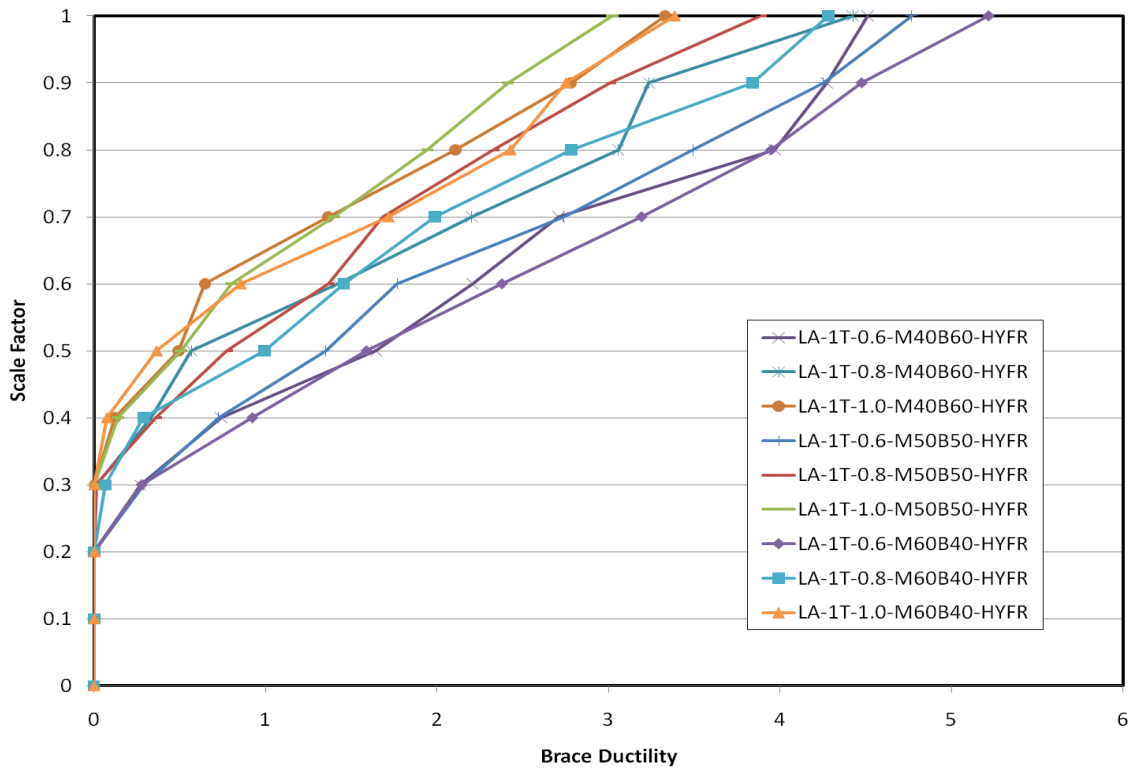


Figure 6-27: HYFR 1T Brace Ductility Response

With a slight sacrifice of moment frame ductility (less than 10%), the M50B50 system with a 1.0 gap size would be the most viable option for a HYFR system. The large gap size allows for significant damping for the lower scale factors. Once again, the major drawback of the system is the moment frame ductility response for the upper scale factors. In comparison to the series systems, moment frame ductility is significantly better but far from ideal. Further solutions need to be investigated for moment frame behavior in the HYFR systems as well.

To demonstrate the differences in responses between the HPCD and HYFR arrangements, a comparison between the two better-performing high-damping rubber systems was made (Figure 6-28). Performance varies across the different response

quantities without a clear advantage for either system. The parallel system offers slightly more moment frame protection in the mid-to-upper scale factors but still yields at 70% of the DBE. Acceleration and base shear responses are very similar for the lower scale factors but the HPCD system has an advantage for the upper scale factors. Brace ductility responses are fairly close, but the HYFR system offers slightly more brace protection across all scale factors. An argument could be made in favor of parallel or series arrangements, but the differences may become clearer after the analysis of the HYFR-VFD systems.

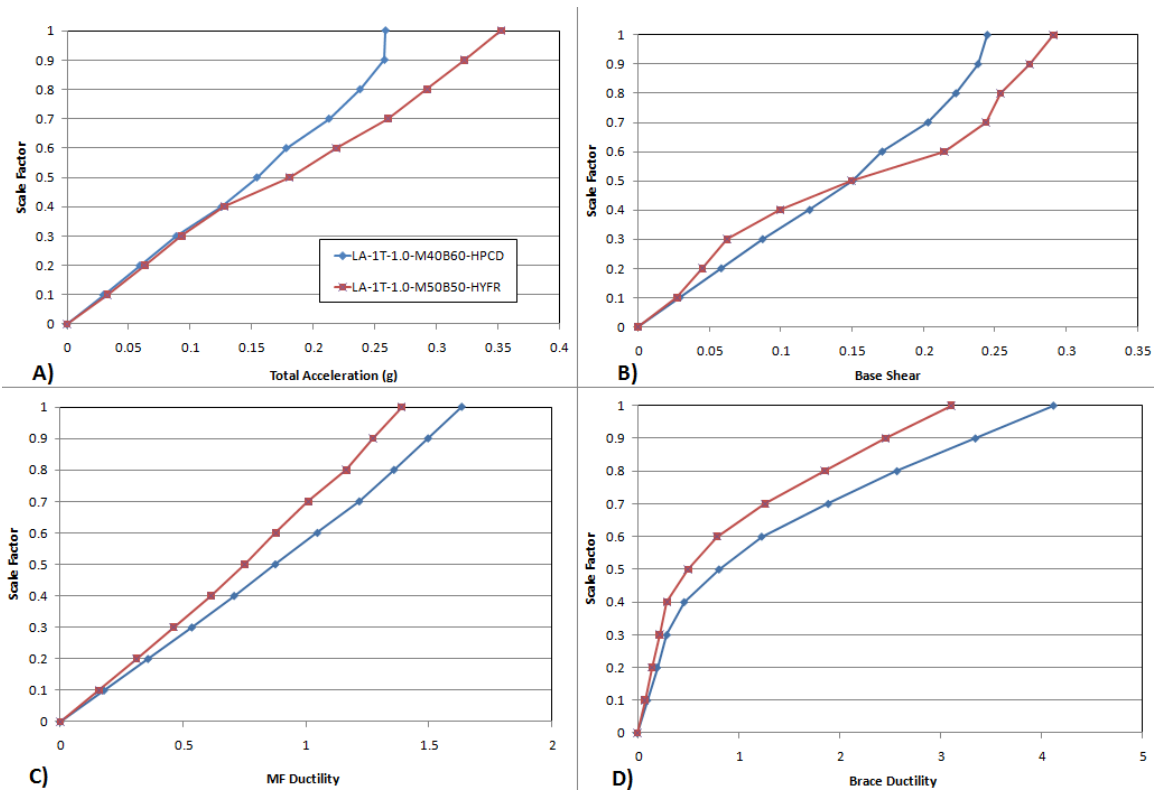


Figure 6-28: HPCD vs. HYFR Performance

6.4.4 HYFR-VFD Analysis

With the HPCD-VFD clearly performing better than the HPCD, as described earlier, the HYFR-VFD offered an intriguing final option for the multi-phase devices. A comparison of the HYFR-VFD system responses to the baseline responses is shown in Figure 6-29.

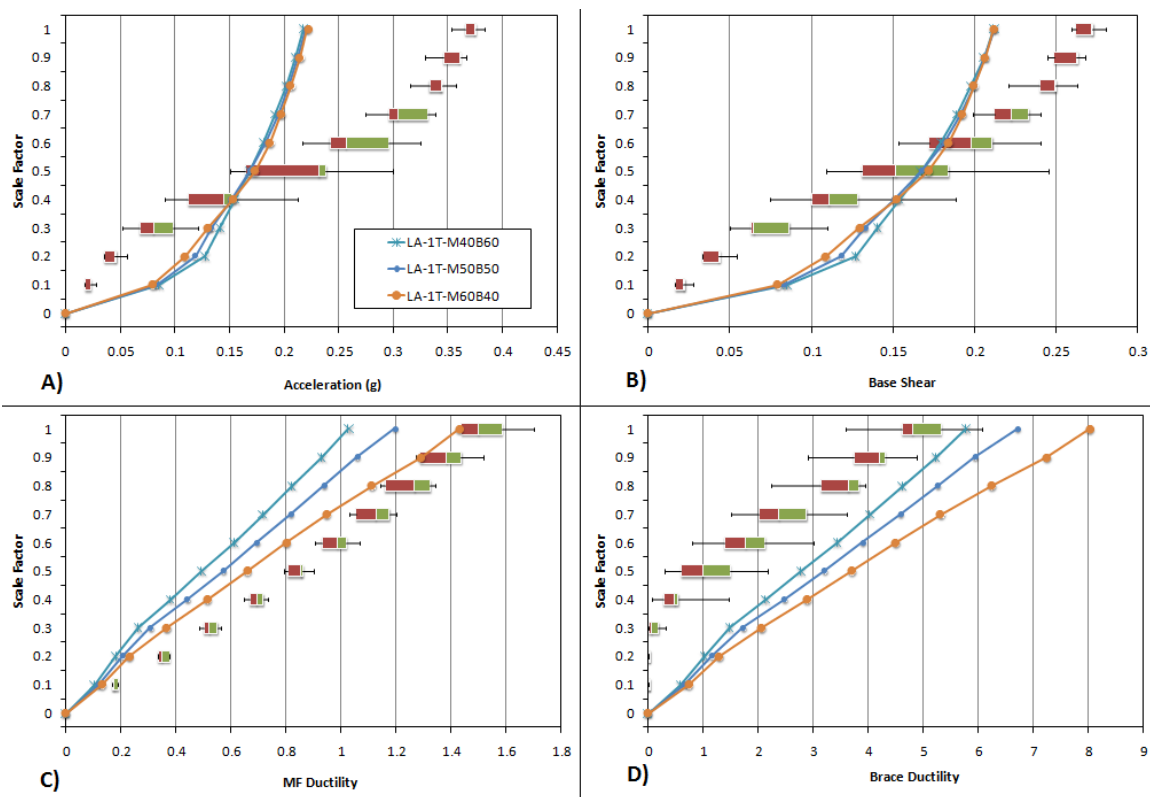


Figure 6-29: HYFR-VFD Comparison to Baselines

The median moment frame ductility was over 20% more than the baseline response at a ductility of about 1.5 times the yield displacement. It appears that yielding of the moment frame for the hybrid system would be expected at about 70% of the DBE,

as opposed to 80% to 100% of DBE for the baselines. Similar to the other multi-phase systems, acceleration and base shear responses were much better for the low scale factors in comparison to the baseline systems. Similar to the other parallel system, the acceleration and base shear performances were relatively poor in comparison to the baselines, with an acceleration response exceeding 70% more than the baseline response at the DBE. Although variable across all the systems, brace ductility performance far exceeded baseline performance across all of the scale factors. The median response indicated that the brace would stay elastic up to 50% of the DBE.

The HYFR-VFD moment frame ductility, presented in Figure 6-30, shows relatively more dispersion in response across all of the systems when compared to the other multi-phase devices. The HYFR-VFD systems with the lower system ratios (M40B60 and M50B50) showed superior performance. Similar to the other multi-phase arrangements, the systems with smaller gap sizes exhibited the best performance for all of the system ratios. The two best performers were the M40B60 with the 0.6 and 0.8 gap sizes.

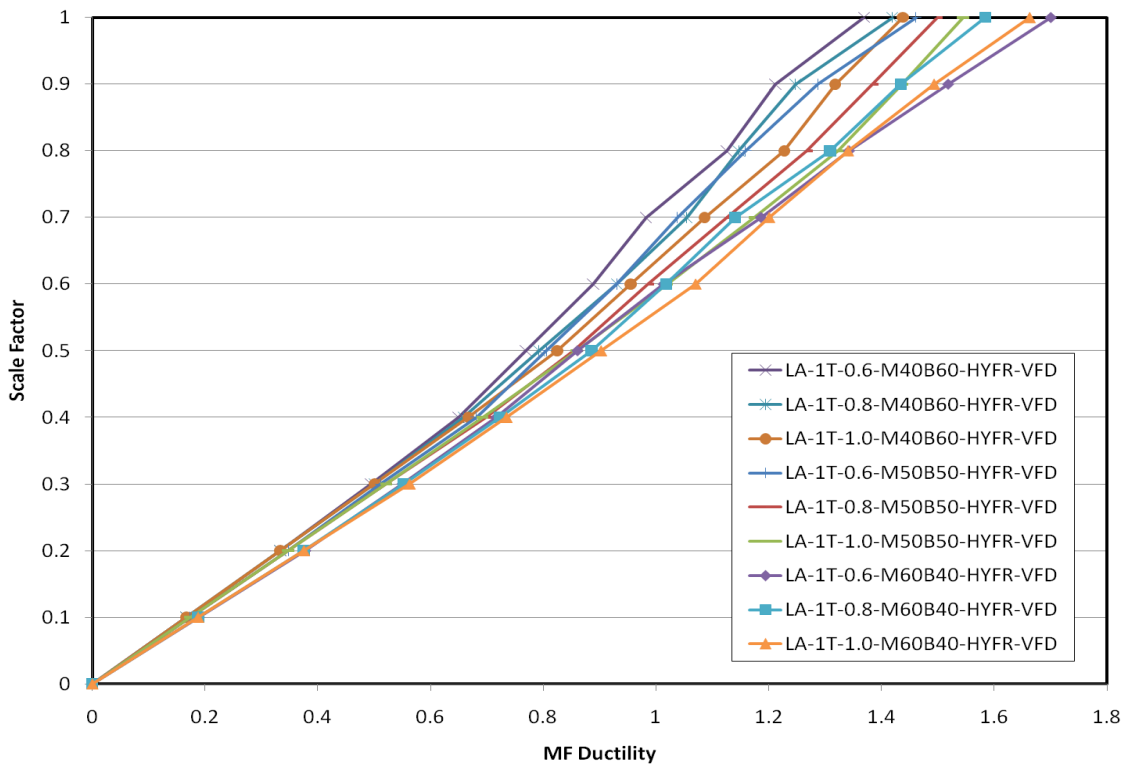


Figure 6-30: HYFR-VFD 1T Moment Frame Ductility

Similar to the HYFR systems, acceleration and base shear responses showed a lot of variability across all of the scale factors, as demonstrated in Figure 6-31 and Figure 6-32. The larger system ratio (M60B40) performed the worst out of the three system ratios. The larger gap sizes allowed for more damping throughout the duration of the multi-phase action and provided better overall response for both acceleration and base shear. With the exception of the upper scale factors in acceleration, the M40B60 system with the 1.0 scale factor consistently performed the best for these selection criteria. This system offers significantly better performance in the low-to-mid factors for both acceleration and base shear.

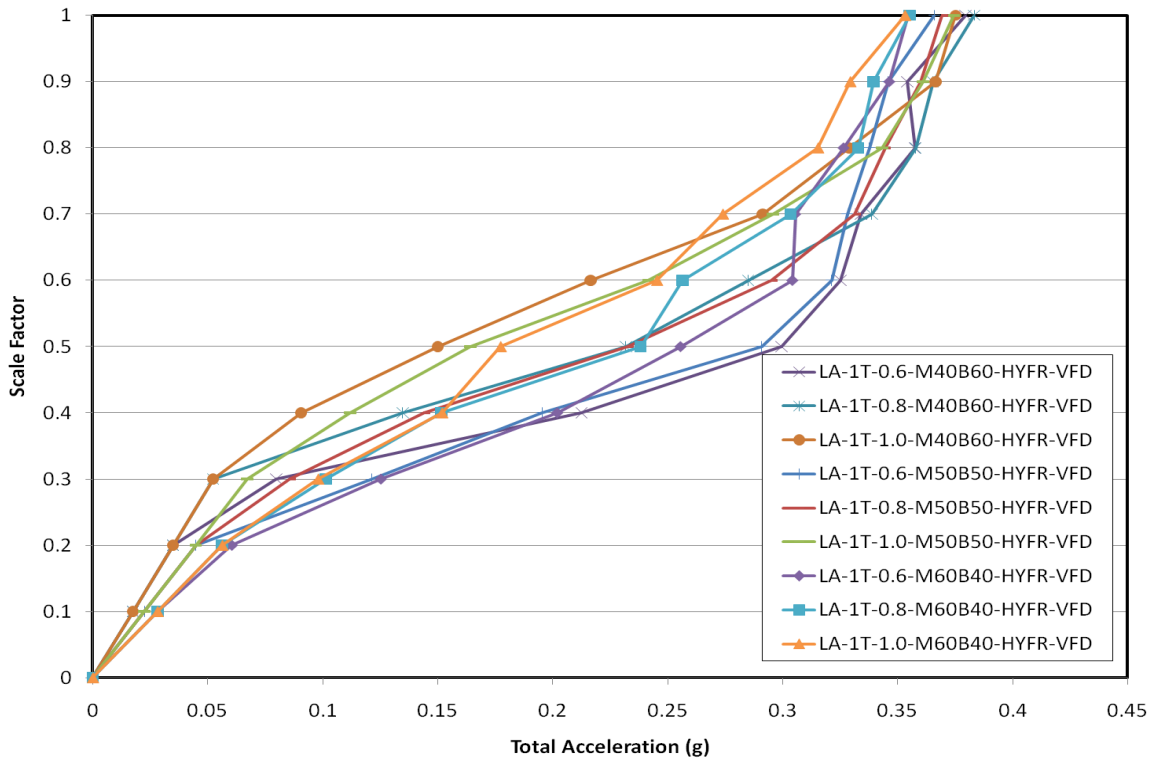


Figure 6-31: HYFR-VFD 1T Acceleration Response

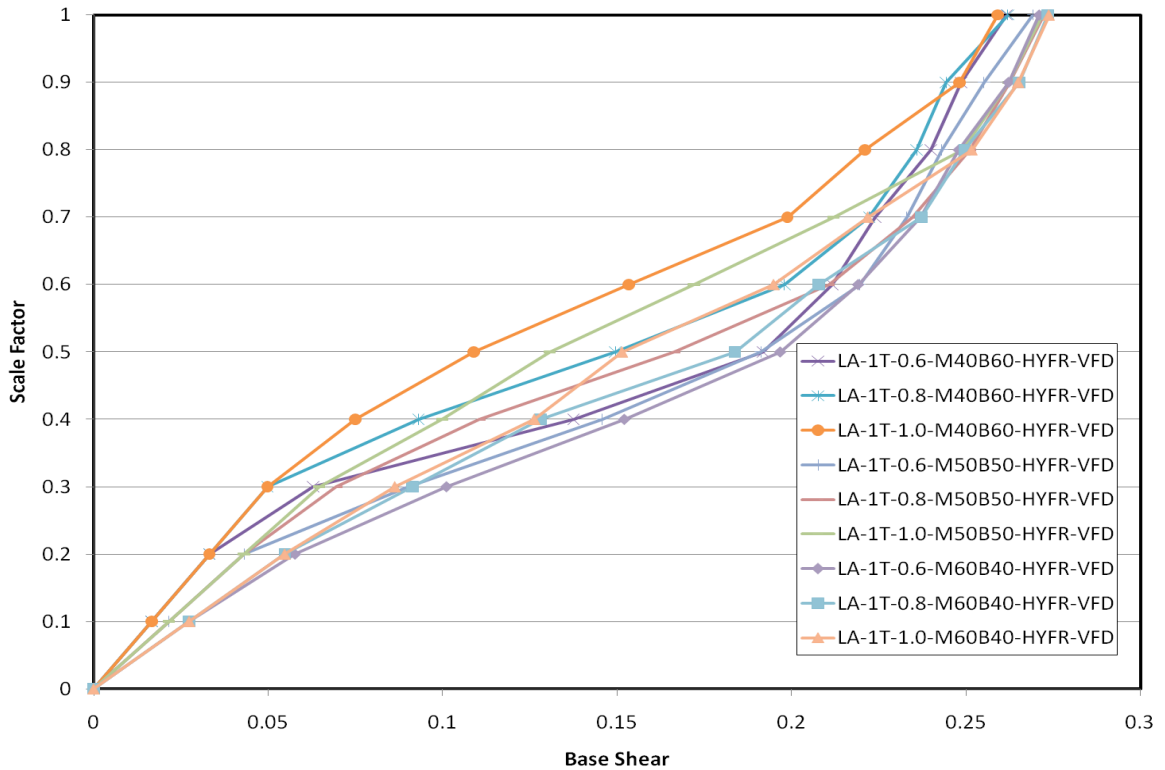


Figure 6-32: HYFR-VFD 1T Base Shear Response

The brace ductility response, presented in Figure 6-33, shows a significant amount of dispersion through the mid-to-upper scale factors. Yielding occurs anywhere from 40% to 70% of the DBE, depending on the system ratio and gap size combination. The brace ductility performance is largely dependent on the gap size, with the largest gap sizes performing the best. Generally speaking, the M60B40 systems perform worse than the M40B60, with the M50B50 performance in the middle. The M40B60 system with the 1.0 gap was consistently the best performer at all scale factors, remaining elastic beyond 60% of the DBE.

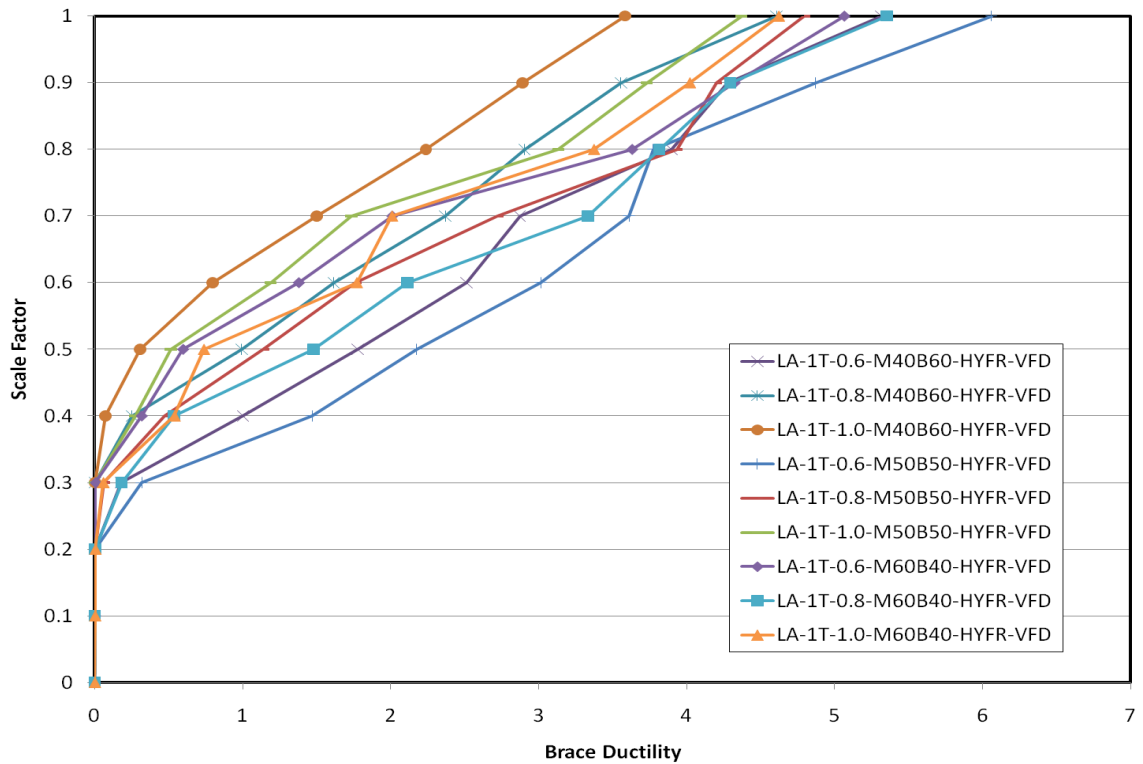


Figure 6-33: HYFR-VFD 1T Brace Ductility

Similar to the two series systems, the M40B60 system with the 1.0 gap size would be the best option for an HYFR-VFD system. The larger gap size allows for significant damping throughout the duration of the ground motion excitement for a parallel system. Like all the other multi-phase systems, the major drawback of the system is the relatively poor moment frame ductility observed in the upper scale factors.

Similarly to the HPCD-VFD systems, the HYFR-VFD systems with a higher damping ratio were evaluated to see if the damping made a significant difference in response (Figure 6-34). Improved performance was seen across all response quantities for the systems with increased damping, especially for the M60B40 system which saw improved performance across all response quantities for all scale factors. Most

importantly, the moment frame ductility performance drastically improved, remaining elastic up to 90% of the DBE. The cost of adding damping may be more worthwhile in the case of the parallel VFD systems than for the series systems. Additionally, larger gap sizes may provide even better performance, while still protecting the moment frame.

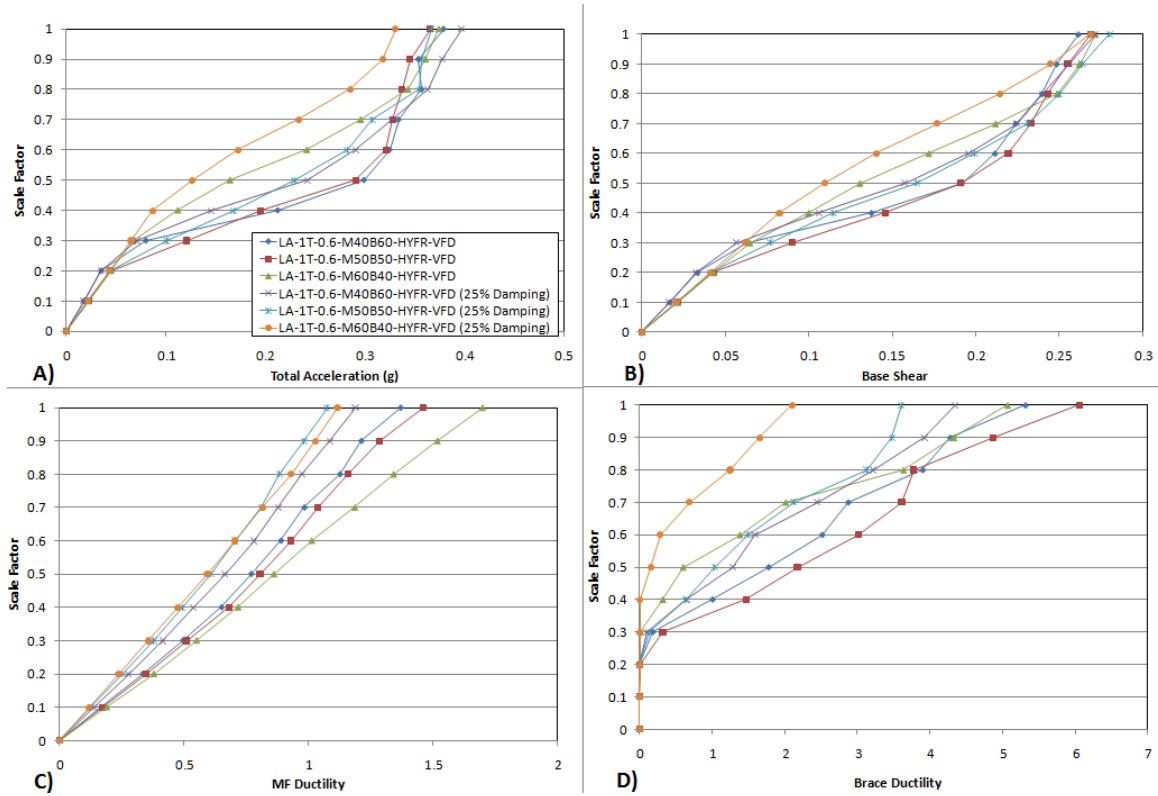


Figure 6-34: HYFR-VFD Damping Ratio Comparison

6.4.5 System Comparison

Although some comparisons were previously made between systems, it is useful to compare them all at once. The four best performing systems identified earlier in the research were all compared with each other in order to make comparisons between system arrangements and damping type (Figure 6-35).

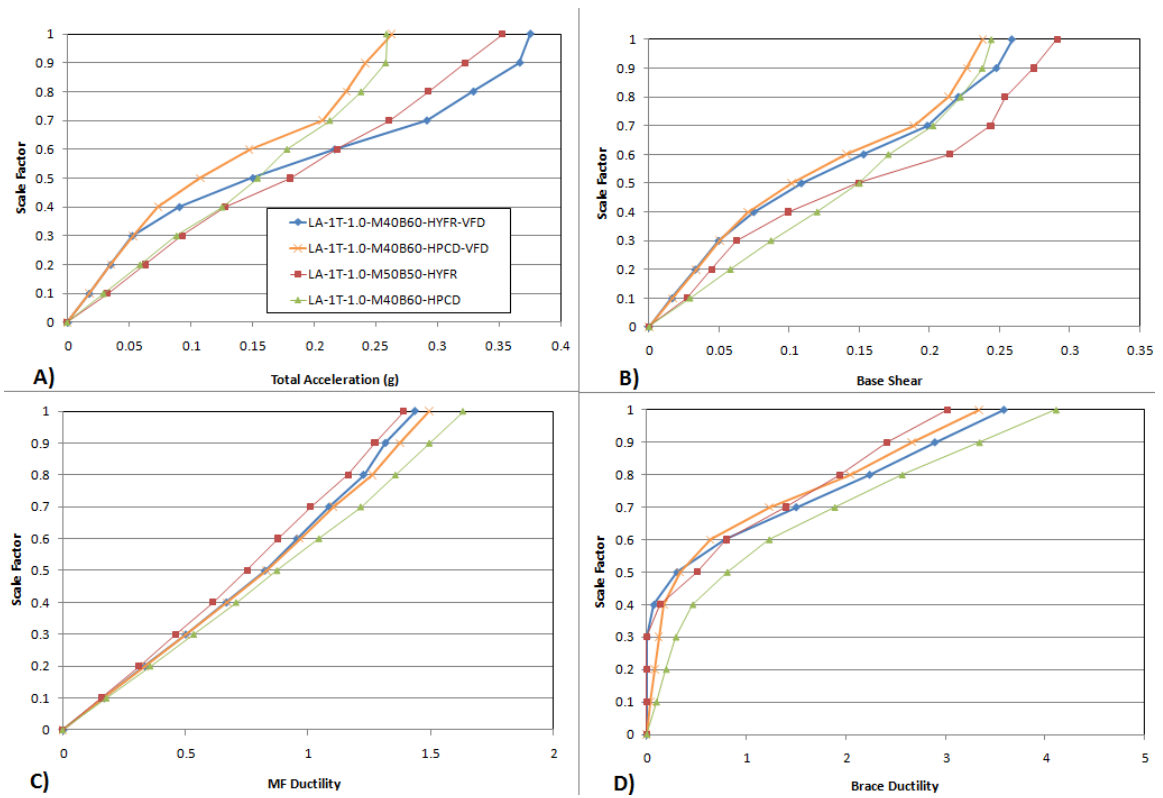


Figure 6-35: System Arrangement Comparison

The moment frames in all four systems were observed to yield anywhere from 60% to 70% of the DBE, with the HYFR system exhibiting the best performance. Acceleration and base shear exhibited the most variability in response from the four systems. The parallel systems both experienced higher responses in the upper scale factors. Brace performance for all of the systems remained elastic until at least 50% of the DBE. The HPCD system was the first to yield, while the other three systems remained elastic until 60% of the DBE.

Overall, the systems offer many benefits in relationship to the baselines. The one major drawback is the poor moment frame ductility behavior, which could potentially be resolved by adding more damping to the systems. Other potential drawbacks of the

multi-phase systems could result from acceleration spikes at the phase transitions. This issue is described in more detail in the next section.

6.5 Acceleration Spikes

The multi-phase systems are possibly subjected to large acceleration spikes as the gap element closes and the system becomes stiffer. These acceleration spikes could be responsible for poor acceleration and base shear responses observed in some of the IDA plots, especially those for the near-field ground motion records. Comparing the acceleration response to the gap link element would give some insight into whether the closing of the gap element was the source of the larger accelerations. If this is the case, further investigation of the stiffness transition region could prove helpful in finding a way to reduce these spikes, and to improve the overall multi-phase system response.

The following is a detailed look at the acceleration spikes for various multi-phase systems and ground motions. The Erzican, Turkey DBE record was chosen to evaluate acceleration spikes for the 0.25 and 1.0 second period systems because it is a near source motion with an acceleration response spectrum similar to design values at the periods of concern. The M40B60-1.0-HYFR-VFD system was evaluated first because of the superior performance it demonstrated earlier in the chapter (Figure 6-36). As alluded to earlier, the poor performance of the 0.25 second multi-phase system could be attributed

to the acceleration spikes.

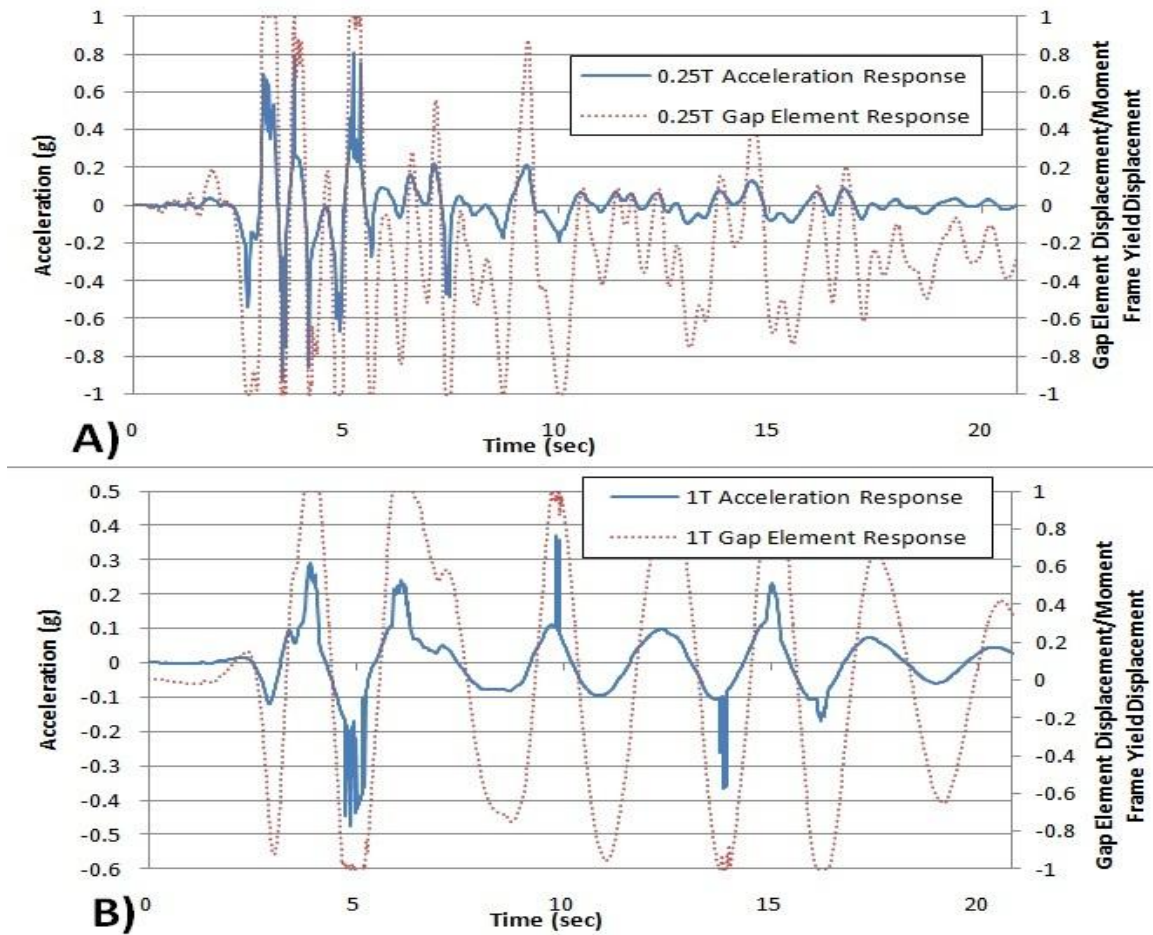


**Figure 6-36: a) HYFR-VFD-0.25T-1.0 Gap-M40B60 Acceleration Response History
b) HYFR-VFD-1T-1.0 Gap-M40B60 Acceleration Response History**

Acceleration and gap element behavior are very closely related. When the gap element is closed, an acceleration spike is sometimes observed. This is apparent in Figure 6-36A; shortly after 5 seconds, the gap closes and the acceleration response has two clear spikes. Figure 6-36B shows multiple instances of acceleration spikes, most notably at 5, 10 and 14 seconds. Although the 0.25 second system goes through more phase transitions, it seems as though the 1 second period system is subjected to more

violent acceleration spikes. This may occur because the duration of the gap closure is longer for the 1 second systems. These spikes may have resulted from an increase in ground motion energy input while the gap is closed rather than a spike caused by the phase transition.

The poor response observed in the 0.25T second systems may be due to the large number of phase transitions rather than acceleration spikes due to phase transitions. Although acceleration spikes would be more likely to occur in a VFD system due to a more drastic stiffness transition, this phenomenon was also investigated for the HPCD systems (Figure 6-37).

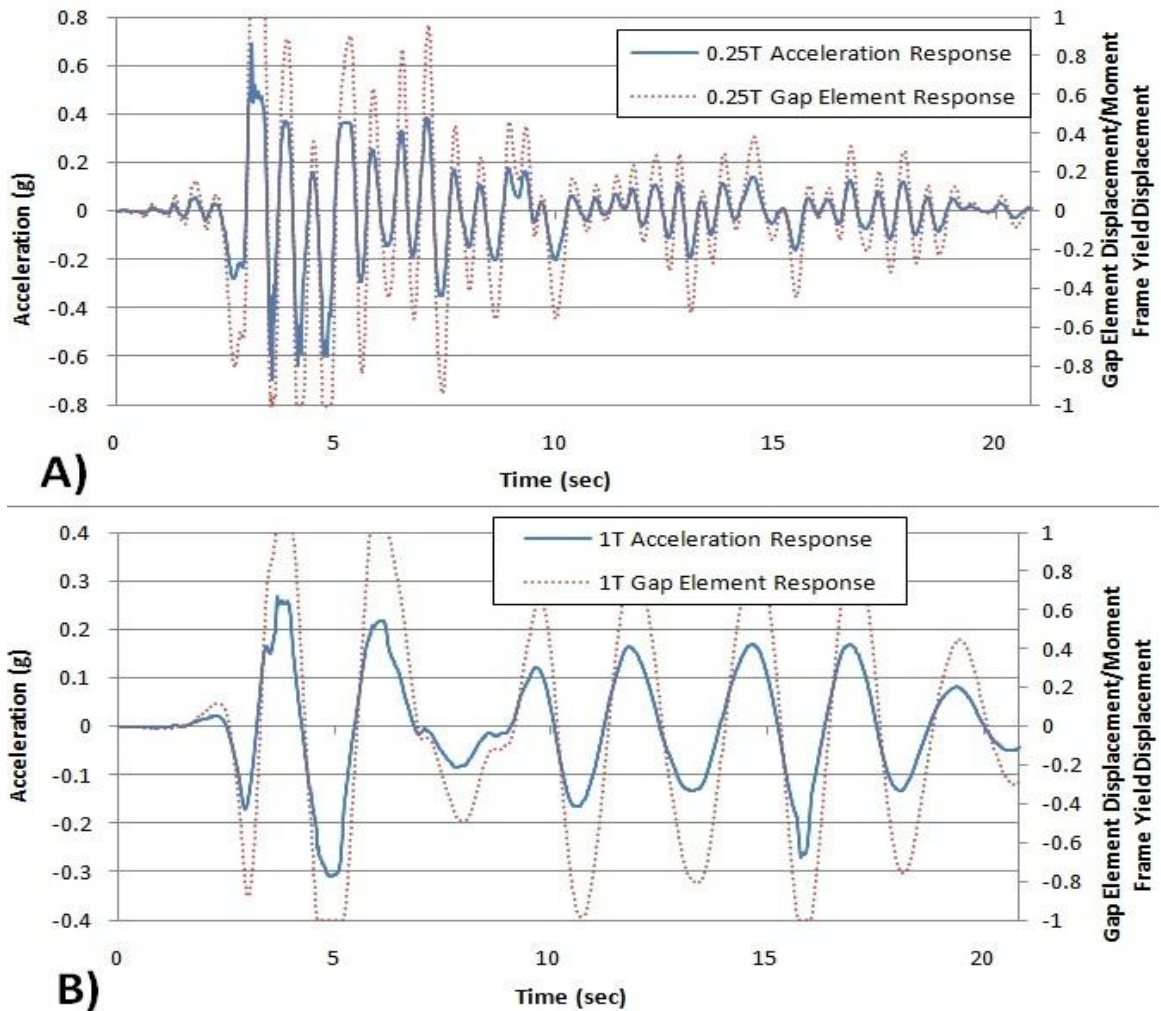


**Figure 6-37: a) HPCD-0.25T-1.0 Gap-M40B60 Acceleration Response History
 b) HPCD-1T-1.0 Gap-M40B60 Acceleration Response History**

Similar to the response observed for the other system, the acceleration and gap element behavior coincided. Records for systems with both periods showed a slight shock at about 4 seconds, but not as substantial as that observed for the VFD systems. The 0.25 second HPCD system also experienced a smaller number of phase transitions than the VFD system, a potentially appealing aspect if an effective solution for multi-

phase behavior is found for lower periods. Overall, it seemed that acceleration spikes did not seem to have a large affect on acceleration response for the HPCD systems.

6.6 Residual Drifts

In addition to investigating the effects of acceleration spikes on the responses of multi-phase systems, it is also important to analyze the residual drifts for the different system arrangements. Inelastic behavior of the buckling restrained brace element or the moment frame could lead to permanent residual deformation in the system. Residual deformation is an important factor in post-event safety of the structure and therefore was investigated for the multi-phase systems. Although residuals may not be directly applicable to a real structure as a SDOF system, the relative residuals for each system can still be compared to demonstrate which multi-phase systems perform the best.

Four ground motions were chosen to evaluate residual deformations for the four best-performing systems (M40B60-1T-1.0-HPCD, M40B60-1T-1.0-HPCD-VFD, M50B50-1T-1.0-HYFR, & M40B60-1T-1.0-HYFR-VFD). Figure 6-38 shows the residual deformations for the four systems. Displacements were normalized by the moment frame yield displacement in order to consistently compare results from the different system ratios. Yield displacements ranged from 7.3 inches to 8.4 inches. Relatively large residual drifts were observed in response to only one ground motion (ERZEW). The HYFR system, which included the parallel arrangement paired with the high-damping elastomeric device, demonstrated self-centering capabilities. This is evident in all of the ground motions by observing the relatively small residual deformations for this system when comparison to the other systems. The HYFR system also is the most effective at damping out the energy after the duration of the ground

motion. The HPCD-VFD and HYFR-VFD behaved very similarly in response to all four ground motions, while the HPCD exhibited the highest overall residual deformations. More research should be performed regarding the minimization of residual deformations in the MDOF system study.

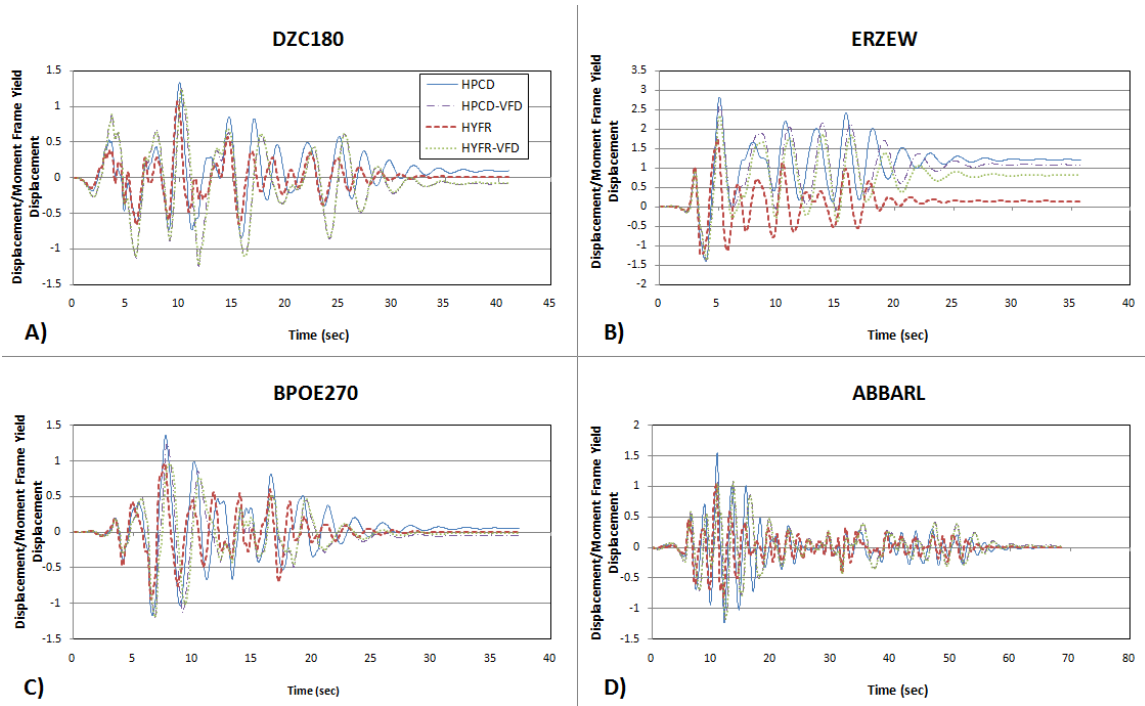


Figure 6-38: Residual Deformations

6.7 Summary

An extensive analysis of the multi-phase behavior of the various hybrid systems was presented in this chapter. Given the range of system parameters that had been narrowed considerably from the initial set, this chapter described the efforts to identify the best performing systems from the remaining systems. In order to demonstrate the benefits of multi-phase behavior, results for the multi-phase systems were compared to

those for baseline systems. Then the multi-phase systems were evaluated to determine the effectiveness at different natural periods. The systems were then divided into system arrangements and their responses were evaluated in detail. Selection criteria were developed to identify the most promising systems considering multiple response quantities. The effects of system ratio and gap size on response were identified and the most desirable systems were chosen. Comparisons were made between damping type and system arrangements. Other aspects of response, such as acceleration spikes and residual deformations, were also considered and compared between systems.

In comparison to the baseline systems, the multi-phase systems offer many benefits. Once the systems were compared in the full factorial analysis, the following four systems were identified as the best-performing systems:

- HPCD: M40B60 with a 1.0 gap size
- HPCD-VFD: M4060 with a 1.0 gap size
- HYFR: M50B50 with a 1.0 gap size
- HYFR-VFD: M40B60 with a 1.0 gap size

Acceleration and base shear for these were largely reduced in the lower scale factors. Their brace behavior remained elastic up 60%-70% of the DBE, compared to 20% for the baseline systems. The major drawback of these systems is poor moment frame ductility performance for the upper scale factors. Moment frame yielding occurs as early as 60% of the DBE, compared to 90%-100% of the DBE for the baseline systems. The beneficial acceleration, base shear, and brace ductility behavior is not useful unless the moment frame can be protected. The inclusion of additional damping was observed to improve the moment frame performance to an acceptable level, but this

option could be costly. Overall, large steps were made towards improving the fundamental understanding of multi-phase passive control systems, but more research needs to be completed to realize the true potential of multi-phase passive control systems.

Chapter 7 Summary and Conclusions

7.1 Summary

The goal of this research was to understand the fundamental behavior of multi-phase passive control devices. The first step was to perform a literature review in order to explore the options for multi-phase systems. A review on active control, semi-active control, and passive control was performed. Within the scope of passive control, possible options for multi-phase systems were analyzed. Other uses of multi-phased devices in past research were also reviewed. Beyond the literature review, the research was split into three primary sections: 1) Parametric development and analysis plan, 2) Model development and nonlinear dynamic SDOF analytical study, and 3) Interpretation of results.

The parametric development and analysis draws from the options presented in the literature review and chooses appropriate parameters for multi-phase use. Two velocity-dependent devices were chosen, a linear viscous fluid damper and viscoelastic high-damping rubber. A buckling-restrained brace was chosen for the displacement dependent device due to the reliable hysteretic behavior and significant energy dissipation capabilities. Relationships between the moment frame strength and hysteretic brace strength were developed for the system design. The transition phase and corresponding gap size was developed as a function of the moment frame yield displacement. Two locations and natural periods were developed in order to test the feasibility of multi-phase systems in different seismic hazards. Once a range of parameters were developed, an

experimental design meant to capture statistical significance and reduce the number of systems was completed.

The next step of the research involved the model development and nonlinear dynamic SDOF study. Important aspects of the response history analysis were established such as the suite of ground motions and the appropriate scaling for the motions. The arrangement of the multi-phase systems and the corresponding modeling details were developed. Appropriate configurations of the multi-phase systems involved multi-linear plastic link elements, multi-linear elastic link elements, and linear viscous dashpots. Four response quantities were developed to compare the performance of the systems. The completion of the model development phase of the research allowed the systems to be run in SAP2000 and the results were interpreted.

The analysis of the results was completed in two phases; the preliminary analysis and a full factorial analysis. Although the preliminary analysis was intended to be the only analysis, the statistical significance was difficult to evaluate due to the inherent nesting of the multi-phase system components. The preliminary analysis did provide valuable insight towards the research and allowed the scope of the analysis to be reduced. Using statistical and empirical observations, the range of variables was able to be reduced to provide 144 systems in a full factorial analysis, a number that was feasible for analysis.

The full factorial analysis provided an extensive look at multi-phase behavior and identified some of the better performing system combinations. Systems were compared to baseline systems in order to demonstrate the benefits of multi-phase behavior. Beyond this comparison, systems were also compared at different natural periods to determine the effectiveness at different natural periods. A detailed look at each system arrangement

was done to identify the key components affecting response. At the completion of this analysis, the systems were compared to each other to identify the effects of damping type and system arrangements. Other aspects of system response, such as acceleration spikes and residual deformations were analyzed to demonstrate other possible benefits or drawbacks of multi-phase behavior.

Overall, the fundamental behavior of multi-phase systems was evident by the end of the research. Multi-phase systems provide an interesting aspect to structural design in that they allow the structure to be more resilient and essentially preprogrammed for ground motion excitement. This idea has been explored in the past, but the implementation using passive control devices is relatively new and appealing for structural design. The work provided in this research provides significant groundwork for multi-phase research in the future. Using the range of variables from this analysis, an MDOF system can be developed and tested analytically. Once the system performance is verified analytically, the study can be tested experimentally and hopefully implemented in design.

7.2 Conclusions

Specific conclusions were given within Chapter 5 and Chapter 6 but this section provides a broader set of conclusions for the multi-phase systems. Compared to the baseline systems, multi-phase passive control devices offer many benefits, especially in the higher periods (1 second to 4 seconds). The first phase provides a significant decrease in acceleration and base shear in the lower scale factors. The brace behavior is another appealing aspect of the multi-phase devices, remaining elastic up to 60%-70% of

the DBE in some cases. As the period decreases (0.25 seconds and 0.5 seconds), the beneficial multi-phase behavior decreases and therefore the extra costs associated with a multi-phase system may not be justified. More research needs to be done to investigate the feasibility of a multi-phase system in lower natural periods.

The major drawback of the multi-phase behavior lies in the protection of the moment frame. The beneficial protection of the brace element is only appealing if the moment frame remains elastic. Variability was not very large for moment frame ductility but was consistently poor in comparison to the baseline systems. Even in the best performing systems, yielding occurs as early as 60% of the DBE compared to 90%-100% for the baseline systems. The two VFD arrangements were analyzed with larger damping ratios for extra moment frame protection. This proved to be very beneficial to the parallel arrangement.

Once the systems were compared to each other in the full factorial analysis, standout performers were noticed for each system arrangement:

- HPCD: M40B60 with a 1.0 gap size
- HPCD-VFD: M4060 with a 1.0 gap size
- HYFR: M50B50 with a 1.0 gap size
- HYFR-VFD: M40B60 with a 1.0 gap size

Other options for multi-phase systems are obviously feasible and could provide similar responses. A range of good performing system traits is evident within each section.

The results presented with this research clearly show the beneficial capabilities of multi-phase behavior. The better performing systems within the research provided elastic behavior of all elements up to 60% of the design basis earthquake which is much better

than the baseline system which experience yielding at 20% of the DBE. In addition to ductility performance, the acceleration and base shear were drastically decreased in the lower scale factors in comparison to the baselines. With the resolution of the poor acceleration, base shear, and moment frame performance in the upper scale factors, multi-phase systems become a very viable option for implementation in design.

Other conclusions drawn are detailed below:

- The statistical analysis of a multi-phase system in which the components are in a hierarchal arrangement is difficult with a limited amount of data. The reduction of the scope of the study into a range in which a full factorial analysis can be performed is a more desirable approach for this research.
- Acceleration spikes did not play as large of a role in response as anticipated. Spikes were present but not always due to the phase transition.
- The HYFR system had the best residual deformation performance but further research into this behavior is required in the MDOF study.
- Overall, the multi-phase systems have a favorable response to increased damping. Generally speaking the VFD systems performed better than the HDR systems. Also, the parallel arrangements had a favorable affect on moment frame performance. A parallel VFD system with the large gap size may be the best option for future research.

7.3 Future Work

Since this research is only meant to provide the groundwork for multi-phase control systems, there is obviously a need for future research. Like most research, assumptions were made and problems arose throughout the duration of the project. These recommendations for future work seek to eliminate these uncertainties and better develop multi-phase systems.

As alluded to many times in the research, this analysis is meant to provide the groundwork for a MDOF system analysis. Although the SDOF analysis offers significant insight towards the fundamentals of the system, it is not a completely accurate representation of structural response. Participation in other modes of vibration in an MDOF system could reduce overall base shears or increase story accelerations and shears. P-delta forces, which were excluded for the SDOF systems, could potentially play a large role in response. The HYFR system which is more effective at reducing residual deformations may become a more appealing system. The MDOF system analysis could be accomplished in the form of a three story shear building and then expanded into a larger analytical model using the multi-phase system recommendations given in this research. Whichever system demonstrates the most appealing behavior in an MDOF study should be further tested experimentally to verify results. Design criteria would also have to be developed if the system were to be implemented into structural design. Other recommendations are detailed below:

- The most pressing issue with the multi-phase systems is moment frame protection. Options were suggested (such as adding more supplemental damping) but further research is needed to investigate this aspect of response.
- A cost-benefit analysis of the systems would also have to be performed to ensure the validity of the multi-phase systems in a practical application.
- A weighted response criterion for the MDOF analysis should be developed. Comparing the four response quantities at 10 different scale factors is a difficult task unless there is a systematic approach developed.
- One of the main issues with the parallel systems is the excessive acceleration and base shear in the upper scale factors most likely due to the strain hardening of the system components and forces from the velocity-dependent device. By implementing a friction device rather than a BRB, the forces would essentially be capped and possibly resolve this issue.
- Linear viscous damping was used in order to reduce the number of variables in the research. Nonlinear viscous damping should also be investigated. In addition, damping values may be able to be increased for the viscous fluid damper and high-damping rubber. Research into feasible damping values should also be performed.
- A detailed analysis was done for the 1 second period although the data was present for 4 natural periods. Although the system behavior was observed to be similar for each period, further research could be performed to find any significant differences if present.

- The focus of this analysis was mostly in the form of an incremental dynamic analysis. Although this is a widely used method of analysis, more conclusions may have been able to be drawn by looking at the individual response history for each ground motion. Some of the better performing systems could be analyzed in more detail for each ground motion.
- The HYFR system involving a compressed elastomeric device is a relatively new concept. More research involving the “slip” behavior of the device should be completed before it is fully implemented in a multi-phase system.
- The phase transition behavior is the most important aspect of the multi-phase device. The reliability of the phase transition mechanism must be evaluated further to ensure adequate behavior.
- The overstrength and response modification factors (2.5 and 8 respectively) used in this study need to be investigated further to see if they are appropriate for multi-phase systems.

These are just a few recommendations for the further development of multi-phase systems. The tendency of design codes is moving towards a performance-based approach which will demand research in the field of multi-phase behavior. Engineers’ ingenuity and creativeness will surely find many uses and make developments for multi-phase passive control devices.

References

Aiken, I. D., Nims, D. K., Whittaker, A. S., & Kelly, J. M. (1993). Testing of Passive Energy Dissipation Systems. *Earthquake Spectra* , 9 (No. 3).

Alehashem, S. M., Keyhani, A., & Pourmohammad, H. (2008). Behavior and Performance of Structures Equipped With ADAS & TADAS Dampers (a Comparison with Conventional Structures). *The 14th World Conference on Earthquake Engineering*. Beijing, China.

Applied Technology Council. (2009). *Quantification of Building Seismic Performance Factors (FEMA P695)*. Washington, D.C.: Federal Emergency Management Agency.

ASCE. (2006). *Minimum Design Loads for Buildings and Other Structures*. Reston, VA: American Society of Civil Engineers.

ASCE/SEI. (2007). *Seismic Rehabilitation of Existing Buildings (ASCE/SEI Standard 41-06)*. Reston, VA: American Society of Civil Engineers.

Asteris, P. G. (2008). On The Structural Analysis and Seismic Protection of Historical Structures. *The Open Construction and Building Technology Journal* , 2, 124-133.

Balendra, T., Yu, C., & Lee, F. L. (2001). An Economical Structural System for Wind and Earthquake Loads. *Engineering Structures* , 23 (5), 491-501.

Chopra, A. K. (2007). *Dynamics of Structures: Theory and Application to Earthquake Engineering* (3rd ed.). Upper Saddle River, New Jersey: Pearson/Prentice Hall.

CSI. (2009). *CSI Analysis Reference Manual* . Berkeley, CA: Computers and Structures, Inc.

Dolce, M., Cardone, D., & Marnetto, R. (2000). Implementation and Testing of Passive Control Devices Based on Shape Memory Alloys. *Earthquake Engineering and Structural Dynamics* , 29, 945-968.

Engineering Seismology Laboratory. (2005). *ESL Home Page*. Retrieved February 2010, from MCEER (SUNY at Buffalo): <http://civil.eng.buffalo.edu/engseislab/>

Fernandez, J. A. (2007). Numerical Simulation of Earthquake Ground Motions in the Upper Mississippi Embayment. Ph.D. Dissertation, Georgia Institute of Technology, Atlanta, GA.

Ghobarah, A. (2001). Performance-based Design in Earthquake Engineering: State of Development. *Engineering Structures* (23), 878-884.

Ibrahim, Y. E., Marshall, J., & Charney, F. A. (2007). A Visco-plastic Device for Seismic Protection of Structures. *Journal of Construction Steel Research* , 63 (11), 1515-1528.

Karavasilis, T. L., Sause, R., & Ricles, J. M. (2010). *Design of Steel Buildings for Earthquake Conditions Using Next-Generation Elastomeric Dampers*. Oxford, U.K.: University of Oxford Department of Engineering Science.

Kim, J., Ryu, J., & Chung, L. (2006). Seismic Performance of Structures Connected by Viscoelastic Dampers. *Engineering Structures* , 28 (2), 183-195.

Krawinkler, H., Zareian, F., Medina, R. A., & Ibarra, L. F. (2006). Decision Support for Conceptual Performance-based Design. *Earthquake Engineering and Structural Dynamics* , 35, 115-133.

Lee, D., & Taylor, D. (2001). Viscous Damper Development and Future Trends. *The Structural Design of Tall Buildings* , 10, 311-320.

Levy, R., Marianchik, E., Rutenberg, A., & Segal, F. (2000). Seismic Design Methodology for Friction Damped Braced Frames. *Earthquake Engineering Structural Dynamics* , 29 (11), 1569-1585.

Lopez, W. A., & Sabelli, R. (2004, July). Seismic Design of Buckling-Restrained Braced Frames. *Steel Tips* .

Marshall, J. D. (2008). Development, Analysis and Testing of a Hybrid Passive Control Device for Seismic Protection of Framed Structures. Ph.D. Dissertation, Virginia Polytechnic Institute and State University, Blacksburg, VA.

Marshall, J. D., & Charney, F. A. (2010). A Hybrid Passive Control Device for Steel Structures, I: Development and Analysis. *Journal of Constructional Steel Research* , 66 (10), 1278-1286.

Midorikawa, M., Okawa, I., Iiba, M., & Teshigawara, M. (2003). Performance-based Seismic Design Code for Buildings in Japan. *Earthquake Engineering and Engineering Seismology* , 4 (1), 15-25.

Montgomery, D. C. (2009). *Design and Analysis of Experiments* (7th ed.). Hoboken, NJ: John Wiley & Sons.

Motlagh, A. Y., & Saadeghvaziri, M. A. (2001). Nonlinear Seismic Response of Stiffening SDOF Systems. *Engineering Structures* , 23, 1269-1280.

NEHRP. (2003). *NEHRP Recommended Provisions for Seismic Regulations for New Buildings and Other Structures*. Washington D.C.: Federal Emergency Management Agency.

Occhiuzzi, A. (2009). Additional Viscous Dampers for Civil Structures: Analysis of Design Methods Based on Effective Evaluation of Modal Damping Ratios. *Engineering Structures* , 31 (5), 1093-1101.

Regents of the University of California. (2000). *PEER Strong Motion Database*. Retrieved February 2010, from <http://peer.berkeley.edu/smcat/>

Reinhorn, A. M., Constantinou, M. C., & Li, C. (1995). Use of Supplemental Damping Devices for Seismic Strengthening of Lightly Reinforced Concrete Frames. *National Institute for Standards and Technology Workshop*. Gaithersburg, MD.

Robinson, K. (2009, November). Specifying Buckling-Restrained Brace Systems. *Modern Steel Construction* .

Sabelli, R., Mahin, S., & Chang, C. (2003). Seismic Demands on Steel Braced Frame Buildings with Buckling Restrained Braces. *Engineering Structures* , 25, 655-666.
SAS Institute Inc. (2009). *JMP Version 8*. Cary, NC: SAS Institute Inc.

Shih, M. H., & Sung, W. P. (2010). A Design Concept of Autonomous Controller for Improving Seismic Proof Capability of Active Control Device. *Experimental Techniques*, 34 (4), 20-26.

Song, G., Ma, N., & Li, H. N. (2006). Applications of Shape Memory Alloys in Civil Structures. *Engineering Structures* , 28, 1266-1274.

Spencer Jr., B. F., & Nagarajaiah, S. (2003). State of Art of Structural Control. *Journal of Structural Engineering* , 129 (7).

Spencer Jr., B. F., & Sain, M. K. (1997). Controlling Buildings: A New Frontier in Feedback. *IEEE Control Systems Magazine on Emerging Technology* , 17 (6), 19-35.

Tehranizadeh, M. (2001). Passive Energy Dissipation Device for Typical Steel Frame Building in Iran. *Engineering Structures* , 23 (6), 643-655.

Tsai, K.-C., Chou, C.-C., Lin, C.-L., Chen, P.-C., & Jhang, S.-J. (2008). Seismic Self-Centering Steel Beam-to-Column Moment Connections Using Bolted Friction Devices. *Earthquake Engineering & Structural Dynamics* , 37 (4), 627-645.

U.S. Geological Survey (2008, April 15). California Has More Than 99% Chance Of A Big Earthquake Within 30 Years, Report Shows. *ScienceDaily*. Retrieved August 19, 2011, from <http://www.sciencedaily.com/releases/2008/04/080414203459.htm>

Vamvatsikos, D., & Cornell, C. A. (2002). Incremental Dynamic Analysis. *Earthquake Engineering and Structural Dynamics* , 31 (3), 491-514.

Weidlinger, P., & Ettouney, M. (1993). Sequential Coupling: New Structural Connection for Seismic Control. *Journal of Structural Engineering* , 119 (1), 181-201.

Appendix A. Preliminary Design

Appendix A presents the results for all of the preliminary design presented in Chapter 5.

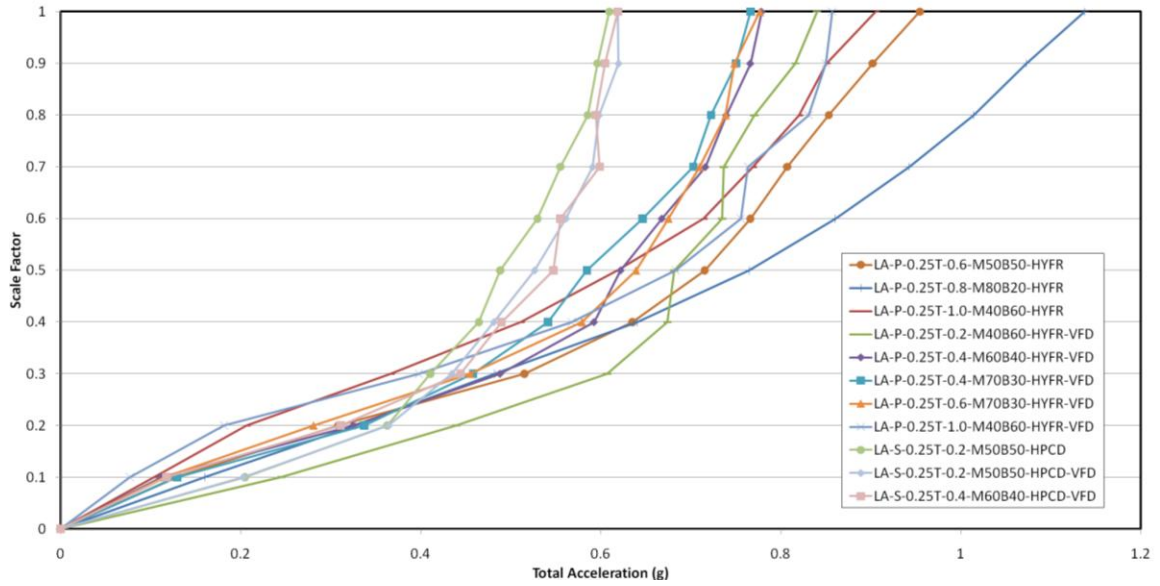


Figure A- 1: Los Angeles 0.25T Acceleration

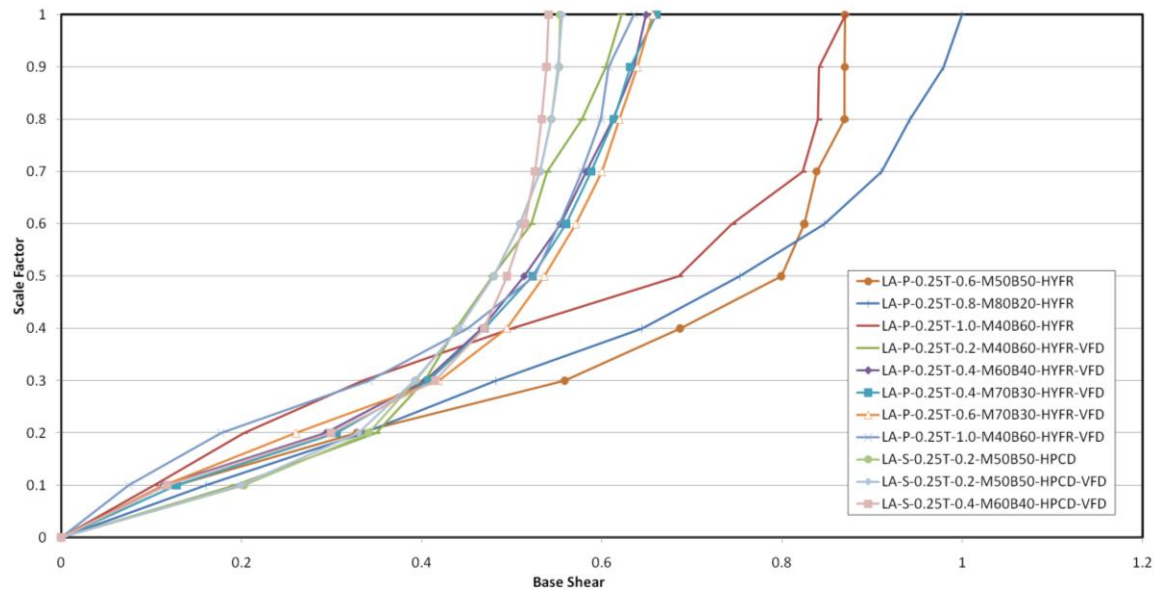


Figure A- 2: Los Angeles 0.25T Base Shear

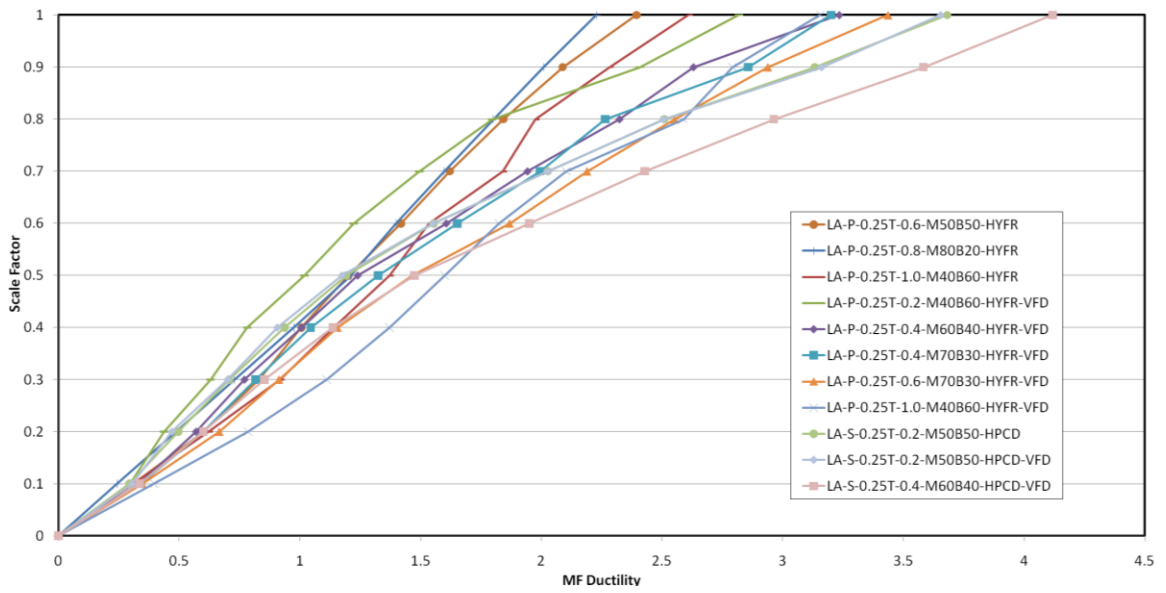


Figure A- 3: Los Angeles 0.25T Moment Frame Ductility

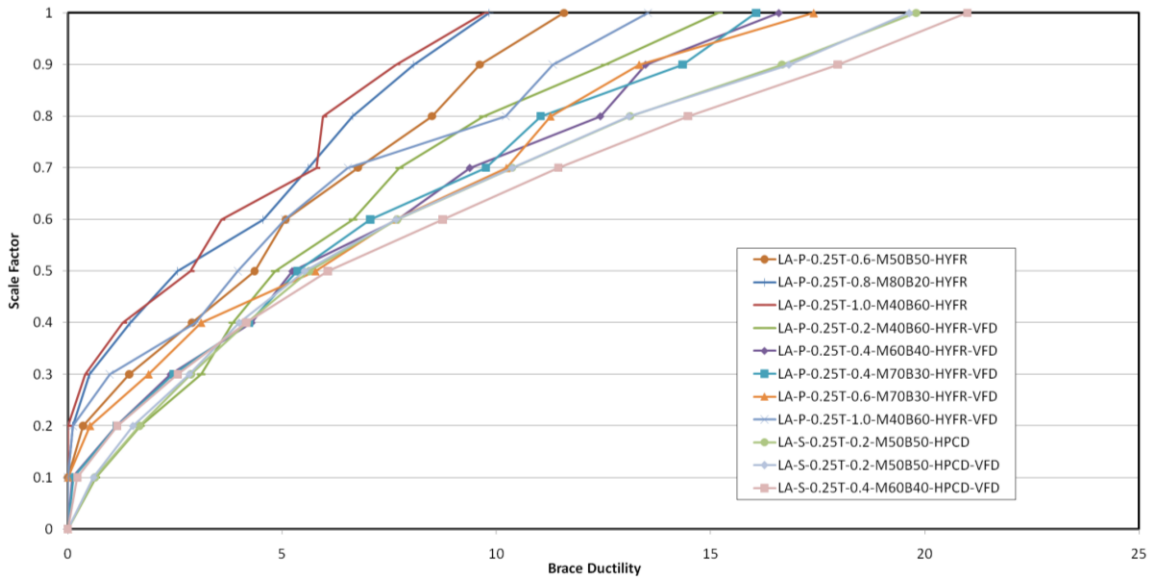


Figure A- 4: Los Angeles 0.25T Brace Ductility

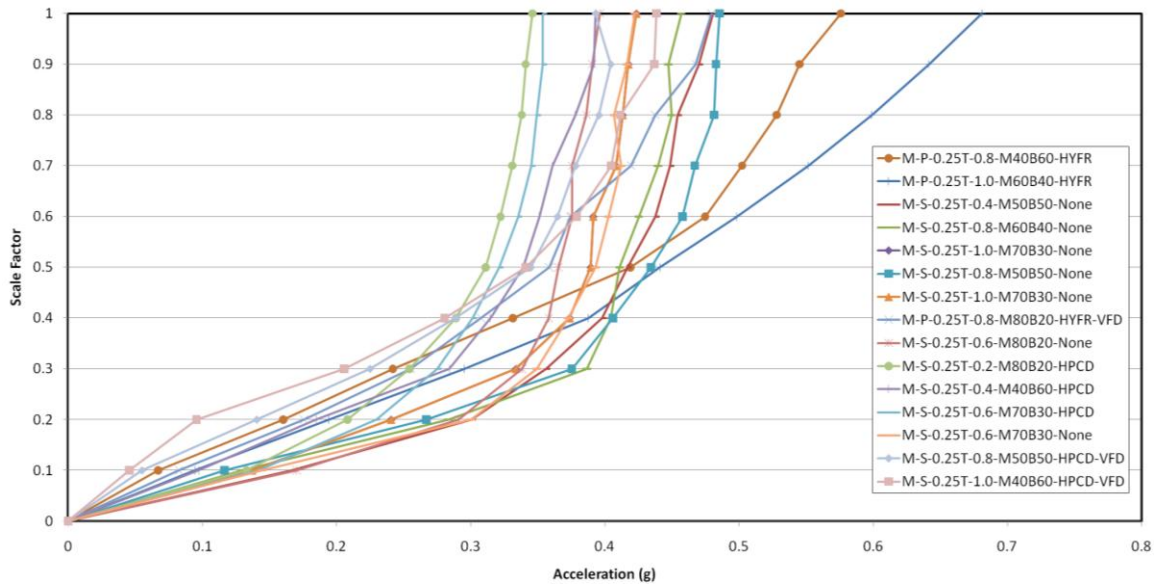


Figure A- 5: Memphis 0.25T Acceleration

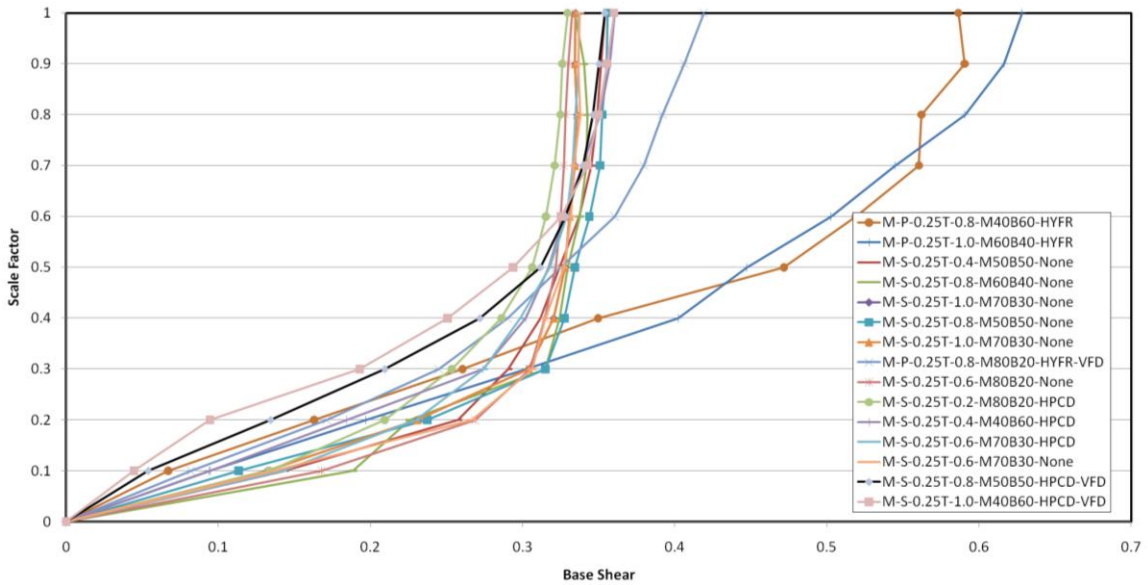


Figure A- 6: Memphis 0.25T Base Shear

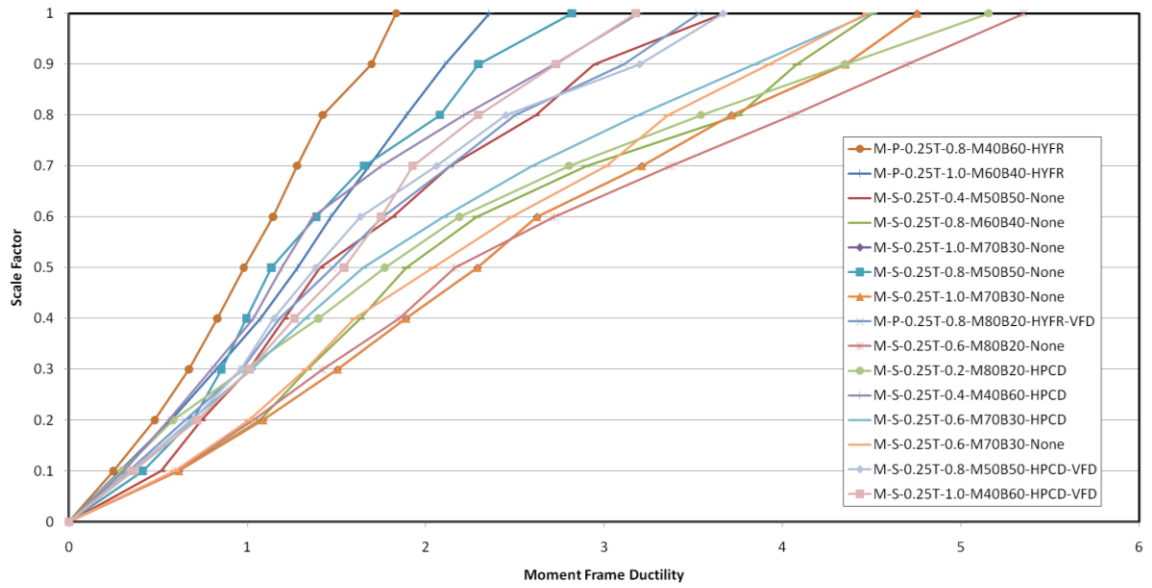


Figure A- 7: Memphis 0.25T Moment Frame Ductility

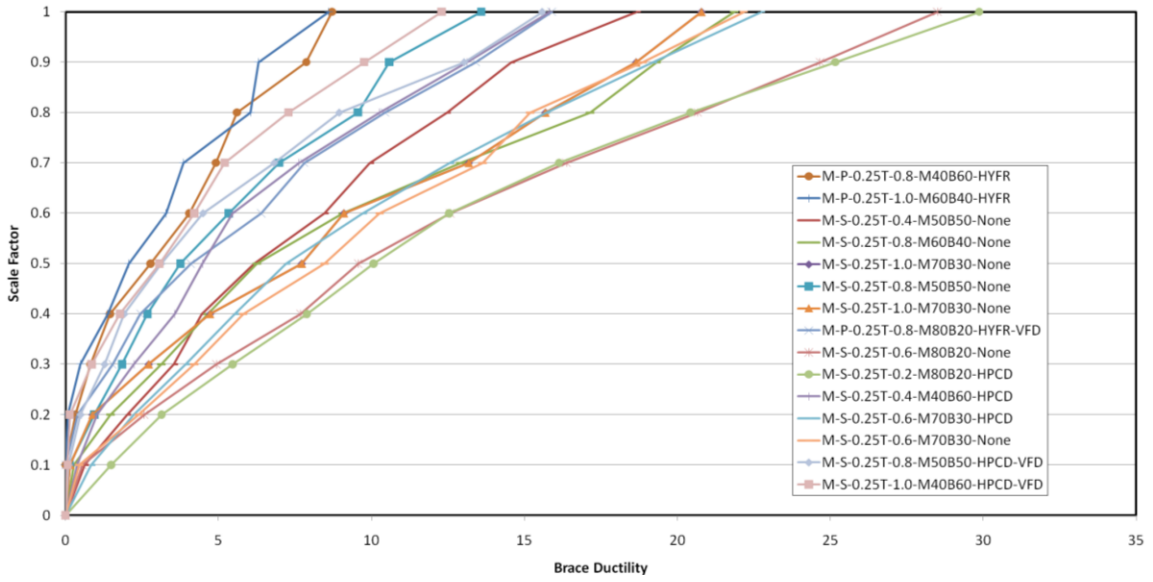


Figure A- 8: Memphis 0.25T Brace Ductility

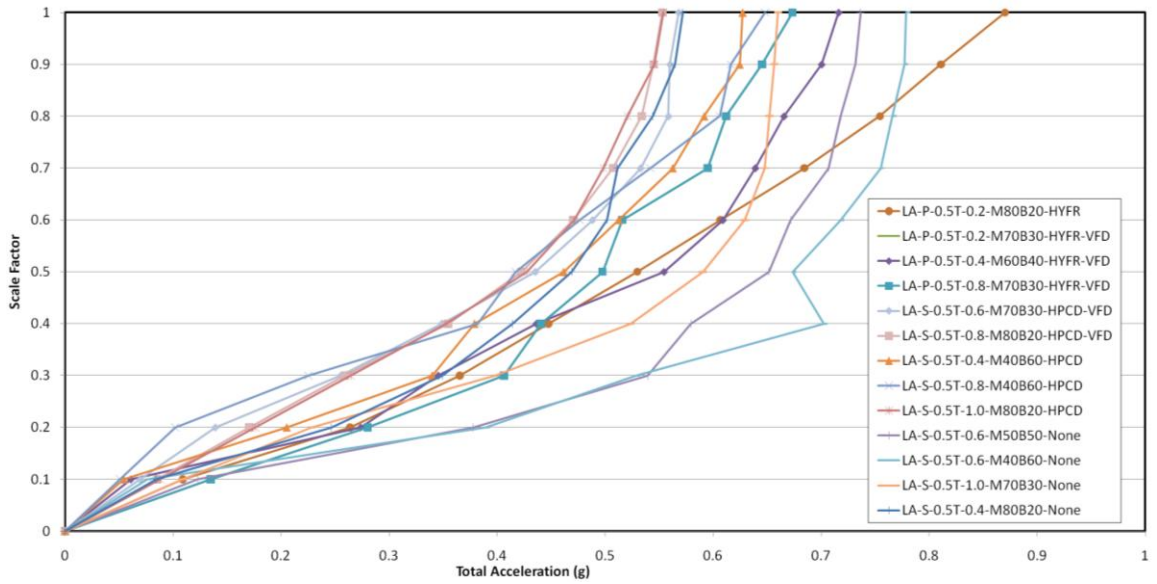


Figure A- 9: Los Angeles 0.5T Acceleration

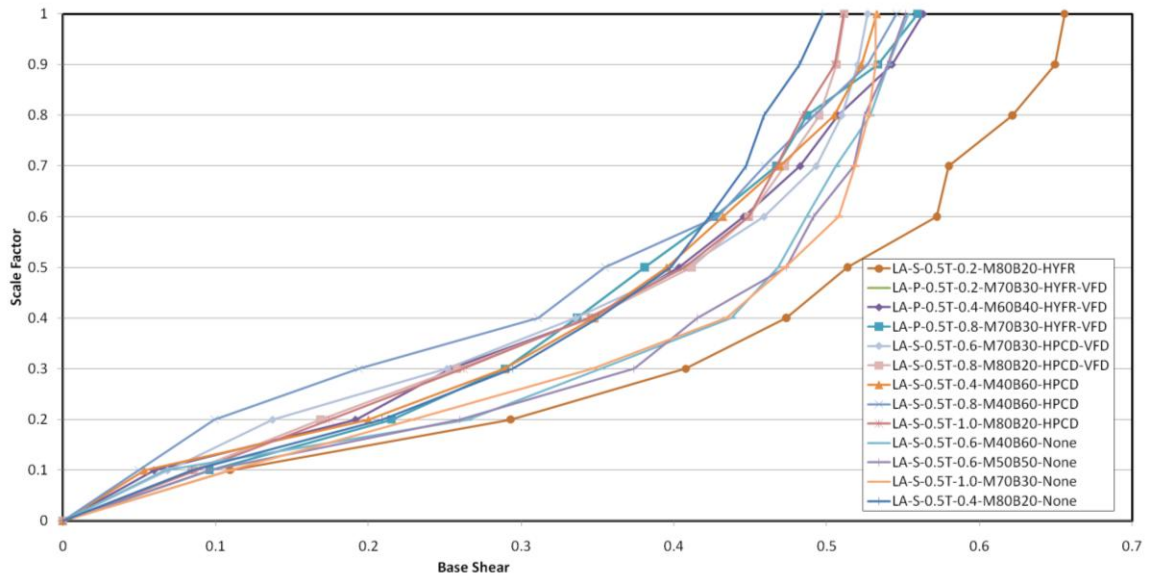


Figure A- 10: Los Angeles 0.5T Base Shear

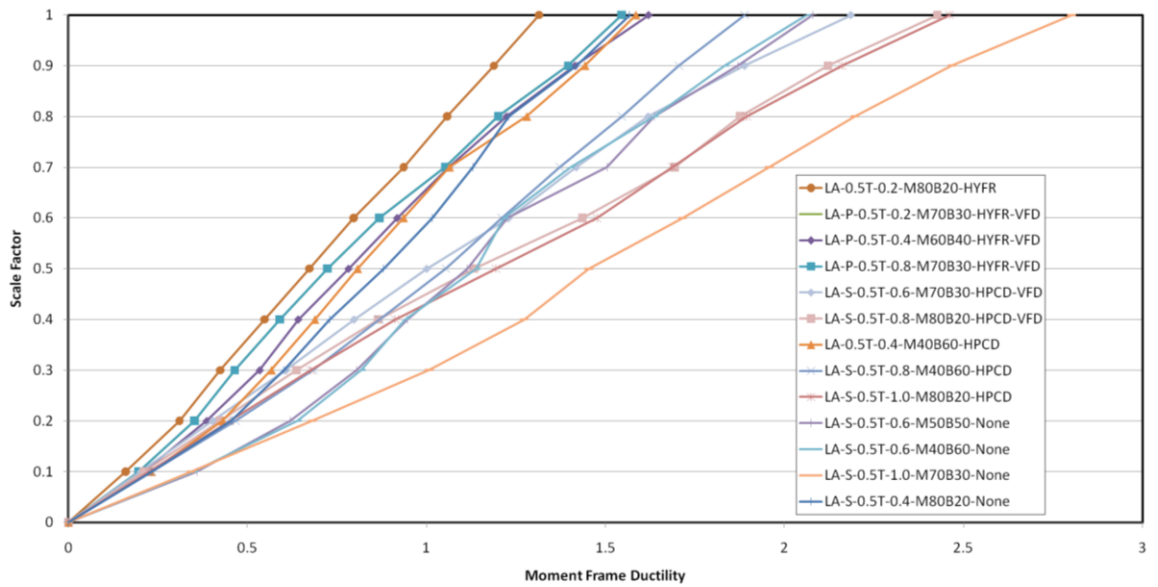


Figure A- 11: Los Angeles 0.5T Moment Frame Ductility

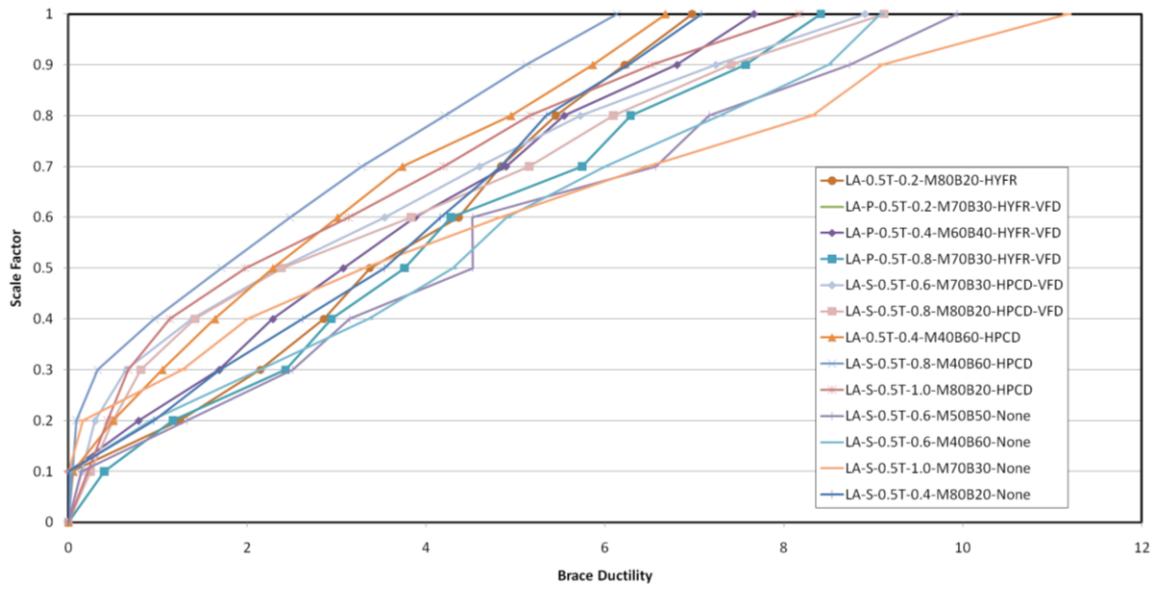


Figure A- 12: Los Angeles 0.5T Brace Ductility

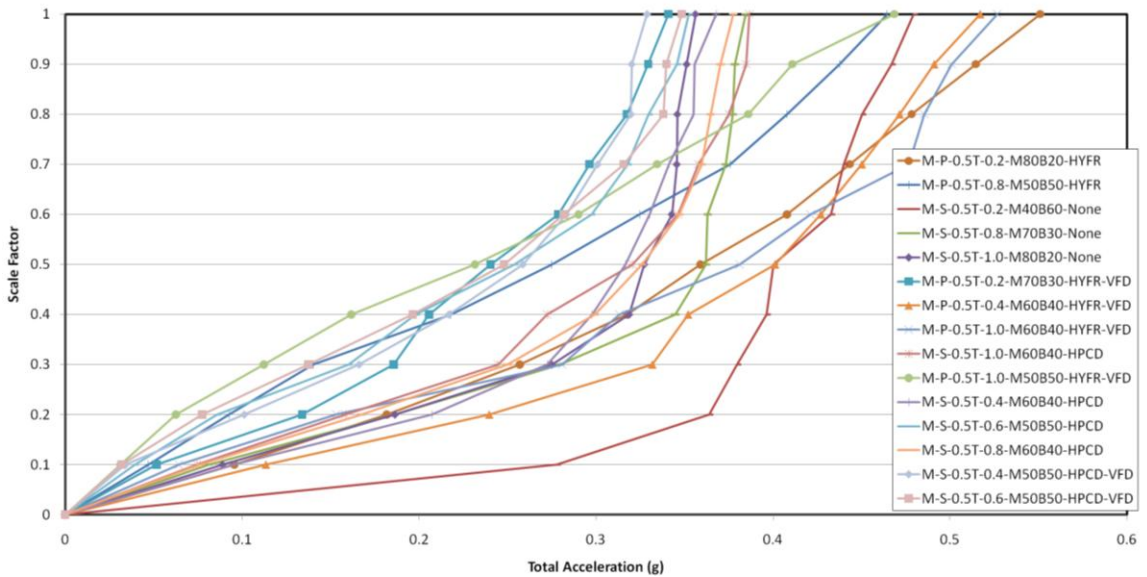


Figure A- 13: Memphis 0.5T Acceleration

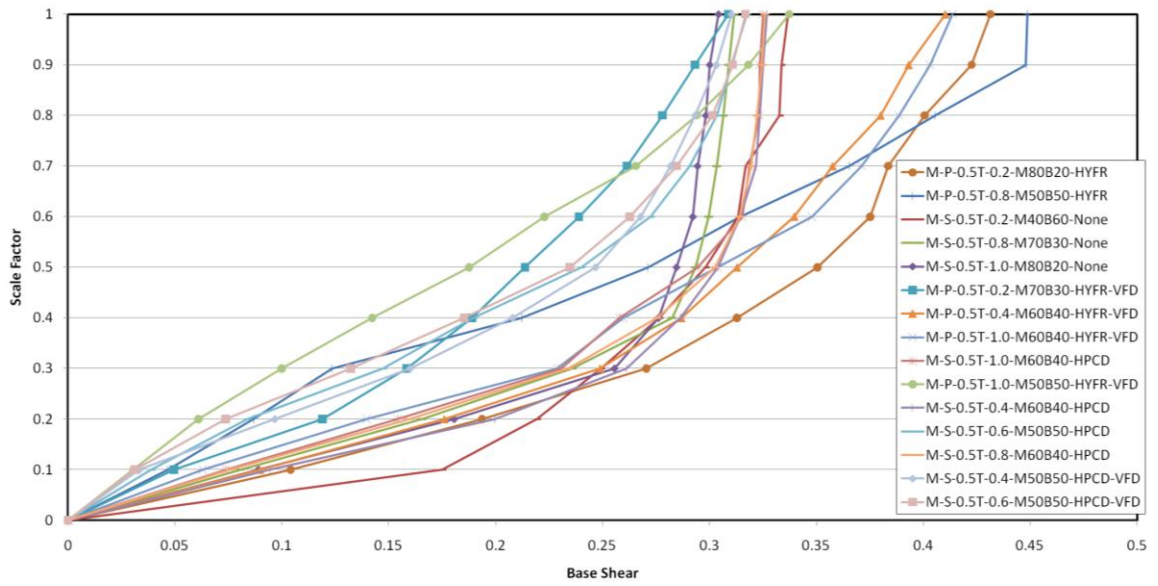


Figure A- 14: Memphis 0.5T Base Shear

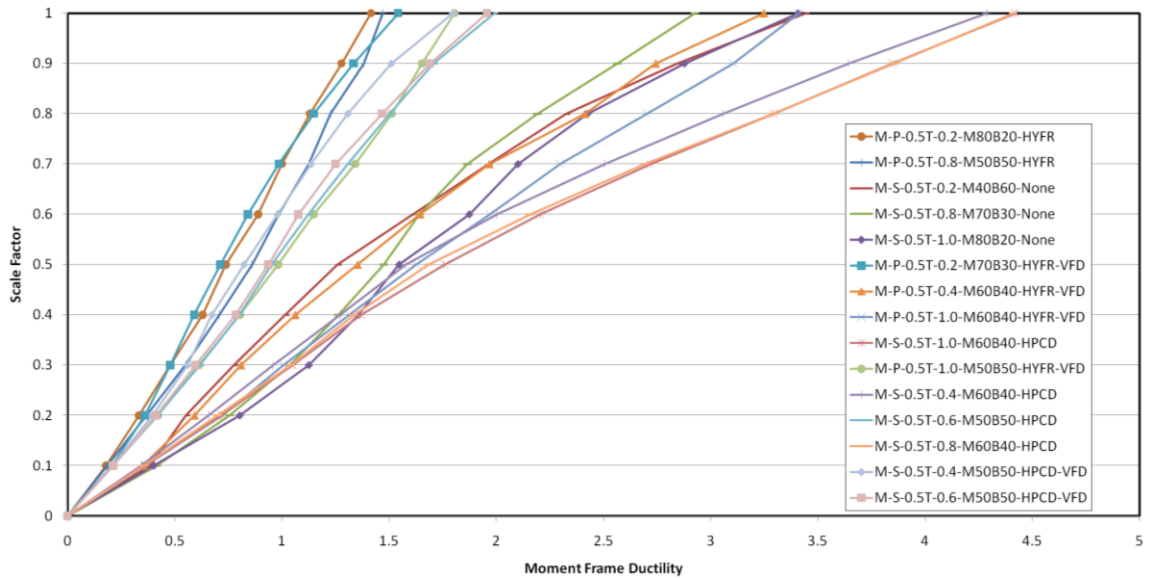


Figure A- 15: Memphis 0.5T Moment Frame Ductility

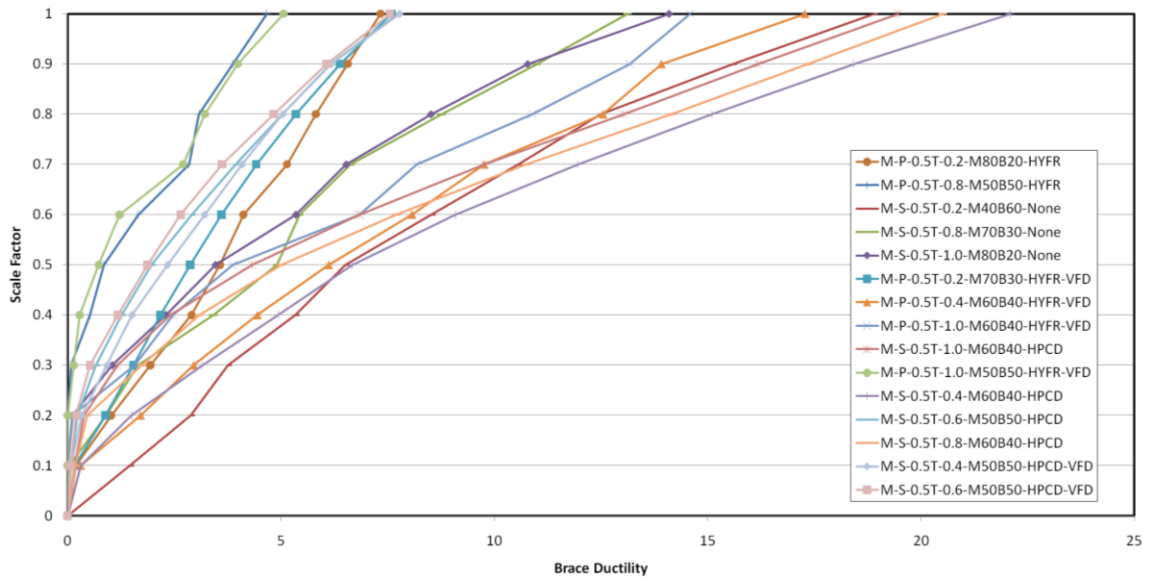


Figure A- 16: Memphis 0.5T Brace Ductility

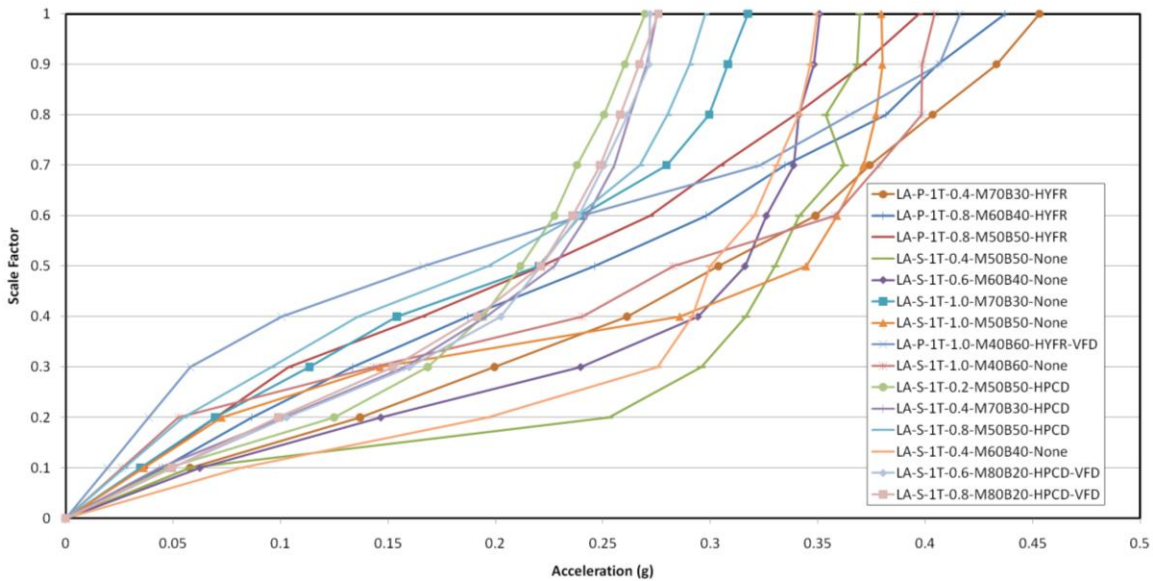


Figure A- 17: Los Angeles 1T Acceleration

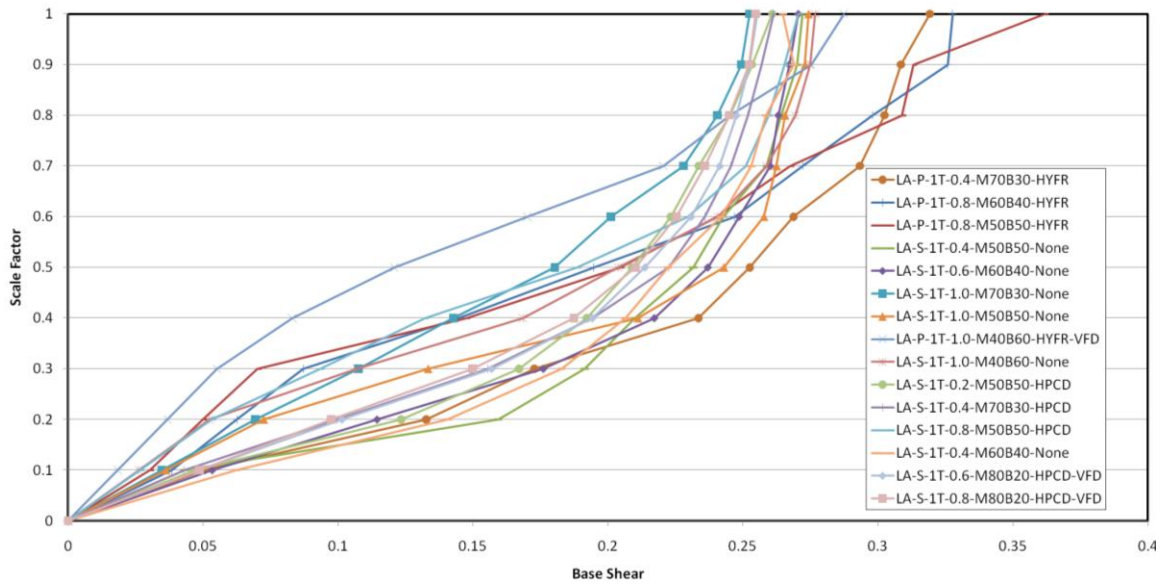


Figure A- 18: Los Angeles 1T Base Shear

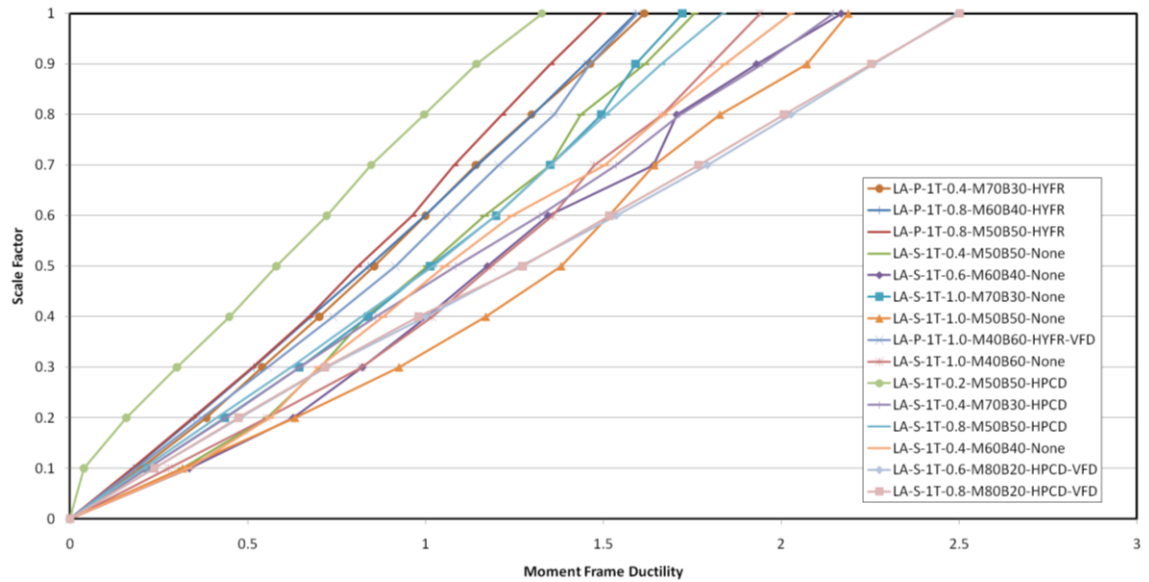


Figure A- 19: Los Angeles 1T Moment Frame Ductility

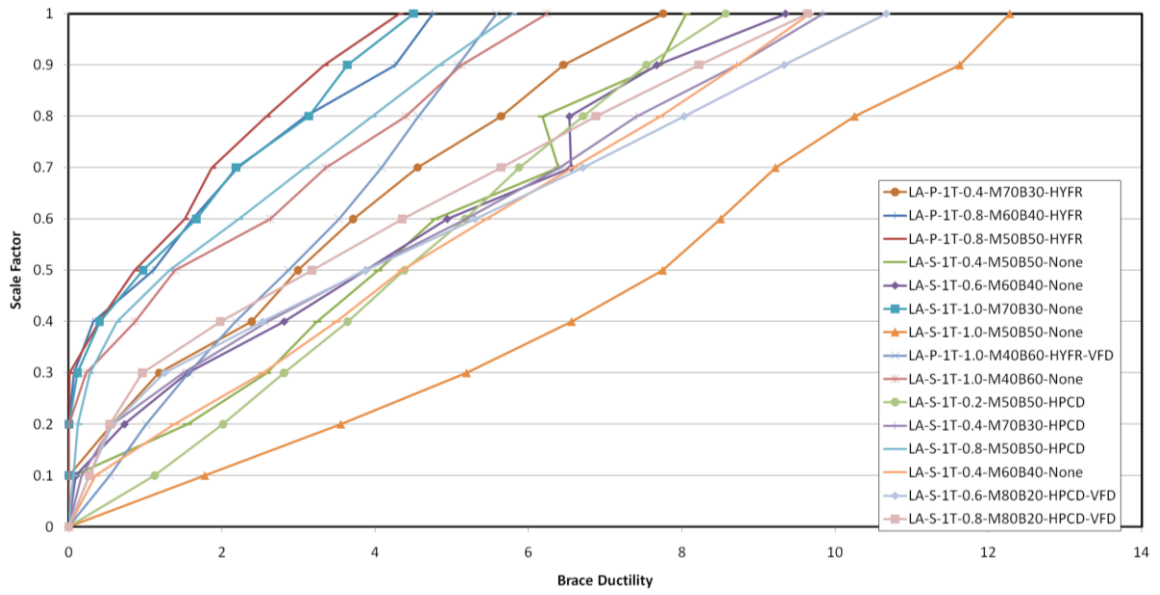


Figure A- 20: Los Angeles 1T Brace Ductility

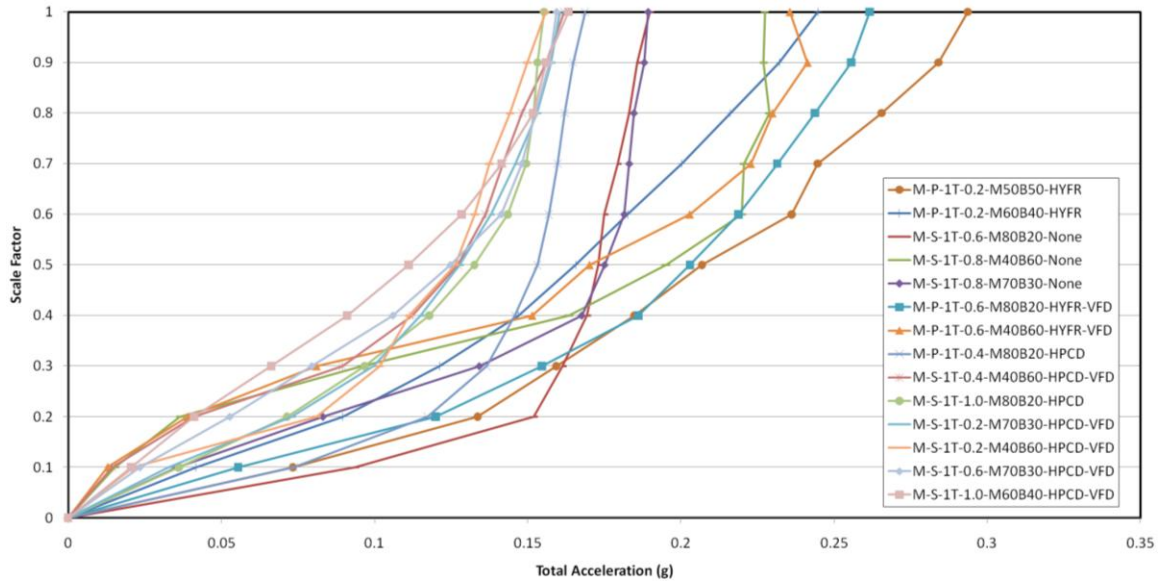


Figure A- 21: Memphis 1T Acceleration

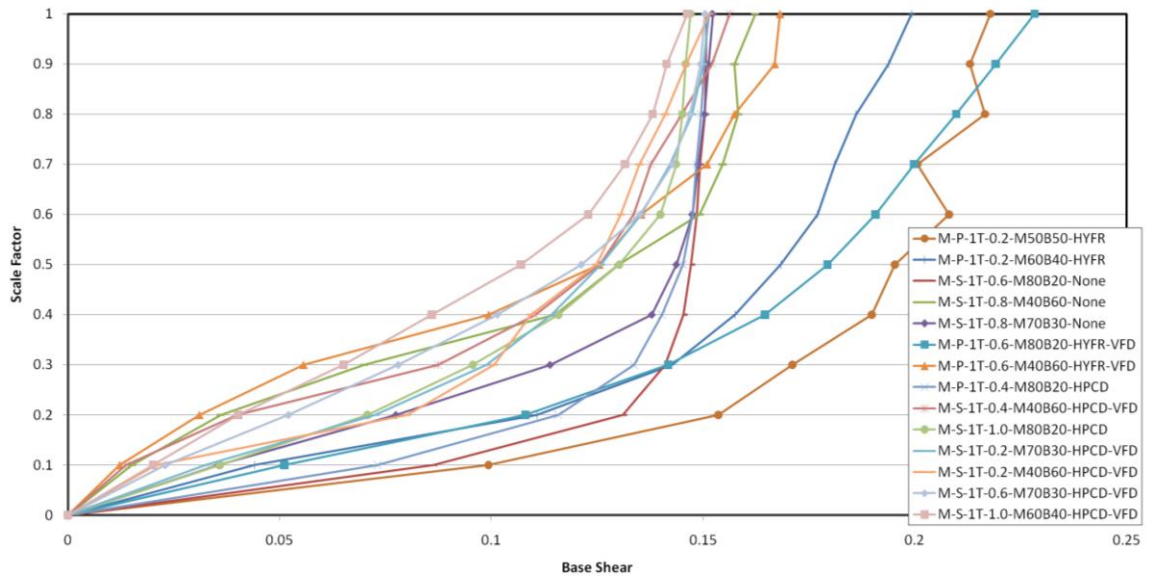


Figure A- 22: Memphis 1T Base Shear

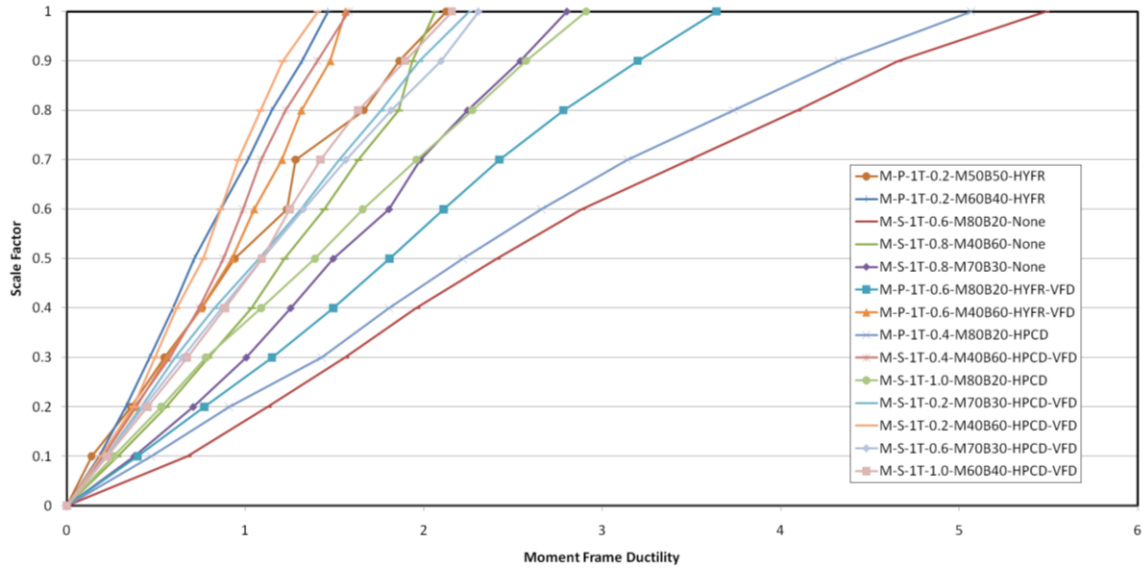


Figure A- 23: Memphis 1T Moment Frame Ductility

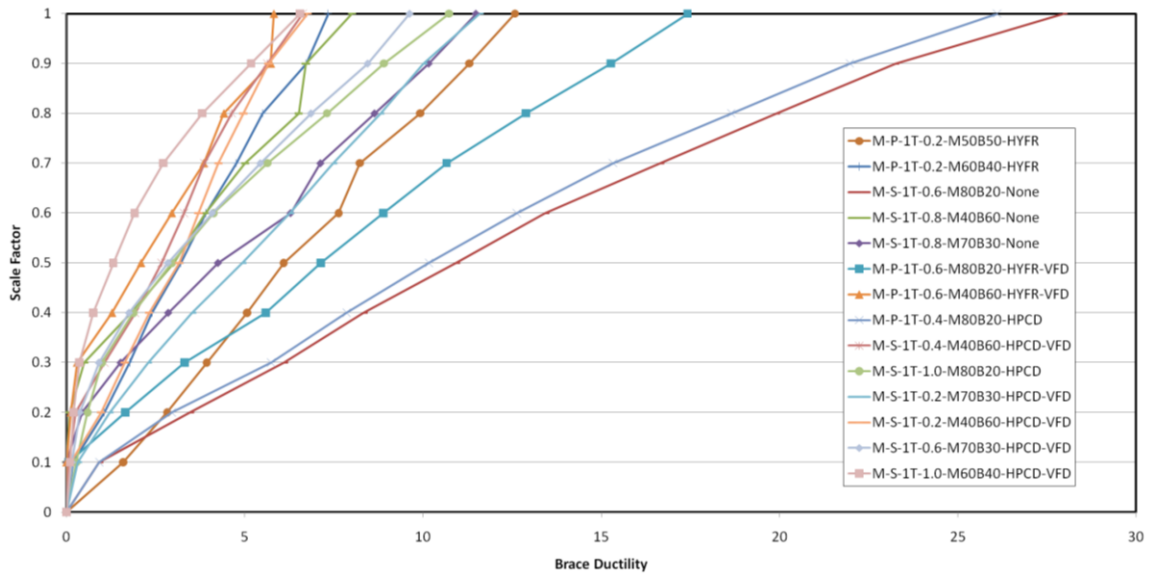


Figure A- 24: Memphis 1T Brace Ductility

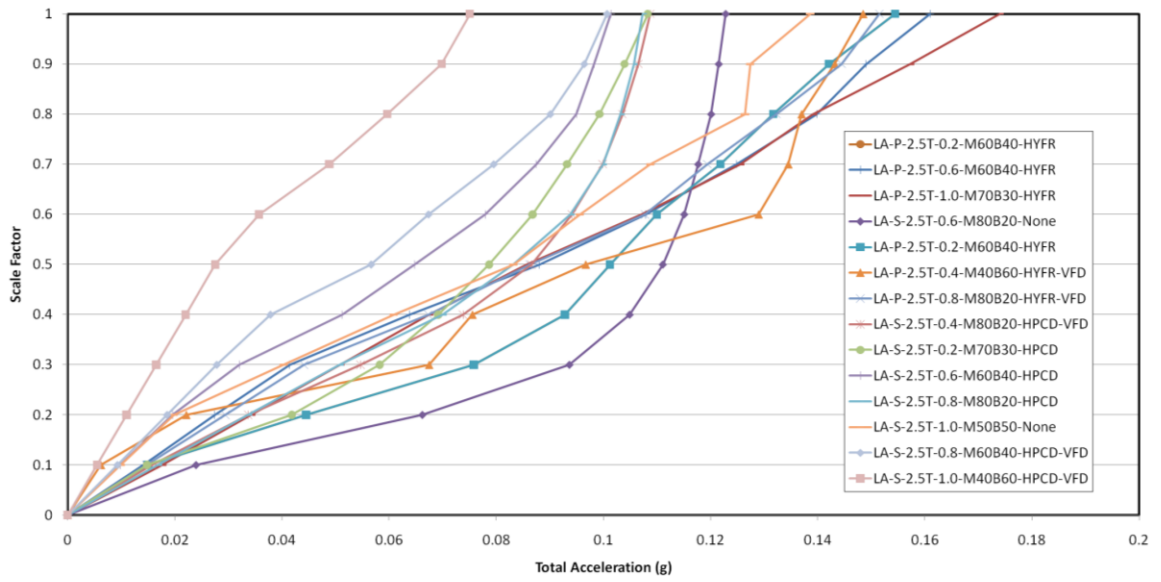


Figure A- 25: Los Angeles 2.5T Acceleration

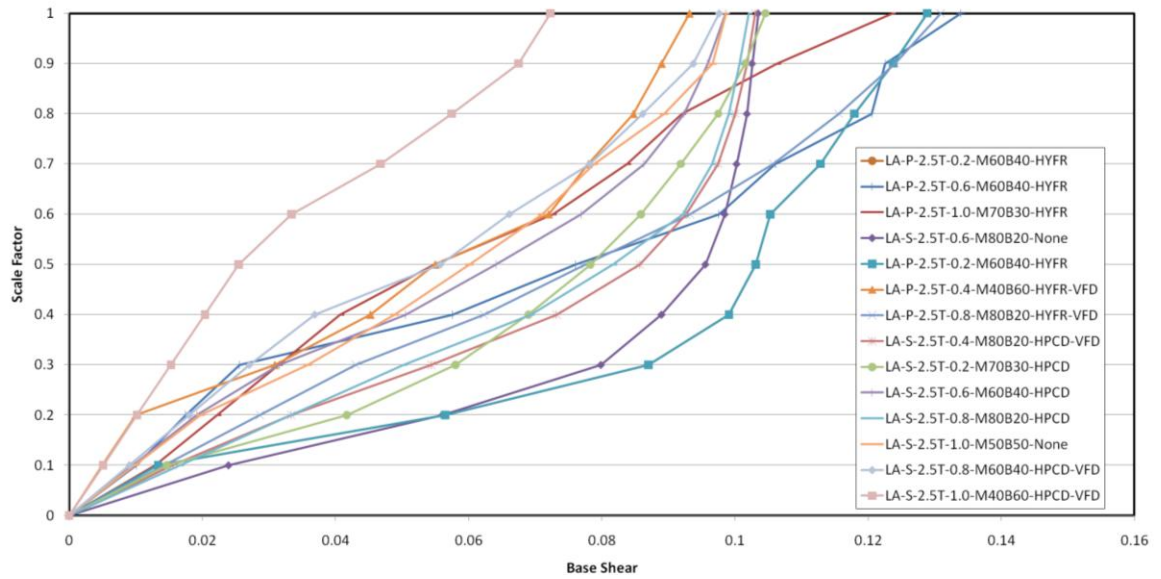


Figure A- 26: Los Angeles 2.5T Base Shear

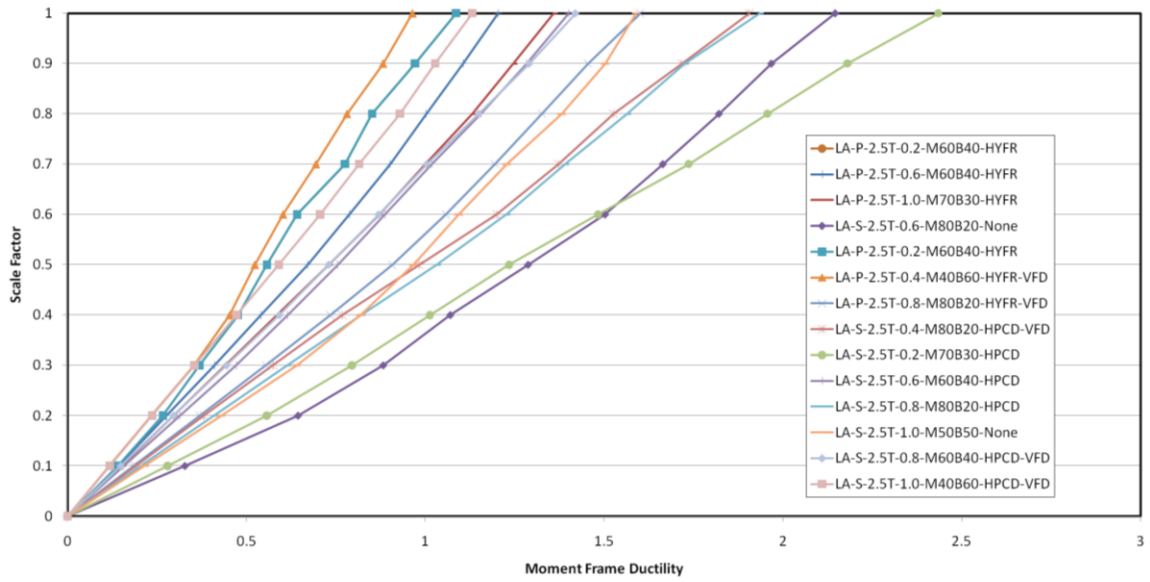


Figure A- 27: Los Angeles 2.5T Moment Frame Ductility

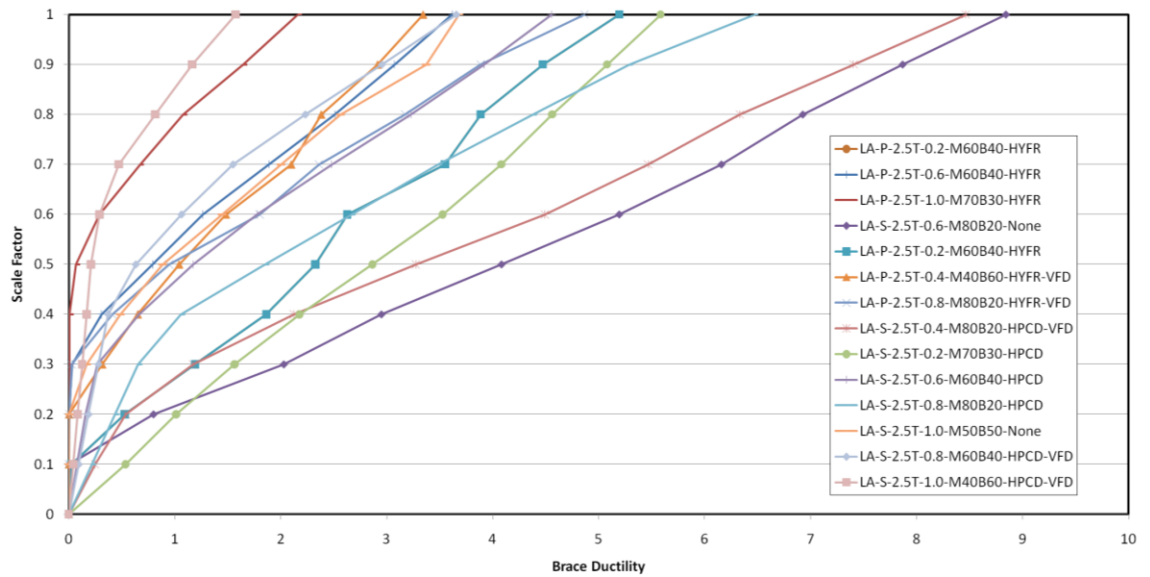


Figure A- 28: Los Angeles 2.5T Brace Ductility

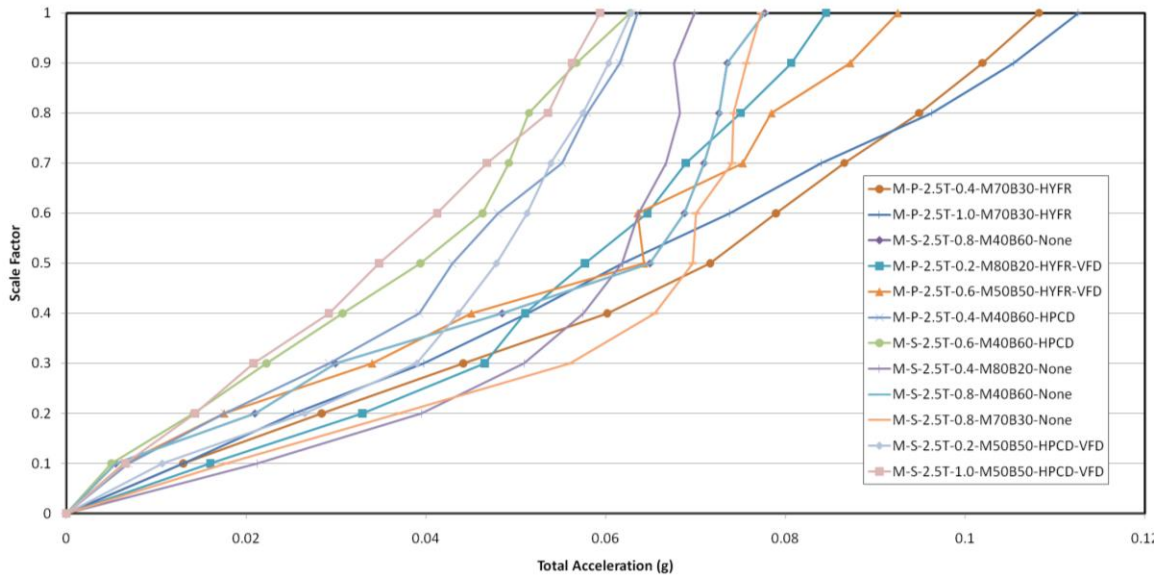


Figure A- 29: Memphis 2.5T Acceleration

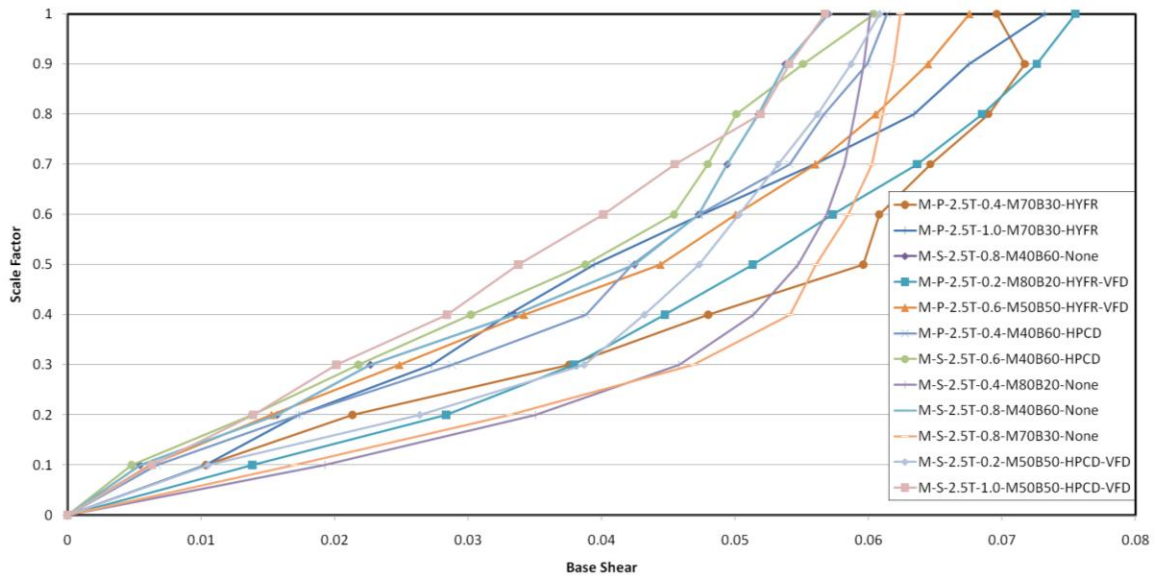


Figure A- 30: Memphis 2.5T Base Shear

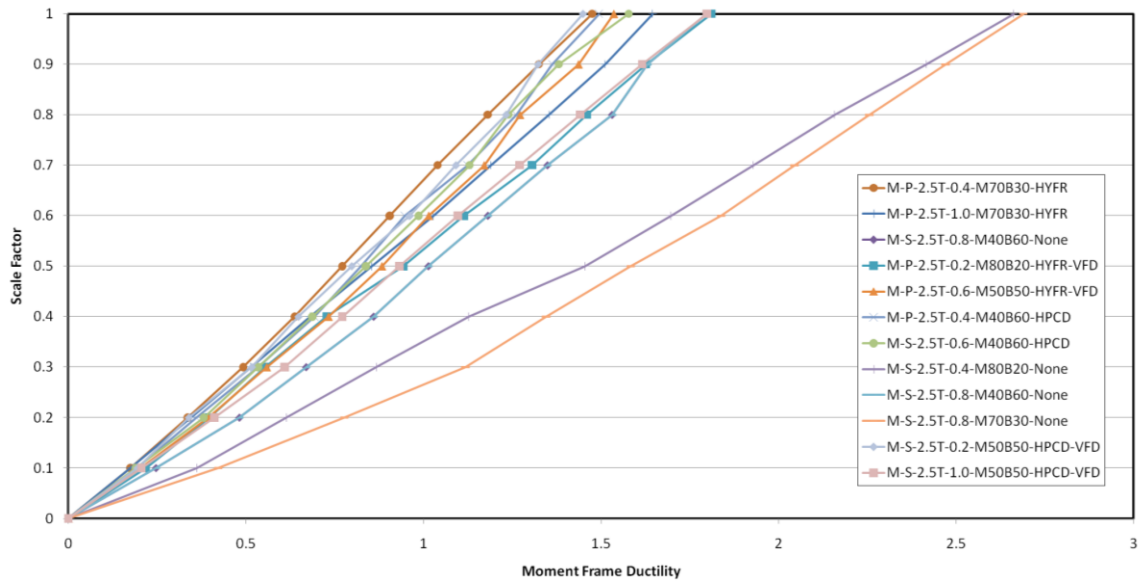


Figure A- 31: Memphis 2.5T Moment Frame Ductility

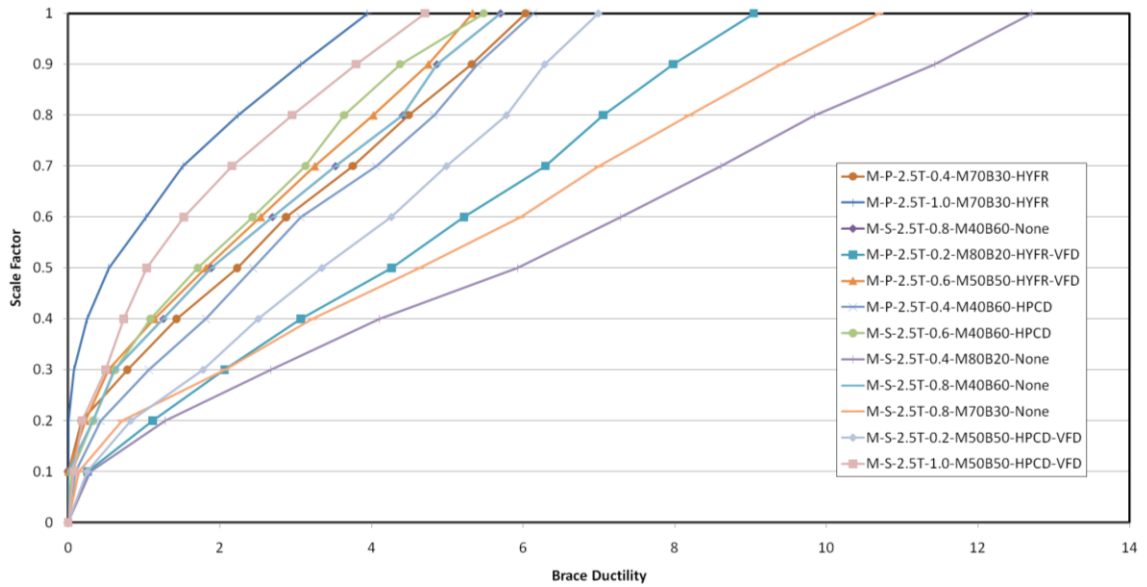


Figure A- 32: Memphis 2.5T Brace Ductility

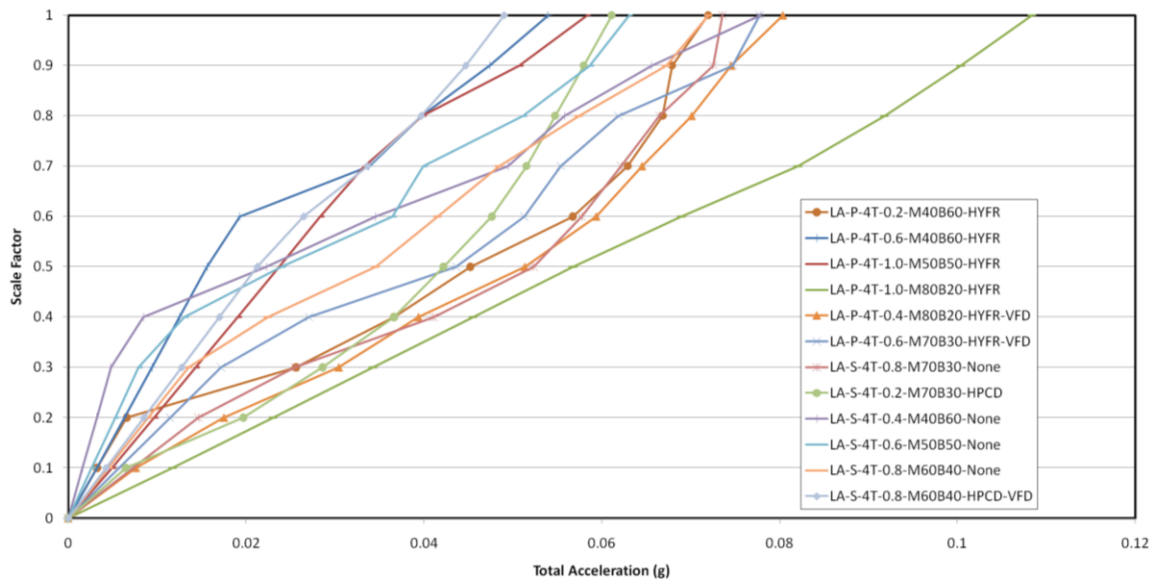


Figure A- 33: Los Angeles 4T Acceleration

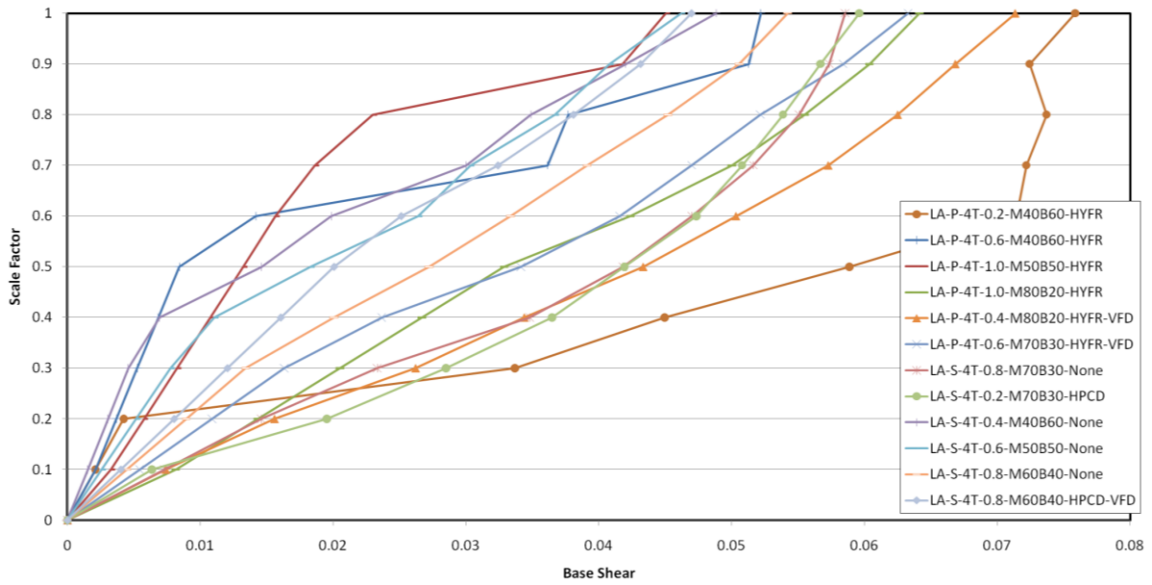


Figure A- 34: Los Angeles 4T Base Shear

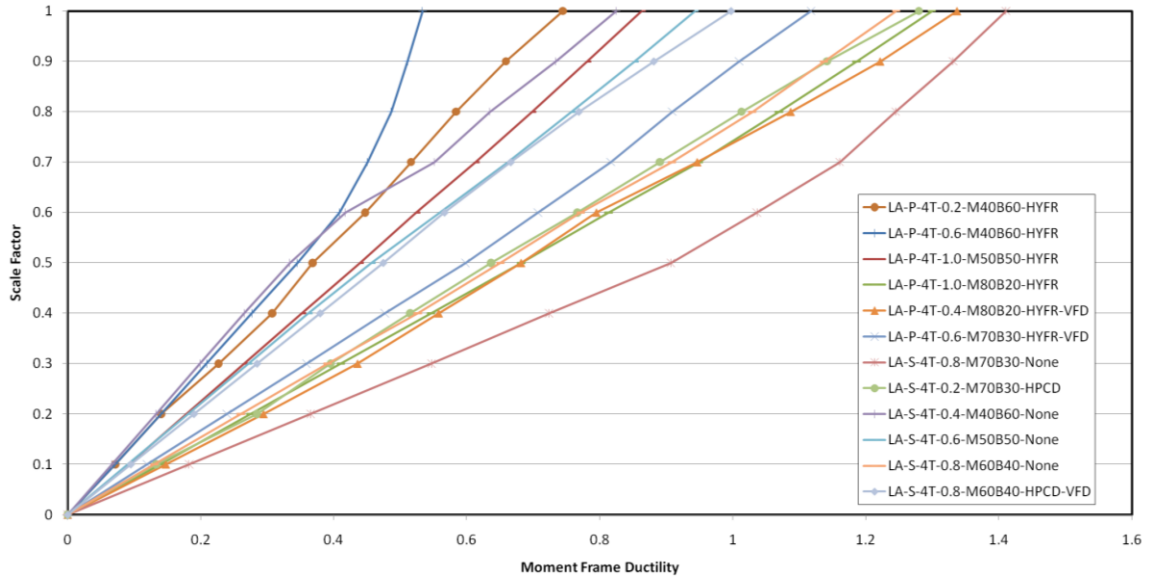


Figure A- 35: Los Angeles 4T Moment Frame Ductility

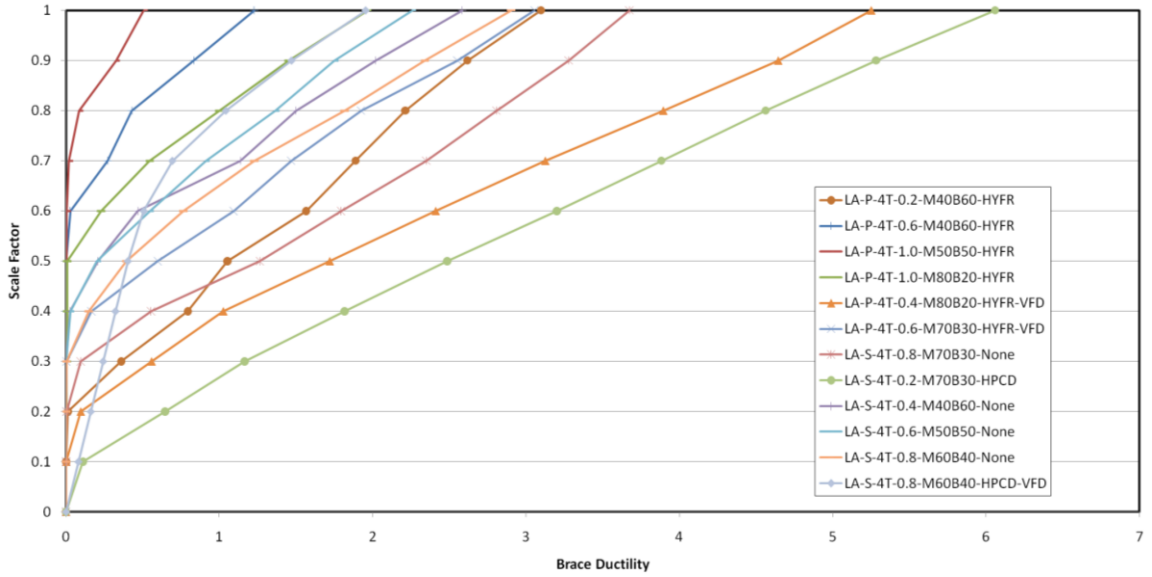


Figure A- 36: Los Angeles 4T Brace Ductility

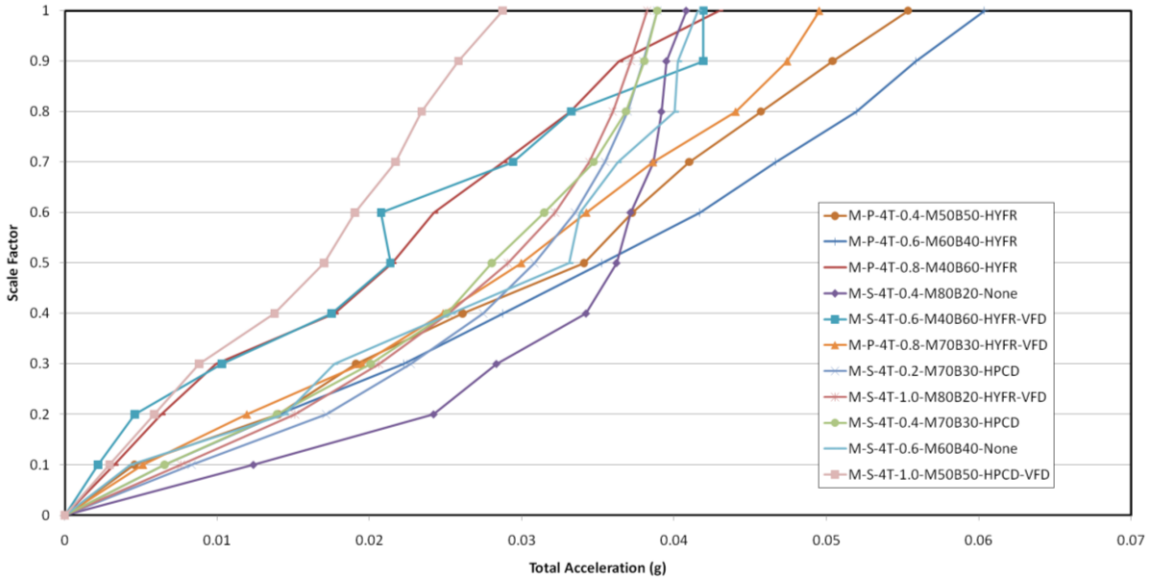


Figure A- 37: Memphis 4T Acceleration

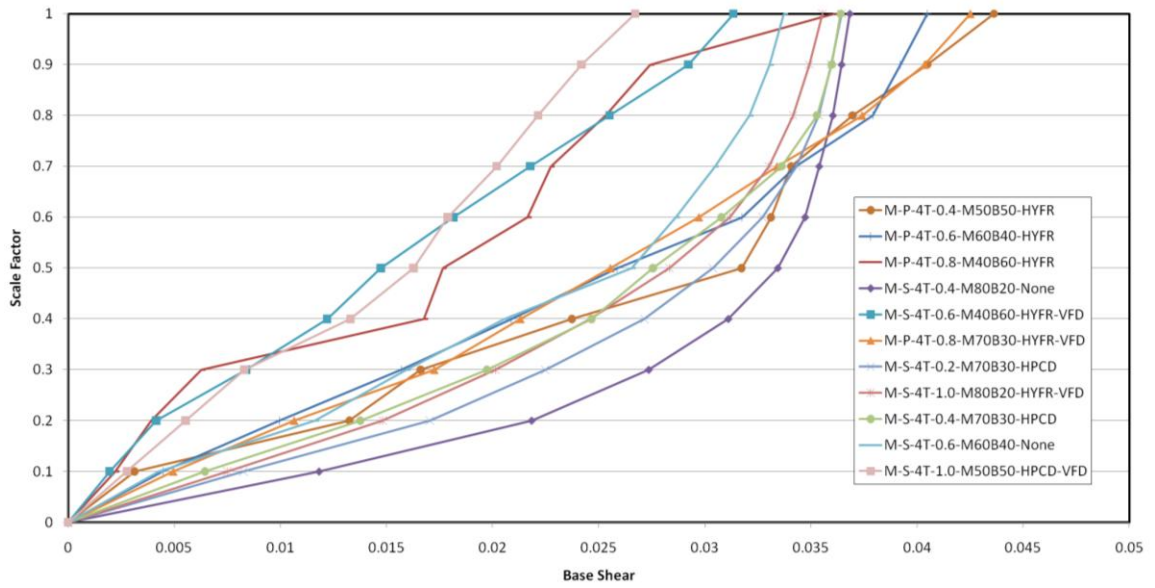


Figure A- 38: Memphis 4T Base Shear

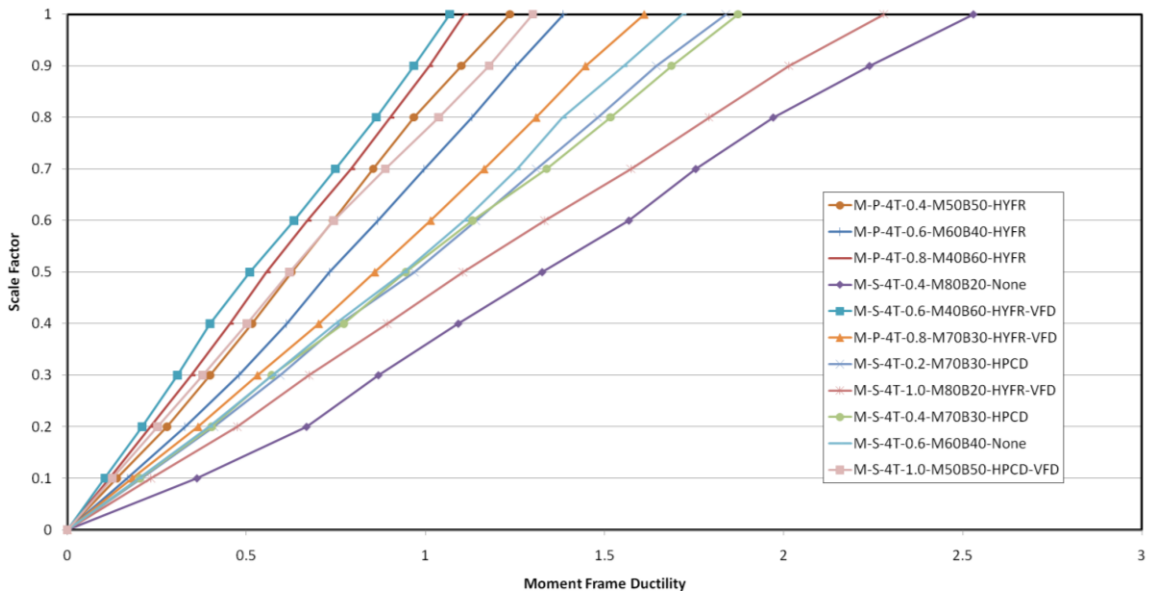


Figure A- 39: Memphis 4T Moment Frame Ductility

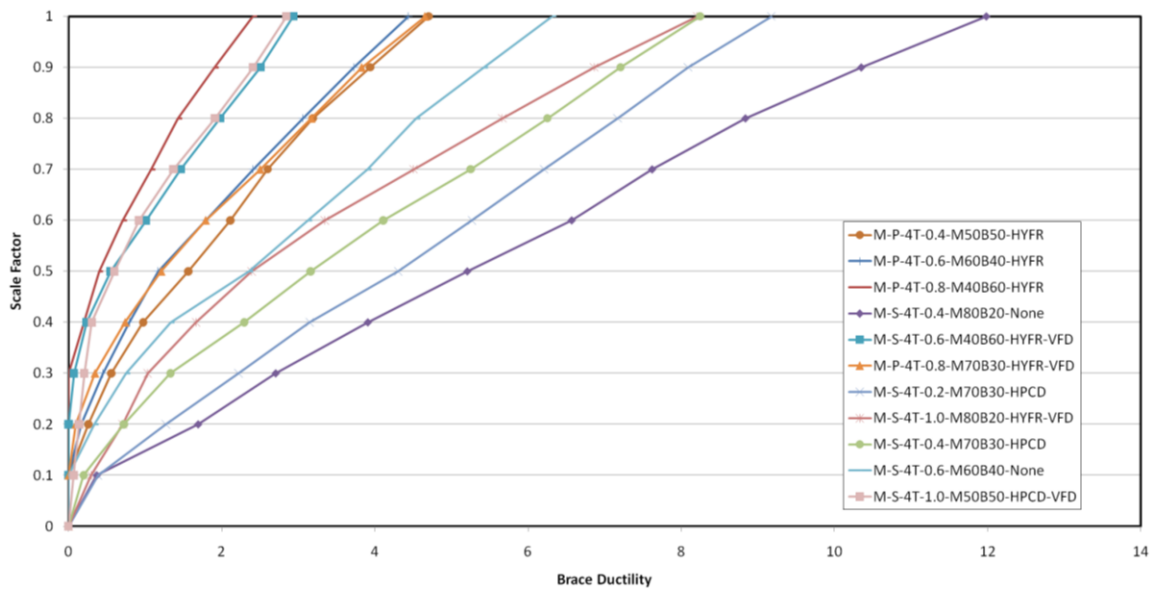


Figure A- 40: Memphis 4T Brace Ductility

Appendix B. Final Design

Appendix B presents the results for all of the full factorial design presented in Chapter 6.

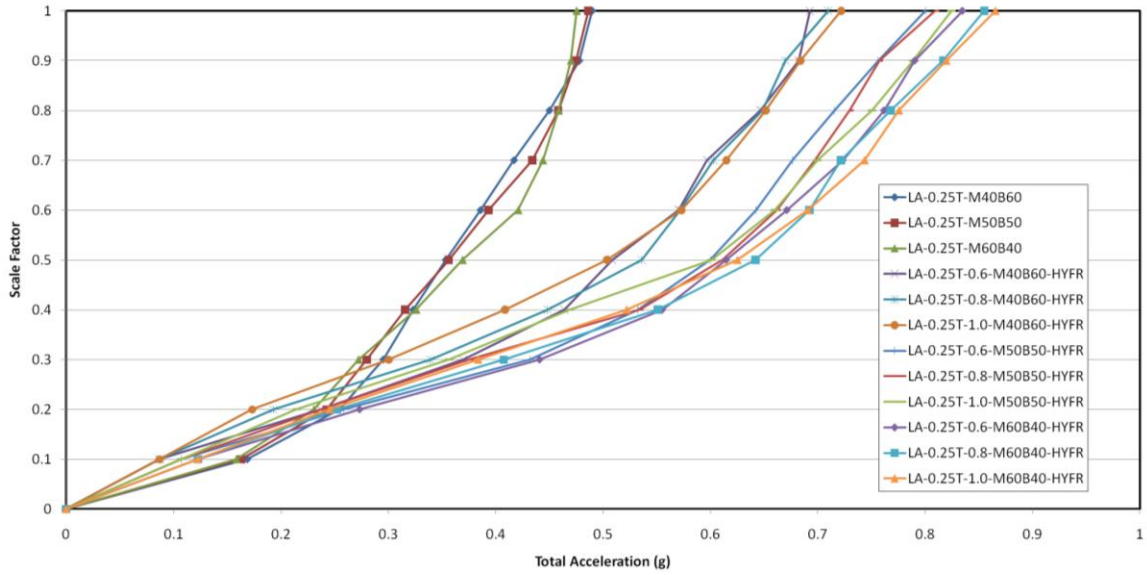


Figure B- 1: Los Angeles 0.25T HYFR Acceleration

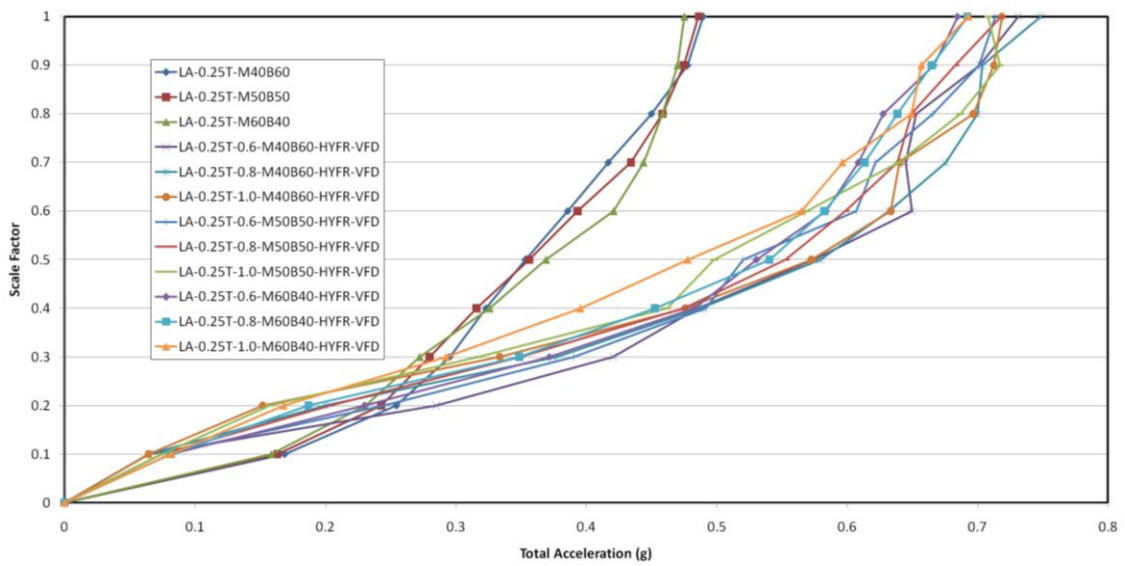


Figure B- 2: Los Angeles 0.25T HYFR-VFD Acceleration

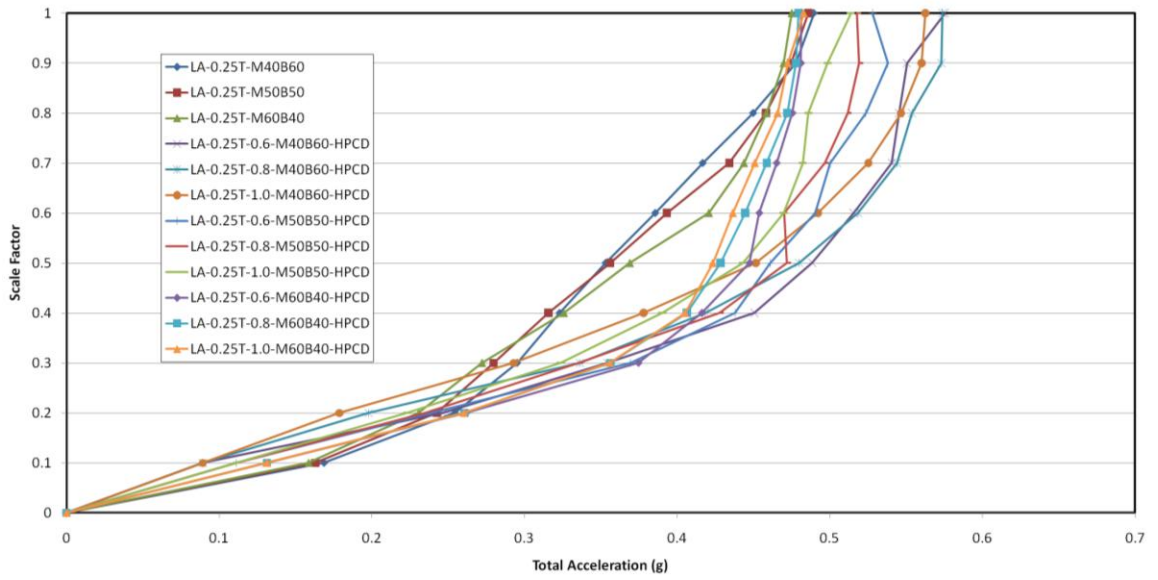


Figure B- 3: Los Angeles 0.25T HPCD Acceleration

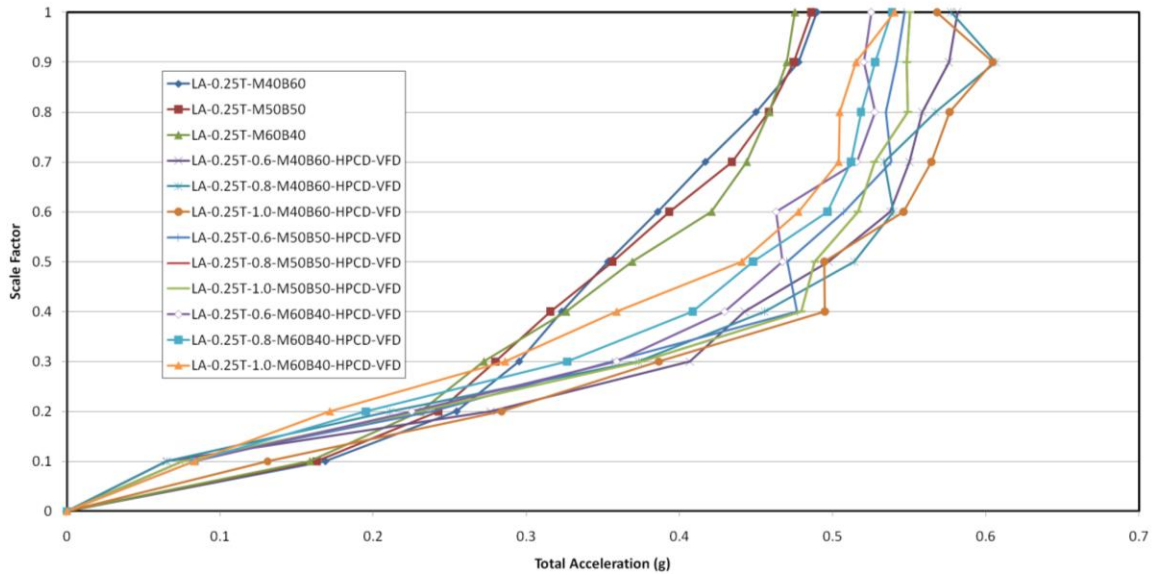


Figure B- 4: Los Angeles 0.25T HPCD-VFD Acceleration

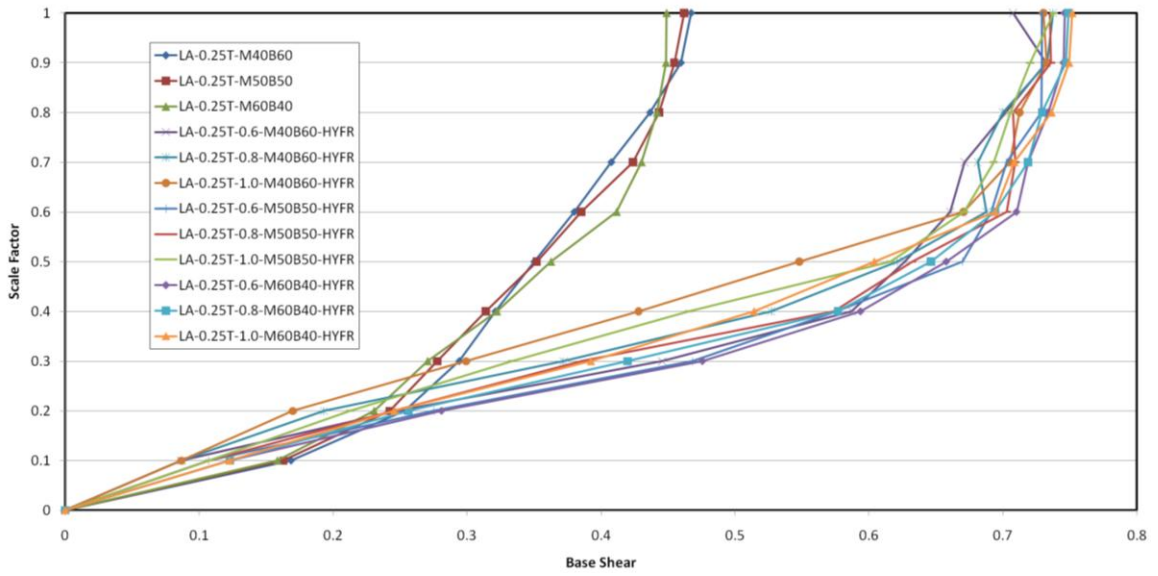


Figure B- 5: Los Angeles 0.25T HYFR Base Shear

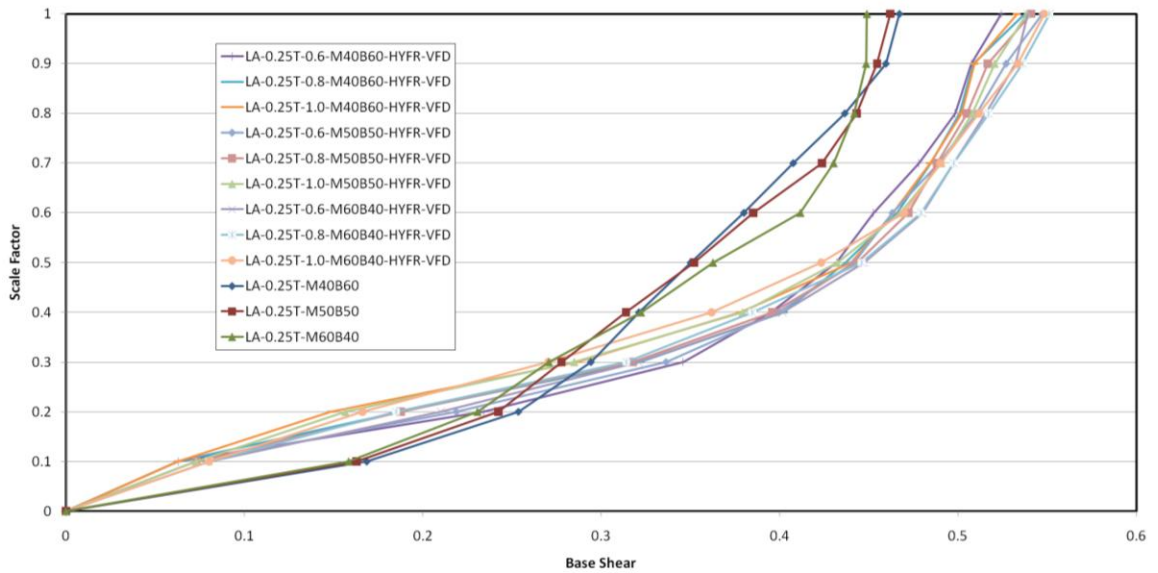


Figure B- 6: Los Angeles 0.25T HYFR-VFD Base Shear

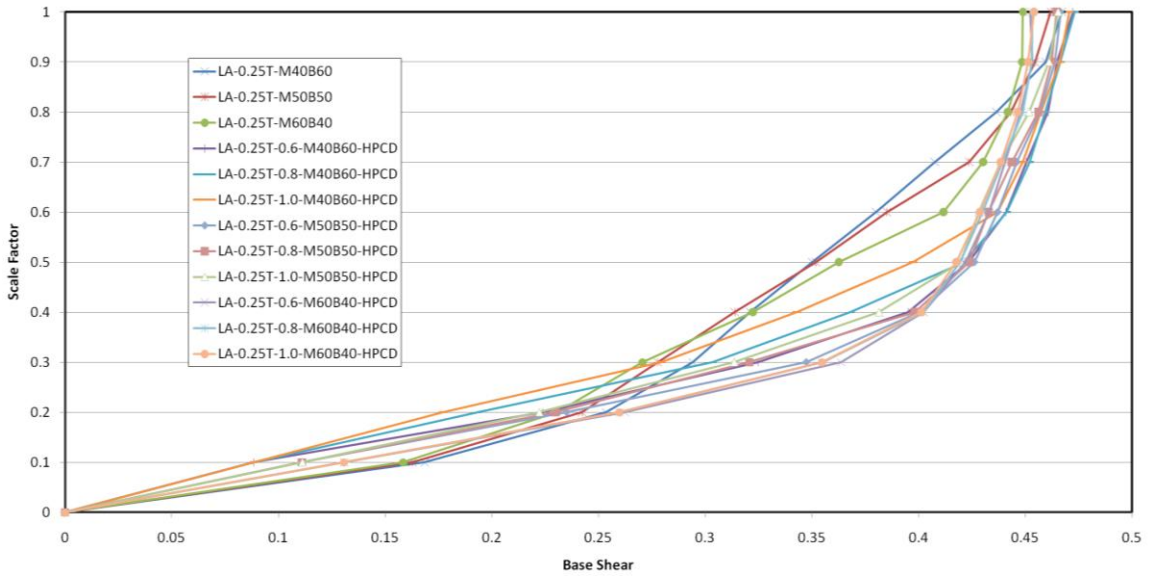


Figure B- 7: Los Angeles 0.25T HPCD Base Shear

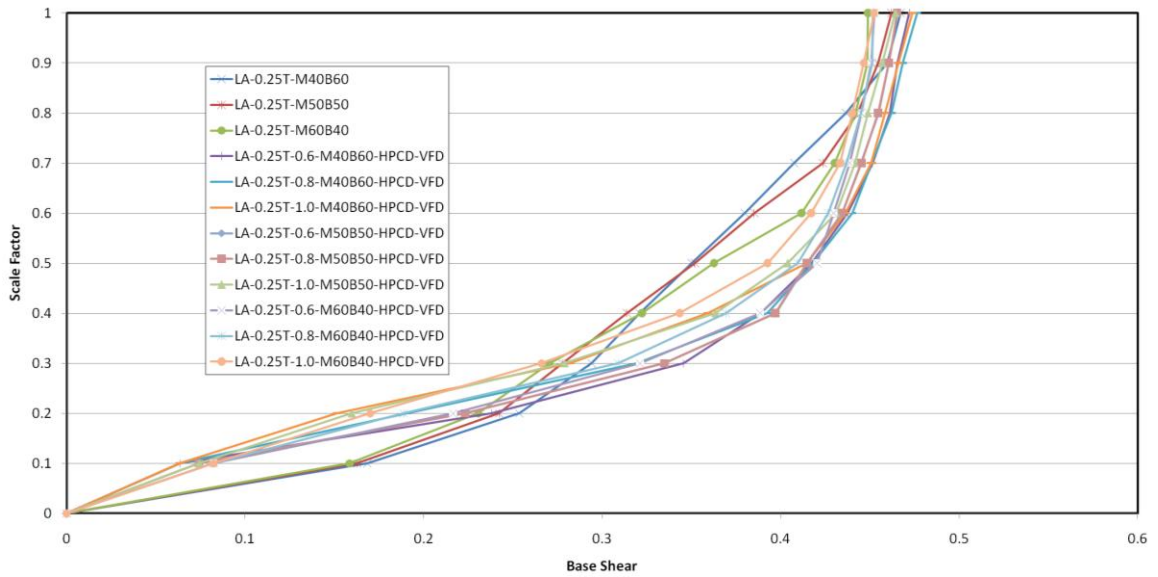


Figure B- 8: Los Angeles 0.25T HPCD-VFD Base Shear

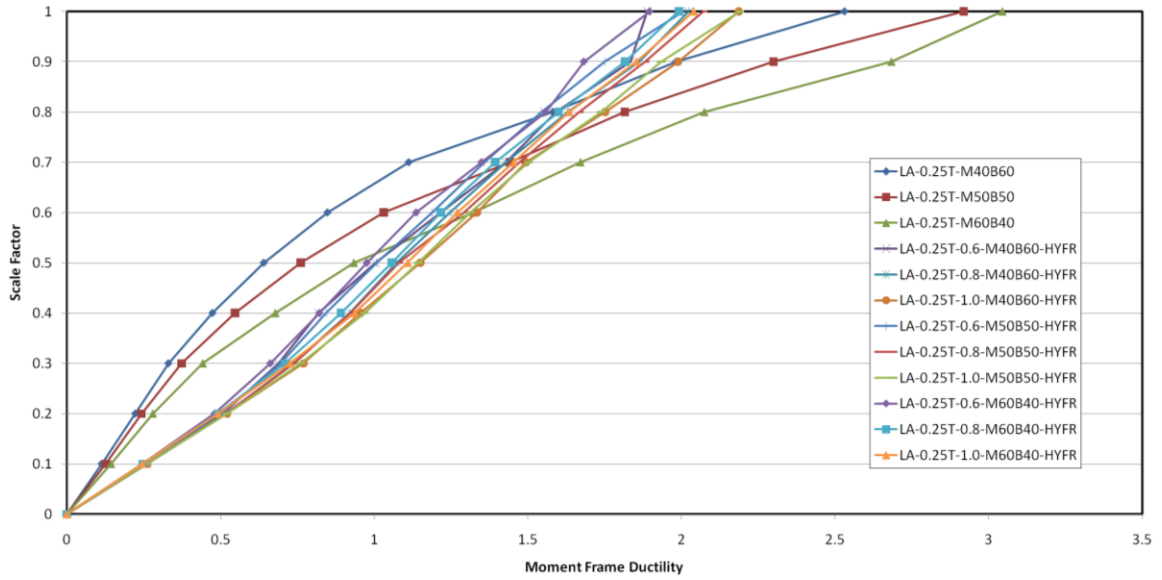


Figure B- 9: Los Angeles 0.25T HYFR Moment Frame Ductility

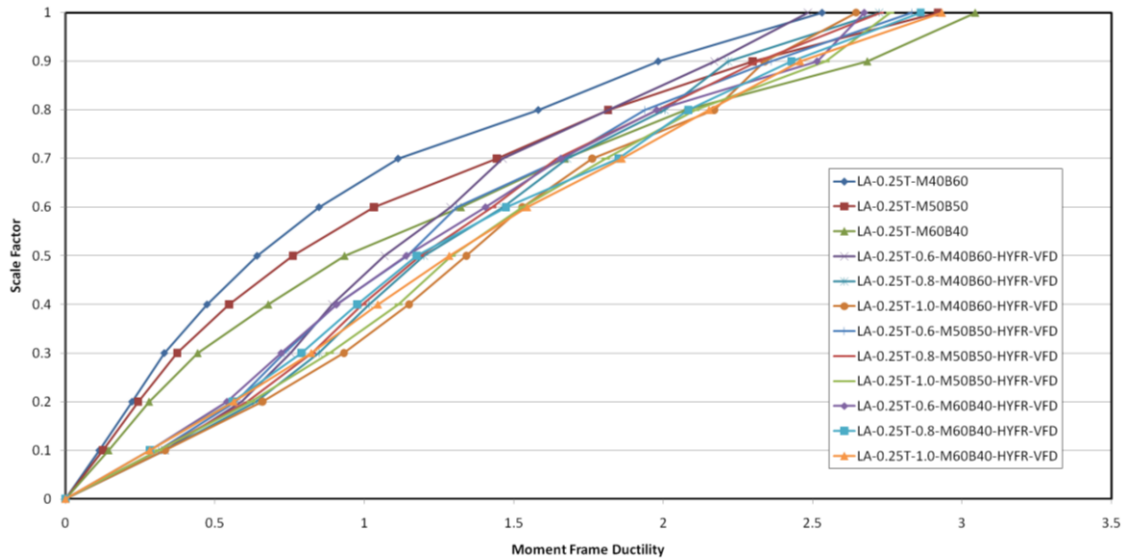


Figure B- 10: Los Angeles 0.25T HYFR-VFD Moment Frame Ductility

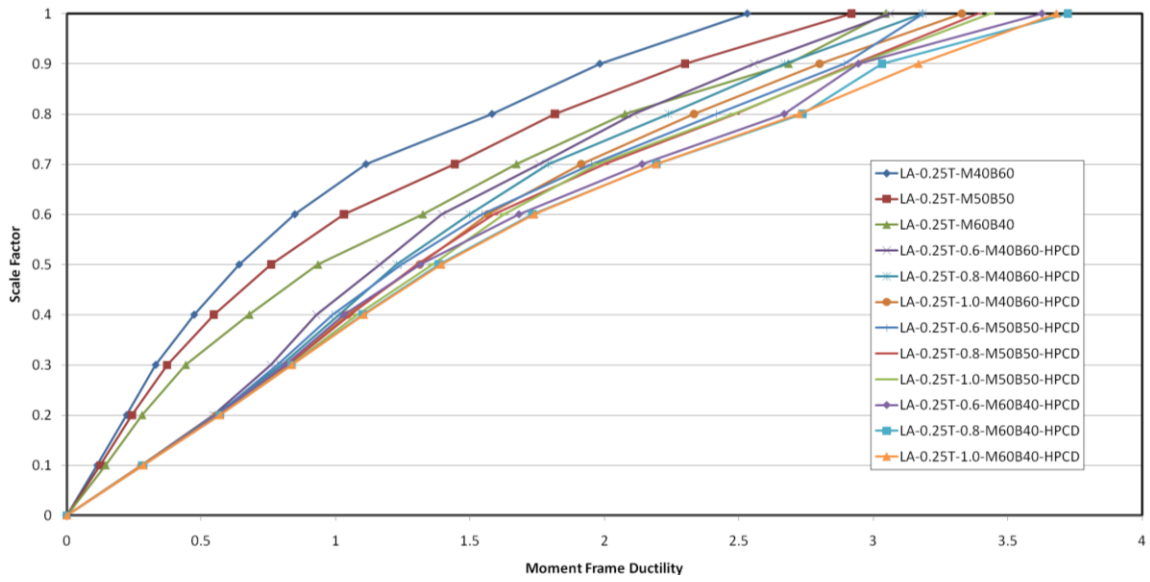


Figure B- 11: Los Angeles 0.25T HPCD Moment Frame Ductility

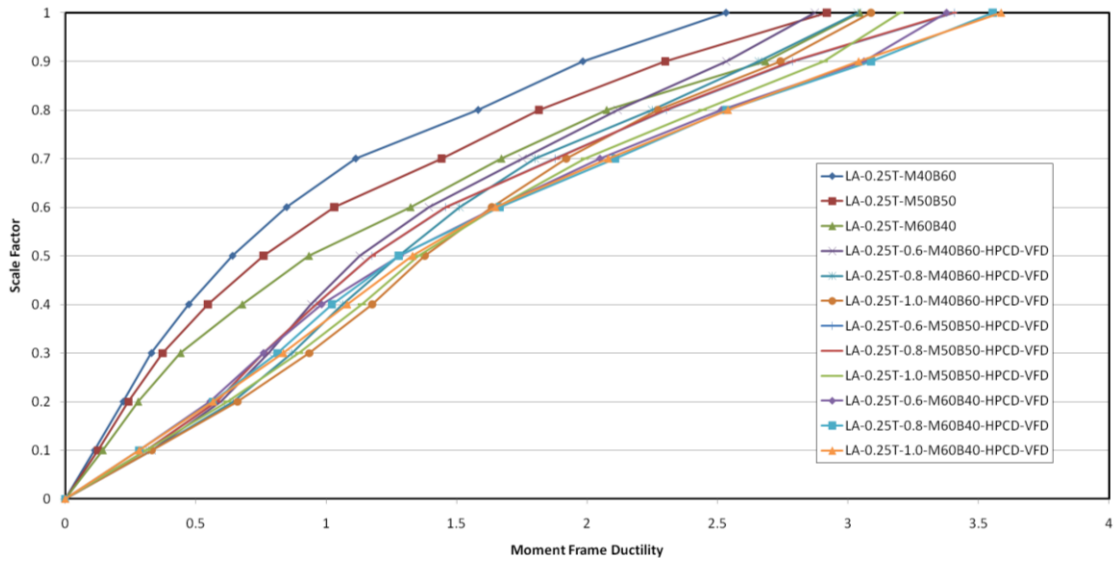


Figure B- 12: Los Angeles 0.25T HPCD-VFD Moment Frame Ductility

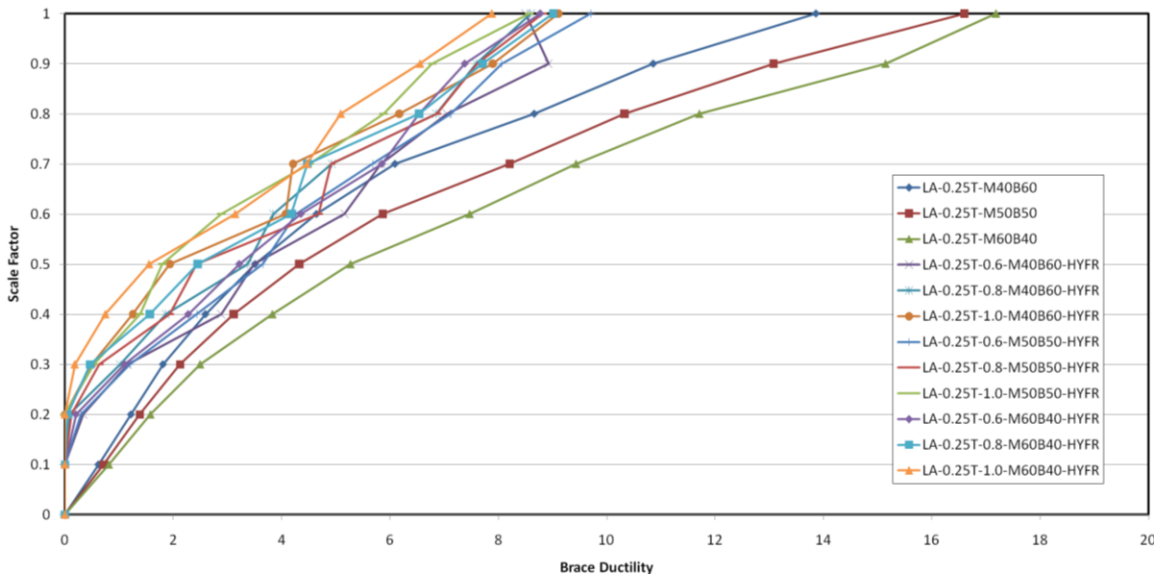


Figure B- 13: Los Angeles 0.25T HYFR Brace Ductility

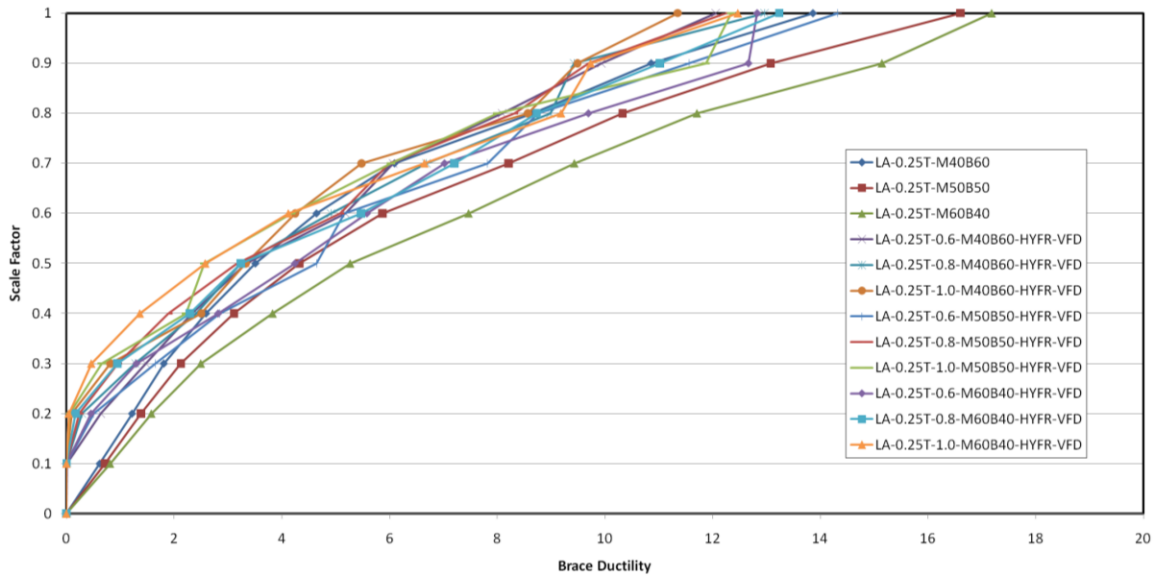


Figure B- 14: Los Angeles 0.25T HYFR-VFD Brace Ductility

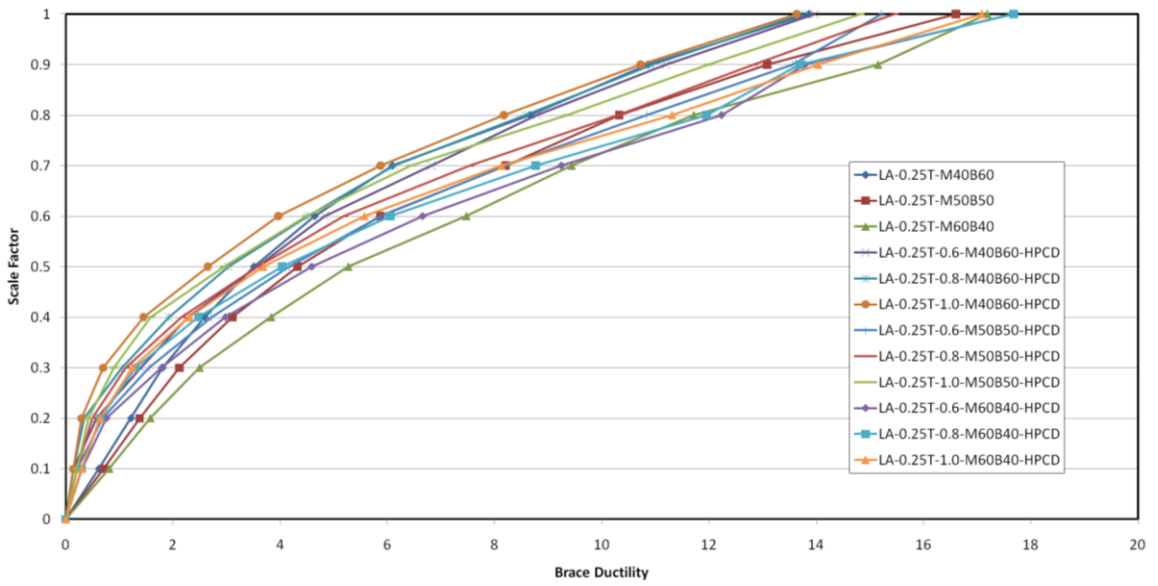


Figure B- 15: Los Angeles 0.25T HPCD Brace Ductility

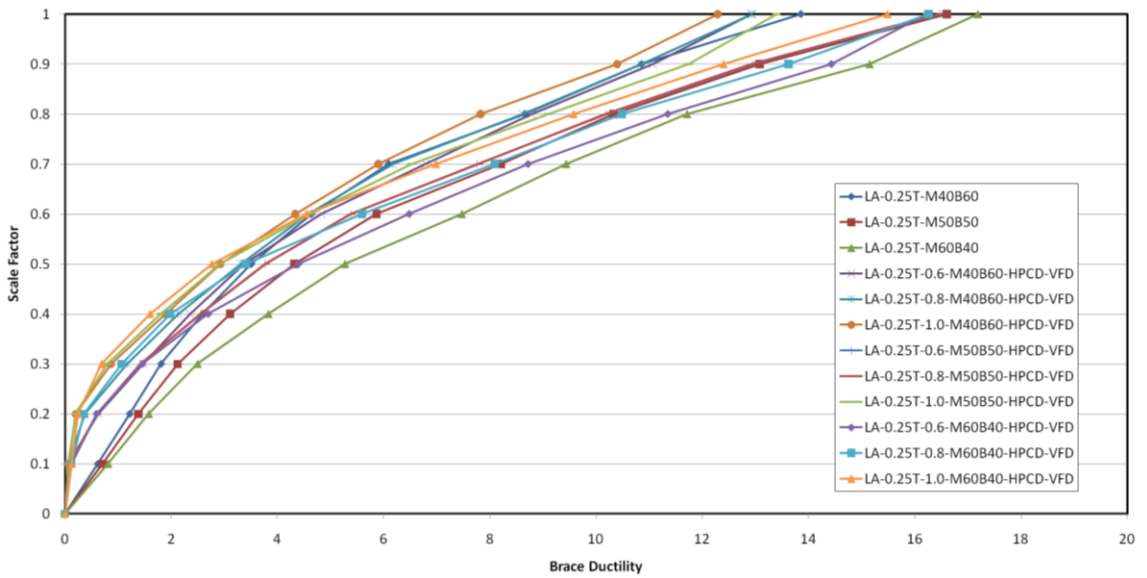


Figure B- 16: Los Angeles 0.25T HPCD-VFD Brace Ductility

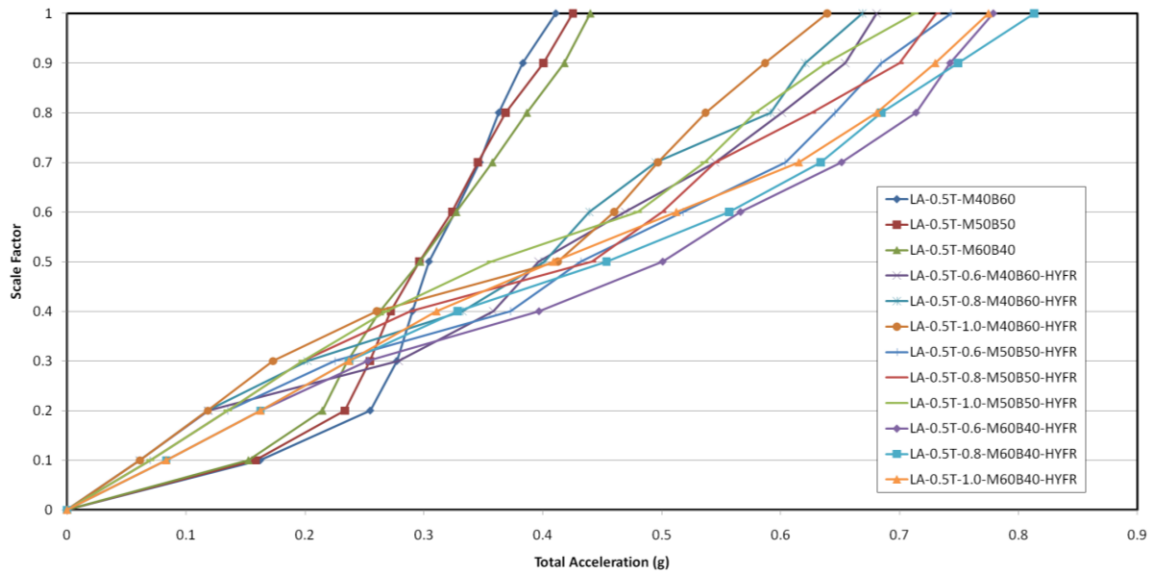


Figure B- 17: Los Angeles 0.5T HYFR Acceleration

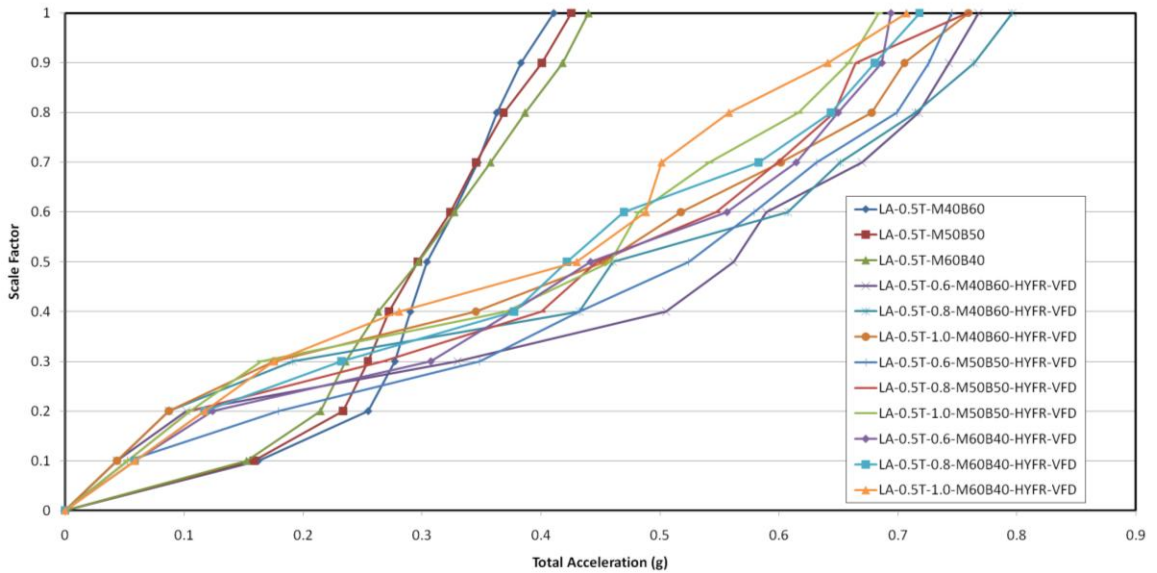


Figure B- 18: Los Angeles 0.5T HYFR-VFD Acceleration

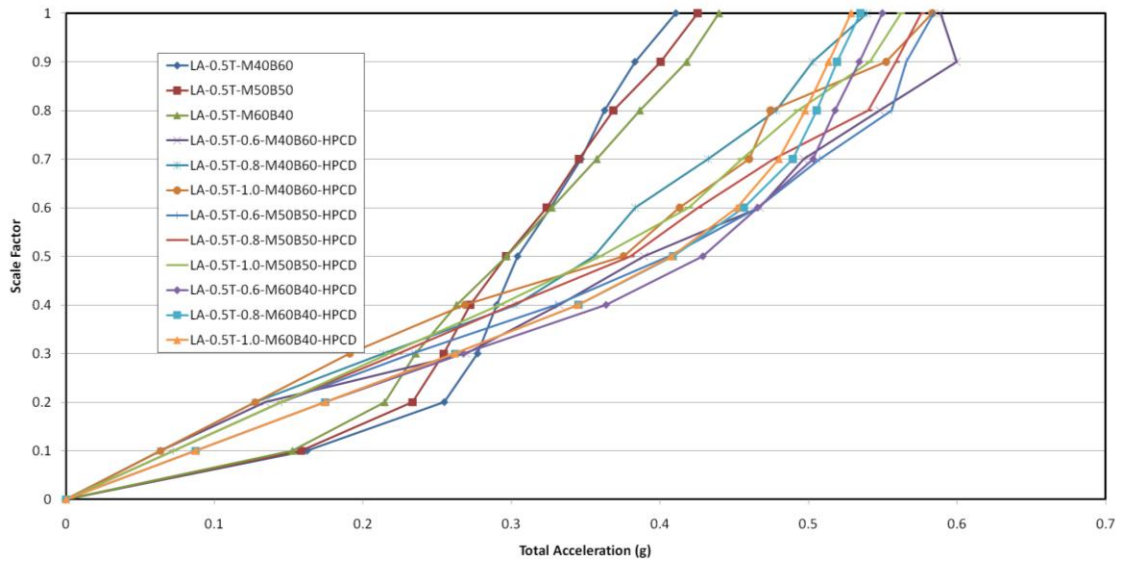


Figure B- 19: Los Angeles 0.5T HPCD Acceleration

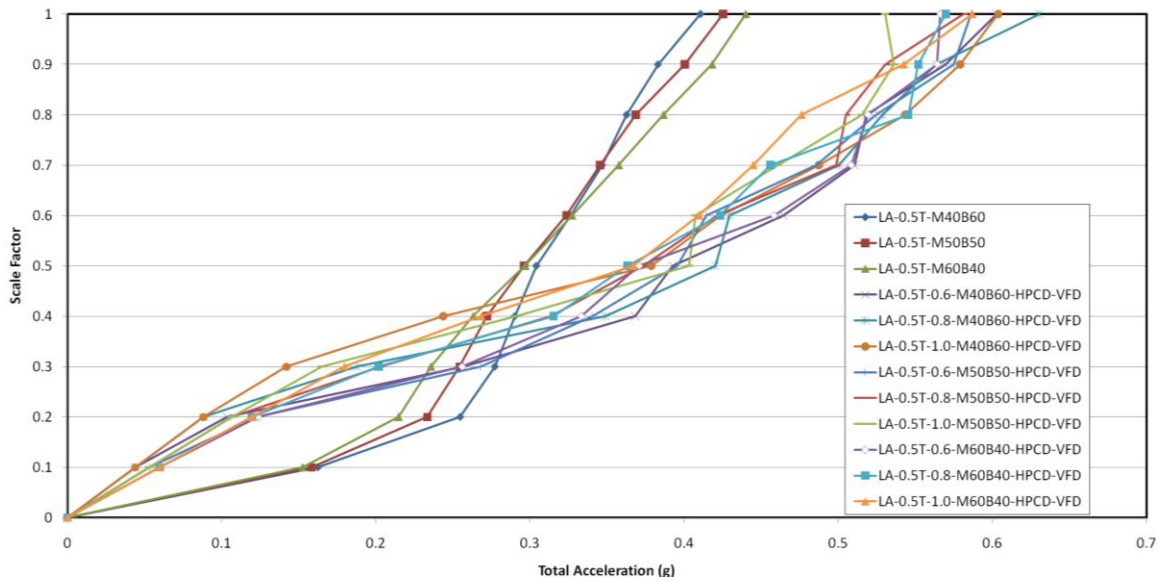


Figure B- 20: Los Angeles 0.5T HPCD-VFD Acceleration

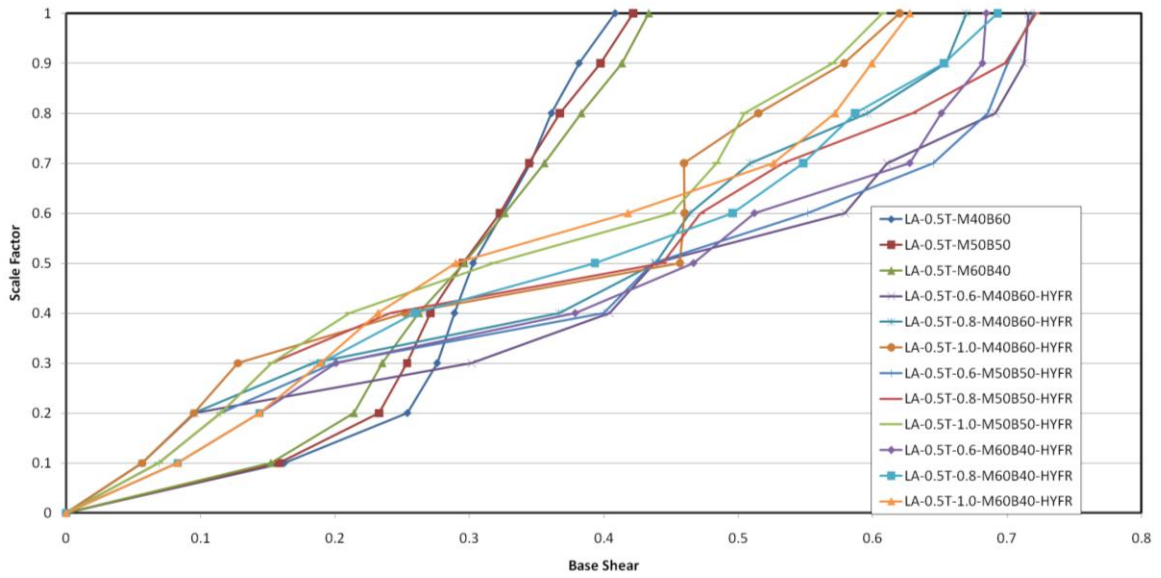


Figure B- 21: Los Angeles 0.5T HYFR Base Shear

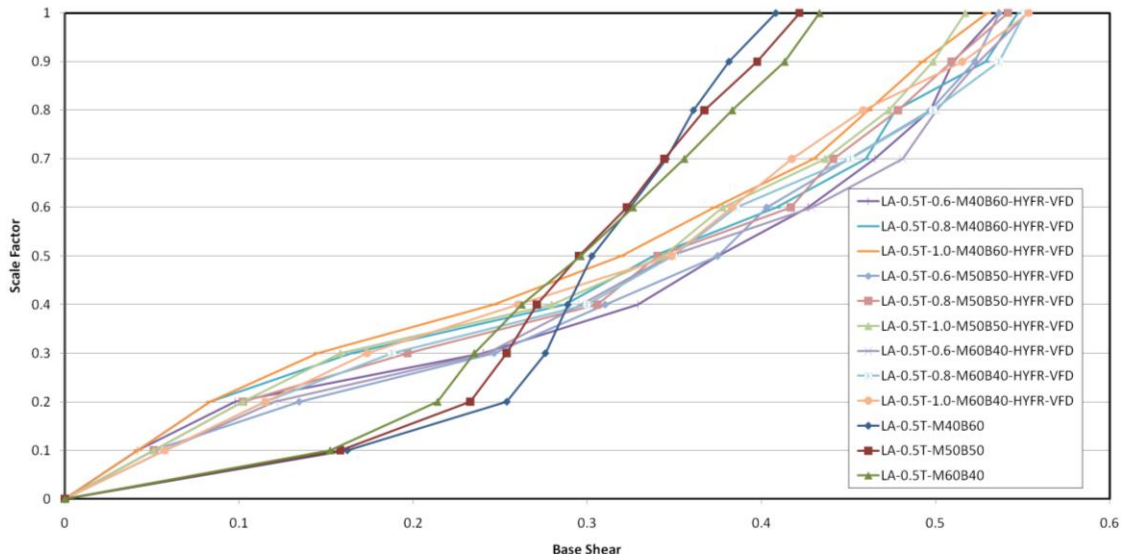


Figure B- 22: Los Angeles 0.5T HYFR-VFD Base Shear

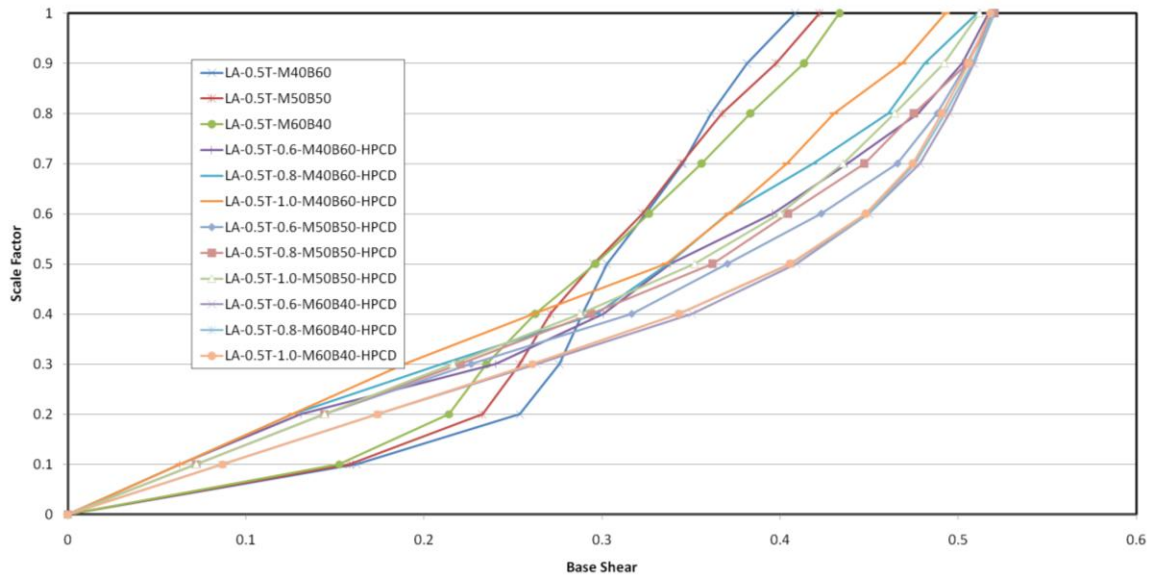


Figure B- 23: Los Angeles 0.5T HPCD Base Shear

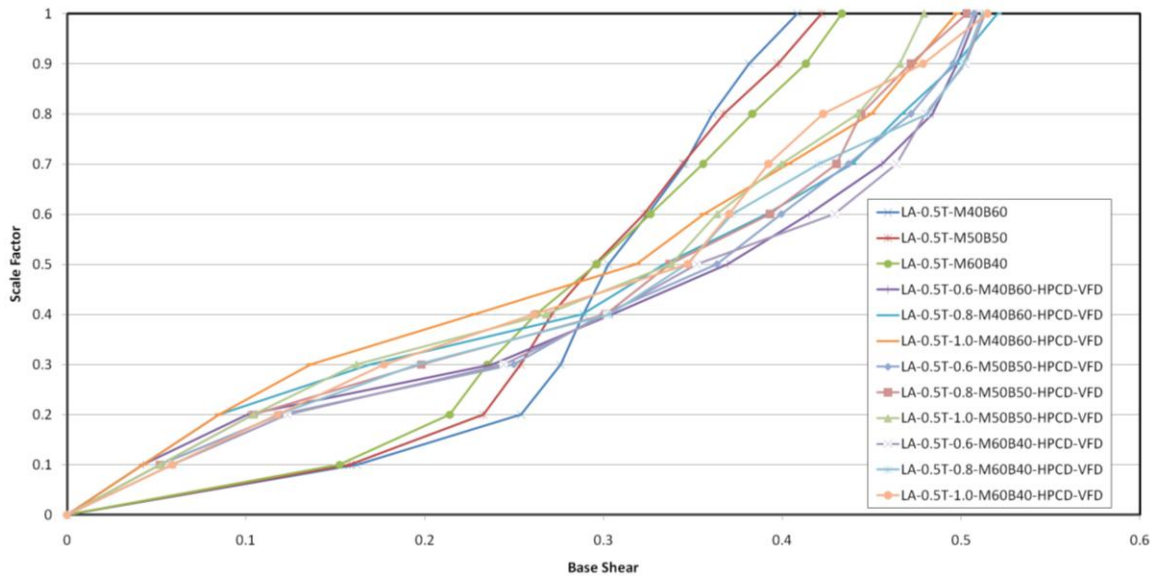


Figure B- 24: Los Angeles 0.5T HPCD-VFD Base Shear

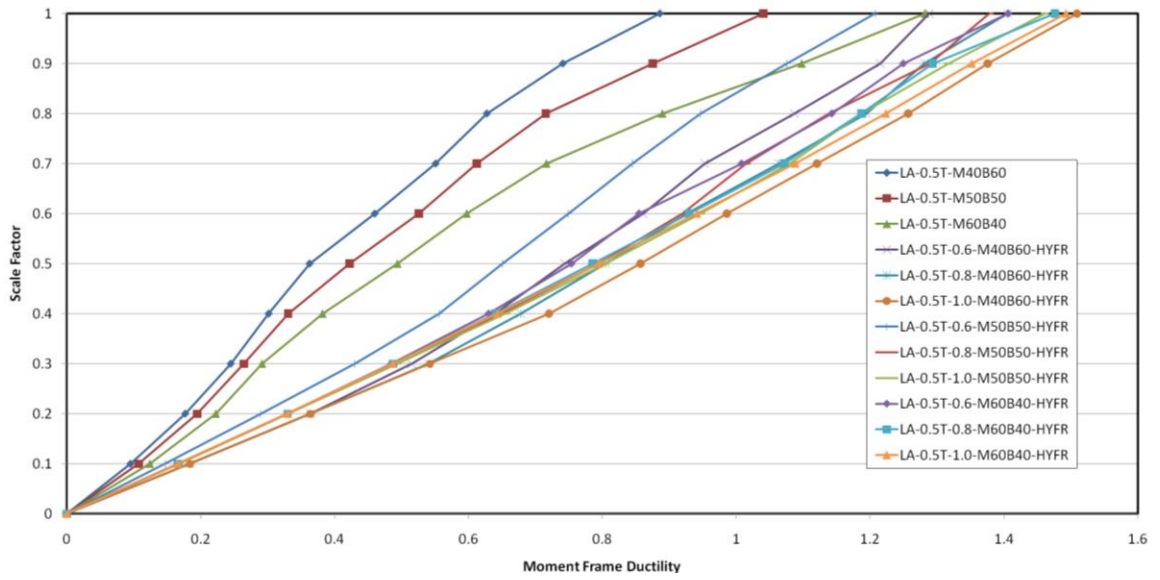


Figure B- 25: Los Angeles 0.5T HYFR Moment Frame Ductility

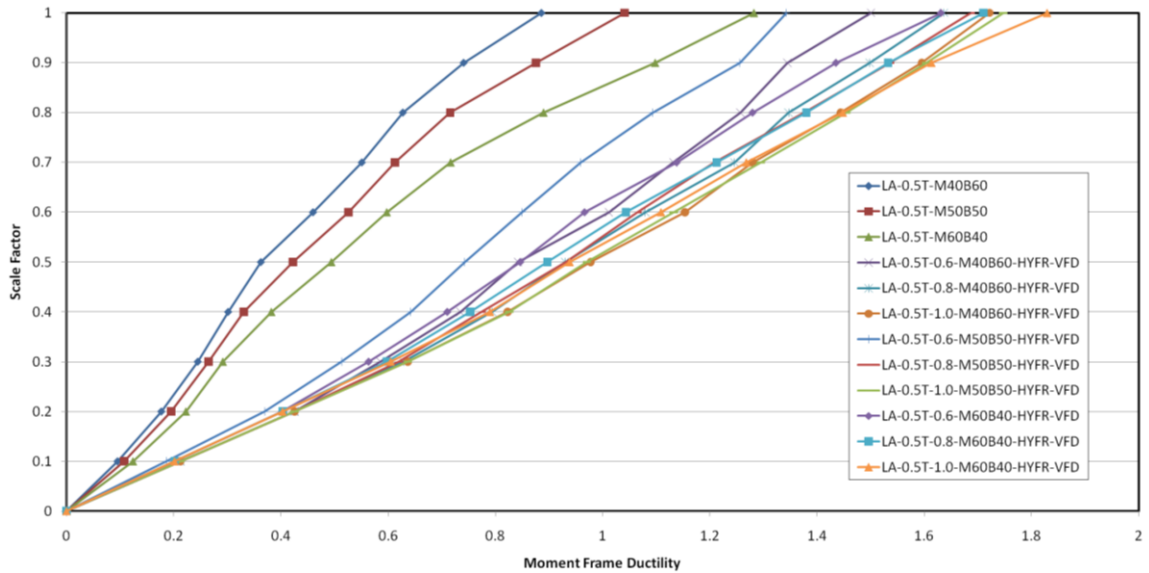


Figure B- 26: Los Angeles 0.5T HYFR-VFD Moment Frame Ductility

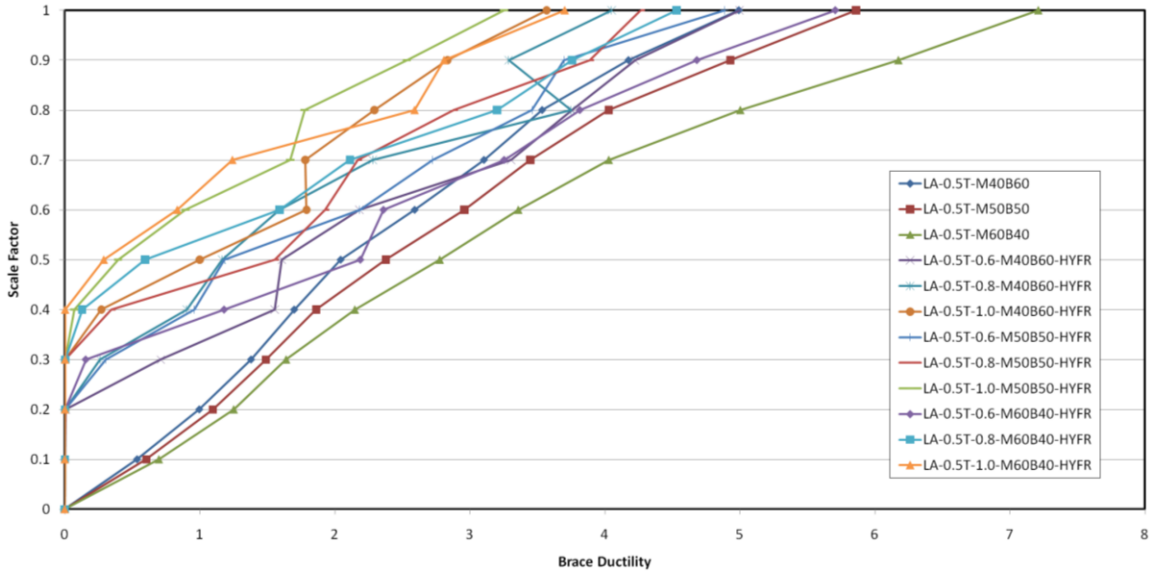


Figure B- 29: Los Angeles 0.5T HYFR Brace Ductility

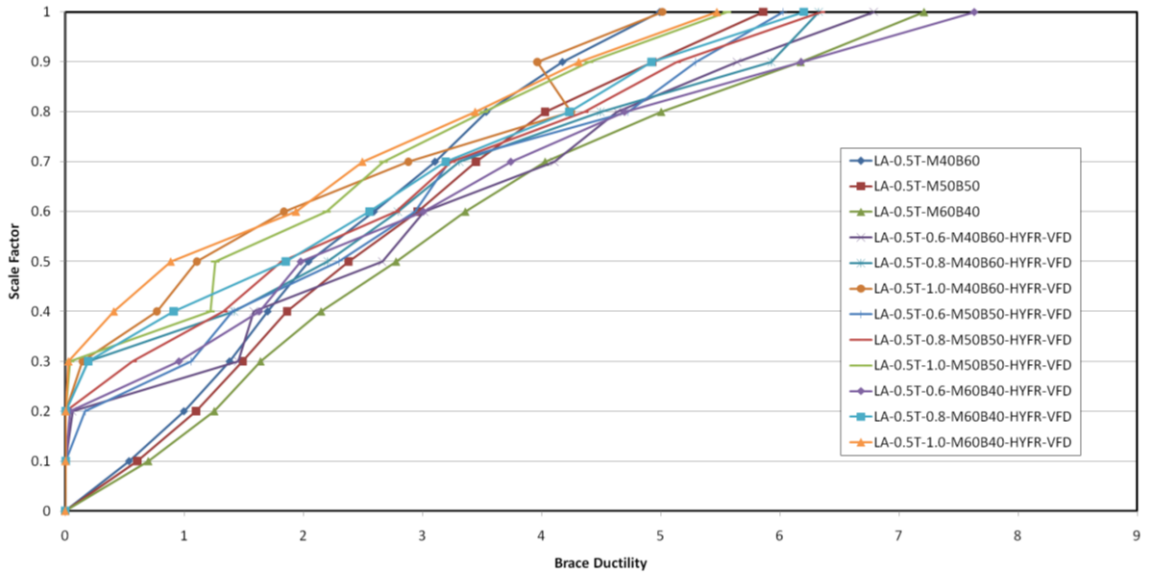


Figure B- 30: Los Angeles 0.5T HYFR-VFD Brace Ductility

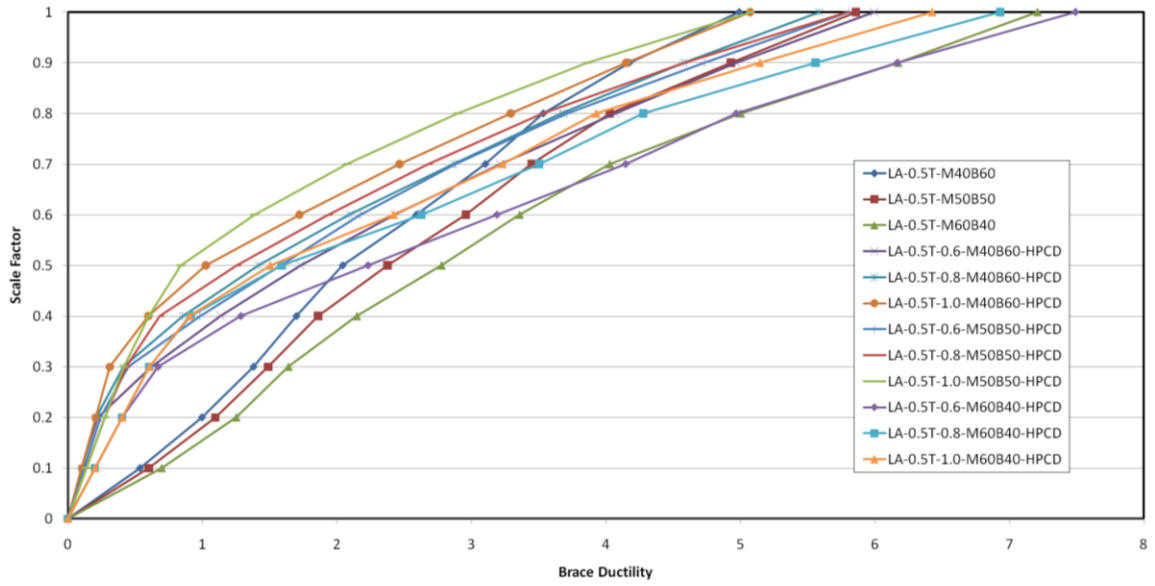


Figure B- 31: Los Angeles 0.5T HPCD Brace Ductility

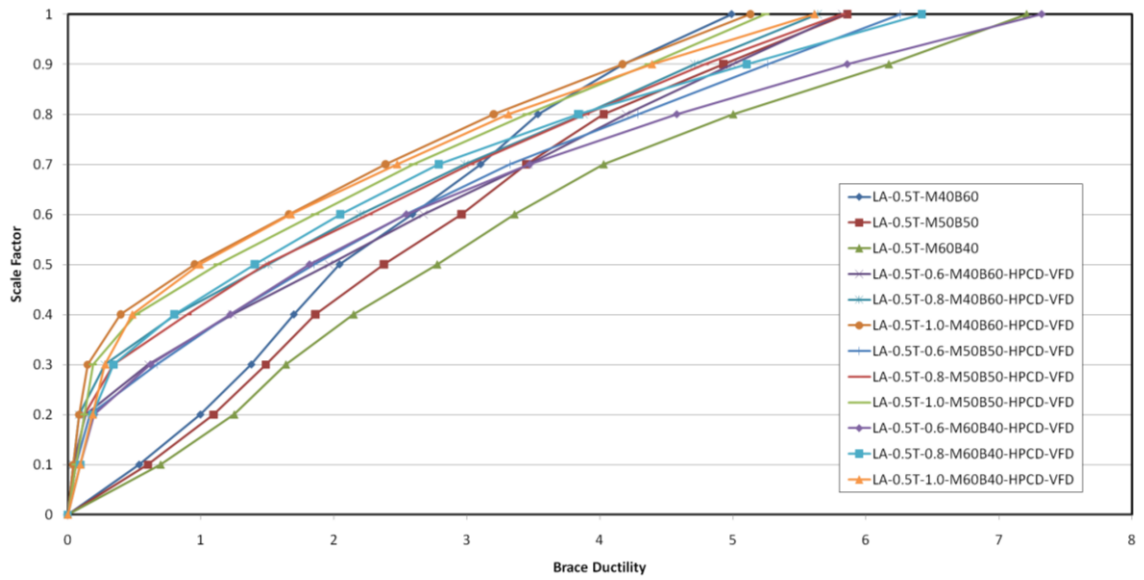


Figure B- 32: Los Angeles 0.5T HPCD-VFD Brace Ductility

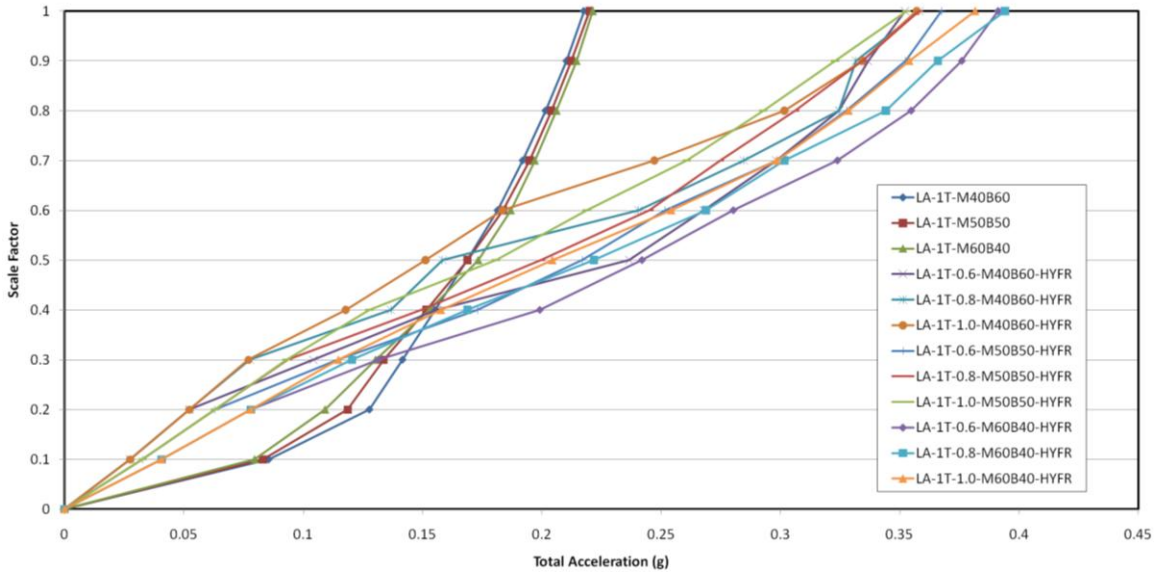


Figure B- 33: Los Angeles 1T HYFR Acceleration

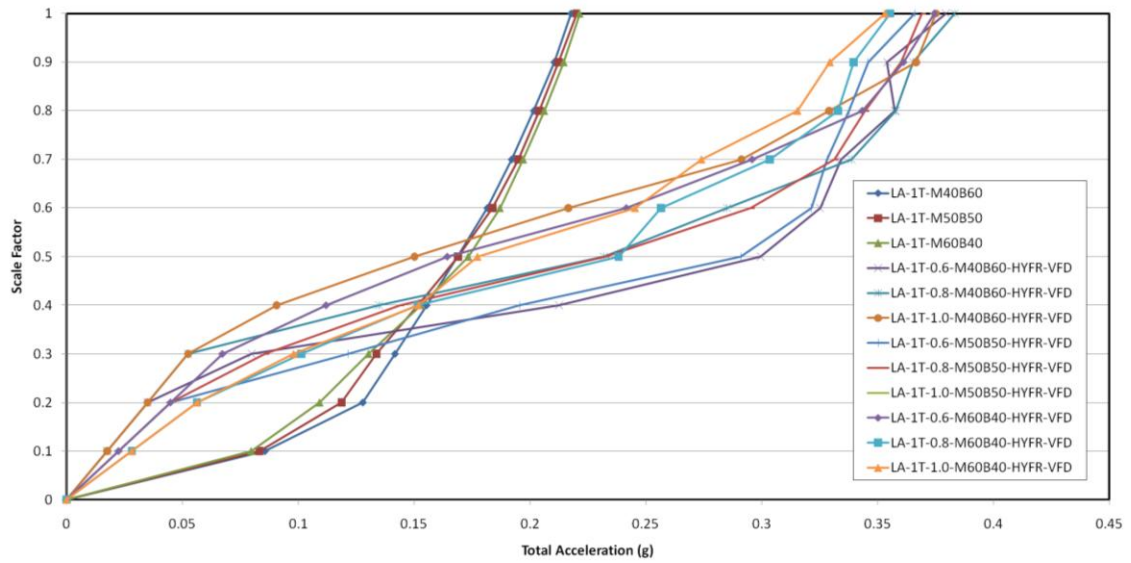


Figure B- 34: Los Angeles 1T HYFR-VFD Acceleration

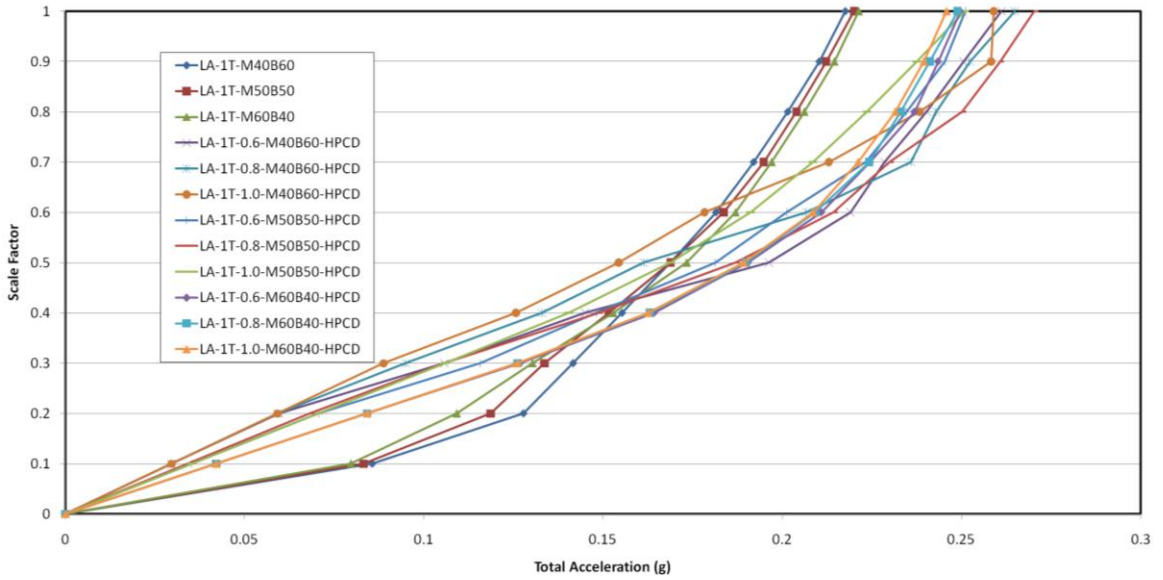


Figure B- 35: Los Angeles 1T HPCD Acceleration

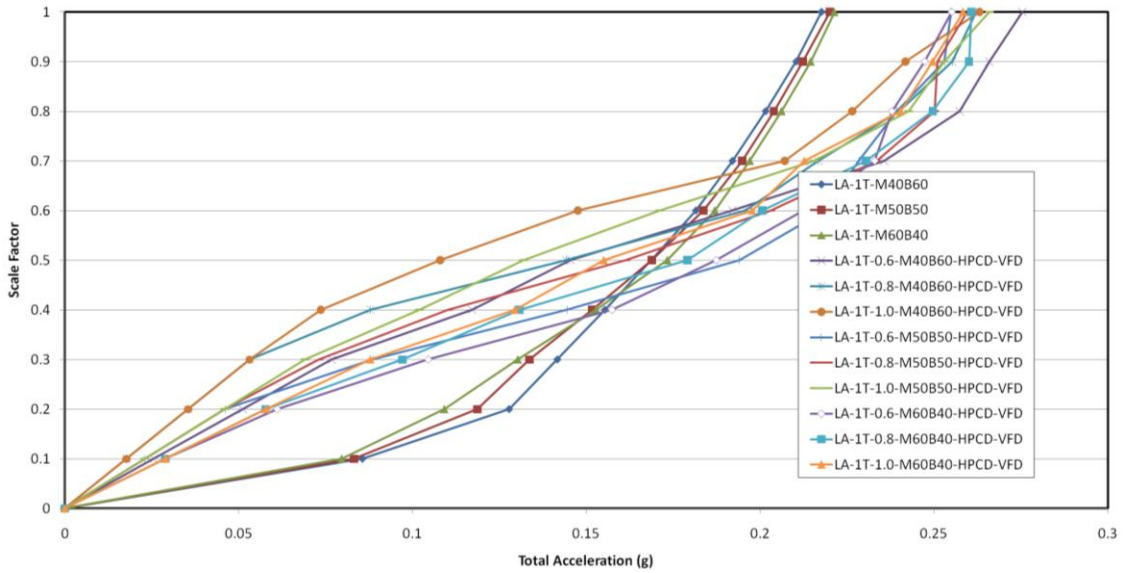


Figure B- 36: Los Angeles 1T HPCD-VFD Acceleration

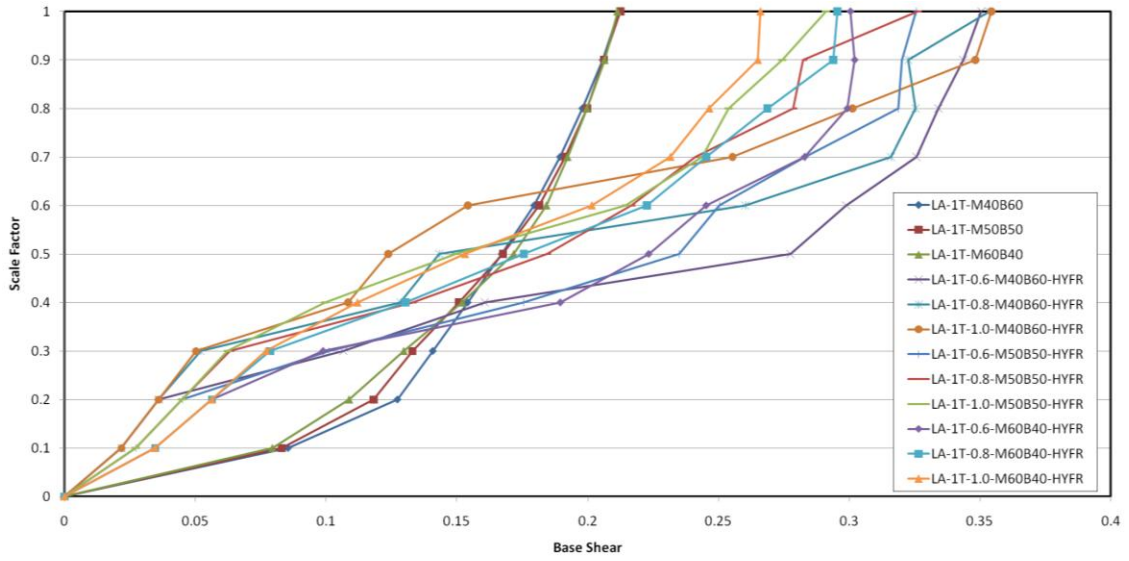


Figure B- 37: Los Angeles 1T HYFR Base Shear

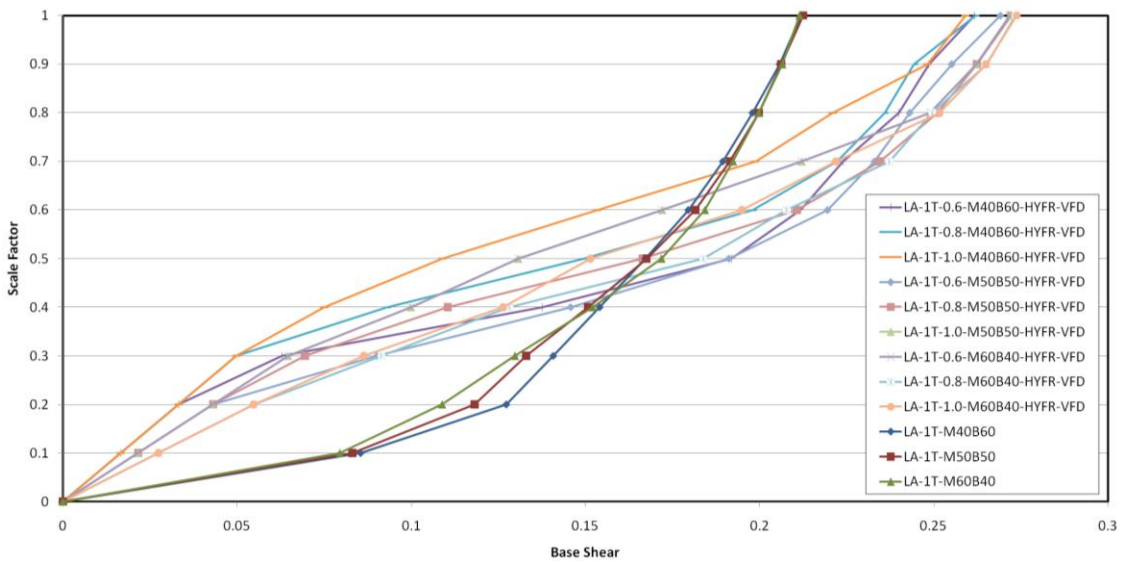


Figure B- 38: Los Angeles 1T HYFR-VFD Base Shear

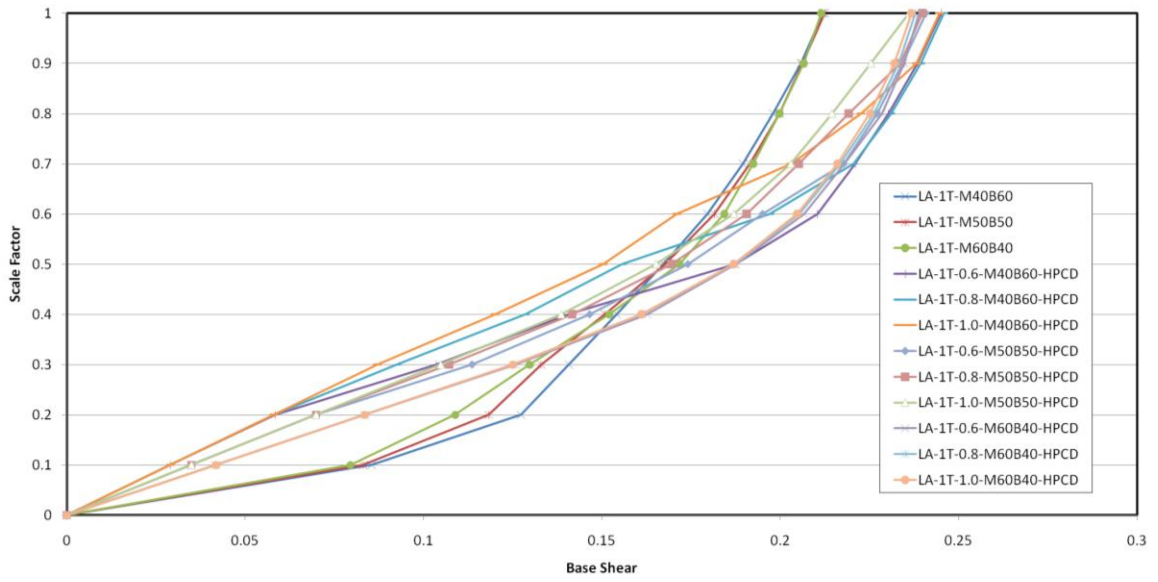


Figure B- 39: Los Angeles 1T HPCD Base Shear

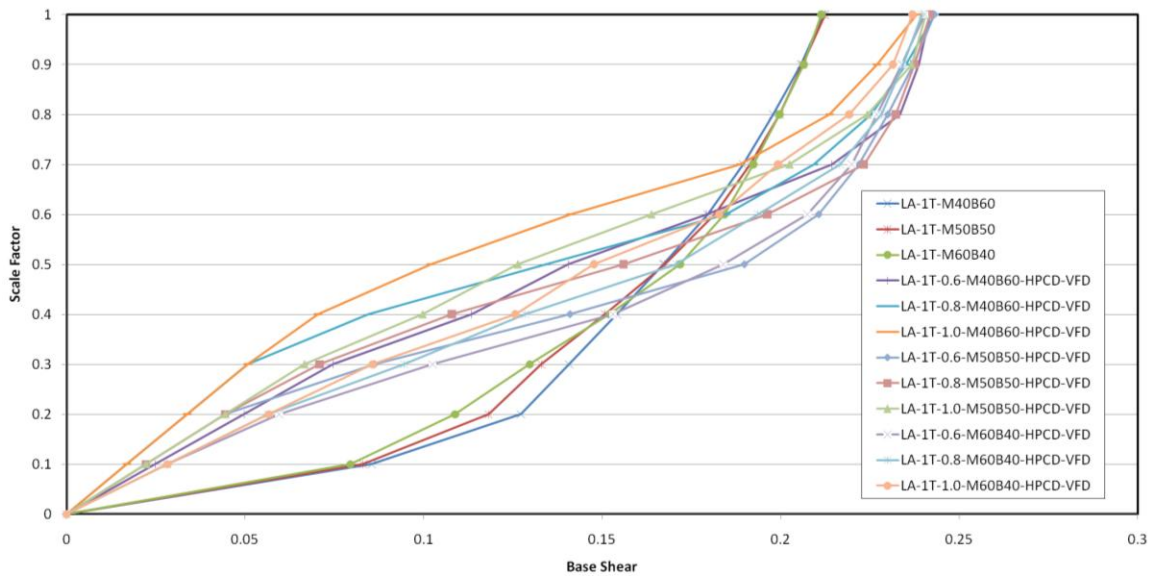


Figure B- 40: Los Angeles 1T HPCD-VFD Base Shear

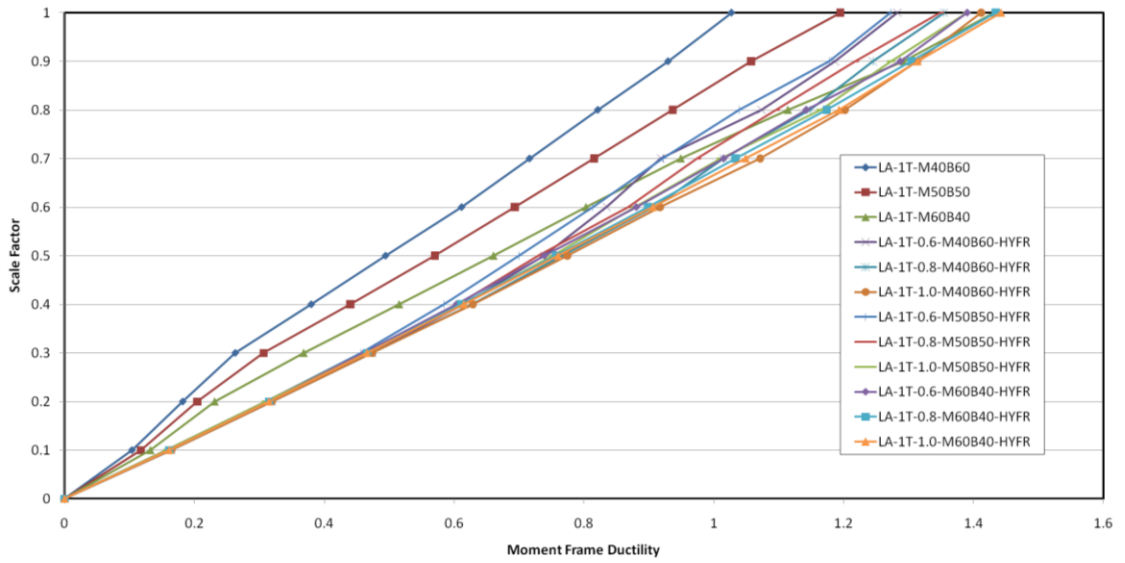


Figure B- 41: Los Angeles 1T HYFR Moment Frame Ductility

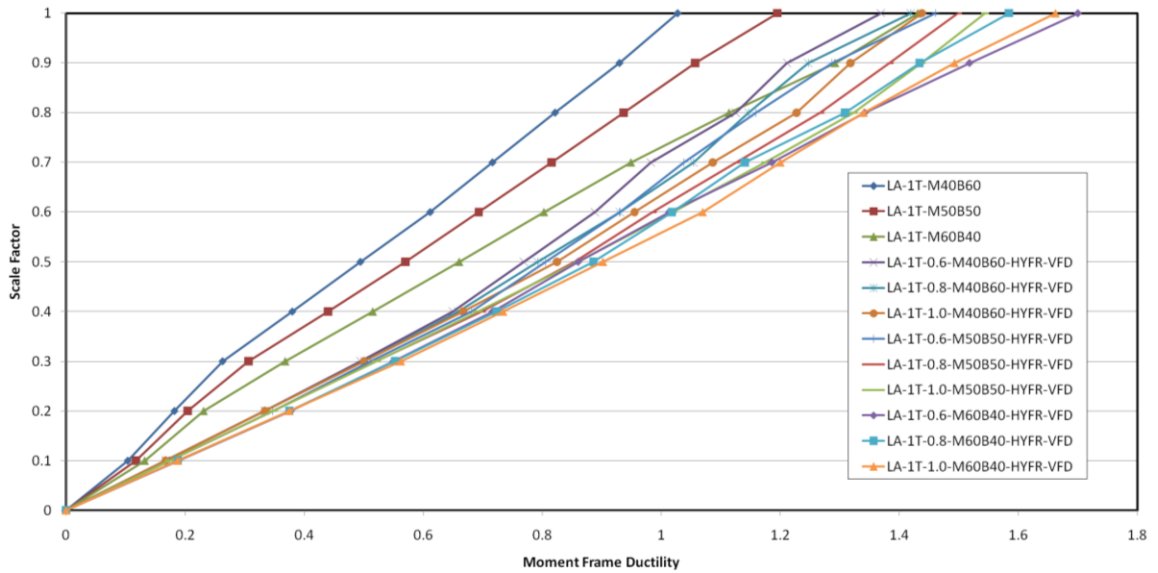


Figure B- 42: Los Angeles 1T HYFR-VFD Moment Frame Ductility

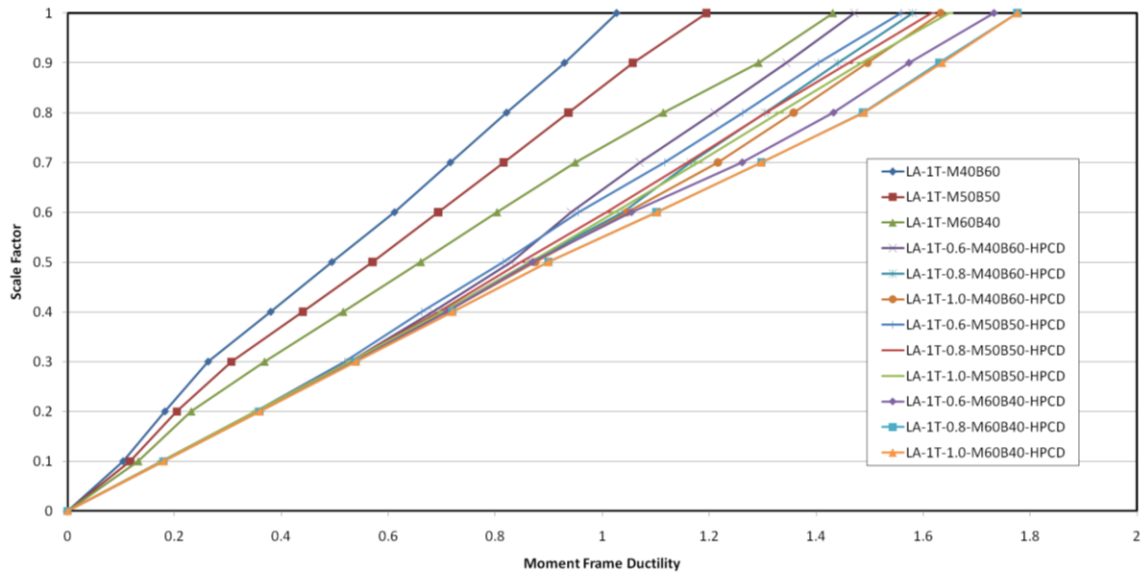


Figure B- 43: Los Angeles 1T HPCD Moment Frame Ductility

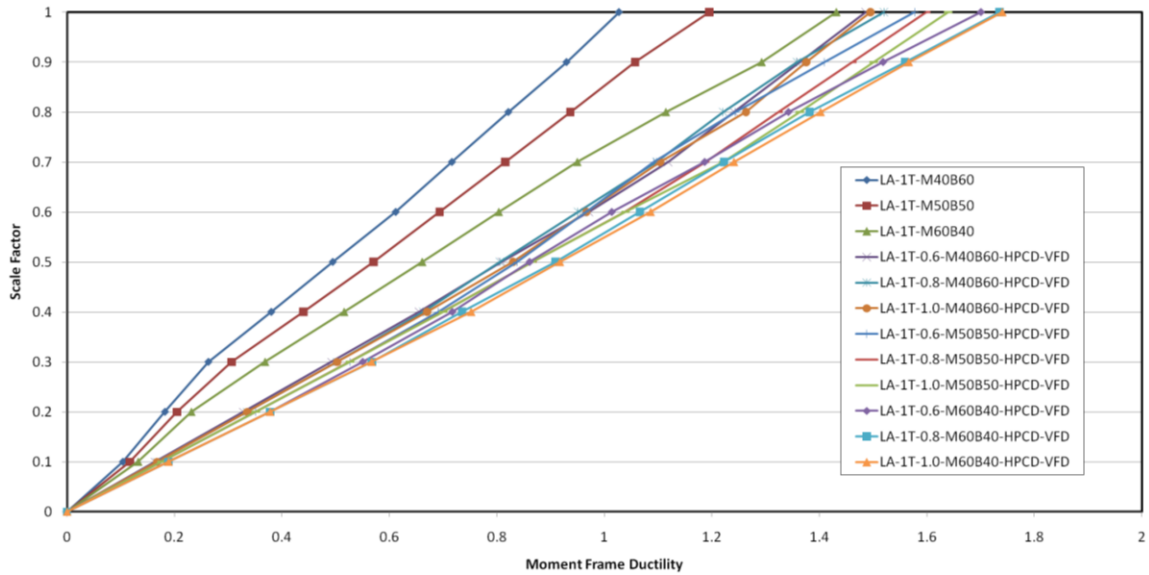


Figure B- 44: Los Angeles 1T HPCD-VFD Moment Frame Ductility

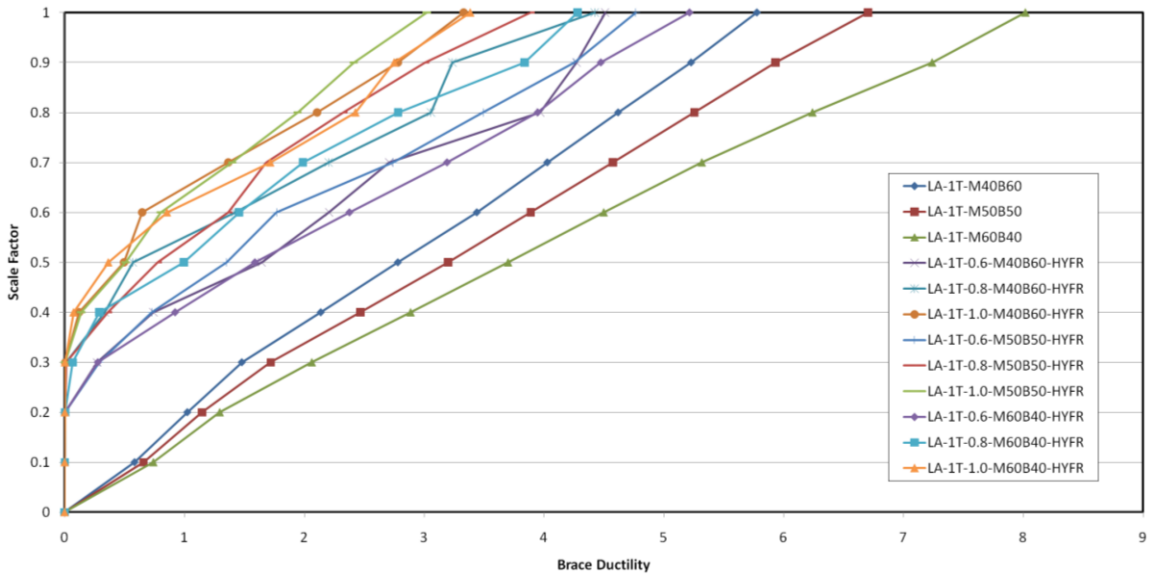


Figure B- 45: Los Angeles 1T HYFR Brace Ductility

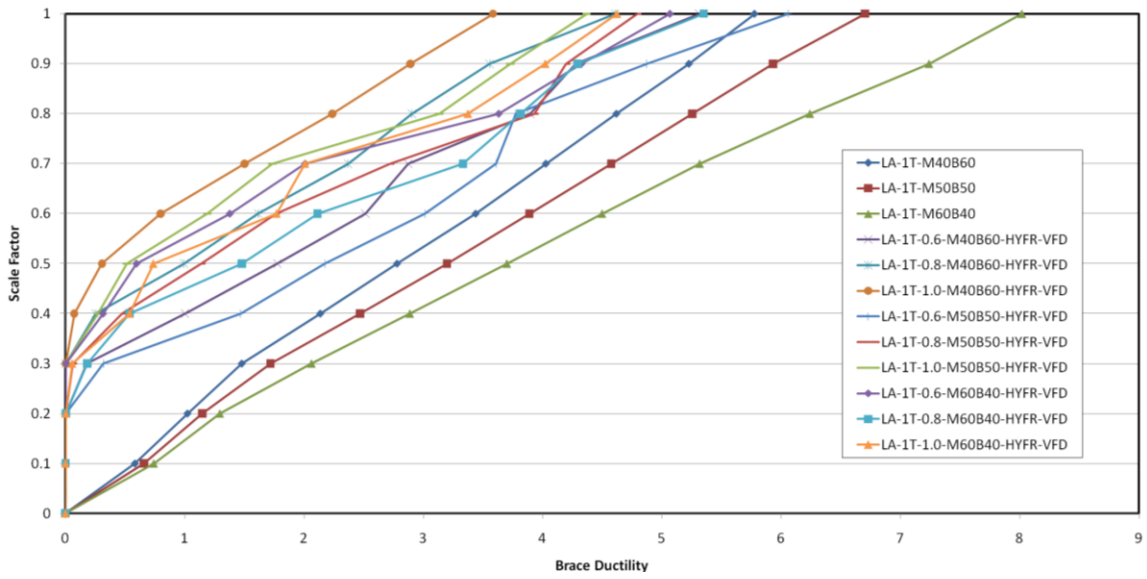


Figure B- 46: Los Angeles 1T HYFR-VFD Brace Ductility

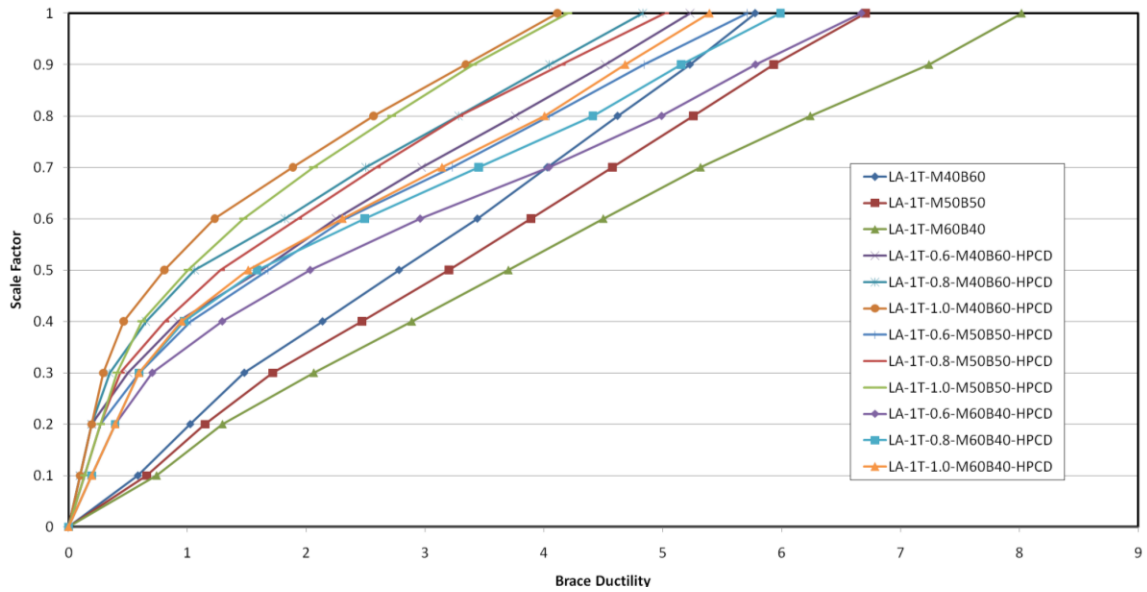


Figure B- 47: Los Angeles 1T HPCD Brace Ductility

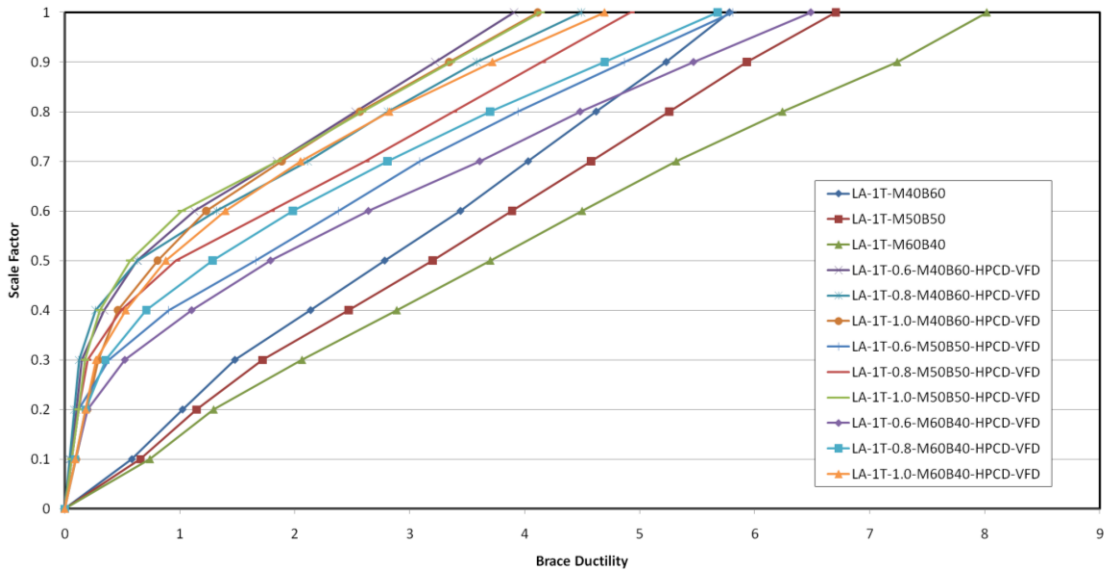


Figure B- 48: Los Angeles 1T HPCD-VFD Brace Ductility

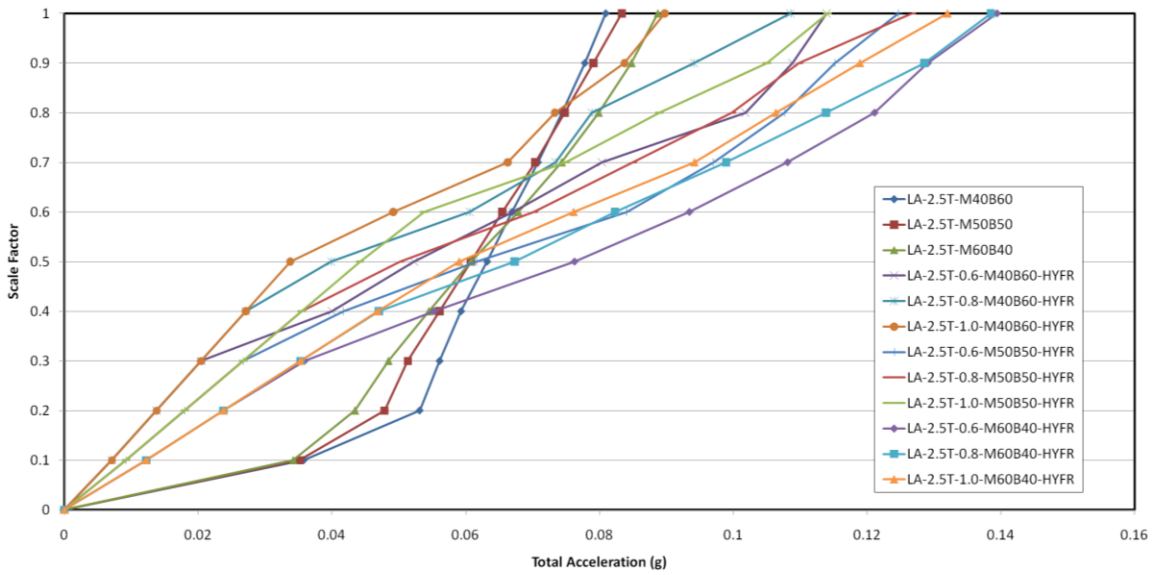


Figure B- 49: Los Angeles 2.5T HYFR Acceleration

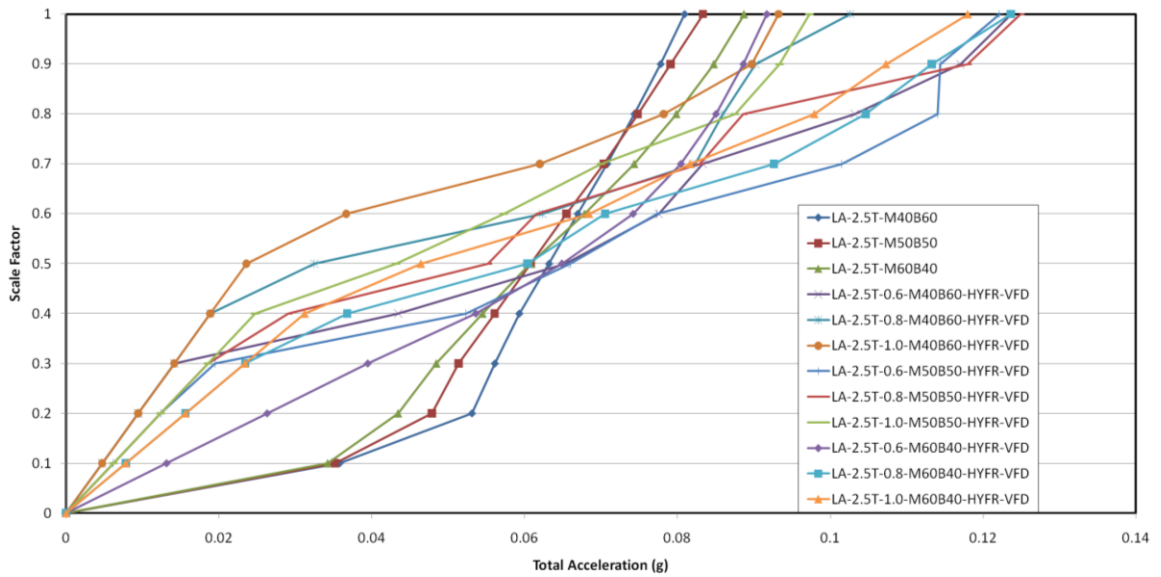


Figure B- 50: Los Angeles 2.5T HYFR-VFD Acceleration

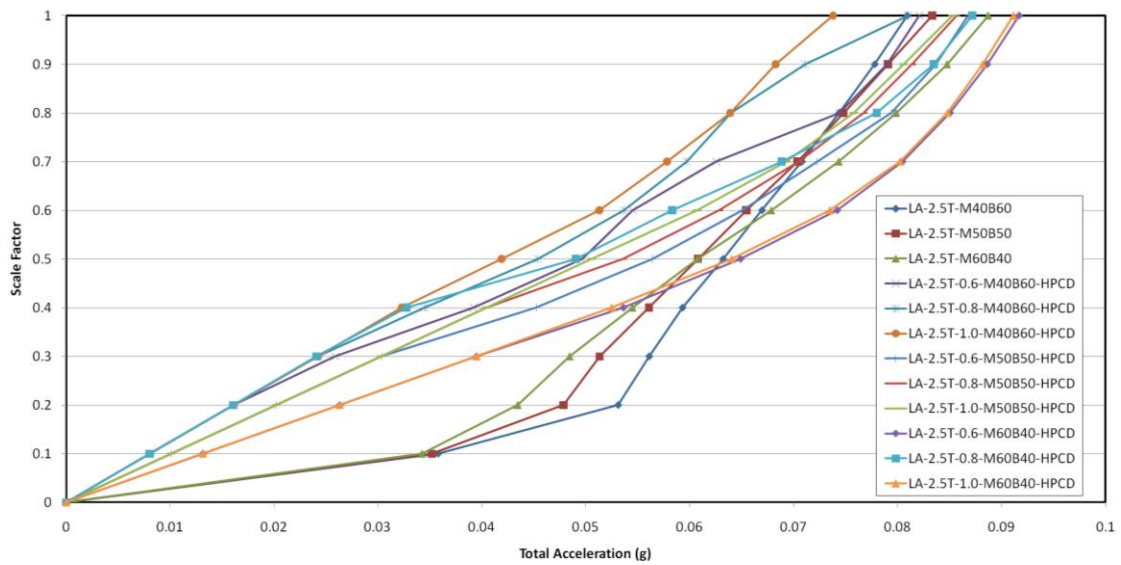


Figure B- 51: Los Angeles 2.5T HPCD Acceleration

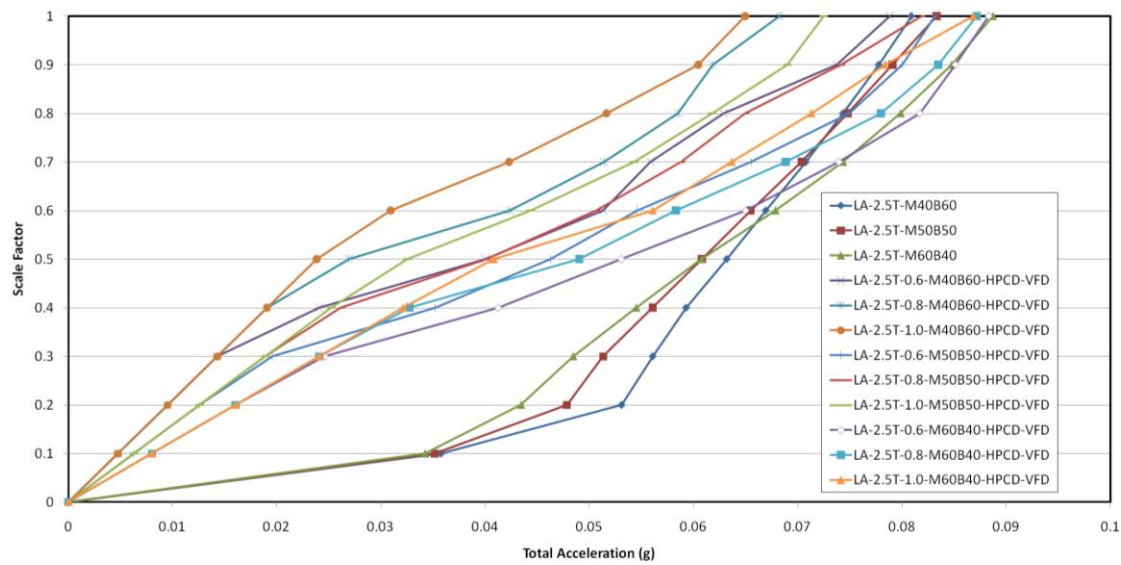


Figure B- 52: Los Angeles 2.5T HPCD-VFD Acceleration

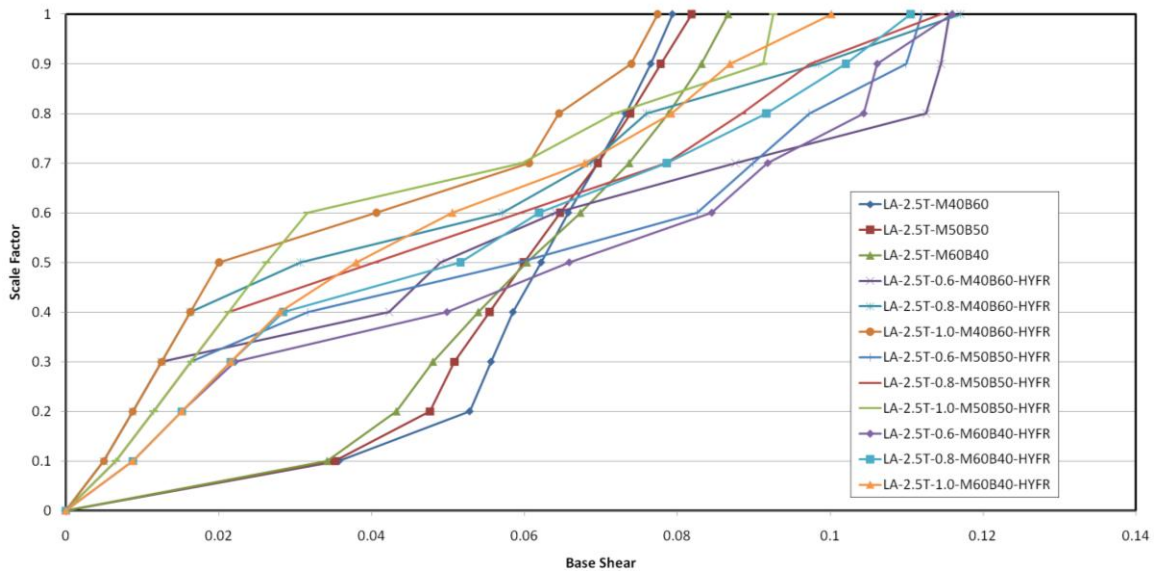


Figure B- 53: Los Angeles 2.5T HYFR Base Shear

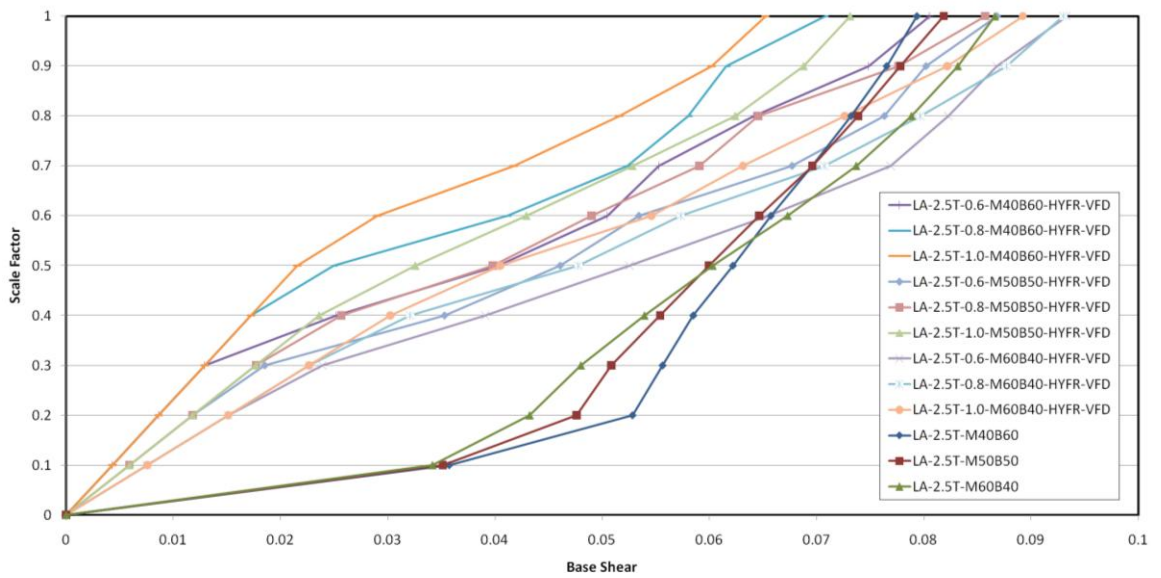


Figure B- 54: Los Angeles 2.5T HYFR-VFD Base Shear

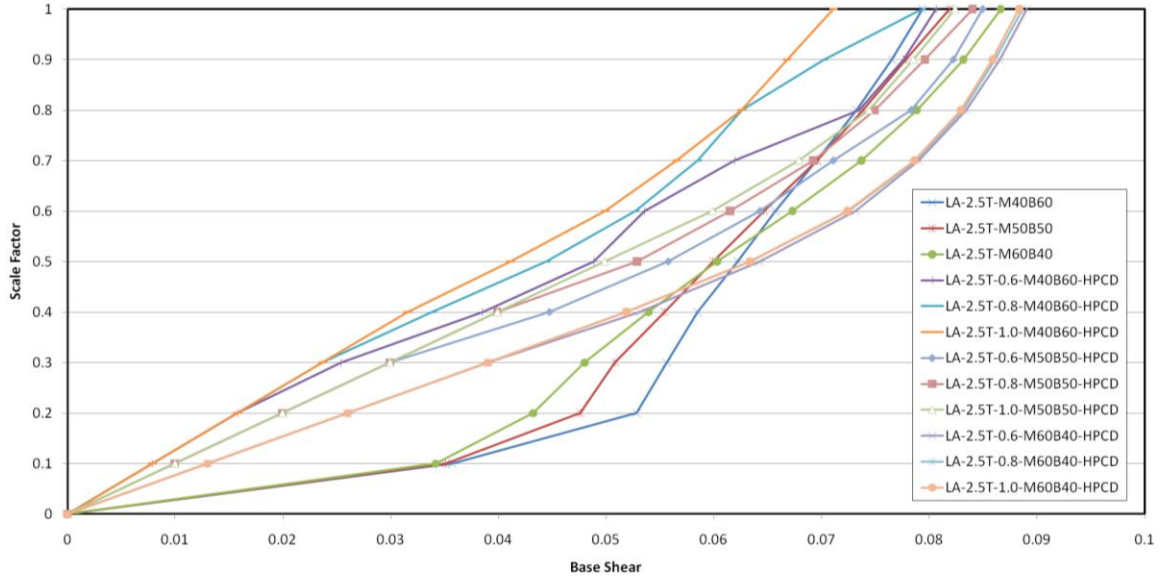


Figure B- 55: Los Angeles 2.5T HPCD Base Shear

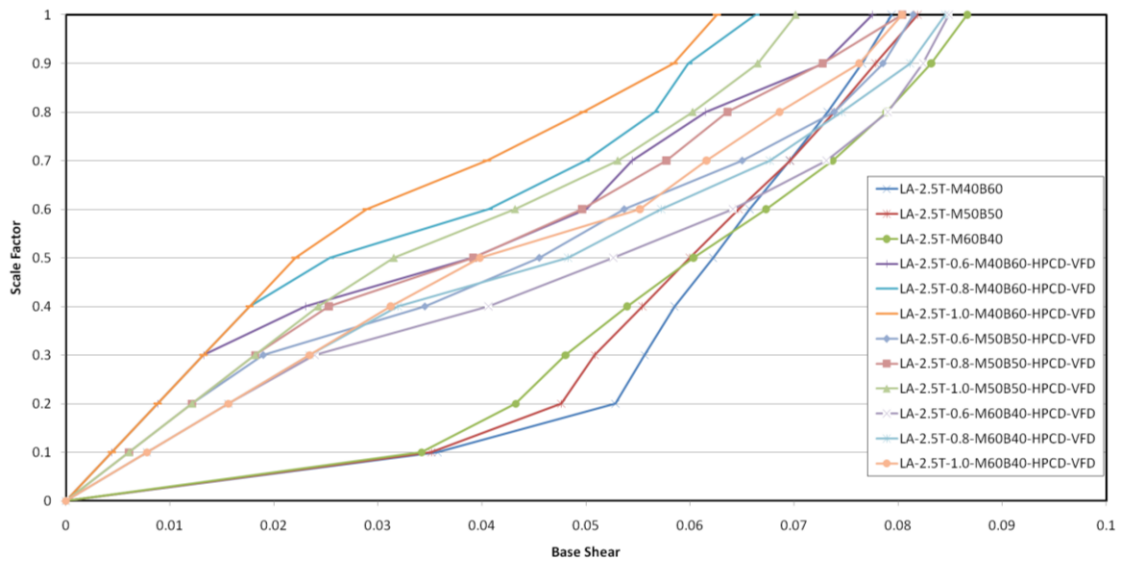


Figure B- 56: Los Angeles 2.5T HPCD-VFD Base Shear

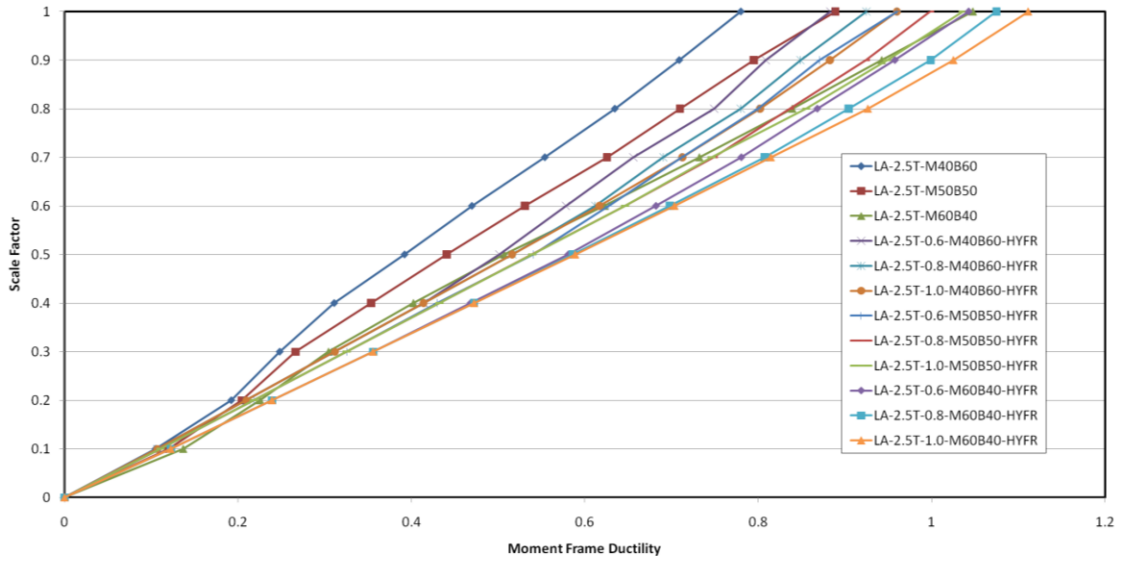


Figure B- 57: Los Angeles 2.5T HYFR Moment Frame Ductility

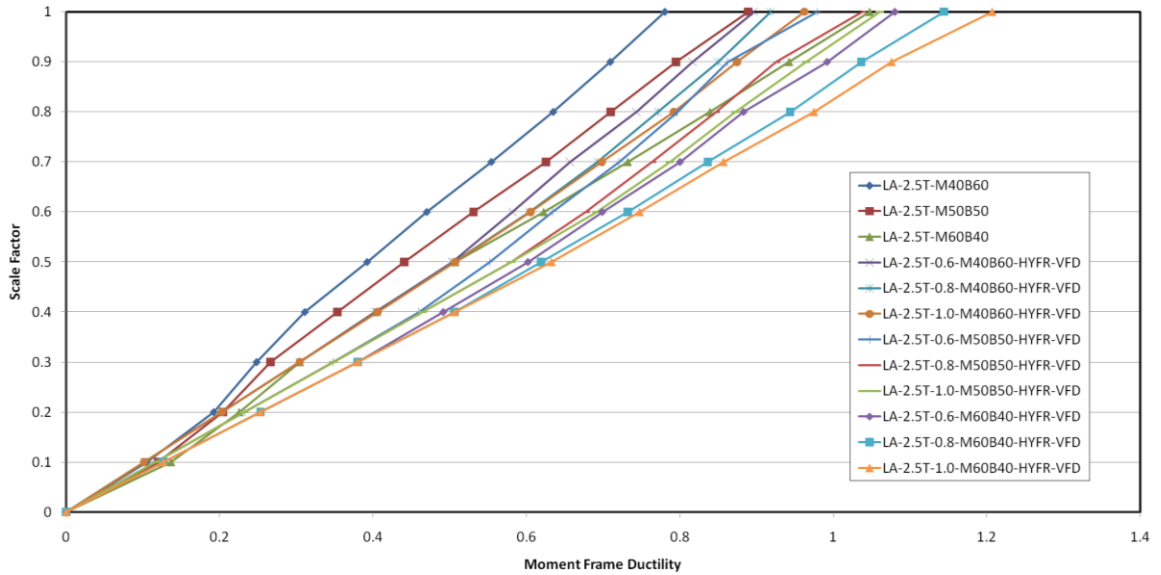


Figure B- 58: Los Angeles 2.5T HYFR-VFD Moment Frame Ductility

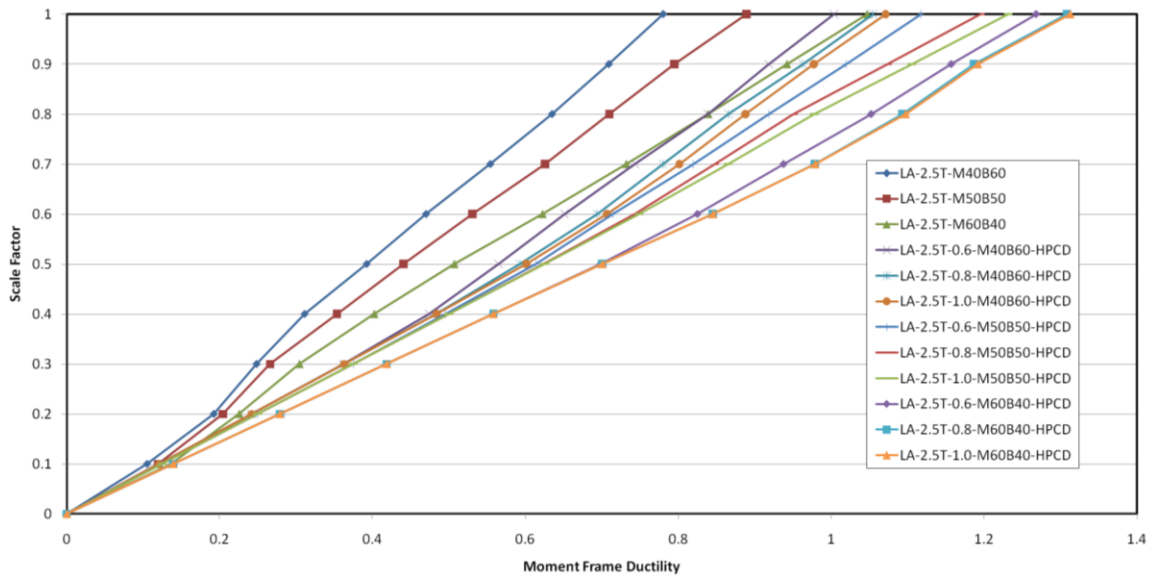


Figure B- 59: Los Angeles 2.5T HPCD Moment Frame Ductility

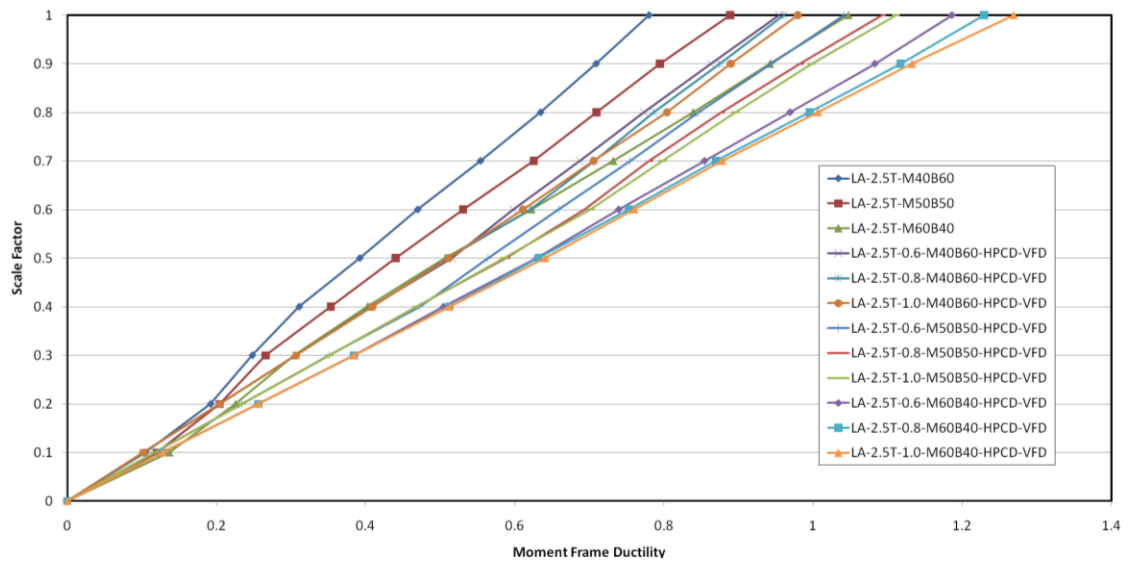


Figure B- 60: Los Angeles 2.5T HPCD-VFD Moment Frame Ductility

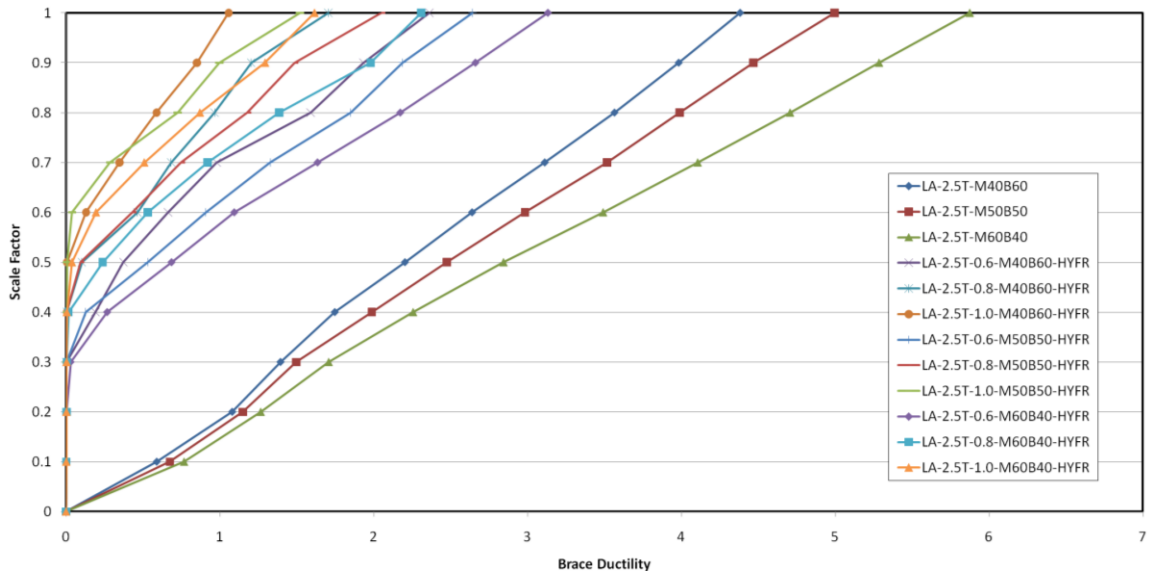


Figure B- 61: Los Angeles 2.5T HYFR Brace Ductility

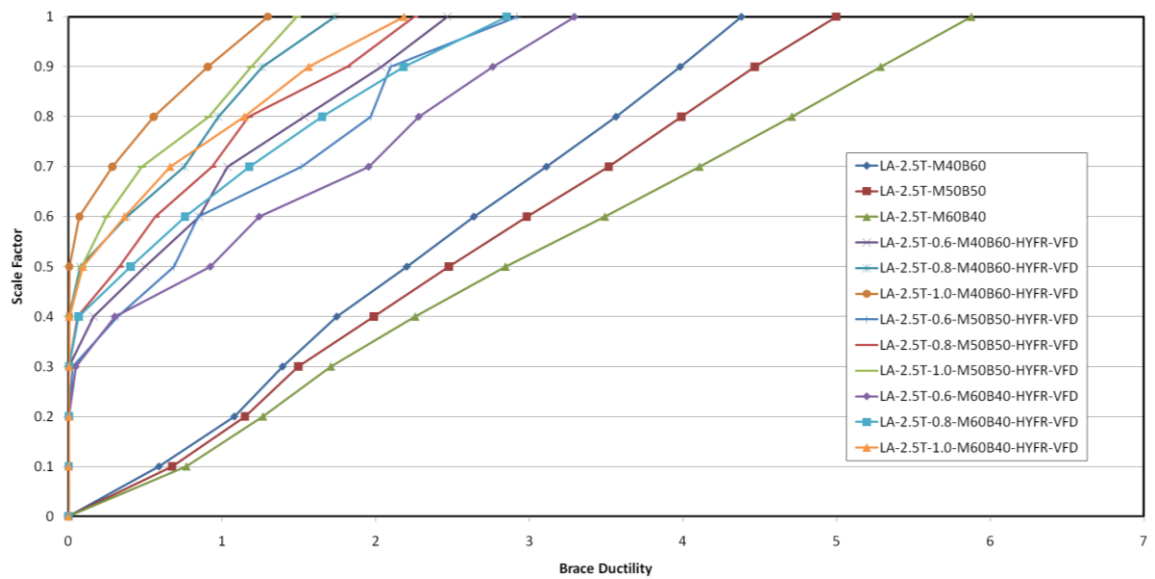


Figure B- 62: Los Angeles 2.5T HYFR-VFD Brace Ductility

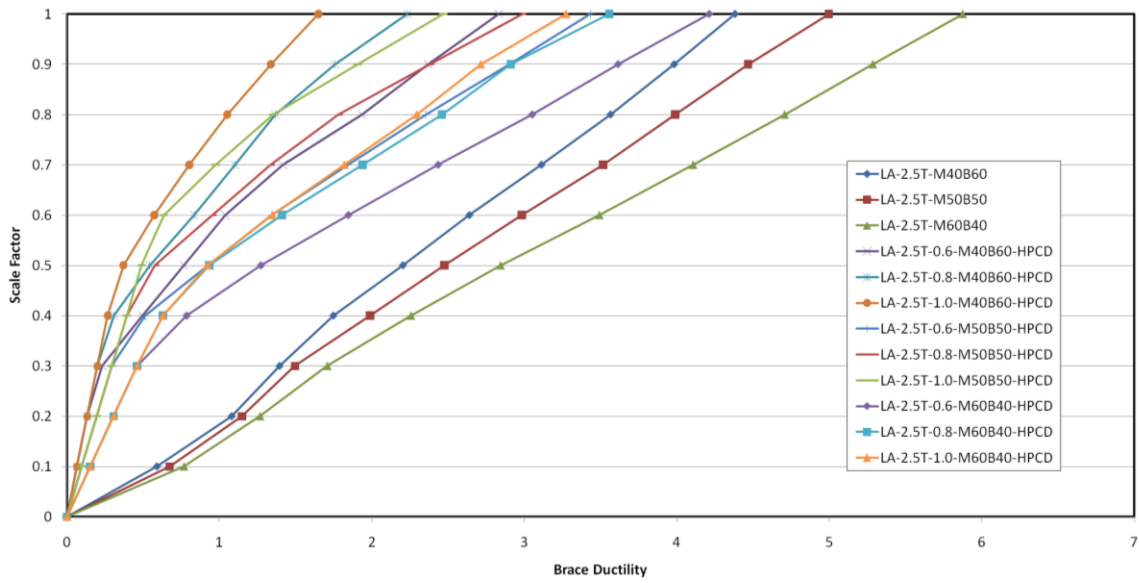


Figure B- 63: Los Angeles 2.5T HPCD Brace Ductility

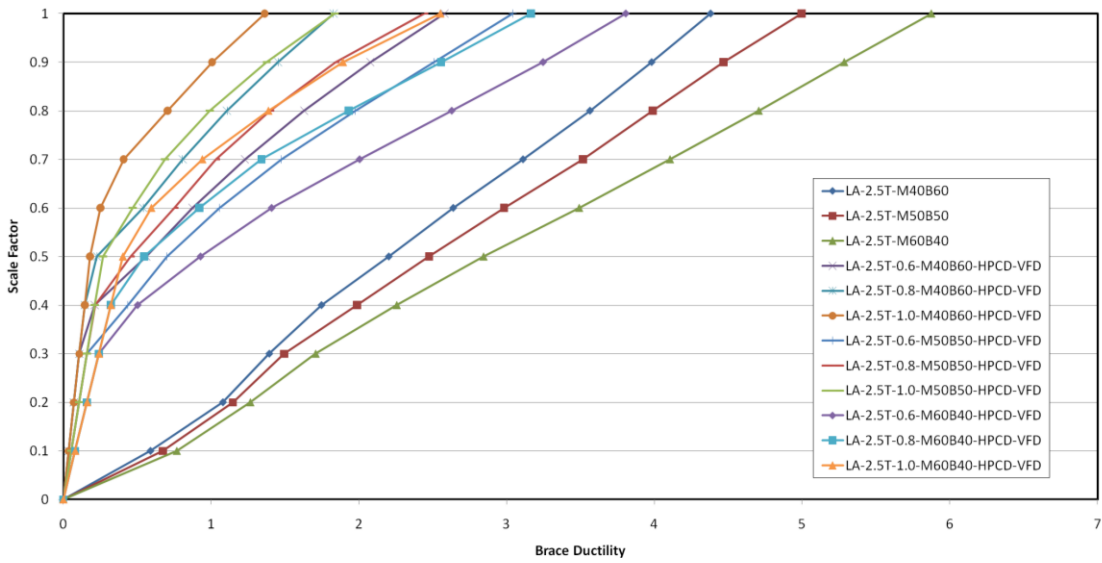


Figure B- 64: Los Angeles 2.5T HPCD-VFD Brace Ductility

